Wayne State University Dissertations

1-1-1999

Effect of cell- and species-differences in the expression of drug metabolism enzymes on chemical-induced injury to the rat and human kidney

Brian S. Cummings

Follow this and additional works at: http://digitalcommons.wayne.edu/oa_dissertations

EFFECT OF CELL- AND SPECIES-DIFFERENCES IN THE EXPRESSION OF
DRUG METABOLISM ENZYMES ON CHEMICAL-INDUCED INJURY TO THE
RAT AND HUMAN KIDNEY

by

BRIAN S. CUMMINGS

DISSERTATION

Submitted to the Graduate School

of Wayne State University,

Detroit Michigan

in partial fulfillment of the requirements

for the degree of

DOCTOR OF PHILOSOPHY

1999

MAJOR: PHARMACOLOGY

Approved by:

_____ 3–5–99
Advisor   Date

_____ 3/23/99

_____ 3/23/99

_____ 3/23/99

_____ 3/23/99

Dedication

This work is dedicated to my wife Jennifer. I could take up pages explaining why, but she already knows why and that's good enough for me.

Acknowledgements

TABLE OF CONTENTS

TABLE OF CONTENTS

LIST OF FIGURES

ABBREVIATIONS

ADP   adenosine 5'-diphosphate

AP   alkaline phosphatase

AOAA   aminooxyacetic acid

ATP   adenosine 5'-triphosphate

α-T   α-tocopherol

BSA   bovine serum albumin

BSP   bromosulfophthalein

CH   chloral hydrate

CDNB   1-chloro-2,4-dinitrobenzene

DCA   dichloroacetic acid

DCVC   S-(1,2-dichlorovinyl)-L-cysteine

DCVG   S-(1,2-dichlorovinyl)glutathione

DMEM   Dulbecco's Modified Eagle's Medium

EDTA   ethylene diamine tetraacetic acid

EGTA   ethylene glycol-bis(β-aminoethyl ether) N,N,N,'N,'-tetraacetic acid

EtOH   ethanol

F12   Ham's F12 Media

FITC   Fluorescein Isothiocyanate

FMO   flavin-containing monooxygenase

GDH   glutamate dehydrogenase

GGCS   γ-glutamylcysteine synthetase

GGT   γ-glutamyltransferase

GPX   glutathione peroxidase

GRD   glutathione reductase

GSH   glutathione

GST   glutathione S-transferase

HEPES	N-(2-hyroxyethyl)piperazine-N'-2-ethenesulfonic acid
HPLC	high-performance liquid chromatography
hPT	human proximal tubular cells
LDH	lactate dehydrogenase
MDH	malate dehydrogenase
NAcDCVC	N-acetyl-S-(1,2-dichlorovinyl)-L-cysteine
NADH	nicotinamide adenine dinucleotide (reduced)
NADPH	nicotinamide adenine dinucleotidediphosphate (reduced)
P450	cytochrome P450 monooyxgenase
PBS	phosphate-buffered saline
RCR	respiratory control ratio
rDT	rat distal tubular cells
rPT	rat proximal tubular cells
ROIs	reactive oxygen intermediates
S3	state 3 rate of oxygen consumption
S4	state 4 rate of oxygen consumption
SCC	succinate cytochrome c oxidoreductase
4-TByA	4-(2-thienyl)butyric acid
TCA	trichloroacetic acid
TCOH	trichloroethanol
TETB	triethyltinbromide
Tri	trichloroethylene
2-TPAA	3-thiopheneacetic acid
3-TPAA	2-thiopheneacetic acid
3-TPEA	2-thiopheneethylamide
2-TPEtOH	2-thiophene ethanol
3-TPEtOH	3-thiophene ethanol

2-TPMeOH   2-thiophene methanol

3-TPMeOH   3-thiophenemethanol

Chapter 1

Issues for Consideration in Chemical-Induced Nephrotoxicity

The mammalian kidney is a complex organ made up of numerous different cell types that function together to facilitate the filtering of blood (Bulger et al., 1982; Tisher and Madsen, 1996). Several physiological functions of the kidneys cause them to be common targets of injury for many drugs and environmental pollutants. These include, but are not limited to, the process of glomerular filtration, the renal microcirculation that enhances delivery of any blood-borne chemical to renal epithelial cells, the high blood flow to the kidney relative to its weight, the presence of transport proteins on the luminal membrane that catalyze the transport of metabolites and ions into epithelial cells, and the ability of the kidney to concentrate urine (Lash, 1996). To support these activities, the kidney relies heavily on cellular ATP and have a high metabolic rate. To support this high metabolic rate the kidney has a high rate of oxygen consumption, which occurs primarily in the mitochondria. When partial reduction of oxygen occurs in the mitochondria, O_2^- and H_2O_2 can be produced. Cells within the kidney with higher rates of oxygen consumption are more susceptible to injury caused by these metabolites. This may result in site-specific chemical-induced injury in the kidneys.

Morphology of the kidneys, as well as their physiology, can contribute to site-specific, chemically-induced nephrotoxicity. For example, rat proximal tubular (rPT) cells are most likely to be the target population for toxicants as they are the first cells to be exposed to blood-borne chemicals that undergo glomerular filtration (Figure 1). Examples of such cell selective toxicity have been demonstrated using cephaloridine, 4-(2-thienyl)butyric acid (4-TByA), trichloroethylene (Tri), and its metabolite S-(1,2-dichlorovinyl)-L-cysteine (DCVC) (Beaune et al., 1994; Lash et al., 1994; Lash and Tokarz, 1995). Furthermore, the concentrating ability of several kidney cell types results in these cells being exposed to higher concentrations of chemicals than non-renal cells.

1

In contrast, some toxicants may cause greater toxicity to rat renal distal tubular (rDT) cells than rPT cells as measured by lactate dehydrogenase (LDH) (EC 1.1.1.27) release (Lash and Tokarz, 1990). Possible explanations for the differences seen with these chemicals include those listed above as well as the presence and absence of several drug metabolizing enzymes such as cytochromes P-450 monooxygenase (P450) (EC 1.14.14.1), flavin-containing monooxygenases (FMO) (EC 1.14.14.1), glutathione-dependent enzymes, N-acetyl-S-transferases (EC 2.3.1.38), cysteine-S-conjugate β-lyase (EC 4.4.1.13), and matrix metalloproteinases (EC 3.4.24.7). The expression and activity of many of these enzymes have been well characterized in kidney microsomes and cytosol and recently studies have produced information about the differences in activity and expression of these enzymes between different sites in the kidney (Figure 1) (Lohr et al., 1998). Despite these studies, little work has been produced describing the differences in the activity and expression of specific drug metabolizing enzymes between different kidney cells within a single species. Even less work has been done studying the differences in these enzymes between similar kidney cells from different species (for example, P450 expression in rPT and rDT cells versus that in human PT and DT cells). These data would be valuable as they would provide information about the mechanism of toxicity of several chemicals and would greatly reduce the uncertainty in the extrapolation of animal data to humans for risk assessment purposes.

As mentioned above, the severity and mechanism of action of a nephrotoxicant is dependent on the location, the physiological function, and the biochemical function of the kidney cells being exposed. Other factors that may play a role in chemical-induced nephrotoxicity include the dose, exposure route, and duration of exposure to the chemical. When such factors are taken into account, it is easy to understand why there exists a large

Figure 1. Regional (A), tubular (B), and subcellular (C) localization of drug metabolizing enzyme systems in the mammalian kidney.

Taken from Lohr et al. (1998).
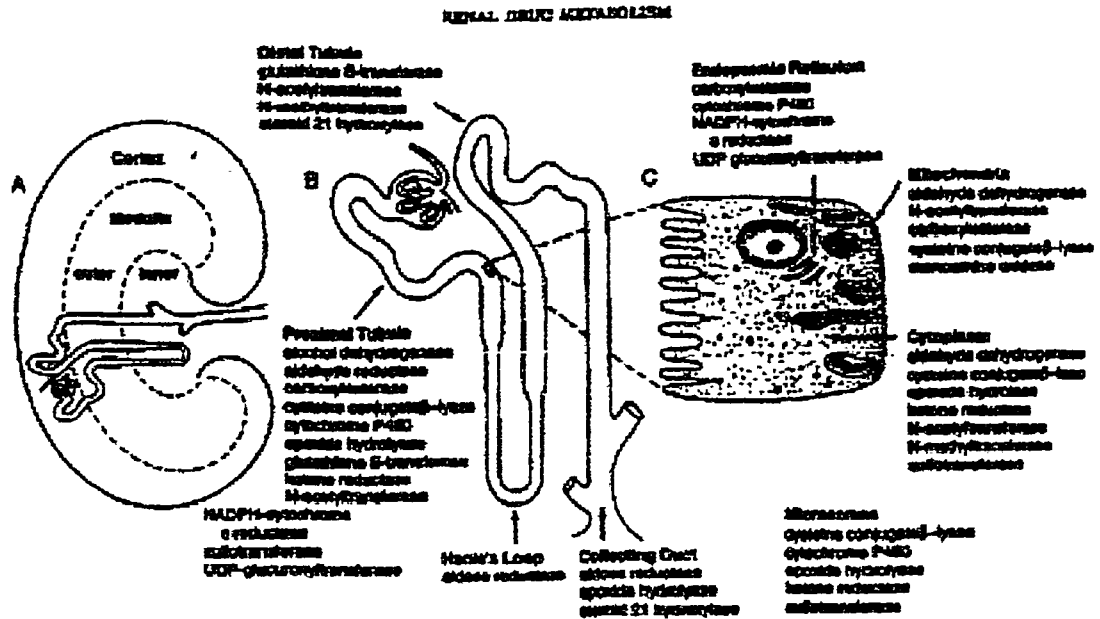
range of responses to toxicant-induced injury between kidney cells of a single species. The possibility for different cellular responses with regards to toxicity is multiplied when the variability of sex-dependent responses is considered. Sex-dependent differences have been observed when Fischer 344 rat renal cells are exposed to Tri and S-(1,2-dichlorovinyl)-L-cysteine (DCVC) (Davidson and Beliles, 1991; Green, 1990; National Cancer Institute, (1976); National Toxicology Program, 1990). For example, male rat kidneys are more sensitive to Tri and DCVC treatment then female rat kidneys (Lash et al., 1995). The mechanism for this was hypothesized to be differences in rates of metabolism by the GSH-dependent conjugation, P450, and cysteine-S-conjugate β-lyase pathways.

Tri is a colorless, volatile liquid and alkenyl halide (Manhn, 1992). The structure of Tri is shown in Figure 2. The lipophilic character, non-flammability, and high boiling point of Tri makes it useful in a variety of industrial processes including metal degreasing and dry cleaning and Tri also was once used as an anesthetic (Davidson and Beliles, 1991). Because of these uses, high amounts of Tri have evaporated into the atmosphere and contaminate ground and surface water and food, raising the possibility of occupational and general human exposure to Tri. The symptoms of toxic Tri exposure include central nervous system depression, abnormal liver function and irritating effects to the skin and mucous membranes of the respiratory tract (Reichert, 1983). Because of these effects, and the fact that Tri was found to be carcinogenic in laboratory animals, Tri is no longer used clinically as an anesthetic.

Variability in toxic insult across species is a great concern, especially for Tri toxicity, as many toxicological tests for drugs meant for human use are done on animals. The existence of certain fundamental differences in the physiology, and sometimes, the basic biochemistry, of humans and other mammals may partially explain differences in responses to toxic insults. For example, Tri produces both acute and chronic toxicity with multiple target organs and its effects have been studied in a wide range of species, including

Figure 2. Schematic of GSH-dependent conjugation of Tri.

Trichloroethylene (Tri) is conjugated to GSH to form S-(1,2-dichlorovinyl)glutathione (DCVG) in both the liver and kidneys. The GST isoforms responsible for the conjugation of Tri to DCVG are not known. DCVG is metabolized by γ-glutamyltransferase (GGT, inhibited by acivicin) and dipeptidase to form S-(1,2-dichlorovinyl)-L-cysteine (DCVC). DCVC can be metabolized by either cysteine-S-conjugate β-lyase to form a reactive sulfhydryl-intermediate (DCVSH) or by N-acetyl-S-transferase, in a reversible process, to form N-acetyl-DCVC (NAcDCVC). NAcDCVC is then either excreted in the urine or it can be deacetylated to reform DCVC.

P-450

P-450 metabolites
(chloral hydrate, tri- and
dichloroacetic acid,
trichloroethanaol)

GSH

GST

DCVG

GGT ← Inhibited by Acivicin

Dipeptidase

DCVC

N-Acetyl-S-
Transferase

β-Lyase

Deacetylation

DCVSH

Reactive intermediate
believed to cause
nephrotoxicity and
nephrocarcinogenicty

NAcDCVC

Metabolite excreted in urine of mice, rats, and humans
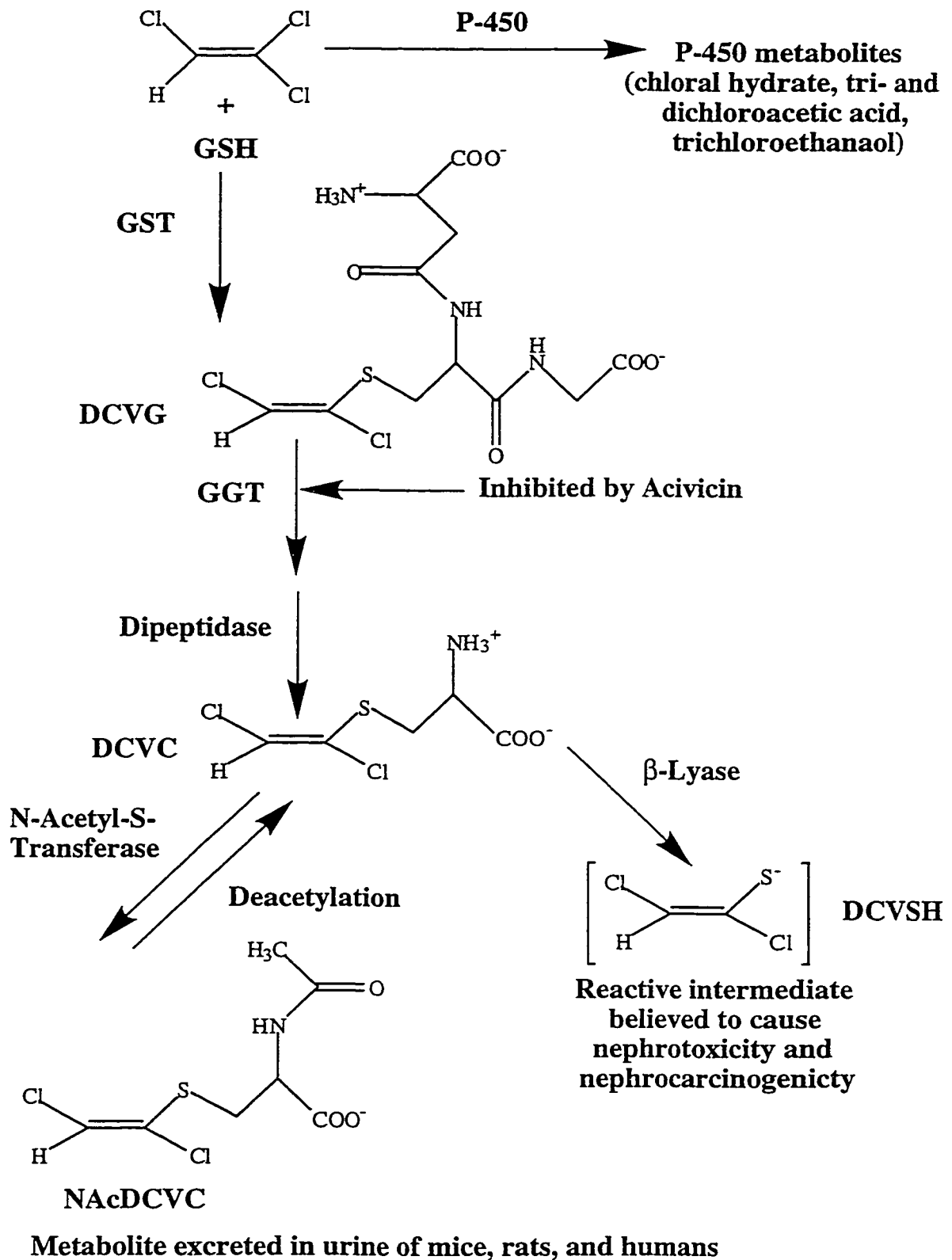
humans (National Cancer Institute, 1976; National Toxicology Program, 1990). Just as there are sex-dependent differences in toxic responses to Tri, there are also species-dependent differences in toxic response to Tri (Brown et. al., 1990; Lash et al., 1995; National Cancer Institute, 1976; National Toxicology Program, 1990; Weiss, 1996). The kidneys are one target organ for Tri, and data from human workers exposed to Tri have indicated that exposure to Tri may increase the risk of kidney cancer in humans (Brown et al., 1990; David et. al., 1989; Henschler et al., 1995; Nagaya et al., 1989; Weiss NS, 1996). Such claims have been recently disputed however, and controversies have arisen surrounding the correlation of human kidney cancer with Tri exposure (Bloemen et al., 1995; Henschler et al, 1995; Swaen, 1995). This controversy has been generated, in part because much of the supporting data on kidney tumorigenesis as a mechanism of action for Tri comes from studies using rats and mice. Some (Abelson, 1993) have questioned the relevance for humans of the renal pathway for Tri metabolism. The specific details of this controversy involve the differences between male rat and human drug metabolism pathways and their role in Tri metabolism.

Tri is metabolized by two distinct pathways, GSH-dependent conjugation and P450-dependent oxidation (Figures 2 and 3, respectively). The former pathway produces S-(1,2-dichlorovinyl)glutathione (DCVG), which can be metabolized further to the cysteine conjugate DCVC. The specific glutathione S-transferase (GST) (EC 2.5.1.18) responsible for the conjugation of Tri to glutathione (GSH) has never been determined. The initial reactions of GSH conjugation to Tri occur predominantly in the liver. DCVG formed in the liver is rapidly secreted into the bile and/or plasma and is eventually delivered to the kidney as DCVG, DCVC, or NAcDCVC through interorgan translocation pathways (Lash et al., 1995b). DCVC rearranges to form potent acylating species. Subsequent acylation of proteins and DNA may lead to cytotoxicity and mutagenesis (Anders et al., 1988; Goeptar et al., 1995). Although NAcDCVC is a detoxification

Figure 3. Schematic of P450 oxidative metabolism of Tri.

Trichloroethylene (Tri) is oxidized by P450 isoforms to a Tri-O-P450 intermediate. P450 isoforms responsible for Tri metabolism in the liver are listed while those responsible for Tri metabolism in the kidney have not been determined. The Tri-O-P450 intermediate can be metabolized further to dichloroacylchloride, which immediately rearranges to form dichloroacetic acid. Dichloroacetic acid can be further processed to monochloroacetic acid or oxalic acid. The Tri P450-O-intermediate can also form chloral hydrate or oxalic acid. Chloral hydrate can be further metabolized to trichloroethanol (which can be metabolized further to trichloroethanol glucuronide) or trichloroacetic acid. Trichloroacetic acid can be processed further to dichloroacetic acid or trichloroethanol.

GSH Conjugation → DCVG, DCVC, NaDCVC

(Tri)

P450 →

<u>Liver</u> <u>Kidney</u>

CYP2E1 ?
CYP2B1/2
CYP2C11
CYP1A1/2

[Tri-O-P450 intermediate]

$Cl_2CH-C(=O)-Cl$

Dichloroacylchloride

$Cl_3C-C(=O)H$

(Cloral Hydrate)

$HO-C(=O)-C(=O)-OH$

Oxalic Acid

$Cl_2CH-C(=O)-OH$

(Dichloroacetic acid)

$Cl_3C-C(=O)-OH$

(Trichloroacetic acid)

Cl_3CCH_2OH

(Trichloroethanol)

$ClCH_2-C(=O)-OH$

Monochloroacetic acid

$HO-C(=O)-C(=O)-OH$

Oxalic acid

$Cl_3CCH_2O\text{-gluc}$

(Trichloroethanol Glucuronide)

product, it can by deacetylated to regenerate DCVC. Due to the tissue distribution of membrane transport systems and γ-glutamyltransferase (GGT) (EC 2.3.2.2), subsequent reactions of the pathway occur within the kidney, thereby generating the reactive toxic species. Previous studies have shown that this entire pathway can occur within the kidney, removing the need for interorgan translocation of DCVG and its derivatives (Lash et al., 1995; 1998). These studies also showed that differences in Tri toxicity correlated with differences in DCVG formation and in GST activity.

In order to understand further the role of both P450 and GST isoforms in the metabolism of Tri, as well as other chemicals, a review of P450 and GST nomenclature is required. P450 monooxygenases are a superfamily of heme-containing proteins that catalyze the carbon hydroxylation, heteroatom oxygenation, dealkylation, and epoxidation of lipophilic endogenous and exogenous compounds (Guengerich et al., 1990; Wrighton and Stevens 1992). Within the last 10 to 15 years a common nomenclature for P450 genes and P450 gene products has been proposed and accepted among researchers in the field. The most current form of the nomenclature system, found in Nelson et al. (1996) will be used in this study. The root symbol (CYP) will be followed by an Arabic number denoting the gene family, a letter representing the subfamily, and an Arabic number representing the individual gene within the subfamily. Members of the same gene family share at least 40% sequence identity, with some exceptions, while members of the same mammalian subfamily share at least 55% sequence identity. P450 genes or gene products can be in the same subfamily and yet be from different species. For example, CYP4A1 denotes the gene 1 in the A subfamily of the 4th gene family of P450. This gene has been found only in rodent species. CYP4A11 represents the 11th gene of the A subfamily of the 4th gene family of P450. To date CYP4A11 has only been identified in humans. These P450 isoforms share at least 55% homology even though they are from different species.

GST isoforms catalyze the general reaction shown below:

$$GSH + R\text{-}X \rightarrow GSR + HX$$
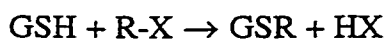
GST isoforms are found in both cytosolic and microsomal fractions of the cell (Armstrong et al., 1997). To date, six genes that encode for at least six individual classes of cytosolic enzymes have been identified. Five of these genes have been found in vertebrates (alpha, mu, pi, kappa, and theta). The cytosolic enzymes studied to date can form either homo- or heterodimeric species, but heterodimers form only between subunits of the same enzyme class (Armstrong et al., 1997). Researchers of the GST gene superfamily have yet to agree on a common nomenclature for all species although several efforts are in progress to do so. A common nomenclature has been chosen for the human GST superfamily and is currently gaining acceptance. The human enzymes are named with respect to the class in which they fall (A, M, P, K, or T for α, μ, π, κ, and τ) with their subunit composition or isoenzyme type designated by Arabic numerals (Armstrong et al., 1997). As an example, a homodimer of human type 1 A subunits is A1-1 and a heterodimer of type 1 and 2 human A subunits is A1-2. In order to minimize confusion when referring to rat and human GST isoforms, the human nomenclature will be followed for all human GST isoforms. When rat GST isoforms are discussed, the Greek symbol will be used instead of the English capital letter. For example, the homodimer of rat type 1 alpha subunits will be called rat GSTα1-1, while the homodimer of human type 1 alpha subunits will be called human GSTA1-1. Designation of the GST isoform will be preceded by the species as well in order to decrease confusion.

The role of renal P450 oxidation of Tri and subsequent processing to its metabolites CH, TCA, DCA, and TCOH (Figure 3) has not been studied extensively. The metabolism of Tri by P450 oxidation in the liver has been studied extensively and reports (Miller and Guengerich, 1983, Nakajima et al., 1985) have shown that in rat liver microsomes CYP2E1, CYP2C11, CYP2B, and CYP1A1 can metabolize Tri. Figure 3 illustrates the metabolism of Tri via P450 oxidation. Tri is first metabolized to a Tri-P450 intermediate, which can rearrange to form dichloroacetyl chloride, which can be further transformed to DCA (Figure

3). The intermediate can also be enzymatically or noneznymatically cleaved to form oxalic acid or rearrange to form CH by catalytic reactions with the Fe (III) on P450. It was proposed that this Tri-P450 intermediate is an epoxide (Butler, 1949; Powell, 1945). These epoxides can readily form acyl chlorides, which are subsequently oxidized to carboxylic acids or reduced to alcohols. Miller and Guengerich (1983) showed that Tri epoxide is not an obligate intermediate in the formation of CH and that Tri epoxide cannot be the intermediate responsible for the irreversible binding to proteins and DNA. Miller and Guengerich (1983) showed further that metabolism of Tri by P450 can inactivate P450 by destruction of the heme group. This inactivation was not a result of interactions with an epoxide metabolite of Tri. This study was supported by the study of Green and Prout (1985), which showed that the major products of an expoxide intermediate of Tri should be CO, CO_2, DCA, and monochloroacetic acid. In contrast CH, TCA, and TCOH are the major metabolites recovered in both in vivo and in vitro studies (Green and Prout, 1985). Assessments that the intermediate of Tri and P450 metabolism must have some degree of chemical stability (unlike an epoxide) have led to the hypothesis that the majority of Tri is believed to undergo a chlorine migration in an oxygenated Tri-P450 transition state. This chlorine migration leads to formation of CH. CH can either be reduced to TCOH by cytosolic NADH-dependent alcohol dehydrogenase (EC 1.1.1.71) or can be oxidized to TCA by mitochondrial or cytosolic NAD^+-dependent aldehyde dehydrogenase (EC 1.2.1.3). Furthermore, TCOH can conjugate with UDP-glucuronic acid to form TCOH glucuronide.

A number of P450 isoforms metabolize Tri in the liver. These include CYP2E1, CYP2B1/2, and CYP2C6/11 (Guengerich, 1991; Guengerich et al., 1991b; Coop et al., 1985; Nakajima et al., 1988, 1990, 1992a, 1992b, 1993). CYP2E1 appears to have the highest affinity for Tri (Guengerich, 1991; Guengerich et al., 1991, Nakajima et al., 1992a) but studies (Miller and Guengerich, 1983) have shown that if other P450 isoforms are induced then they may alter metabolism of Tri by CYP2E1. For example, Miller and

Guengerich (1983) showed that induction of CYP2B1/2 by phenobarbital increased the affinity of CYP2B1/2 for Tri and decreases the amount of Tri metabolized by CYP2E1 in rat liver. Most of the work done on oxidative metabolism of Tri has been done in the liver. To date, no study has been published studying the oxidative metabolism of Tri in the kidney and it is not known if isoform selectivity exists for Tri in different tissues. Furthermore, P450 isoform specificity in different animal species has not been thoroughly studied. Differences among animal species, like differences among different cell types, may cause differences in metabolism and toxicity of many chemicals, including Tri.

Although marked sex- and species-dependent differences exist in P-450-dependent metabolism of Tri, there is no evidence that bioactivation by P-450 plays a role in the renal effect of Tri. These effects of Tri exposure have been attributed to reactive metabolites generated from DCVC. The mechanism of DCVC-induced nephrotoxicity has been thoroughly studied, with proposed mechanisms including oxidative stress with lipid peroxidation and GSH depletion (Chen et al., 1990, 1992, 1994; Groves et al., 1991; Groves et al., 1993; Lash and Anders, 1987), alterations in cellular calcium ion homeostasis (Chen et al., 1992, 1994; Groves et al., 1993; Lash and Anders, 1987; Lash et al., 1986; Vamvakas et al., 1990; Vamvakas et al., 1992; Yu et al., 1994; and Hayden et al., 1990), inhibition of mitochondrial function (Chen et al., 1992, 1994; Groves et al., 1993; Lash and Anders, 1987; Lash et al., 1986; 1994; Hayden et al., 1990, 1992; Vamvakas et al., 1990, 1992), covalent binding of reactive metabolites to protein (Chen et al., 1992, 1994; Eyre et al., 1995a; Groves et al., 1993; Lock et al., 1990; Wallin et al., 1992; Yu et al., 1994), oncogene activation (Chen et al., 1992; Vamvakas et al., 1992), and stimulation of cellular proliferation or repair processes (Eyre et al., 1995b; Hatzinger et al., 1988; Kays et al., 1995; Vamvakas et al., 1989). While the mechanism of action of DCVC has been extensively studied, the correlation of renal toxicity with Tri exposure has yet to be fully characterized. Significant controversy exists concerning exactly how much DCVG can be formed after exposure to Tri. One important factor in this controversy is the amount of Tri conjugated to GSH (via

the GST conjugation pathway) versus the amount metabolized by the P450 pathway. A model system that could measure the activity of one of these pathways while in the presence of the other would greatly advance our understanding of this question.

As mentioned above, the human health hazard of Tri toxicity has been subject to some controversy mostly because the flux of Tri through the GSH conjugation pathway is thought to represent only a small fraction of Tri metabolism (Davidson and Beliles, 1991). Recent studies have shown that humans are capable forming detectable levels of DCVG after exposure to small doses of Tri (Lash et al., 1999a). Furthermore, recent reports (Brüning et al., 1998) of cases involving acute Tri poisoning have demonstrated that the products of the GSH-conjugation pathway can be formed in humans. Finally, the metabolites generated from Tri by the P-450 pathway (CH, DCA, TCA, and TCOH) are chemically stable, making quantification of these metabolites relatively straightforward. Metabolites generated from Tri by GSH conjugation and subsequent cysteine-S-conjugate β-lyase are chemically unstable and hard to measure (Anders et al., 1988). Thus, it is possible that small amounts of these unstable metabolites may produce a high degree of toxicity. The recovery and identification of NAcDCVC as a urinary metabolite of Tri in rats, mice, and humans (Birner et al., 1993; Commandeur and Vermeulen, 1990; Dekant et al., 1986, 1990) suggests that the kidney is a primary site for the accumulation of DCVG and formation of its subsequent metabolites. This correlates with the activity of GST and GSH-conjugate metabolism within the liver and kidneys. Despite knowledge of this correlation, little work has been done to determine the specific isoform responsible for GSH conjugation of Tri. This knowledge would significantly advance our ability to assess the relative human health hazard of not only Tri but of many other chemicals that are metabolized by these enzymes.

Variability in toxic injury between animals and humans can also be seen with tienelic acid, a thiophene-containing compound. Although thiophene-containing compounds have not received as much study as Tri, the pathways for their metabolism are similar.

Thiophene-containing compounds are oxidized by P450 and conjugated to GSH, resulting in the excretion of N-acetyl-S-(2-thienyl)-L-cysteine in the urine after the GSH conjugate is processed to the cysteine conjugate (Beaune et al., 1994; Dansette et al., 1990, 1992; Neau et al., 1990). Compounds bearing thiophene structural groups (e.g., cephaloridine, 4-TByA, and tienilic acid) are toxic to liver and/or kidney (Lash and Tokarz, 1995; Lopez-Garcia et al., 1993; Tune and Fravert, 1980; Tune et al., 1986; Zimmerman et al., 1984). Cephaloridine and 4-TByA exert cell selective toxicity to rPT cells. Differences in drug metabolizing enzyme activity between rPT and rDT cells have been suggested as a reason for 4-TByA cell selective cytotoxicity (Lash and Tokarz, 1995). Human P450 metabolism of thiophenes by CYP2C9 and CYP2C10 occurs in the liver by the hydroxylation of the fifth carbon of the thiophene ring (Dansette et al., 1993, Beaune et al., 1994; Lopez-Garcia et al., 1993; Zimmerman et al., 1984). P450-dependent oxidation of tienilic acid by human CYP2C9 and rat CYP2C11 results in decreased tienilic acid hydroxylation in a manner that corresponds to decreases in CYP2C9 and CYP2C11 activity, supporting the hypothesis that tienilic acid can act as a mechanism-based inhibitor of certain P450 isoforms (Beaune et al., 1994; Lopez-Garcia et al., 1993; Zimmerman et al., 1984). Tienilic acid has been implicated in a form of hepatitis induced in humans, which results in the formation of anti-LKM$_2$ autoantibodies (for review see Beaune et al., 1994). Thus, alteration in drug metabolizing activities may be another mechanism for thiophene-induced toxicity

Tienilic acid did not show any toxicity in laboratory animals when first studied and was first marketed in Europe in 1976 and the United States in 1979, under the name of Ticrynafen®, a uricosuric diuretic used in treatment of hypertension but was quickly recalled in 1980 because of the possibility of hepatotoxicity (Zimmerman et al., 1984). Further studies utilizing tienilic acid revealed that differences in toxic response to this compound between rat and humans could be due to the presence of a protein in humans (CYP2C9) that is absent in laboratory animals. The nephrotoxicity of thiophene-containing compounds has not been studied extensively and warrants further study. Furthermore, the

presence of a toxicological model allowing for the increased testing of the toxicity of tienilic acid in humans might have resulted in Ticrynafen® never having been introduced to the market. Detailed knowledge of the differences between rat and human CYP2C metabolism of Ticrynafen® might also have prevented its introduction to the market.

Both Tri and Ticrynafen® display species variability in repose to toxic injury, resulting in conflicting views on the mechanism of toxicity and risk to human health of these compounds. Further testing of laboratory animals more similar to humans (such as primates) and more intense phase III clinical trials might have resulted in increased information on the toxicity of these compounds. A deeper understanding of the differences between animal and human drug metabolism with respect to specific organs would provide valuable information about the mechanism of toxicity of each compound and increase our ability to extrapolate animal data to humans for risk assessment purposes.

When considering toxicity testing of any chemical, both in vivo and in vitro models should be considered. The benefits of an in vivo model are obvious but the drawbacks are also numerous. These drawbacks include expense, variability, lack of human models, and that most of the measurements that can be made in humans are non-invasive (glucose excretion in the urine, blood urea nitrogen, proteinurea, blood pressure, etc). Furthermore, assessment of target organ toxicity can usually only be made after sacrifice of the model. (This makes human models rare indeed). Despite this, several in vivo models for toxicity testing, including those using Tri (Lash et al., 1999a), have been presented. These models usually involve analysis of the presence of the parent compound and metabolite in the urine or blood. This usually means that background knowledge on the metabolism of the compound must be available. In vitro models for toxicity testing are numerous and like in vivo models, they have many advantages and disadvantages. The advantages include the fact that they are relatively inexpensive compared with in vivo models and have reduced variability. The results from in vitro studies are also easier to reproduce than in vivo studies, and there are usually less ethical concerns surrounding the use of in vitro models than are

encountered with both animal and human in vivo models. Drawbacks of in vitro models include the issue that the route of exposure of a chemical is usually not considered nor are compartmentalization and first pass effects. Further drawbacks include lack of similarity to the in vivo state and the fact that dedifferentiation and genetic alterations may occur, especially in models employing cultures of established cell lines.

Numerous in vitro models have been proposed and used to study mechanisms of nephrotoxicity of Tri, DCVC, thiophenes, and other compounds. Most of these models have used laboratory animals such as the rat and each has its own advantages and disadvantages, which limits their applicability. For example, while microsomes and cytosol fractions are invaluable for studying of the metabolism of various compounds, they are not useful in the study of nephrotoxicity. Furthermore, microsomal fractions do not contain many of the GSH-dependent enzymes, which are usually found in the cytosol (e.g., cytosolic GST isoforms). On the other hand, cytosolic fractions do not contain P450 isoforms, which are microsomal in origin. Though valuable and often critical, information can be obtained with these models they cannot be used to study the simultaneous metabolism of compounds by both cytosolic and microsomal enzyme systems.

Freshly isolated cells are often used to study chemical-induced injury. Liver cells are often used for toxicity and are good models as the concentration of P450 and GST isoforms are often highest in the liver, allowing for easy measurement of metabolism. The homogeneity of the liver, compared to the kidney, also allows for a uniform response to toxic insult. The heterogeneous morphology of the kidney combined with the low level of drug metabolizing enzymes expressed in the kidney combine to make assessment of chemical-induced injury to the kidney difficult. The lack of knowledge about what drug metabolizing enzymes are expressed in the kidneys further hampers this problem. Finally, the toxicity of many chemicals, including Tri, is believed to be a result of chronic exposures. Cell cultures are predominately the model of choice for chronic toxicity studies. However, as explained above, because established cell lines are immortalized they may have

undergone dedifferentiation or have genetic alterations that make them invalid for comparison with toxicity responses in freshly isolated cells or in vivo (Wilson et al., 1986). Primary cell culture can theoretically avoid such problems and should better represent in vivo conditions.

Three critical issues in development and application of primary cell culture to renal cells are: i) cellular material used as seed material should have as high a degree of homogeneity as possible; ii) fibroblast growth should be prevented; and iii) differentiated phenotype and function should be maintained. In this case, differentiated phenotype refers to the maintenance of specific cell markers and function for rPT and rDT cells. For this work, dedifferentiation refers to the state where rPT and rDT cells lose both cellular makers and function as compared with freshly isolated cells. These criteria are often difficult to satisfy with epithelial tissues because they readily undergo phenotypic and genotypic changes when grown in culture. Taub and colleagues (Aleo et al., 1989; Chung et al., 1982; Miller et al., 1986; Taub et al., 1989) pioneered the development and use of serum-free, hormonally-defined media for the primary culture of renal PT cells from rabbit. Much of the primary cell culture work for renal epithelial cells has been done with rabbit, rather than rat, because rPT cells have a much more limited growth capacity as compared with rabbit renal PT cells (Miller, 1986). However, it is important to develop such primary cell culture procedures for rPT cells to take advantage of the large database of toxicology studies using the rat. Furthermore, rats are a significantly less expensive and more convenient animal model as compared with the rabbit. Several groups (Boogaard et al., 1990; Chen et al., 1989; Detrisac et al., 1984; Elliget and Trump, 1991; Hatzinger and Stevens, 1989; Lash et al., 1995b; Miller, 1986) have recently developed procedures for primary culture of rPT cells using serum-free, hormonally-defined media. Although serum-free media produce less rapid cell division and growth, they generally result in better maintenance of differentiated properties and prevent the growth of fibroblasts.

Although most toxicological studies with primary renal cell cultures have used

animal tissue, this methodology has also been applied in a few limited cases to primary culture of PT cells from human kidney (Chen et al., 1990; Trifillis et al., 1985). However, human PT cells have not been characterized extensively in terms of drug metabolism enzyme expression. Determination of the drug metabolizing enzymes present in both rat and human PT cells would allow direct comparison of biochemical and physiological responses in renal cells from human tissue and from a commonly used animal model, namely the rat. We have recently developed a model for the study of chronic toxicity in cell culture for rat renal PT and DT cells (Lash et al., 1995b). This model is able to sustain levels of constitutive enzymes (GGT, alkaline phosphatase (EC 3.1.3.1)), mitochondrial activities, low LDH activity, expression of cytokeratins and be used for the study of acute cytotoxicity of numerous compounds. The expression of other drug metabolizing enzymes in these cultures such as P450 isoforms has not been determined. The availability of human PT cells for culture will allow direct comparison of not only the bioactivation and detoxification pathways in rat and human kidney but will also allow for comparisons of time- and dose-dependent responses to Tri, DCVC, and thiophenes. Prior to establishment of cultures of both these cell types the expression of drug metabolizing enzymes in freshly isolated rPT and human PT (hPT) cells must first be determined. These data will be compared to those generated in primary cultures of both cell types, to determine the extent of dedifferentiation, if any, that occurs in these cells as a result of culture. Successful establishment of cultured rPT and rDT cells and hPT cells will decrease the uncertainty involved in risk assessment with Tri, DCVC, and thiophenes as well as other toxicants.

In summary, study of chemically–induced injury to the mammalian kidney is of importance due to the role of the kidneys in maintaining normal physiological function of the body. Because of both their specialized physiological and biochemical functions, the kidneys are common targets for many drugs and environmental pollutants. Examples of such drugs are first generation antibiotics such as cephaloridine and other thiophene-containing drugs. Examples of environmental pollutants include Tri, which causes

nephrotoxicity and nephrocarcinogenicity to rodents with controversial studies being reported for humans. These studies are controversial due to the lack of knowledge about the flux of Tri through the GSH-conjugation pathway versus the P450 oxidation pathway, and the fact that the GST isoforms responsible for the metabolism of Tri have never been studied. Controversies have also arose concerning Tri toxicity because the differences between rats and humans in terms of the drug metabolizing enzymes responsible for the metabolism of Tri in the kidney have never been thoroughly studied. Furthermore, models testing the toxicity and metabolism of Tri in both the rat and human kidneys are extremely limited, being performed mostly in freshly isolated tissue. Determination of the differences in drug metabolizing enzymes expressed in both rat and human kidneys would aid greatly in evaluating the human health risk of Tri. Once these differences are established, studies of Tri toxicity and metabolism in freshly isolated rat and human tissues could be done utilizing these differences to increase our understanding of renal injury induced by both Tri and other chemicals. These data also could be used to develop cell culture models that more closely mimic the in vivo state of rat and human kidney cells. Development of these cell culture models would allow for testing of the long-term effects of Tri and other chemicals. Comparison of data generated in cultures of rat kidney cells to those from cultures of human kidney cells will decrease the uncertainty involved in risk assessment would not only Tri, DCVC, and thiophenes, but with other toxicants as well.

The specific aims of this study were:

1.   Determine if freshly isolated rPT and rDT cells differ significantly enough in the expression of drug metabolism enzymes to be of use for the testing of chemically-induced nephrotoxicity.

2.   Determine the expression and distribution of P450 and GST isoforms in rPT and rDT cells, and assess how these differences effect chemically-induced nephro-toxicity in these cells.

3.   Establish, characterize, and validate primary cultures of rPT and rDT cells for use in

testing of chemically-induced toxicity.

4.   Determine the expression of drug metabolism enzymes in freshly isolated and primary cultures of hPT cells. Correlate differences in the expression of drug metabolism enzymes in these cells to differences in the toxicity and metabolism of chemicals tested in rPT and rDT cells.

Data resulting from completion of these objectives was used to test the hypothesis that differences in the toxicity of chemicals to rat and human kidney cells are caused by cell- and species-dependent differences in drug metabolizing enzymes.

Chapter 2

Material and Methods

Materials. Tri (reported to be 99.9% pure, as judged by electron ionization mass spectrometry), collagenase type I (EC 3.4.24.3), bovine serum albumin (BSA) (fraction V), acivicin, and L-γ-glutamyl-L-glutamate were purchased from Sigma (St. Louis, MO). DCVG was synthesized as previously described (Elfarra et al., 1986). Purity (> 95%) was determined by HPLC analysis, and identity was confirmed by proton NMR spectroscopy. Antibodies for CYP2C11, CYP2E1, and CYP3A were purchased from Oxford Biomedical (Oxford, MI). The CYP4A antibody was a gift from Dr. Raymond F Novak while the CYP4A11 antibody was a gift from Dr Jerome M Lasker. Individual isoforms for GSTα1-1, 1-2, and 2-2 were purchased from Detroit R&D (Detroit, MI) while antibodies for GSTα, GSTΠ, and GSTμ were purchased from Oxford Biomedical. Antibodies to human GSTT and GSTα1, and GSTα2 were purchased from Biotrin Inc. (Newton, MA). Bromosulfopthalein (BSP) was purchased from Sigma (St Louis, MO) while triethyltin bromide (TETB) was purchased from Aldrich.

Animals. Male Fischer 344 rats (150-250g; Charles River laboratories, Wimington, MA) were used in these studies, and animals were housed in a controlled room on a 12-hr light/dark cycle and were given commercial rat chow and water *ad libitum.*

Isolation of rat hepatic and human and rat renal microsomes and cytosolic fractions. Liver and kidney microsomes, regardless of origin, were isolated as described by Sharer et al. (1992). Animals were anesthetized with i.p. injections of pentobarbital (0.11 mL/100 g body weight of rats). Rats were injected with 0.2 mL of 0.2% (w/v) heparin in 0.9% NaCl (saline) into the tail vein, the abdomen was opened, and the liver or kidneys, were removed, rinsed with buffer (250 mM sucrose, 10 mM triethanolamine, 1 mM ethylenediamine tetraacetic acid disodium (EDTA·Na$_2$, pH 7.6), and homogenized in

3 mL of buffer/g tissue. Homogenates were initially centrifuged at 9,000 x g for 20 min. The supernatant was filtered through cheesecloth and then centrifuged for 60 min at 105,000 x g. The resulting supernatant (cytosol fraction) was used for enzymatic and western blot analysis and was stored at -80°C until use. The resulting pellets were resuspended in buffer and were centrifuged an additional 60 min at 105,00 x g to produced "washed" microsomes. The microsomal pellets were resuspended in buffer containing 10% (v/v) glycerol and were stored at -80°C until used. Enzymatic activities were normalized to protein concentrations, which were determined as explained below. The same procedure essentially was followed for human renal cortical slices except tissue was received from the Human Tissue Resources Core from the Department of Pathology, Harper Hospital (Detroit, MI).

Isolation of mitochondria from renal cortical homogenates. Mitochondria were isolated from renal cortical homogenates by differential centrifugation, essentially as described by Johnson and Lardy (1967), except that the buffer used was 20 mM triethanolamine/HCl, pH 7.4, containing 225 mM sucrose, 3 mM potassium phosphate (pH 7.4), 5 mM MgCl$_2$, 20 mM KCl, and 0.1 mM phenylmethylsulfonyl fluoride to inhibit proteolysis. Ethylene glycol-bis(β-amino ethyl) N,N,N',N'-tetraacetic acetic acid (EGTA) (2 mM) was included in all preparatory stages, except the final resuspension, to remove calcium ions. Briefly, homogenates were initially centrifuged at 600 x g for 10 min. The supernatant was centrifuged at 15,000 x g for 5 min. The resulting pellets (mitochondria) were washed twice with the buffer and washed mitochondria were resuspended in the buffer without EGTA. Purity of mitochondria was estimated by measurement of activity of a marker enzyme (i.e., citrate synthase (EC 4.1.3.28); spectrophotometric assay according to Srere, 1969).

Preparation of freshly isolated rat renal cortical, rPT, and rDT cells. Isolated renal cortical cells were obtained by collagenase perfusion (Jones et al., 1979) from male Fischer 344 rats. To obtain enriched populations of renal PT and DT cells, cortical cells

23

were subjected to density-gradient centrifugation in Percoll as previously described (Lash and Tokarz, 1989). Briefly, after anesthesia with pentobarbital (0.11 mL/100 g body weight), rats were injected with 0.3 mL of 0.2% (w/v) heparin in 0.9% saline. The aorta below the renal arteries was then cannulated with a 19-gauge steel cannula and subjected to initial recirculating perfusion at 8 mL/min with a calcium-free, EGTA-containing Hanks' Buffer (Hanks' I; 25 mM $NaHCO_3$, 25 mM N-(2-hydroxyethyl)piperazine-N'-2-ethanesulfonic acid) (HEPES), pH 7.4, 0.5 mM EGTA, and 0.2% (w/v) BSA. All buffers were continuously bubbled with 95% O_2/5% CO_2 and were maintained at 37°C. The kidneys were perfused with Hank's buffer supplemented with 4 mM $CaCl_2$ and collagenase (0.1% w/v), in a recirculating manner at 5 mL/min for 13-18 min. Cells were dispersed by mechanical disruption. The cortical cells were collected by low speed centrifugation (100 x g for 30 sec) and subjected to density-gradient centrifugation in Percoll (20 %, v/v) as previously described (Lash and Tokarz, 1989). Marker enzyme activity and functional assays were used to confirm the identity and purity of the two cell populations (Lash and Tokarz, 1989). Cell concentrations were determined in the presence of 0.2% (w/v) trypan blue in a hemacytometer, and cell viability was estimated by measuring the fraction of cells that excluded trypan blue.

Primary culture of rPT and rDT cells. Primary cultures of rPT and rDT cells were prepared following the method Lash et al. (1995b). Isolation of rPT and rDT cells was achieved as explained above except sterile conditions were used (i.e., all instruments and glassware were autoclaved and all buffers were filtered through a 0.2 µm filter). After isolation, cells were resuspended in 2 mL of Krebs-Henseleit Buffer I (118 mM NaCl, 4.8 mM KCl, 0.96 mM KH_2PO_4, 0.12 mM $MgSO_4 \cdot 7H_2O$, 25 mM $NaHCO_3$, 25 mM HEPES, and, BSA (2% w/v)) and diluted to 30 mL with media. Basal media was a 1:1 mixture of DMEM:F12. Standard supplementation for both rPT and rDT cells included 15 mM HEPES, pH 7.4, 20 mM $NaHCO_3$, antibiotics for day 0 through day 3 only (192 IU penicillin G/mL + 200 µg streptomycin sulfate/mL) to inhibit bacterial growth, 2.5 µg

amphotericin B/mL to inhibit fungal growth, 5 µg bovine insulin/mL, 5 µg human transferrin/mL, 30 nM sodium selenite, 100 ng hydrocortisone/mL, and 100 ng epidermal growth factor/mL. rPT cells also received 7.5 pg 3,3',5-triiodo-DL-thyronine/mL, while rDT cells received 5 ng thyrocalcitonin/mL. Cells were seeded at densities of 50-100 µg protein per cm^2 (0.5-1.0 x 10^6 cells/mL) in polystyrene culture dishes. Cultures were grown at 37°C in a humidified incubator under an atmosphere of 95% O_2/5% CO_2 at pH 7.4. Cultures were allowed to attach and grow for at least 24 hr prior to treatment with any agent. Cells were harvested from the dishes by either scrapping the plates with a Teflon scraper or by brief incubation with 0.05% (w/v) trypsin (EC 3.4.21.4)/EDTA (0.2%, w/v) in Ca^{2+}- and Mg^{2+}-free Hanks' buffer.

Isolation of microsomes and cytosol from rat renal cortical, rPT, and rDT cells. Cytosol and microsomes were prepared from freshly isolated rat renal cortical, rPT, and rDT cells by homogenization of the cells in a Polytron ultrasonic homogenizer followed by centrifugation at 11,000 x g for 20 min to spin pellet nuclei, mitochondria and cellular debris. Supernatant from this step was centrifuged in a tabletop ultracentrifuge at 105,000 x g for 90 min at 4°C. The resulting supernatant is the cytosol while the pellet is the microsomal fraction.

Isolation and primary culture of hPT cells. The method of Todd et al. (1995) was used to isolate and culture hPT cells from human renal tissue cortical slices (obtained through the Human Tissue Resources Core, Department of Pathology, Harper Hospital, Detroit, MI). This method results in highly pure hPT cells using methods involving digestion of minced cortical tissue with collagenase followed by a filtering step to remove tissue fragments and by a low speed differential centrifugation step (Detrisac et al., 1984; Kempson et al., 1989). The fibrous renal capsule was removed from human renal cortical slices and the slice was weighed. The slices were then washed with sterile PBS, minced, and the pieces were placed in a trypsinization flask filled with 30 mL Hanks' solution [same as used for isolation of rPT and rDT cells except BSA was absent

while gentamicin (50 μg/mL), collagenase (1.3 mg/mL), and CaCl$_2$ (0.59 mg/mL) was added and the solution was filtered prior to use]. Minced cortical pieces were subjected to enzymatic disassociation for 15 min, after which the supernatant was filtered through 70-μm mesh to remove tissue fragments, centrifuged at 150 g for 7 min, and the pellet resuspended in Krebs Henseleit Buffer I similar to that used for isolation of rPT and rDT cells. These steps were repeated until complete digestion of the tissue was achieved (usually 4-5 cycles). Resuspensions were combined and centrifuged at 150 x g for 7 min, pellets were washed with Krebs Henseleit Buffer I, centrifuged at 150 x g for 7 min, and the final pellet (hPT cells) was resuspended in Krebs Heinseleit Buffer II (same as Krebs Henseleit Buffer I except no BSA was added). For primary culture, hPT cells were diluted in the same media used for culture of rPT cells. Cells were seeded at 0.5 to 1.0 x 10^6 cells/mL. Approximately 70 x 10^6 cells were obtained from 1 g of human renal cortical tissue.

Assay of Tri metabolism by the P450 oxidation pathway. Measurement of P450 metabolites of Tri was done according to Elfarra et al., (1998) and EPA method number 151. All incubations were carried out in 1-mL glass vials at 37°C for the indicated amount of time (typically 15 or 30 min depending on tissue type). Tissue (0.5 to 2.0 mg/ml) was resuspended in 0.5 mL to 1.0 mL of 50 μM Tris-HCl buffer (pH 7.4). Triton X-100 was then added to lyse the cells (not done with tissue) at a concentration of 0.1% (v/v). Tri (0-20 mM) in acetonitrile (0.5% v/v) was then added and the reaction was incubated at 37°C for 3 min after which NADPH (1 mM final) was added to initiate the reaction. For experiments testing the effect of P450 inhibitors, samples were preincubated with either 250 μM SKF-525A or 1 mM chlorzoxazone for 15 min prior to the addition of Tri. Reactions were allowed to proceed for the indicated amount of time, stopped by flash freezing in a dry ice acetone bath, thawed, and 1 μL a of 1,000-fold diluted solution of dibromopropanol (DBP) (Aldrich Chemicals, St. Louis, MO) was added as an internal standard. Samples were then extracted with 0.25 mL ethyl acetate.

Sample analysis was carried out with a Perkin Elmer Autosystem XL gas chromatograph fitted with a PE-210 30 m x 0.25 mm ID, 0.5 µM thickness column (Perkin Elmer) and an electron-capture detector. Metabolites were analyzed by injection of the ethyl acetate extracts into a split injector set at 200°C with a detector temperature of 300°C and a He flow rate of 24.8 cm/sec. The initial oven temperature was 35°C for 11 min. Temperature was increased at 10°/min to 120°C, where it was held for 19 min. Retention times for Tri and CH were approximately 3.9 and 6 min, respectively. Retention times for DCA, TCA, TCE, DBP, and TCE were approximately 2.5, 9, 14, 16, and 19 min, respectively.

Assay of Tri metabolism by GSH conjugation pathway. All incubations were performed in 25-ml polypropylene Erlenmeyer flasks on a Dubnoff metabolic shaking incubator (60 cycles/min) at 37°C. Isolated rPT and rDT cells were preincubated for 15 min with 0.25 mM acivicin to inhibit GGT activity before performing incubations to measure DCVG formation. Cells were then incubated with 0 to 20 mM concentrations of Tri. With isolated cells, Triton X-100 (0.1%, v/v, final concentration) was added to solubilize the plasma membrane. After incubations for various lengths of time, reactions were terminated by addition of perchloric acid (10%, w/v, final concentration), and samples were processed for analysis of DCVG as described previously (Lash et al., 1995b) using the HPLC method described by Farris and Reed (1987). This method involved measurement of the GSH S-conjugate of Tri (DCVG) in acid-soluble supernatants after derivatization with 1-fluoro-2,4-dinitrobenzene and analysis by ion-exchange high-performance liquid chromatography (HPLC) on an amine column. An aliquot (0.5 mL) from the metabolism assay mixture was treated by adding 0.05 mL of 1.5 mM γ-L-glutamyl-L-glutamic acid (prepared in 0.3%, v/v, perchloric acid) as an internal standard, 0.05 mL of 15 mM bathophenanthrolinedisulfonic acid (as an antioxidant) and 0.1 mL of 70% (v/v) perchloric acid. Treated samples were then mixed on a vortex mixer and centrifuged for 2 min in a microcentrifuge at room temperature. Samples were derivatized by taking 0.5 mL of the supernatant and adding 0.05 mL of 0.1

M iodoacetic acid. The acidic solution was brought to pH 9 by addition of 0.5 mL of KOH (2 M)-KHCO$_3$ (2.4 M) and the solution was incubated for 10 min at room temperature. 1-Fluoro-2,4-dinitrobenzene [1.0 mL of 1%, v/v, in ethanol (EtOH)] was then added. The reaction mixture was capped, mixed on a vortex mixer, and stored overnight in the dark at 4°C. HPLC analysis was essentially as described by Lash and Jones (1985). Thiol-containing compounds were separated on an amine column by reverse-phase, ion-exchange HPLC. Buffer conditions were: mobile phase 80% Buffer A (80% methanol), 20% Buffer B (0.5 M sodium acetate in 64% methanol) for 5 min at 1.5 mL/min, then a 10-min linear gradient to 20% A and 80% B until the last compound is eluted, followed by a 1-min linear gradient to 80% A and 20% B to re-equilibrate at initial conditions. Peaks were identified and quantified by comparison with standards. For P450 inhibition assays, cells were preincubated in the presence or absence of the general P-450 inhibitor SKF-525A (0.25 mM) or chlorzoxazone (1 mM) for the indicated amount of time. Reactions were allowed to proceed as explained above. For all microsomal and cytosolic fractions, assays were performed as explained above except that they were performed in 1.5 mL polypropylene microcentrifuge tubes at 30°C instead of 37°C. The lower temperature was chosen for assays with subcellular fractions and purified enzyme because more consistent results were obtained than at the higher temperature used with intact cells. Neither purified enzyme or rPT and rDT cytosol were preincubated with acivicin because these biological samples do not contain significant GGT activity (Lash et al., 1998b). Reactions were performed in Krebs-Henseleit Buffer III (pH 7.35) buffer minus BSA as this was the buffer used for the cellular reactions. Reactions were allowed to proceed for the indicated amount of time, stopped, and processed by HPLC analysis as described above.

Assay of cytotoxicity. Cell viability was estimated by determining the release of LDH from cells after various incubations and at various times (Lash, 1989). The LDH release assay involves measurement of NADH oxidation spectrophotometrically at 340

nm after addition of pyruvate and NADH to an aliquot of cells, first in the absence, and then in the presence, of 0.1% (v/v) Triton X-100. The ratio of the slopes of the rates of decrease in absorbance at 340 nm in the two cases gives the fraction of damaged cells. For cytotoxicity assays in primary cultures of rPT and rDT cells, LDH release from cells was measured by determining LDH activity in media and, after removal of media, washing cells with PBS and solubilization of cells with 0.1% (v/v) Triton X-100, in total cells. The fraction of LDH release was an index of irreversible injury:

%LDH release = LDH activity in media/(LDH activity in media + LDH activity in total cells) x 100%.

DNA and enzyme assays. DNA content was measured as the relative fluorescence of the DNA-diamidinophenylindole complex with 360-nm excitation and 450-nm emission according to Sorer and Germinario (1983), with double-stranded, calf thymus DNA as a standard.

Glutamate dehydrogenase (GDH) (EC 1.4.1.3) activity was measured as NADH oxidation ($\varepsilon = 6220$ $M^{-1}cm^{-1}$) in the presence of 2-oxoglutarate by following the decrease in absorbance at 340 nm according to Schmidt and Schmidt (1993).

GGT activity was measured at 410 nm by monitoring p-nitroanilide formation ($\varepsilon = 8800$ $M^{-1}cm^{-1}$) with γ-glutamyl-p-nitroanilide and glycylglycine as substrates according to Orlowski and Meister (1963).

Alkaline phosphatase (AP) (EC 3.1.3.1) activity was determined according to Bessey et al., (1946) with p-nitrophenylphosphate as a substrate and was quantitated as p-nitrophenol ($\varepsilon = 9600$ $M^{-1}cm^{-1}$) formation by measuring the increase in absorbance at 410 nm.

Malice dehydrogenate (MDH) (EC 1.1.1.37) activity was determined spectrophotometrically by the measuring the reduction in absorbance of NADH ($\varepsilon = 6220$ $M^{-1}cm^{-1}$) at 340 nm using oxaloacetate (7.6 mM) as a substrate (Ochoa, 1955).

Succinate cytochrome C oxidoreductase (SCC) (EC 1.3.1.6) activity was

determined spectrophotometrically by measuring the oxidation of ferricytochrome c (1% v/v) ($\varepsilon = 0.0185$ $M^{-1}cm^{-1}$) in the presence of succinate (20 mM) at 550 nm (Fleischer and Fleischer, 1967).

GST activity was determined by measuring the turnover of 1-Chloro-2,4-dinitrobenzene (CDNB, 1 mM) ($\varepsilon = 6220$ $M^{-1}cm^{-1}$) and 1 mM GSH as substrates, spectrophotometrically at 340 nm as described by Habig et al. (1974).

Glutathione disulfide (GSSG) reductase (GRD) (EC 1.6.4.2) activity was measured spectrophotometrically by observing the decrease in NADPH (0.1 mM) ($\varepsilon = 6220$ $M^{-1}cm^{-1}$) absorbance at 340 nm in the presence of GSSG (Eklow et al., 1984).

GSH peroxidase (GPX) (EC 1.11.1.9) activity was measured spectrophotometrically by recording the change in absorbance of NADPH (0.2 mM) ($\varepsilon = 6220$ $M^{-1}cm^{-1}$) in the presence of GRD (1 U/mL), NaN_3 (1 mM), GSH (1 mM), and H_2O_2 (0.25 mM) at 340 nm as described by Lawrence and Burk (1976).

γ-Glutamylcysteine synthetase (GGCS) (EC 6.3.2.2) activity was determined indirectly by determining the decrease in absorbance of NADH ($\varepsilon = 6220$ $M^{-1}cm^{-1}$) as oxidized by pyruvate generated by the formation of adenosine 5'-diphosphate (ADP) from L-glutamate (10 mM) and L-α-aminobutyrate (10 mM) in the presence of Mg-adenosine 5'-triphosphase (ATP) (20 mM) (Seelig and Meister, 1984).

Hexokinase (EC 2.7.1.1) activity was determined by measuring the increase in NADPH absorbance at 340 nm as catalyzed by glucose-6-phosphate dehydrogenase (EC 1.1.1.49) (2 U/ml) ($\varepsilon = 6220$ $M^{-1}cm^{-1}$) in the presence of ATP (50 mM), and glucose (15 mM) (Joshi and Jagannathan, 1966).

Toxicity of Tri in isolated rPT and rDT cells. The toxicity of Tri in isolated rPT and rDT cells was determined by release of LDH into the media. Total cellular LDH activity was determined spectrophotometrically by measuring the oxidation of NADH by the decrease in absorbance at 340 nm ($\varepsilon = 6220$ $M^{-1}cm^{-1}$). For P450 inhibition assays, cells were preincubated with 0.25 mM SKF-525A or 0.25 mM metyrapone, another

general P450 inhibitor.

Cytochrome P450 assays. CYP2E1 activity was determined by measuring chlorzoxazone 6-hydroxylase activity as described previously (Peter et al., 1986), using 6-hydroxychlorzoxazone (Ultra Fine Chemicals, Glasgow, UK) as a standard. Rat liver microsomes were used as a positive control. Briefly, the indicated tissue (0.5 to 1.0 mg protein) was incubated in 50 mM potassium phosphate buffer (pH 7.4) along with chlorzoxazone (500 μM final) for 3 min at 37°C, after which NADPH (1 mM final) was added to initiate the reaction. After 20 min, the reaction was stopped by addition of 50 μL phosphoric acid (53%, v/v) and 50 μL of benzoxazolone (0.1 mg/mL stock solution) was added as an internal standard. Samples were then extracted with 2 mL methylene chloride and centrifuged at 3,000 x g for 10 min. The organic layer was then transferred to a clean test tube and evaporated to dryness under N_2. Samples were brought up in 100 μL acetonitrile:water (40:60) and sonicated. Chlorzoxazone and 6-hydroxychlorzoxazone formation were determined by injection onto a C_{18} column (150 mm x 2 mm) (Microsorb, Huntington WV), and isocratic elution using acetonitrile:phosphoric acid (37%:0.31%) at 1.8 mL/min for 30 min, at 287 nm. The limit of detection for this assay was at least 1 pmol of metabolite. Alternatively, CYP2E1 activity was determined by the amount of *p*-nitrophenol hydroxylase activity as measured spectrophotometrically by measuring the absorbance of 4-nitrocatechol at 510 nm. This assay was only used for liver and kidney microsomes from whole tissue homogenates due to its low sensitivity (typically no less than 100 pmol of product formed) compared with the chlorzoxazone HPLC assay. CYP4A activity was determined by measuring the formation of ω and ω-1 metabolites of lauric acid by HPLC as described previously (Miranda et al., 1990; Salhab et al., 1987). Briefly, 0.5 to 1 mg of tissue protein was incubated in 0.5 mL of 50 mM Tris-HCl buffer with 1 mM NADPH and 100 μM [^{14}C]-lauric acid. Liver microsomes were used as a positive control. The reactions were stopped by addition of 100 μL of 10% (v/v) H_2SO_4 and 5 μL of 1 mM tolbutamide was

added as an internal standard. Lauric acid and its metabolites were then extracted twice

in diethyl ether followed by evaporation to dryness under N_2. Samples were resuspended

in 150 μL of HPLC-grade MeOH and injected onto a reverse-phase, μBondapack C_{18} 10-

μM cartridge (10 cm x 8 mm) (Waters Associates, Milford, MA). Peaks for lauric acid

and ω-lauric acid were identified by comparison with authentic standards. The presence

of (ω-1)-lauric acid was determined on the basis of both its retention time and

radiometric labeling. Retention times of ω- and ω-1-lauric acid, and lauric acid itself

were 8, 16-20, and 48 min, respectively. ω- and ω-1-Lauric acid were eluted isocratically

by a mobile phase consisting of 62% MeOH, 37.8% H_2O, and 0.2% acetic acid for 40

min at 0.7 mL/min. Lauric acid was then eluted isocratically by a mobile phase

consisting of 100% MeOH for 20 min. This method was able to measure amounts of

metabolite formation as low as 1 pmol.

Measurement of intracellular content of 4-TByA. Intracellular content of 4-(2-

thienyl)butyric acid (4-TByA) was measured by incubating cells (1.5 to 4.0 x 10^6

cells/mL) in the presence of 4-TByA (10 mM) alone, 4-TByA and SKF525A, or 4-TByA

and α-tocopherol (α-T) in the presence of SKF525A. Cells were preincubated with the

indicated chemical or appropriate control (EtOH, 1%v/v) for 15 min at 37°C in 25-mL

polypropylene Erlenmeyer flasks. At the specified times, 0.5-mL aliquots of cell

suspensions were layered on 1 mL of 20% (v/v) Percoll in saline in 1.5-mL

microcentrifuge tubes and the tubes were centrifuged for 30 sec at 10,000 x g. Cell

pellets were resuspended in saline, 0.25 mL of 3.0 M perchloric acid was added, and

samples were centrifuged in a microcentrifuge for 2 min at 10,000 x g. Acid-soluble

supernatants (0.6 mL) were neutralized by addition of 60 μL each of 1 M potassium

phosphate and 10 M KOH. Supernatants were assayed for 4-TByA by HPLC on a

μBondapack C_{18} 10 μm cartridge (10 cm x 8 mm) (Waters Associates, Milford, MA) with

a Waters Model 600E multisolvent delivery system. Separation was achieved under

isocratic conditions at a flow rate of 1 mL/min with an acetonitrile/water/acetic acid

(20:79:1) mobile phase. 4-TByA exhibited an absorbance maximum at 232 nm (ε^{232} = 1870 $M^{-1}cm^{-1}$). Detection was at 244 nm (ε^{244} = 1070 $M^{-1}cm^{-1}$) due to interference from excessive noise at the lower wavelength, and was performed on a Waters Model 490 variable wavelength detector with quantitation with respect to standard using a Waters Model 745 Data Module. The retention time for 4-TByA was 15 to 17 min.

Flow cytometry analysis of DNA. Flow cytometry of cells was performed following the methods of Ashwell et al. (1987), Dean (1987), Deniger et al. (1983), and Pluzink et al. (1984). After treatment with the indicated agent for the indicated time, cultures were washed twice with sample buffer (PBS plus glucose (1g/L) filtered through a 0.22-μm filter), dislodged by trypsin/EDTA (0.1% w/v) incubation, centrifuged at 400 x g for 10 min and resuspended in sample buffer. Cell concentrations were adjusted to 1 to 3 x 10^6 cells/mL with sample buffer and 1 mL of the cell suspension was centrifuged at 400 x g for 10 min. All of the supernatant except 0.1 mL/10^6 cells was removed and the remaining cells were mixed on a vortex mixer in the remaining fluid for 10 sec. Next, 1 mL of ice-cold EtOH (70% v/v) was added to the sample drop by drop, with samples being mixed for 10 sec between drops. The tubes were capped and fixed in EtOH at 4°C. After fixing, the cells were stained in propidium iodide (PI, 50 μg/ml) containing RNase A (100 U/mL). Samples were then mixed, centrifuged at 1,000 x g for 5 min and all the EtOH except 0.1 mL was removed. Cells were mixed in the residual EtOH and 1 mL of the PI staining solution was added to each tube. After mixing again, cells were incubated at room temperature for at least 30 min. Samples were analyzed within 24 hours by flow cytometry using a Becton Dickinson FACS*Calibur* Flow Cytometer.

Northern blot analysis. Total RNA was isolated from rat liver and kidney homogenates or rPT and rDT cells by acid phenol extraction using the Trizol extraction kit (Gibco BRL, Gaithersburg, MD). Blots were then incubated with probes to CYP2E1, CYP3A1, and CYP4A1 mRNA as described previously (Zangar et al., 1995). Total RNA (10 μg/lane) was fractionated on a formaldehyde/agarose gel, transferred to a nylon

membrane, probed with cDNAs complementary to the indicated mRNA, or stripped and reprobed with a cDNA to mouse 7S RNA to standardize mRNA loading, autoradiographed, and band density was determined by scanning laser densitometry.

Western blot analysis of individual P450 and GST isoforms. The expression of individual P450 and GST isoforms in all tissues was done by subjecting the indicated tissue to SDS-PAGE on a 7% or 10% gel followed by transfer of the gel to nitrocellulose. Nitrocellulose membranes were then exposed to the indicated antibodies. Alkaline phosphatase-conjugated secondary enzymes and substrate were used to detect protein bands. Band densities were determined by scanning laser densitometry. For CYP4A detection in rats, the method of Okita et al. (1998) was used to achieve separation of CYP4A into its individual isoforms. This method involves subjecting small amount of microsomes to SDS-PAGE after pre-running the gel for 4 hours at 25 mA. After loading, samples were allowed to migrate until the 40 kD marker band was approximately 10% (10 mm) from the bottom of the gel. The gel was then transferred to a nitrocellulose membrane and processed as described above.

Immunohistochemical staining for cytokeratins and vimentins. Cultures of rPT, rDT, and hPT cells were grown on 35 mm polystyrene dishes. Cytokeratins were monitored as an epithelial cell marker by indirect immunofluorescent staining as described by Chopra et al. (1987). Vimentins were monitored as an endothelial cell marker and should not be present in control cells (Vamvakas et al., 1988). After fixation with 3.7% (v/v) formalin in PBS, cells were washed several times with PBS containing saponin (0.1% w/v), then incubated with α-keratin conjugated to FITC antibody from guinea pig or a mouse anti-donkey vimentin antibody (Sigma Chemical Co.). After 1 hr, cultures were washed with PBS and viewed under a Carl Zeiss Laser Microscope at the Confocal Imaging Core Facility in the School of Medicine at Wayne State University (Detroit, MI). For vimentin, cultures were incubated with a secondary antibody solution conjugated to Texas Red.

Measurement of state 3 and 4 oxygen consumption rates in isolated mitochondria. Mitochondrial oxygen consumption was measured with a Gilson 5/6H oxygraph in a thermostated, air-tight, 1.6-mL chamber at 20°C. The electrode was a Clark-type electrode, which was calibrated with air-saturated buffer at 20°C, which contains about 265 μM oxygen (Estabrook, 1967). State 3 rates were measured by addition of 3.3 mM succinate and 0.3 mM ADP in the presence of 5 μM rotenone in EtOH (Final concentration = 0.3%, v/v) to the chamber with 0.5 mL mitochondrial sample and 1 mL of mitochondrial buffer. State 4 rates were measured as the rate of oxygen consumption after exhaustion of ADP. Respiratory control ratios (RCR = state 3 rate/state 4 rate) > 5.0 or 3.0 , for mitochondria for liver or kidney, respectively, were used as criteria for functional integrity.

Protein determination and data analysis. Protein determination was done using the BCA protein determination kit from Sigma. All values are means $\pm$ SD of measurements made on the indicated number of separate preparations. Significant differences between means for data were first assessed by a one-way analysis of variance. When significant F values were obtained, the Fisher's protected least significance t test was performed to determine which means were significantly different from one another, with two-tail probabilities < 0.05 considered significant.

Chapter 3

Cell Selective Toxicity of Thiophene-Containing Compounds

Effect of polarity, position, and chain length on thiophene cytotoxicity. Freshly isolated renal rPT and rDT cells were incubated with 0 to 10 mM thiophene, 2- or 3-thiophene methanol (2- and 3-TPMEOH), or 2- or 3-thiophene ethanol (2- and 3-TPEtOH) and LDH release was measured after incubations of 1 hr or 2 hr to assess relative cytotoxicity in the two cell populations (Tables 1 and 2). Thiophene itself was not toxic to rPT cells. The other compounds tested produced intermediate levels of toxicity, causing 40% to 50% LDH release. Toxicity was time-dependent (data not shown) but the concentration dependence for many of the compounds was not straightforward. 3-TPMeOH caused greater toxicity at 2 mM than at 10 mM while 2-TPEtOH caused approximately equal toxicity at 2 and 10 mM. While most of the compounds tested produced significant increases in toxicity as compared with thiophene, there was no apparent pattern of toxicity that seemed to be influenced by altering the chain length, polarity, or position, of the R substituent. The only pattern of toxicity observed was that the compounds that possessed side chains were generally more toxic than unmodified thiophene.

In rDT cells, thiophene caused the greatest amount of toxicity (Table 2). 2-TPMeOH did not produce a significant increase in LDH release over that of the control incubation and 3-TPMeOH, 2-TPEtOH, and 3-TPEtOH all caused moderate increases in toxicity. Increasing the chain length of the R substituent seemed to increase the toxicity in rDT cells, as the LDH release from rDT cells incubated with 10 mM 2- or 3-TPEtOH (47.8% or 43.6%, respectively) was greater than that from 2- or 3-TPMeOH (24.0% or 40.0%, respectively). However, thiophene itself was more toxic than any of these compounds. Unlike in rPT cells, the addition of an R substituent group did not seem to be necessary for thiophene toxicity.

Table 1. Effect of position, chain length, and polarity on LDH release from rPT cells incubated for 2 hr with thiophenes.

Freshly isolated rPT cells (2 to 3 x 10^6 cells/mL) were incubated at 37°C with either solvent control or the indicated concentrations of thiophenes for 2 hr. Cell viability was assessed by measurement of LDH release. Results are the means ± SD of measurements from 3 cell preparations. [a]Statistically significant ($P < 0.05$) difference from corresponding control cells (0 mM). [b]Statistically significant ($P < 0.05$) difference from thiophene at the same concentration. [c]Statistically significant ($P < 0.05$) difference from same thiophene compound with the same R substituent group at the alternate carbon atom (2 or 3 carbon).

mM	Thiophene	2-TPMeOH	3-TPMeOH	2-TPEtOH	3-TPEtOH
0	25.5 ± 9.4	20.9 ± 4.2	22.8 ± 7.1	26.2 ± 6.5	23.8 ± 4.2
1	20.2 ± 8.8	29.2 ± 5.6	16 ± 4.1	28.9 ± 1.2	28.9 ± 5.1
2	25.6 ± 6.5	27.6 ± 6.8	40.4 ± 6.8[b, c]	44.4 ± 7.0[b, c]	24.9 ± 6.4
5	29.4 ± 6.6	22.2 ± 2.9	29.2 ± 4.2	20.3 ± 4.0	41.2 ± 3.8[a, b, c]
10	29.8 ± 7.0	44.6 ± 3.2[a, b, c]	30.9 ± 4.1	44.6 ± 4.2[a, b, c]	53.7 ± 2.7[a, b, c]

Table 2. Effect of position, chain length, and polarity on LDH release from rDT cells incubated for 2 hr with thiophenes.

Freshly isolated rDT cells (2 to 3 x 10^6 cells/mL) were incubated at 37°C with either solvent control or the indicated concentrations of thiophenes for 2 hr. Cell viability was assessed by measurement of LDH release. Results are the means ± SD of measurements from 3 cell preparations. [a]Statistically significant ($P < 0.05$) difference from corresponding control cells (0 mM). [b]Statstically significant ($P < 0.05$) difference from thiophene at the same concentration. [c]Statistically significant ($P < 0.05$) difference from the same thiophene compound with the same R substituent group at the alternate carbon atom (2 or 3 carbon).

mM	Thiophene	2-TPMeOH	3-TPMeOH	2-TPEtOH	3-TPEtOH
0	21.9 ± 6.2	14.2 ± 3.4	15.3 ± 2.8	15.8 ± 2.8	27.7 ± 1.6
1	28.4 ± 5.1	22.4 ± 3.4	25.4 ± 1.2	18.2 ± 2.9	29.9 ± 5.3
2	41.8 ± 8.2[a]	20.7 ± 1.2[b]	31.3 ± 1.6[a,b,c]	23.4 ± 3.4[b]	32.8 ± 5.7[c]
5	36.9 ± 4.3[a]	24.9 ± 6.9[b]	32.5 ± 5.7[a,c]	20.7 ± 4.9[b]	35.8 ± 3.6[c]
10	50.7 ± 4.9[a]	24.0 ± 3.8[b]	40.0 ± 2.6[a,b,c]	47.8 ± 2.4	43.6 ± 5.4[b]

Effect of charge on thiophene cytotoxicity. Freshly isolated rPT and rDT cells were incubated with 0 to 10 mM thiophene, 4-TByA, 2-thiopheneethylamide (2-TPEA), and 2- or 3-thiopheneacetic acid (2- and 3-TPAA) and LDH release was measured after incubations of 1 hr or 2 hr to assess relative cytotoxicity in the two cell populations (Tables 3 and 4). The toxicity of these compounds increased with increasing concentrations and was time-dependent (data not shown). In rPT cells, 4-TByA induced the greatest amount of cytotoxicity (81.2%) while thiophene and 4-TByA induced equal levels of cytotoxicity to rDT cells (50.7% and 49.0%, respectively). 2-TPEA induced a moderate increase in cytotoxicity in rPT cells but exhibited less cytotoxicity in rDT cells than thiophene. In rPT cells, 2-TPAA, but not 3-TPAA was more cytotoxic than thiophene while both 2- and 3-TPAA were less cytotoxic than thiophene in rDT cells. Thus, in rPT cells a charged R substituent on the thiophene ring increased cytotoxicity of thiophene. Whereas in rDT cells, a charged R substituent on the thiophene ring decreased the cytotoxicity of thiophene.

Effect of thiophene-containing compounds on mitochondrial function. Because previous studies (Lash et. al., 1994; Lash and Tokarz, 1995) showed that cellular respiration is decreased when rPT and rDT cells are incubated with 4-TByA or cephaloridine for 30 min, the ability of thiophene-containing compounds to cause mitochondrial dysfunction was assessed (Tables 5 and 6). Rat renal cortical mitochondria were incubated with the various thiophene-containing compounds for 15 min at concentrations of 0, 1, 2, 5, and 10 mM at 20°C. After the 15-min incubation period, state 4 (S4) and state 3 (S3) rates of oxygen consumption were measured and used to calculate RCR values (Table 5). None of the compounds tested produced significant changes in S4 respiration rates at any concentration (data not shown) and only 4-TByA produced a significant decrease in S3 rates when used at 10 mM (data not shown). Modest decreases in S3 rates were also observed with 2- and 3-TPEtOH. When the RCR value was calculated, it was found that incubation of mitochondria with 4-TByA for 15 min at

Table 3. **Effect of charge on LDH release from rPT cells incubated for 2 hr with thiophenes.**

Freshly isolated rPT cells (2 to 3 x 10^6 cells/mL) were incubated at 37°C with either solvent control or the indicated concentrations of thiophenes for 2 hr. Cell viability was assessed by measurement of LDH release. Results are the means ± SD of measurements from 3 cell preparations. [a]Statistically significant ($P < 0.05$) difference from corresponding control cells (0 mM). [b]Statistically significant ($P < 0.05$) from thiophene at the same concentration. [c]Statistically significant ($P < 0.05$) difference from the same thiophene compound with the same R substituent group at the alternate carbon atom (2 or 3 carbon).

mM	Thiophene	4-TByA	2-TPEA	2-TPAA	3-TPAA
0	25.5 ± 7.3	29.3 ± 7.3	35.2 ± 4.8	23.4 ± 3.2	25.7 ± 3.7
1	20.2 ± 6.8	33.6 ± 8.2	30.1 ± 9.4	30.5 ± 4.5	18.9 ± 5.9
2	25.6 ± 6.5	42.8 ± 4.1[a,b]	43.9 ± 4.1[a,b]	31.3 ± 11.0	44.5 ± 6.3[a,b,c]
5	29.4 ± 4.5	66.6 ± 10.5[a,b]	39.9 ± 4.8[b]	44.5 ± 6.3[a,b,c]	20.5 ± 1.1
10	29.8 ± 5.0	81.2 ± 11.4[a,b]	48.7 ± 6.4[a,b]	50.1 ± 3.0[a,b,c]	23.1 ± 4.4

Table 4. Effect of charge on LDH release from rDT cells incubated for 2 hr with thiophenes.

Freshly isolated rDT cells (2 to 3 x 10^6 cells/mL) were incubated at 37°C with either solvent control or the indicated concentrations of thiophenes for 2 hr. Cell viability was assessed by measurement of LDH release. Results are the means ± SD. of measurements from 3 cell preparations. [a]Statistically significant ($P < 0.05$) difference from corresponding control cells (0 mM). [b]Statistically significant ($P < 0.05$) difference from thiophene at the same concentration. [c]Statisically significant ($P < 0.05$) difference from same thiophene compound with the same R substituent group at the alternate carbon atom (2 or 3 carbon).

mM	Thiophene	4-TByA	2-TPEA	2-TPAA	3-TPAA
0	21.9 ± 4.3	19.2 ± 7.5	27.2 ± 7.3	25.2 ± 4.0	14.9 ± 1.0
1	28.4 ± 3.1	24.5 ± 7.4	33.6 ± 2.9	14.2 ± 1.8[b]	15.5 ± 2.3[b]
2	41.8 ± 6.3[a]	35.6 ± 7.6	27.3 ± 2.1[b]	17.7 ± 4.3[b]	30.2 ± 1.6[a,c,c]
5	36.9 ± 2.1[a]	43.0 ± 6.5[a]	29.7 ± 3.6	30.1 ± 2.0	32.7 ± 1.9[b]
10	50.7 ± 2.4[a]	49.0 ± 13.2[a]	42.3 ± 8.8	32.7 ± 1.9[b]	39.3 ± 2.3[a,c]

Table 5. RCR values for mitochondria incubated for 15 min with thiophenes.

Isolated renal cortical mitochondria were incubated at 20°C with either solvent control or the indicated concentrations of thiophene-containing compounds for 15 min. Table 15A measures the affect of charge on mitochondrial toxicity. Table 15B measures the affect of chain length on mitochondrial toxicity. Mitochondrial function was assessed by calculation of the RCR from the S3 and S4 rates of oxygen consumption (RCR = S3/S4). Results are the means ± SD of measurements from 3 mitochondrial preparations. [a]Statistically significant ($P < 0.05$) difference from corresponding control cells (0 mM). [b]Statistically significant ($P < 0.05$) difference from thiophene at the same concentration. [c]Statistically significant ($P < 0.05$) difference from same thiophene compound with the same R substituent group at the alternate carbon atom (2 or 3 carbon).

A.

mM	Thiophene	4-TByA	2-TPEA	2-TPAA	3-TPAA
0	3.1 ± 0.4	2.5 ± 0.4	3.4 ± 0.3	2.6 ± 0.5	3.7 ± 0.4
1	3.1 ± 0.2	2.5 ± 0.1	3.0 ± 0.2	2.0 ± 0.2[b,c]	3.5 ± 0.5
2	3.0 ± 0.5	1.8 ± 0.2[b]	2.8 ± 0.4	2.2 ± 0.5	3.0 ± 0.5
5	3.1 ± 0.4	1.9 ± 0.1[a,b]	2.7 ± 0.3	1.8 ± 0.3[b,c]	2.6 ± 0.2[a]
10	3.1 ± 0.6	1.2 ± 0.1[a,b]	3.4 ± 0.3	2.5 ± 0.4	3.2 ± 0.2

B.

mM	Thiophene	2-TPMeOH	3-TPMeOH	2-TPEtOH	3-TPEtOH
0	3.1 ± 0.4	3.0 ± 0.4	3.5 ± 0.1	2.9 ± 0.1	4.4 ± 0.4
1	3.1 ± 0.2	2.2 ± 0.2[b,c]	2.4 ± 0.4	2.3 ± 0.2[b,c]	3.3 ± 0.8
2	3.0 ± 0.5	1.8 ± 0.1[a,b]	2.5 ± 0.4	2.3 ± 0.2	2.4 ± 0.5[a]
5	3.1 ± 0.4	2.7 ± 0.4	2.6 ± 0.5	2.2 ± 0.2[a,b]	2.2 ± 0.2[a,b]
10	3.1 ± 0.6	1.9 ± 0.2[a,b,c]	3.2 ± 0.3	2.4 ± 0.1[a,b]	2.4 ± 0.2[a,b]

concentrations of both 5 and 10 mM produced a significant decrease in RCR from the control ([dimethylsulfoxide] <1%, v/v Table 5). Furthermore, 3-TPAA, 2-TPMeOH, and 2 and 3-TPEtOH also produced significant decreases in RCR from control values. 3-TPAA and 2-TPMeOH only caused a significant decrease at 5 mM. 2-TPEtOH caused a significant decrease in RCR from control at both 5 and 10 mM. There were no detectable differences in patterns of mitochondrial toxicity, as measured by increases in S4 or decreases in S3 and RCR, between thiophene compounds that differed with respect to the 2- and 3-position of the substituent on the thiophene ring. The charge of the R substituent on the thiophene ring also did not seem to alter mitochondrial toxicity and there was no detectable effect on toxicity by altering polarity of the R substituent. In contrast, increasing the chain length of the R substituent seemed to increase the toxicity as both 2- and 3-TPEtOH caused larger decreases in S3 and RCR than the corresponding TPMeOH compounds.

To understand further the effects of thiophene-containing compounds on mitochondrial function, mitochondria were incubated with each of the thiophenes (5 mM) at 20°C for 15 min and S3 and S4 rates were measured and RCR values were calculated (Table 6). The use of all the compounds at one concentration allowed for direct comparisons of the toxicity of thiophenes to one another with a common control, thus avoiding problems with variation in control rates of oxygen consumption among sets of experiments. The concentration of 5 mM was chosen because not all of these compounds followed a straightforward, concentration-dependent pattern of toxicity, as shown in Table 5. None of the thiophene compounds tested at 5 mM were able to cause significant decreases in S3 or S4 rates of oxygen consumption, and only 4-TByA and 3-TPAA caused a significant decrease in RCR over that of the control. The addition of a functional group to the thiophene ring resulted in a significant decrease in RCR for all of the compounds tested as compared with thiophene.

Table 6. State 3, state 4, and RCR values for mitochondria incubated with 2 mM thiophene-containing compounds with a common control.

Isolated renal cortical mitochondria were incubated at 20°C with either solvent control or 5 mM of the indicated thiophene compound for 15 min. Mitochondrial function was assessed by measurement of S3 and S4 rates of oxygen consumption and calculation of RCR values (RCR = S3/S4). Results are the means ± SD of measurements from 3 mitochondrial preparations. [a]Statistically significant ($P < 0.05$) difference from corresponding control cells (0 mM). [b]Statistically significant ($P < 0.05$) difference from thiophene at the same concentration. [c]Statistically significant ($P < 0.05$) difference from the same thiophene compound with the same R substituent group at the alternate carbon atom (2 or 3 carbon).

Treatment	State 4 (nmol O_2/min per mg protein)	State 3 (nmol O_2/min per mg protein)	RCR
Control	20.2 ± 4.1	75.7 ± 7.7	3.5 ± 0.2
Thiophene	20.2 ± 0.8	68.2 ± 4.7	3.8 ± 0.3
4-TByA	24.9 ± 4.7	55.2 ± 4.8	2.3 ± 0.3[a,b]
2-TPEA	28.0 ± 2.1	67.0 ± 5.3	2.4 ± 0.4[b]
2-TPAA	25.9 ± 2.2	67.4 ± 2.2	2.6 ± 0.2[b]
3-TPAA	29.0 ± 2.0	57.7 ± 4.0	2.0 ± 0.2[a,b]
2-TPMeOH	24.9 ± 7.5	63.5 ± 3.5	2.5 ± 0.2[b]
3-TPMeOH	23.1 ± 2.8	61.5 ± 5.6	2.6 ± 0.4[b]
2-TPEtOH	25.2 ± 3.2	66.2 ± 3.6	2.6 ± 0.3[b]
3-TPEtOH	24.6 ± 3.5	66.5 ± 2.0	2.6 ± 0.4[b]

Roles of oxidative stress, cytochrome P450-dependent metabolism, and transport in thiophene-induced cytotoxicity. Because 4-TByA produced the greatest difference in cytotoxicity between rPT and rDT cells, this compound was used to study further the differences in metabolism and uptake between rPT and rDT cells. The ability of 4-TByA to cause LDH release in rPT and rDT cells after inhibition of P450 by SKF-525A, and after addition of GSH, was assessed (Figure 4A and B). rPT and rDT cells were incubated with acivicin (0.25 mM) for 15 min and then with SKF-525A (0.25 mM) and/or GSH (5 mM) for another 15 min at 37°C prior to addition of 4-TByA (10 mM), and LDH release was measured at 0, 1, and 2 hr. For rPT cells (Figure 4A), 4-TByA produced LDH release that was significantly above control levels at both 1 and 2 hr and the addition of SKF-525A modestly increased LDH release further. The addition of GSH to rPT cells treated with 4-TByA reduced LDH release only at 1 hr and had no effect at 2 hr. The ability of GSH to reduce LDH release caused by 4-TByA at 1 hr was negated when SKF-525A was included in the incubation medium. Previous studies have already demonstrated that SKF-525A alone did not significantly increase LDH release from either rPT or rDT cells (Lash and Tokarz, 1995). The ability of 4-TByA to produce increases in LDH release in rDT cells was significantly increased in the presence of SKF-525A (Figure 4B). rDT cells preincubated with SKF-525A prior to the addition of 4-TByA exhibited LDH release levels comparable to those of rPT cells. As in rPT cells, preincubation of rDT cells with GSH prior to addition of 4-TByA lowered the LDH release to control levels at 1 hr but not at 2 hr. Unlike rPT cells, preincubation with GSH and SKF-525A prior to the addition of 4-TByA significantly lowered LDH release from rDT cells preincubated with 4-TByA and SKF-525A alone.

α-Tocopherol (α-T), an antioxidant, has previously been shown to partially protect rPT and rDT cells from 4-TByA-induced toxicity (Lash and Tokarz, 1995), but whether or not this protection occurs before or after metabolism of 4-TByA was not determined. Isolated rPT and rDT cells were incubated with either SKF-525A (0.25 mM) or α-T (20

μM) for 15 min at 37°C prior to addition of 4-TByA. As shown in Figure 5, preincubation of rPT cells with SKF-525A prior to the addition of 4-TByA produced modest increases in LDH release compared with rPT cells treated with 4-TByA alone at both 1 and 2 hr (Figure 5A). Preincubation of rPT cells with α-T resulted in protection after only 2 hr. Pretreatment of rPT cells with both SKF-525A and α-T did not result in protection from increases in 4-TByA-induced LDH release. In fact, LDH release in rPT cells pretreated with both α-T and SKF-525A was higher than that in rPT cells pretreated with SKF-525A alone at both 1 and 2 hr. For rDT cells (Figure 5B), preincubation of cells with SKF-525A prior to the addition of 4-TByA once again resulted in an greater LDH release at levels comparable to those measured in rPT cells. In contrast to rPT cells, when rDT cells were preincubated with SKF-525A and α-T, the levels of LDH release were not changed at either 1 or 2 hr as compared with rDT cells that were pretreated with 4-TByA and SKF-525A alone.

To determine how the intracellular content of 4-TByA was affected by the inhibition of P450 and addition of GSH, intracellular 4-TByA concentrations in cells incubated for 2 hr at 37°C with 4-TByA (10 mM) were measured (Figure 6). Isolated rPT and rDT cells were preincubated for 15 min with acivicin (0.25 mM) at 37°C and then with either solvent controls, SKF-525A (0.25 mM), GSH (5 mM), or SKF-525A and GSH. 4-TByA (10 mM) was then added and cells were incubated for another 2 hr at 37°C, after which the intracellular acid extracts were isolated as described in Chapter 2. When cells were treated with 4-TByA alone, rPT cells had intracellular 4-TByA levels almost twice those of rDT cells. When cells were pretreated with SKF-525A, there was a slight significant difference in intracellular 4-TByA content in rPT cells, but intracellular 4-TByA content in rDT cells more then doubled. Pretreatment of rPT and rDT cells with GSH resulted in a significant decrease in intracellular 4-TByA content in rPT cells but had no effect in rDT cells. Finally,

Figure 4. Effect of SKF525A and GSH on the cytotoxicity of 4-TByA in freshly isolated rPT and rDT cells.

rPT (A) and rDT (B) cells were incubated with acivicin (0.25 mM) for 15 min and then SKF-525A (0.25 mM) and/or GSH (5 mM) for another 15 min at 37°C prior to addition of 4-TByA. LDH release was measured at 0, 1, and 2 hr. LDH release was determined as explained in Chapter 2. %LDH release in control rPT cells was 7.3 ± 2.7% and that of control rDT cells was 6.3 ± 3.3% (n =3). Results are the mean ± SD or at least 3 separate preparations. *Significantly different from cell incubated with 4-TByA only. †Significantly ($P < 0.05$) different from cells preincubated with SKF-525A. ‡Significantly ($P < 0.05$) different from cells preincubated with SKF-525A.

A. PT Cells
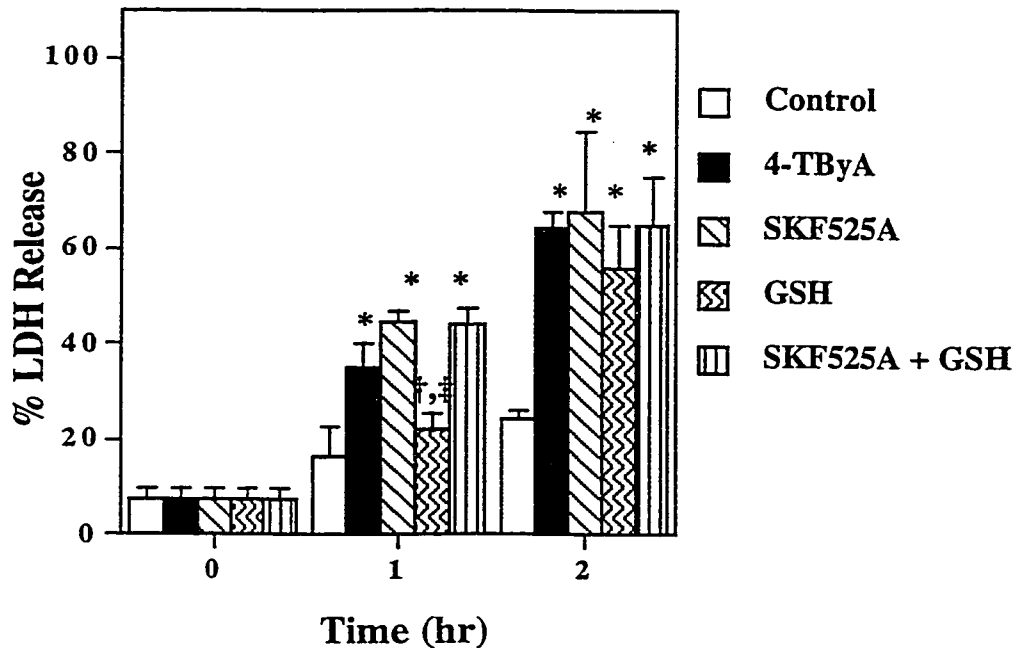
B. DT Cells
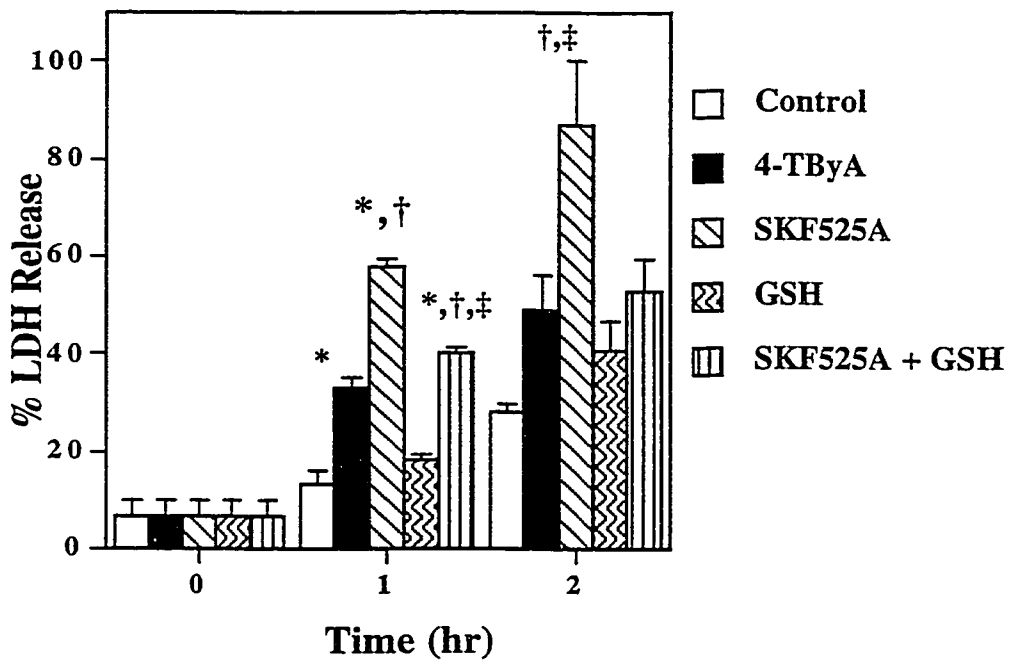
Figure 5. Effect of SKF525A on protection from 4-TbyA-induced cytotoxicity by α-tocopherol in freshly isolated rPT and rDT cells.

rPT (**A**) and rDT (**B**) cells were incubated with SKF525A (0.25 mM) at 37°C for 15 min and then 4-TByA (10 mM) and α-tocopherol (0.25 mM) or buffer was added. LDH release was measured at 0, 1, and 2 hr. LDH release was determined as explained in Chapter 2. %LDH release in control rPT cells was $9.0 \pm 3.5\%$ and that of control rDT cells was $6.0 \pm 2.5\%$ (n =3). Results are the mean $\pm$ SD of at least 3 separate preparations. *Significantly different from cell preincubated with buffer followed by treatment with 4-TByA only. †Significantly ($P < 0.05$) different from cells incubated with SKF-525A ‡Significantly ($P < 0.05$) different from cells incubated with SKF-525A and GSH.

A. PT Cells

B. DT Cells

Control

4-2-TByA

SKF525A

α-T
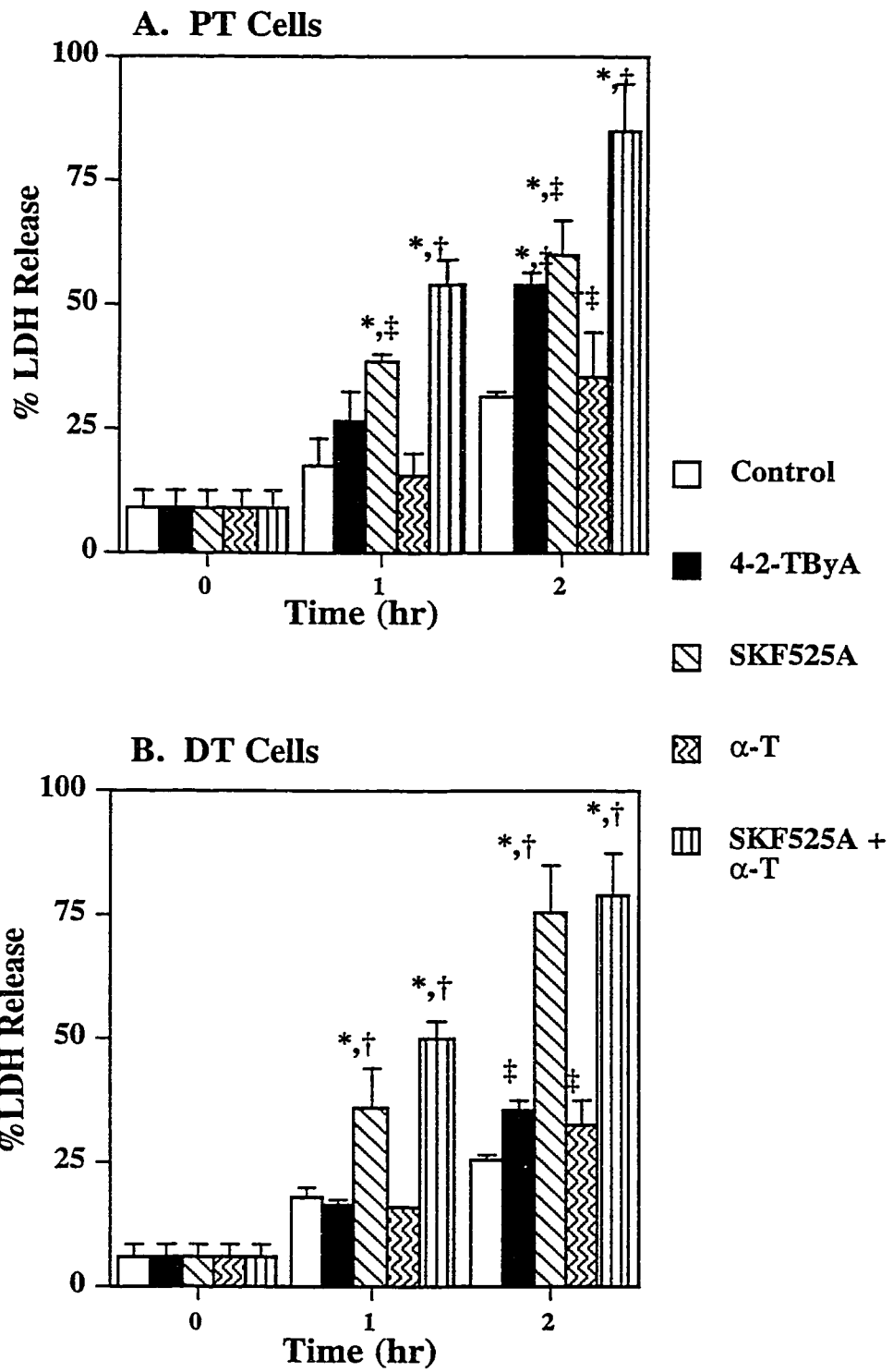
SKF525A +
α-T

Figure 6. Effect of SKF525A and GSH on intracellular content of 4-TByA in freshly isolated rPT and rDT cells.

Isolated rPT (A) and rDT (B) cells were preincubated for 15 min with acivicin (250 μM) at 37°C and then with either solvent control, SKF-525A (0.25 mM), GSH (5 mM), or SKF-525A and GSH. 4-TByA (10 mM) was then added and cells were incubated for another 2 hr at 37°C, after which the intracellular acid extracts were isolated as described in Chapter 2. Results are the mean ± SD of at least 3 separate preparations. Within each cell population, bars with different letters are significantly ($P < 0.05$) different from one another.
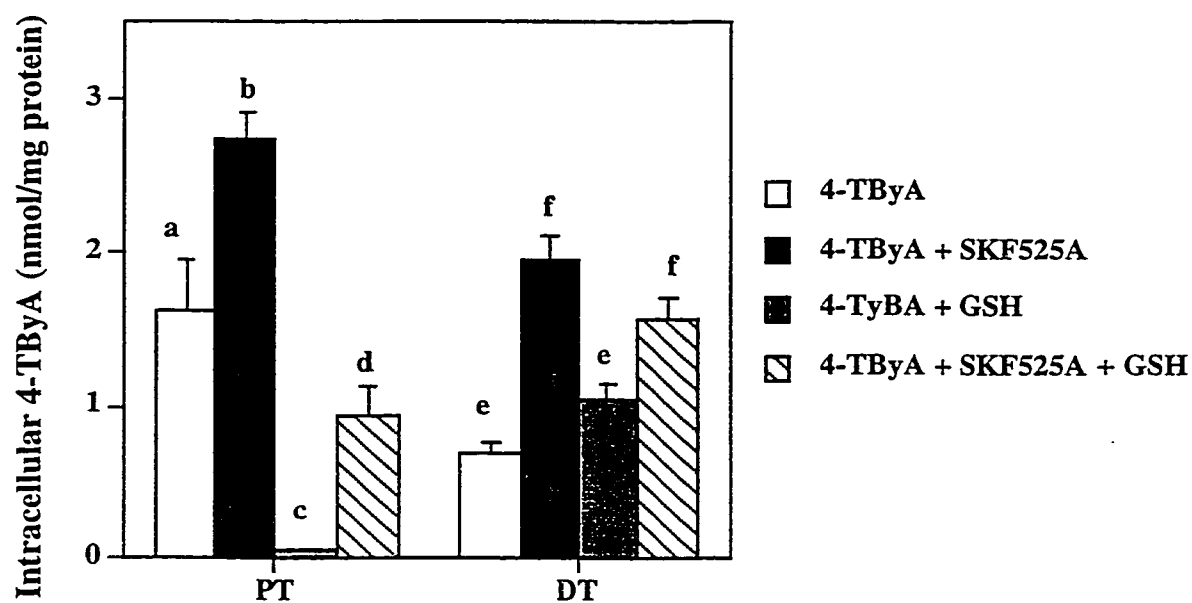
pretreatment of PT cells with SKF-525A and GSH together resulted in a slight change in intracellular 4-TByA content over 4-TByA treatment alone. In contrast, rDT cells pretreated with SKF-525A and GSH prior to the addition of 4-TByA exhibited higher intracellular 4-TByA content than DT cells treated with only 4-TByA.

In summary, data from these studies indicated that significant differences exist in the drug metabolism ability of rPT and rDT cells. Data on the affect of inhibition of P450 on 4-TByA toxicity and metabolism suggests that significant differences exist in P450 expression in these cells. These possibilities are tested in Chapter 4.

Discussion.

Thiophenes are important compounds in both the chemical and pharmaceutical industries. In addition, the thiophene derivative tienilic acid has been studied intensely as it has been implicated in tienilic acid-induced hepatitis (Beaune et al., 1987; Lopez-Garcia et al., 1993). Thiophene-containing compounds such as cephaloridine are also nephrotoxicants (Lash et al., 1994) and metabolism on the thiophene functional group was hypothesized to play a role in cephaloridine-induced nephrotoxicity (Tune, 1986). Previous work (Lash and Tokarz, 1995) showed that a thiophene derivative, 4-TByA, was cytotoxic to freshly isolated rPT and rDT cells. This work proposed that the mechanism for 4-TByA-induced toxicity might involve oxidative stress. This was supported by the fact 4-TByA also increased malondialdehyde formation in both rPT and rDT cells. Finally, the possibility that the mechanism of 4-TByA toxicity may involve mitochondrial dysfunction was proposed, since 4-TByA decreased cellular respiration in both rPT and rDT cells.

In the present study, the ability of nine different thiophene-containing compounds, differing only in the R substituent on the 2- or 3-position, to cause cytotoxicity and mitochondrial dysfunction was determined. 4-TByA was the most toxic compound in both rPT cells and mitochondria (Tables 1, 3, 5, and 6). In contrast, several of the other thiophene-containing compounds caused modest cytotoxicity in rDT cells. (Tables 2 and 3).

Differences in the R substituent of the thiophene ring allowed for the study of the chemical specificity of cytotoxicity. In rPT cells the addition of an R substituent to the thiophene ring generally resulted in increased toxicity relative to unmodified thiophene. In contrast, in rDT cells the addition of an R substituent to the thiophene ring generally resulted in lower toxicity relative to unmodified thiophene. Unlike rPT cells, increasing the chain length of the R substituent on the thiophene ring seemed to lead to increased toxicity in rDT cells.. Finally, the presence of a charged R substituent on the thiophene ring resulted in greater toxicity of thiophenes in rPT cells but less toxicity of thiophenes in rDT cells.

Two possible explanations that can account for the difference in thiophene-induced cytotoxicity between rPT and rDT cells are the difference in drug metabolizing enzymes in rPT and rDT cells and that the toxicity of thiophenes in both rPT and rDT cells is modulated by cellular transport mechanisms. The former explanation seems plausible since both qualitative and quantitative differences in many drug metabolism enzyme activities among cell populations along the nephron have been documented (Guder and Ross, 1984; Lash and Tokarz, 1990). This suggests that rDT cells may metabolize 4-TByA differently than rPT cells, thus altering the nature and/or rate of generation of reactive metabolites. Evidence from the present study suggests that it may be the presence and not the absence of key drug metabolizing enzymes in the rDT cells that accounts for the decreased toxicity of 4-TByA to rDT cells and the different response of these cells to a P450 inhibitor. This possibility is supported by data in Figure 4, which showed that when cells were pretreated with SKF-525A, 4-TByA-induced increases in LDH release were unaltered in rPT cells but were markedly increased in rDT cells. These data suggest that 4-TByA may be detoxified by a P450 isoform in rDT cells that is absent in rPT cells and that this could account for the greater toxicity of 4-TByA to rPT cells. Thus, the decreased toxicity of a thiophene with an R substituent in rDT cells may occur because the R substituent makes the thiophene more likely to be metabolized by P450.

It is possible that the difference in the cytotoxicity of thiophenes to rPT and rDT

cells is a result of differences in activity of enzymes that mediate oxidative stress. However, the inability of GSH and α-T to fully protect cells against 4-TByA-induced toxicity lends support to the possibility that the mechanism of toxicity of thiophene-containing compounds cannot be fully explained by oxidative stress. While GSH was protective at 1 hr in both rPT cells and rDT cells, it was not protective at 2 hr. Furthermore, GSH was not protective in the presence of SKF-525A in either rPT or rDT cells (Figure 4). Data presented in Figure 5 showed that α-T also failed to protect rPT and rDT cells against 4-TByA-induced toxicity in the presence of SKF-525A. The fact that GSH and α-T seemed to protect against 4-TByA-induced toxicity at 1 hr in both rPT and rDT cells indicates that the metabolism of thiophenes or their interaction with cellular molecules may lead to the generation of reactive oxygen intermediates (ROIs). Indeed, data have been published on the metabolism of thiophene-containing compounds that support this possibility (Dansette et al., 1992); the authors proposed that the toxicity of thiophene is linked to the hydroxylation of its ring to form 5-hydroxythiophene via an epoxide intermediate. They also proposed that thiophene was conjugated with GSH and excreted in the urine as the mercapturate, N-acetyl-S-(2-thienyl)-L-cysteine. Recent studies from Valadon et al. (1996) provided evidence for intermediate formation of a reactive, electrophilic thiophene sulfoxide in the metabolic activation of 3-aroylthiophenes, such as tienilic acid, in rat liver microsomes. The presence of a thiophene sulfoxide was demonstrated further by trapping experiments with thiol-containing trapping agents and GSH. Therefore, the presence of GSH should be beneficial to rPT and rDT cells as it should enhance the detoxification of thiophene to its mercapturic acid. This may be the reason for the protective effect of GSH seen after 1 hr incubation of rPT and rDT cells with 4-TByA.

Reasons for the inability of GSH to protect rPT and rDT cells from 4-TByA-induced toxicity after 2 hr could be that GSH is either depleted or that 4-TByA is exerting toxicity through another pathway that is independent of P450-dependent metabolism or oxidative stress. Indeed, it appears that the toxicity of 4-TByA in rPT cells is dependent on

4-TByA metabolism, as α-T was not an effective protective agent when cytochrome P450 isoforms were inhibited. However, since the toxicity of 4-TByA to rPT cells only changed modestly after P450 inhibition, it can be argued that the toxicity of 4-TByA in rPT cells is not dependent on metabolism by P450 and the protection afforded to these cells by α-T is occurring by some manner other then a scavenging of ROIs generated by this metabolism. α-T did not protect against 4-TByA-induced toxicity in rDT cells and inhibition of P450 resulted in an increase in the toxicity of 4-TByA. This is different than the results in rPT cells, suggesting that thiophene metabolism differs in the two cell populations.

It is also possible that the mechanism of toxicity of unmetabolized 4-TByA involves oxidative stress. Therefore, the metabolism of the parent compound by a P450 isoform present in rDT cells and not rPT cells could result in a decrease in ROIs generated by 4-TByA, rendering α-T ineffective in DT cells. Further studies need to be performed to examine differences in the distribution of specific P450 isoforms in PT and DT cells to substantiate this possibility.

Another possibility for the difference in cytotoxicity of 4-TByA in rPT and rDT cells is differences in amounts of cellular uptake and accumulation of 4-TByA. The present findings (Figure 4) support this possibility by showing that when GSH was added to rPT and rDT cells, the amount of 4-TByA in rPT cells, but not in rDT cells, was significantly decreased. The GSH-dependent decrease may be the result of increased conjugation of 4-TByA to GSH in rPT cells. The absence of this effect of GSH in rDT cells could be due to differences in metabolism, such as lower GST activity (Guder and Ross, 1984; Lash and Tokarz, 1990), or the formation of a metabolite that is less likely to conjugate to GSH. The increase in 4-TByA levels after P450 inhibition supports the conclusion that 4-TByA is metabolized by P450 isoforms in the kidney and also corresponds well to the greater LDH release and toxicity seen after P450 inhibition (Figure 4). Therefore, the data presented in this paper support the possibility that 4-TByA is transported into rPT and rDT cells, is metabolized differently by P450 isoforms in the two cell populations, and is conjugated with

GSH primarily in rPT cells to be ultimately excreted as a mercapturic acid. Again, the presence of an R substituent on the thiophene ring could alter the uptake of thiophene into the cell. In this case, the presence of the R substituent enhances its transport into the cell via a specific transporter. Further experiments need to be done to validate or refute this possibility.

Experiments examining the effects of GSH and α-T treatment on 4-TByA-induced LDH release were done to determine if the mechanism of toxicity involves oxidative stress. These experiments showed that only partial protection of cells was afforded by GSH and α-T treatments, suggesting that other mechanisms may be involved, particularly in mitochondria.

The patterns of mitochondrial toxicity seen with the various compounds, which differed in the R substituent on the thiophene ring, generally paralleled those seen in cells. There was a pattern of increasing toxicity as an result of increasing chain length of the R substituent seen in mitochondria and rDT cells, but not rPT cells. It is unlikely that the mechanism of toxicity of thiophene-containing compounds to mitochondria involves the generation of ROIs as neither GSH nor α-T were able to significantly reduce the toxicity.

The present study has explored the renal cellular and mitochondrial toxicity of several thiophene-containing compounds to examine structural requirements for toxicity. Potential modulators of toxicity were tested to uncover factors that are responsible for cell type specific patterns of toxicity in the kidneys, thereby elucidating the mechanism of action of thiophenes. Data from this study showed that the two most important factors in the determination of thiophene toxicity in freshly isolated rPT and rDT cells are the presence of a side chain on the thiophene ring and the difference in P450 activity between the two cell populations. It is possible that the presence of a side chain group on the thiophene ring alters its metabolism by P450. The difference in toxicity between rPT and rDT cells may be, therefore, a result of the presence and absence of the P450 isoforms responsible for the metabolism of thiophene (CYP2C11 in the rat; Dansette et al., 1990). To better understand

how differences in P450 expression may affect cell selective toxicity of thiophenes and other compounds, the P450 isoforms expressed in rPT and rDT cells need to be determined.

In summary, the present study showed that rPT and rDT cells differ significantly in their susceptibility to thiophene compounds. Data from this study showed that this difference can be attributed, in part, to differences in expression of drug metabolism enzymes, mainly P450. Thus these data partially supports the hypothesis that differences in cell selective toxicity of chemicals to different renal cell populations are a result of differences in the activity of drug metabolizing enzymes. To further prove this hypothesis, it must be shown that rPT and rDT cells actually do differ in the expression and activity of critical drug metabolism enzymes.

Chapter 4

Expression and Distribution of Cytochrome P450
and GST Isoforms in rPT and rDT Cells

Introduction

As mentioned in Chapter 1, the expression of P450 isoforms in rPT and rDT cells has not been studied extensively. This information would aid greatly in the determination of a number of mechanisms of chemically-induced nephrotoxicity caused by chemicals such as Tri and thiophenes. Furthermore, some of the P450 isoforms found in the kidney are believed to affect physiological function. For example, CYP4A isoforms participate in the arachidonic acid cascade in the kidney and thereby alter blood pressure (Escalante et al., 1991; Hirt et. al.; 1991). To better understand the metabolism and toxicity of both Tri and thiophenes in freshly isolated rPT and rDT cells, the expression of several P450 isoforms was determined. The isoforms studied are those that are involved in both Tri and thiophene metabolism in the rat liver and include CYP2B1/2, CYP2C11, CYP2E1, CYP3A1/2, and CYP4A isoforms (See Chapter 1).

Results

CYP2E1 Expression. To determine if CYP2E1 expression differed between rat renal PT and DT cells, western blot analysis was performed. Microsomes from cortical, rPT, and rDT cells from at least 3 rats were isolated, combined, lysed, and subjected to western blot analysis using a polyclonal anti-rat CYP2E1 antibody (Figure 7A). The expression of CYP2E1 in liver and kidney microsomes was also determined for comparative purposes. The expression of CYP2E1 was higher in liver microsomes than in kidney microsomes and microsomes isolated from cortical and rDT cells expressed higher levels of CYP2E1 than microsomes isolated from rPT cells. Densitometric analysis of these

Figure 7. Expression of CYP2E1 protein and mRNA in rat liver and kidney.

A. Representative western blot using a polyclonal anti-rat CYP2E1 antibody showing expression of CYP2E1 in 5 μg of pyridine-induced rat liver microsomes (lane 1) and kidney microsomes (lane 2), or 60 μg of rat cortical (lane 3), rPT (lane 4), and rDT (lane 5) microsomes. **B.** Densitometric analysis of CYP2E1 protein expression. **C.** Northern blots of CYP2E1 and 7S RNA. Total RNA (10 μg/lane) was fractionated on a formaldehyde/agarose gel, transferred to a nylon membrane, probed with a cDNA complementary to rat CYP2E1 or mouse 7S RNA (loading standard) and autoradiographed. **D.** Densitometric analysis of CYP2E1 mRNA expression in rPT and rDT cells.
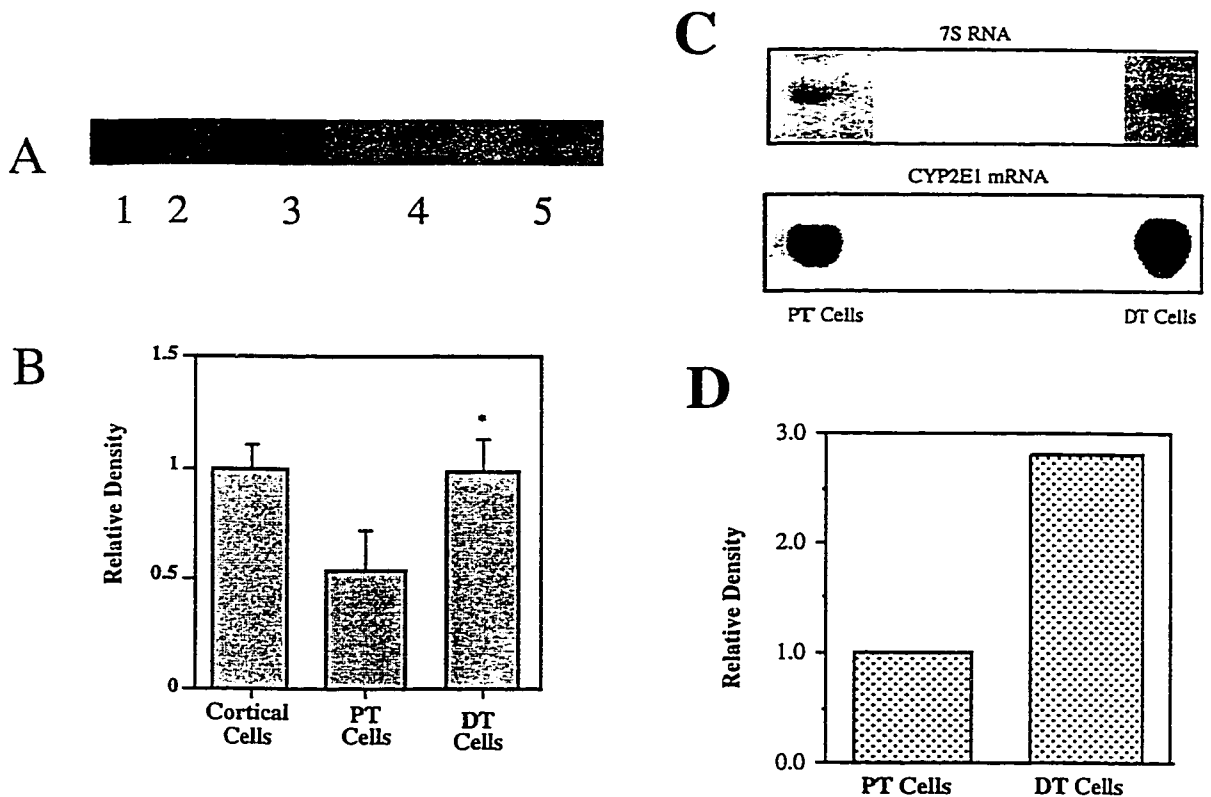
Table 7. Chlorzoxazone hydroxylation activity in liver and kidney samples from Fischer 344 rats.

Microsomes from liver and total kidney cortical homogenates or from cortical, rPT, and rDT cells were isolated from male Fischer 344 rats. Activity of chlorzoxazone hydroxylase was determined by formation of the hydroxylated metabolite by HPLC, with detection at 285 nm. Results are the means ± SD of measurements from 3 to 5 tissue or cell preparations. *Significant difference ($P < 0.05$) from activity in PT cells.

Sample	Chlorzoxazone 6-Hydroxylation (pmol/min per mg protein)
Liver microsomes	682 ± 92
Kidney cortical microsomes	131 ± 5
Cortical cell microsomes	104 ± 18
Proximal tubular cell microsomes	62.0 ± 3.2
Distal tubular cell microsomes	23.0 ± 8.0*

blots demonstrated that CYP2E1 protein levels in microsomes from cortical and rDT cells were approximately equal, but CYP2E1 protein levels were almost twofold higher in rDT cells than in microsomes isolated from rPT cells (Figure 7B). Northern blot analysis of total RNA from rPT and rDT cells revealed that the expression of CYP2E1 mRNA was 2- to 3- fold higher in rDT cells than PT cells (Figure 7C and 7D). This was not due to differences in loading as there was no apparent difference in 7S mRNA levels (Figure 7C).

To determine if the level of expression of CYP2E1 between rPT and rDT microsomes paralleled differences in CYP2E1 activity, 6-chlorzoxazone hydroxylase activity was examined in rPT and rDT microsomes (Table 7). Rates of chlorzoxazone hydroxylation were 5-fold higher in liver microsomes than in renal cortical microsomes and were 2.7-fold higher in microsomes from rPT cells than in microsomes from rDT cells. This lack of correlation in cell type distribution between chlorzoxazone hydroxylation activity and CYP2E1 expression suggests that other enzymes are contributing to chlorzoxazone hydroxylation activity in rPT microsomes.

CYP2C11 expression. Western blot analysis of kidney and liver tissues using a monoclonal anti-rat antibody demonstrated that CYP2C11 was expressed in both tissues. CYP2C11 expression was detected in kidney microsomes and cortical and rPT microsomes but was undetectable in rDT microsomes (Figure 8A). The level of expression in kidney microsomes was approximately 10% of that detected in the liver. CYP2C11 expression in rPT microsomes was twice that of cortical microsomes, as determined by densitometric analysis (Figure 8B).

CYP3A1/2 expression. Western blot analysis of liver and kidney tissues using a monoclonal anti-rat CYP3A1 antibody, which also recognizes CYP3A2, demonstrated that CYP3A1/2 was expressed in liver and kidney microsomes but not in cortical, rPT, or rDT microsomes (Figure 9). The expression of CYP3A1/2 in kidney microsomes was

Figure 8. Expression of CYP2C11 protein in rat liver and kidney.

A. Representative western blot using a monoclonal anti-rat CYP2C11 antibody showing expression of CYP2C11 in 5 μg of rat liver microsomes (lane 1) and kidney microsomes (lane 2), or 60 μg of rat cortical (lane 3), rPT (lane 4), and rDT (lane 5) microsomes. **B.** Densitometric analysis of CYP2C11 protein expression.
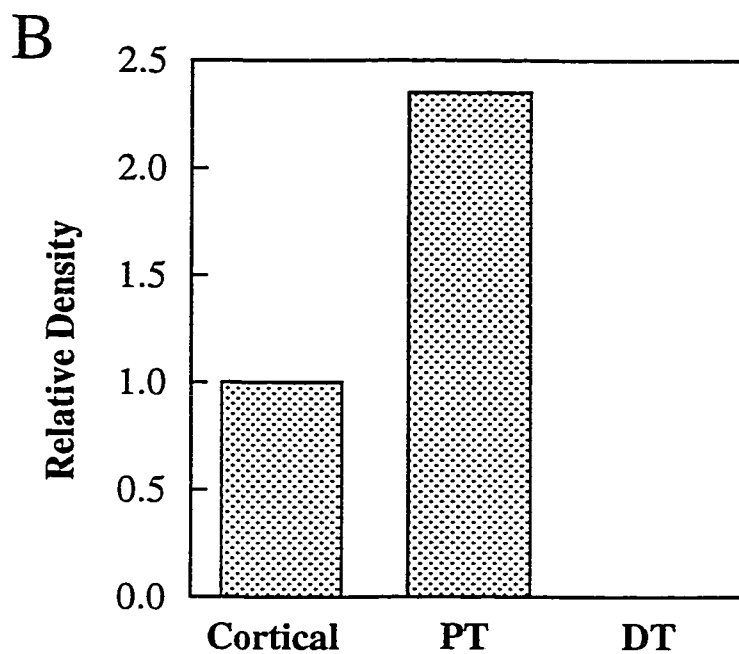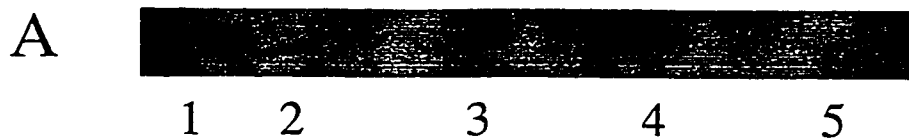
Figure 9. Expression of CYP3A1/2 protein in rat liver and kidney.

Representative western blot using a monoclonal anti-rat CYP3A1 antibody, which also recognized CYP3A2, showing expression of CYP3A1/2 in 5 µg of rat liver microsomes (lane 1) and kidney microsomes (lane 2), or 60 µg of rat cortical (lane 3), rPT (lane 4), and rDT (lane 5) microsomes.

1   2   3   4   5

approximately 10% of that seen in liver microsomes (data not shown). CYP3A1 mRNA was not detected in either rat cortical, rPT, or rDT cells (data not shown).

CYP2B expression. Western blot analysis of liver and kidney tissues using a polyclonal anti-rat CYP2B antibody, which recognizes both CYP2B1 and CYP2B2, revealed that CYP2B was expressed in both liver and kidney microsomes (Figure 10A), with the kidney expressing lower levels than the liver. A single band was observed in the blot of liver and renal microsomes and it is unclear if this represents CYP2B1, CYP2B2, or both. Treatment of rats with the peroxisomal proliferator clofibrate (0.2 g/kg per day; 3 days) induced the expression of CYP2B1/2 approximately 4-fold in both liver microsomes and kidney microsomes (Figure 10C). CYP2B1/2 expression was detected in rat renal cortical, rPT, and rDT microsomes (Figure 10B, arrow) as well, but clofibrate did not elevate CYP2B1/2 levels in these microsomes (data not shown). Rat renal cortical, rPT, and rDT microsomes from untreated rats expressed comparable levels of CYP2B1/2 (Figure 10B). An additional band with increased mobility was detected in both kidney microsomes and rPT and rDT microsomes using this antibody (Figure 10A and 10B). The identity of this band remains unknown.

Expression of CYP4A. Western blot analysis of liver and kidney microsomes from untreated rats resulted in the detection of CYP4A in both liver and kidney tissues (Figure 11A). Clofibrate treatment increased the expression of CYP4A in both tissues approximately 5-fold. Using the method of Okita et al. (1998), multiple bands were detected in liver, renal cortical, rPT, and rDT microsomes (Figure 11B). Multiple bands were also detected in kidney microsomes (data not shown). The migration of these bands in rat cortical, rPT, and rDT microsomes (Figure11B: lanes 1-6) was comparable to that observed in liver microsomes (Figure11B: lane 7). Okita et al. (1998), using rat liver microsomes from male Fisher F344, identified these bands as CYP4A2 (lower band) and CYP4A3 (top band). Expression of CYP4A2/3 appeared to be equal in untreated rat

Figure 10. Expression of CYP2B1/2 protein in rat liver and kidney.

A. Representative western blot using a polyclonal anti-rat CYP2B1 antibody, which recognizes both CYP2B1 and CYP2B2, showing expression of CYP2B1/2 in 5 μg of rat liver microsomes (lanes 1 and 2) and 30 mg of kidney microsomes (lanes 3 and 4). Lanes 1 and 3 are with microsomes from untreated rats and lanes 2 and 4 are with microsomes from clofibrate-treated rats. **B.** Representative western blot showing expression of CYP2B1/2 in 60 μg of rat cortical (lane 1), rPT (lane 2), and rDT (lane 3) microsomes. **C.** Densitometric analysis of CYP2B1/2 protein expression in untreated and treated liver and kidney microsomes. **D.** Densitometric analysis of CYP2B1/2 protein expression in untreated rat cortical, rPT, and rDT cells.
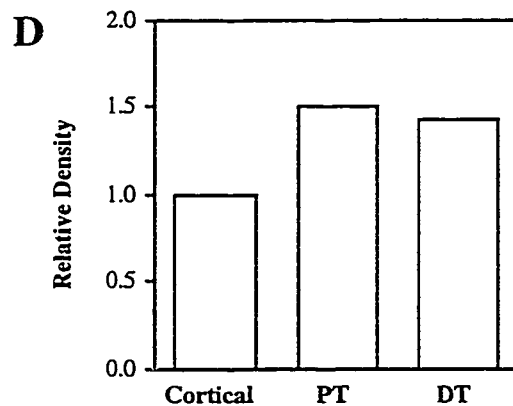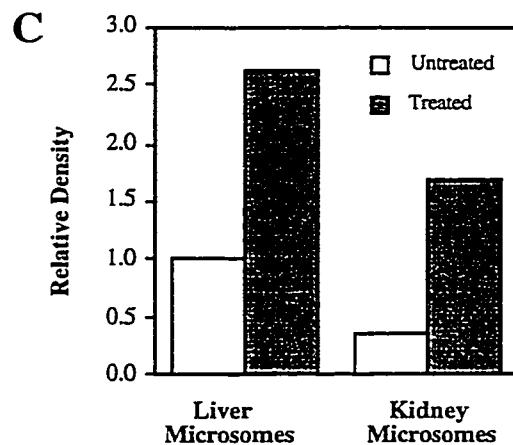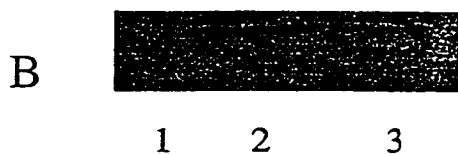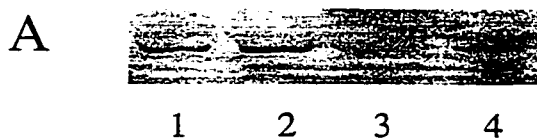
Figure 11. Expression of CYP4A2/3 protein and mRNA in rat liver and kidney.

A. Representative western blot using a polyclonal anti-rat CYP4A antibody showing expression of CYP4A2/3 in 5 μg of rat liver microsomes (lane 1 and 2) and 30 μg kidney microsomes (lane 3 and 4). Lanes 1 and 3 are from untreated rats and lanes 2 and 4 are from clofibrate-treated rats. **B.** Representative western blot showing expression of CYP4A2/3 in 60 μg of rat cortical (lanes 1 and 2), rPT (lanes 3 and 4), and rDT (lane 5 and 6) and 1 μg of liver (lane 7) microsomes. Lanes 2, 4, and 6 represent microsomes from clofibrate-treated animals whereas lanes 1, 3, 5, and 7 are from untreated animals. **C.** Densitometric analysis of CYP4A2/3 protein expression in untreated and treated rat cortical, rPT, and rDT microsomes. **D.** Northern blot analysis of CYP4A mRNA. Total RNA (10 μg/lane) was fractionated on a formaldehyde/agarose gel, transferred to a nylon membrane, probed with a cDNA complementary to rat CYP4A1 mRNA or mouse 7S RNA (loading standard) and autoradiographed.
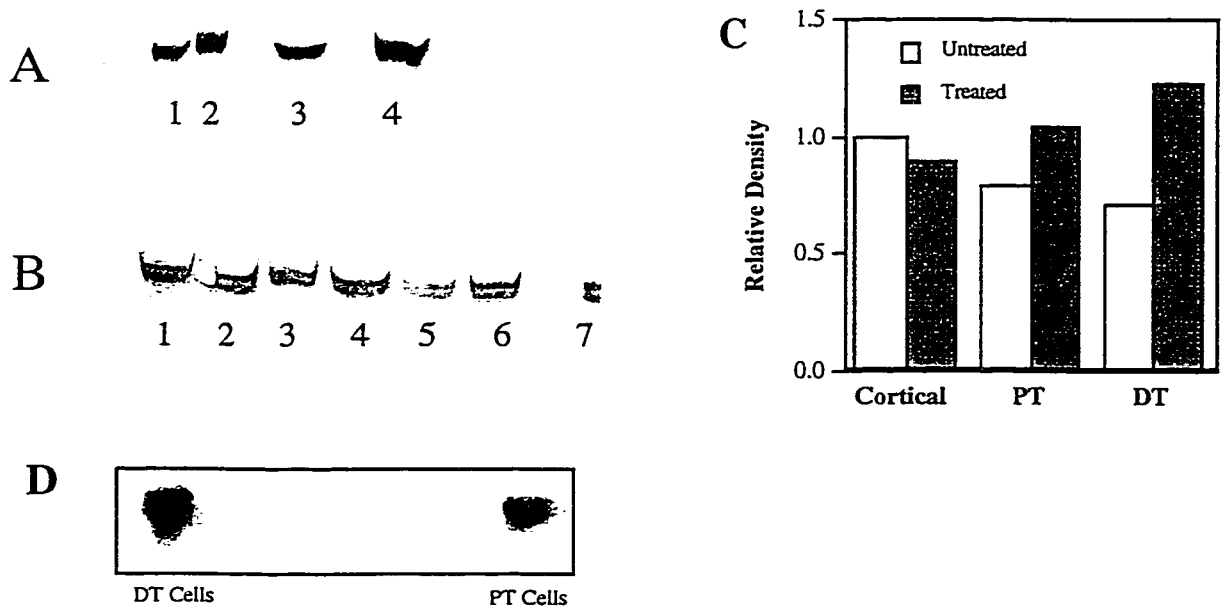
Table 8. Activity of CYP4A in liver and kidney cortical microsomes and in renal cells as measured by lauric acid hydroxylation. Activity of CYP4A was determined by analysis of the appearance of two metabolites of lauric acid (ω and ω-1) by HPLC. Results are the means $\pm$ SD of measurements from 3 separate preparations of microsomes or cells. For isolated cells, material from two animals was combined and was used for a single experiment. No significant differences ($P < 0.05$) were observed between rPT and rDT cells.

Sample	ω (nmol/min per mg protein)	ω-1
Liver microsomes	1.48 ± 0.24	0.29 ± 0.07
Kidney cortical microsomes	1.19 ± 0.01	0.23 ± 0.05
Cortical cells	1.14 ± 0.15	0.21 ± 0.07
Proximal tubular cells	0.79 ± 0.07	0.20 ± 0.02
Distal tubular cells	0.77 ± 0.08	0.18 ± 0.02

renal cortical and rPT microsomes, with slightly lower levels of CYP4A isoforms being expressed in untreated rDT microsomes (Figure 11B: lanes 1, 3, and 5). Treatment of rats with clofibrate resulted in a slight increase in expression of these bands in rPT microsomes (Figure11B: lane 4) and an even greater increase in rDT microsomes (Figure11B: lane 6), and no increase in rat renal cortical microsomes (Figure 11B: lane 2). Northern blot analysis of total RNA extracted from rPT and rDT cells isolated from untreated rats demonstrated that CYP4A mRNA levels were higher in rDT cells than in rPT cells (Figure 11D).

There was no significant difference in CYP4A activity between liver and kidney microsomes from untreated rats, as assessed by the hydroxylation of [^{14}C]lauric acid (Table 9). The rate of formation of ω-lauric acid in liver microsomes was 1.47 ± 0.23 nmol/min per mg protein and 1.19 ± 0.01 nmol/min per mg protein in kidney microsomes while the formation of the ω-1 metabolite was 0.29 ± 0.07 and 0.22 ± 0.5 in liver and kidney microsomes, respectively. Furthermore, there was no significant difference in lauric acid hydroxylation between rat cortical, rPT, and rDT cells.

Expression of GST isoforms. Western blot analysis of cytosol isolated from rat renal cortical, rPT, and rDT cells using polyclonal antibodies to human GSTα and rat GSTμ, and GSTπ revealed that GSTα was expressed in all cell types at very high levels (Fig. 12, Panel α, lanes 2-4). A small amount of GSTμ was detected in cortical and DT cells while no GSTπ was detected in any cell type (Fig. 6, Panels μ and π, respectively). All of these antibodies detected bands in rat liver cytosol (lane 1). The polyclonal GSTμ, and GSTπ antibodies did not cross-react with purified rat GSTα2-2. However, a strong band was detected when GSTα2-2 was cross-reacted with the polyclonal rat GSTα antibody (Fig. 12, Panels α, μ, and π; lane 2). Western blot analysis of rat liver and kidney cytosol using a rabbit anti-human antibody to GSTT did not result in detection of the GST isoform (data not shown).

Figure 12. Expression of GST isoforms in cytosol isolated from freshly isolated rat renal PT and DT cells.

Cytosol was isolated as described in **Materials and Methods** and approximately 50 µg of protein was subjected to SDS-PAGE, transferred to a nitrocellulose membrane, and exposed to polyclonal antibodies to human GSTA, or rat GSTµ and GSTπ. Lane 1: Cytosol from liver homogenates used as a positive control; Lane 2: Purified rat GSTα2-2 used as a positive and negative control; Lane 3: Cytosol isolated from freshly isolated rat renal cortical cells; Lane 4: Cytosol isolated from freshly isolated rat renal PT cells; Lane 5: cytosol isolated from freshly isolated rat renal DT cells.
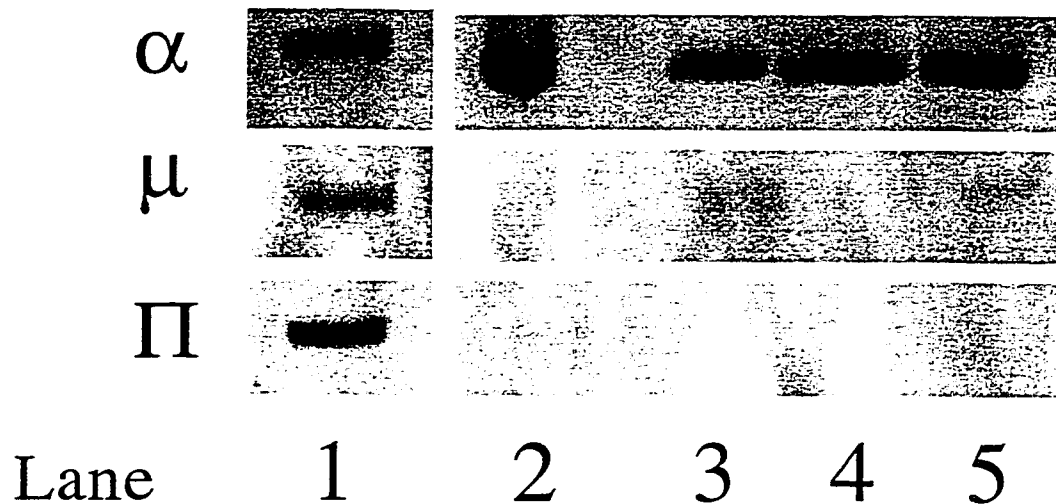
Discussion

A majority of studies characterizing the expression of P450 in the kidney have been done using microsomes prepared from whole tissue homogenates (Okita et al., 1998; Bebri et al., 1995). Much less work has been devoted to the determination of the distribution of renal P450 isoforms within specific cell types. Some studies have been done using immunohistochemistry on whole kidney slices (Bebri et al., 1995; Hotchkiss et al., 1995; Schuetz et al., 1992) or studying the expression of P450s in rPT cells only (Cui et al., 1991). Very little is known concerning the expression of P450 forms in rDT cells. This study demonstrates that several P450s are indeed expressed in both rPT and rDT cells, determines the distribution of these P450s, and studies the effect of clofibrate on the expression of CYP4A and CYP2B isoforms in these cells.

CYP2E1 was expressed in total kidney, cortical, rPT, and rDT microsomes with slightly higher amounts being measured in microsomes from rDT cells (Figure 7). Studies using immunohistochemistry have shown that CYP2E1 is expressed in rPT and rDT cells in Sprague Dawley and Fischer 344 rats (Hotchkiss et al., 1995; Ronis et al., 1998) but the differences in expression between these two cell types were not quantified. Data from this study confirm the above results. This slightly greater expression may play a role in the rDT cell selective toxicity seen with certain nephrotoxicants (Lash and Tokarz, 1995; Lash et al., 1994). Caution should be taken when comparing toxicity and metabolism studies of CYP2E1 substrates between the rat and human because recent work with tissue from 18 patients reported that CYP2E1 was not detected in human kidney microsomes (Amet et al., 1997a).

The difference in the renal cellular pattern of chlorzoxazone hydroxylase activity and levels of CYP2E1 protein and mRNA expression in rPT and rDT microsomes suggests that CYP2E1 is not the only P450 form responsible for chlorzoxazone hydroxylase activities in these cells. Rather, recent reports on the selectivity of chlorzoxazone hydroxylation as a marker for CYP2E1 activity showed that both CYP3A isoforms (Gorski et al., 1997;

Jayyosi et al. 1995) and CYP1A1 (Jayyosi et al., 1995; Yamazaki et al., 1995) can catalyze this activity. The possibility that enzymes other than CYP2E1 can metabolize chlorzoxazone in rPT and rDT microsomes is supported by the inability of chlorzoxazone to fully inhibit p-nitrophenol hydroxylation in rPT and rDT cells (data not shown). It should be noted that the levels of chlorzoxazone hydroxylation reported in this study are within the range reported previously for rat kidney microsomes (Amet et al., 1997b). However, Amet et al. (1997b) did not specifically measure chlorzoxazone hydroxylation in rPT and rDT cells. A role for both CYP2E1 and CYP3A in the hydroxylation of p-nitrophenol has also been suggested (Zerilli et al., 1997, 1998).

Both kidney microsomes and cortical and rPT microsomes expressed CYP2C11 (Figure 8), while expression was undetectable in rDT microsomes. Renal CYP2C11 functions in the metabolism of both exogenous chemicals, such as thiophene or cephaloridine, and endogenous chemicals, such as testosterone. Activity of CYP2C11 (as measured by the 2α-hydroxylation of testosterone) corresponded to the expression of CYP2C11 in rPT and rDT microsomes (data not shown). Thus, it is possible that the metabolism of cephaloridine and 4-(2-thienyl)butyric acid by CYP2C11 is responsible for the cell-type selective toxicity demonstrated by these chemicals (Lash and Tokarz, 1995; Lash et al., 1994). The role of CYP2C11 in the metabolism of testosterone or other endogenous substrates in the kidney has not been studied extensively. Other studies (Sundseth and Waxman, 1992), however failed to detect CYP2C11 mRNA in the kidney of male Fischer 344 rats.

Testosterone is also metabolized by CYP3A isoforms to 6β-hydroxytestosterone (Waxman et al., 1987). The expression of isoforms of CYP3A in the kidney has been studied extensively and investigators have found that rat CYP3A1, CYP3A2, and human CYP3A5 are expressed in kidney microsomes (Bebri et al., 1995; Schuetz et al., 1992). Data from this study showed the presence of CYP3A1/2 in both liver and kidney microsomes but not in cortical, rPT, or rDT microsomes. Thus, it is likely that CYP3A1 and

CYP3A2 are expressed in other areas of the kidney such as the glomeruli. Formation of 6β-hydroxytestosterone was also demonstrated in incubations with liver and kidney microsomes and analysis by HPLC (data not shown). It is possible that other isoforms of CYP3A are expressed in either rPT or rDT cells, and the possible presence and identity of these are currently under investigation.

CYP2B1/2 was detected in liver and kidney microsomes, and low levels of expression were detected in cortical, rPT, and rDT microsomes (Figure 10A and B). CYP2B isoforms hydroxylate testosterone primarily at the 16α and 16β positions. CYP2B1/2 was induced by clofibrate in both liver and kidney microsomes but not in cortical, rPT, or rDT microsomes. Possible reasons for these differences are difficult to determine because of uncertainties about the mechanism of CYP2B induction in general. Clofibrate or similar compounds have been reported to increase rat hepatic CYP2B (Kocarek et al., 1993; Sundseth and Waxman, 1992; Zangar et al., 1995) but no data could be found examining the effect of these compounds on renal CYP2B. Sundseth and Waxman (1992) found a 13-fold increase in male rat hepatic CYP2B1/2 mRNA after 3 days of treatment with 40 mg of clofibrate/0.2 ml of corn oil per 100 g of body weight, but expression of renal CYP2B1/2 was not examined. Data from the present study demonstrated that CYP2B1/2 protein levels were increased in both liver and kidney microsomes as a result of clofibrate treatment. Furthermore, clofibrate-mediated increases in rat renal CYP2B1/2 appeared to be specific to other renal cell types besides those studied, as increases in CYP2B1/2 levels were not detected in microsomes from either cortical, rPT, or rDT cells.

CYP4A isoforms have been previously reported to be expressed in rPT cells (Carroll et al., 1990; Escalante et al., 1989; Ito et al., 1998; Makita et al., 1996; Romero et al., 1991). Ito et al. (1998) showed significant expression of CYP4A2 and CYP4A3 mRNA in all nephron segments tested, including the glomerulus, proximal convoluted and straight tubules, medullary and cortical thick ascending limbs, cortical collecting duct, and inner and

outer medullary collecting ducts but only found small, but detectable levels of CYP4A8 mRNA in cortical but not in medullary nephron segments. In contrast, Sundseth and Waxman (1992) and Okita et al. (1998) reported that neither CYP4A1 mRNA nor CYP4A1 protein were expressed in male Fischer 344 rat kidneys, although Ito et al. (1998) found CYP4A1 mRNA in total kidney homogenates, but not in single nephron segments of Sprague-Dawley rats. Both Sundseth and Waxman (1992) and Okita et al. (1998) identified CYP4A2 and CYP4A3 protein in kidney microsomes from male Fischer 344 rats, with CYP4A2 being present in higher amounts. Ito et al. (1998), using a polyclonal antibody raised against CYP4A1, but that cross-reacts with CYP4A1, CYP4A2, and CYP4A3, found strong expression of CYP4A proteins in glomerular, rPT, and medullary thick ascending limb segments. Using the same antibody and methods used by Okita et al. (1998), we were able to detect multiple bands in all tissues tested. Based on the above studies, it appears that the lower band in Figure 11B is CYP4A2 and the higher band is CYP4A3. CYP4A2 and CYP4A3 proteins were expressed equally in both rPT and rDT microsomes (Figure 11). Thus, although Ito et al. (1998) described the distribution of CYP4A mRNAs and proteins in many, but not all, nephron segments, this is the first time that expression of CYP4A2/3 has been shown in rat renal DT cells.

Similar to the results on clofibrate induction of renal CYP2B1/2, clofibrate induction of renal CYP4A2/3 expression did not occur in all cell types tested. Significant increases in CYP4A2/3 were detected only in rDT cells, suggesting that clofibrate induction of CYP4A isoforms in the kidney is cell type-specific. CYP4A2/3 expression correlated well with the activity of lauric acid hydroxylation in these tissues (Table 2). The level of ω- and ω-1 lauric acid hydroxylation in rat kidney microsomes agreed with that reported previously (Amet et al., 1997b; Ronis et al., 1998). The activity of CYP4A in rat renal microsomes, as measured by lauric acid hydroxylation, reported here is within the range of values reported in human kidney microsomes (Amet et al., 1997a), suggesting that the rat may serve as a valid model for the study of CYP4A-dependent substrate metabolism in humans. The

distribution of CYP4A isoforms between human renal PT and DT cells has not been studied.

The role of CYP4A in the kidney has been studied extensively and a role for this P450 family in the arachidonic acid cascade has been cited previously. A potential role for CYP4A in the subsequent metabolism of reaction products of other P450 isoenzymes has also been suggested. For example, certain metabolites of Tri may be substrates for CYP4A (Hanioka et al., 1997), and a role for CYP4A in the genesis of Tri-induced nephrotoxicity has been proposed (Davidson and Beliles, 1991). Thus, a role for renal CYP4A isoforms in the metabolism of both physiological and toxicological substrates should be considered.

In conclusion, this study showed that there are differences in the expression of P450 isoforms between two renal cell populations. CYP2E1, CYP2C11, and CYP2B1/2 were expressed at low levels in the rat kidney relative to rat liver, while CYP4A2/3 was expressed at comparable levels in the two tissues. CYP2E1 was expressed at slightly higher levels in rDT microsomes than in rPT microsomes while CYP2C11 expression was highest in rPT microsomes. CYP2B1/2 was expressed in comparable amounts in rPT and rDT cells and CYP3A1 was not detected in either cell type. CYP4A2/3 expression was detected in cortical, rPT and rDT microsomes. Both renal CYP2B1/2 and CYP4A2/3 expression were increased by clofibrate treatment, but these increases were not observed in all renal cell types tested. The significance of these results in terms of both the nephrotoxicity of several chemicals and renal physiology warrants further investigation.

Chapter 5

Toxicity and Metabolism of Tri in Freshly Isolated rPT and rDT cells

Introduction

As mentioned in Chapter 1, Tri is common ground water pollutant and is used extensively in industry as a metal degreasing and dry-cleaning agent. Tri, like thiophenes, is also metabolized by P450 isoforms. Tri is also metabolized by GST isoforms. The human health hazard of Tri toxicity, using the kidney as a target organ, has been subject to some controversy, mostly because the flux of Tri through the GSH conjugation pathway is thought to represent only a small fraction of Tri metabolism (Davidson and Beliles, 1991). However, humans form DCVG at detectable levels after exposure to small doses of Tri (Lash et al., 1999). Furthermore, recent reports (Brüning et al., 1998) of cases involving acute Tri poisoning demonstrated that the products of the GSH-conjugation pathway can be formed in humans. Finally, the metabolites generated from Tri by the P450 pathway (CH, DCA, TCA, and TCOH) are chemically relatively stable. In contrast, metabolites generated from Tri by GSH conjugation and subsequent reactions are chemically unstable and thus, difficult to measure accurately (Anders et al., 1988). It is also possible that small amounts of these unstable metabolites may produce a high degree of toxicity.

To better understand the role of both GSH conjugation and P450 oxidation in Tri toxicity and metabolism, the differences in Tri toxicity and metabolism, in freshly isolated rPT and rDT cells, were studied.

Results

Cytotoxicity of Tri in freshly isolated rPT and rDT cells. Freshly isolated rPT and rDT cells were incubated in the presence of 0 to 10 mM Tri or solvent control (acetone < 1.0% (v/v) for 0, 1, or 2 hr (Figure 13). Toxicity was measured as % LDH release from the cells compared with the total LDH activity within the cells. Tri did not inhibit LDH

activity in either cell type (data not shown). Tri was modestly cytotoxic to rPT and rDT cells only at the highest concentration tested, causing approximately 20% increases in LDH release.

Preincubation of rPT and rDT cells with metyrapone (0.25 mM), a general P450 inhibitor, increased Tri cytotoxicity in rDT cells only (Figure 14). The same results were seen when 0.25 mM SKF-525A, another general P450 inhibitor, was used instead of metyrapone (data not shown). These data indicate that the cytotoxicity of Tri in rPT and rDT cells is influenced by the expression of P450 isoforms within these cells.

Metabolism of Tri to DCVG in freshly isolated rPT and rDT Cells. Tri (10 mM) conjugation to GSH was measured in freshly isolated rPT and rDT cells by measuring the formation of DCVG by HPLC analysis. In the absence of P450 inhibition, DCVG formation was detected only in rPT cells at approximately 1-2 nmol/min per mg protein (Figure 15). DCVG formation in rPT cells was approximately linear throughout 60 min of incubation. Preincubation of cells with SKF-525A resulted in significant increases in DCVG formation in both rPT and rDT cells. Inhibition of P450 in DT cells resulted in DCVG formation at levels comparable to those of rPT cells. DCVG formation decreased significantly after 60 min of incubation in the presence of P450 inhibitors. Data from Chapter 4 showed that rDT cells express slightly higher levels of CYP2E1 than rPT cells. Preincubation of both cell types with chlorzoxazone, a competitive substrate for CYP2E1, significantly increased DCVG formation in both rPT and rDT cells. These increases were measured only after 30 min and DCVG content decreased to control levels by 60 min. Larger increases were measured in rDT cells than in rPT cells. This increased DCVG formation in rDT cells, compared with rPT cells, correlates with the levels of expression of CYP2E1 in these cells. Furthermore, the increase in DCVG formation in rDT cells after P450 inhibition with SKF-525A correlated with the increases in Tri cytotoxicity in rDT cells after P450 inhibition.

Figure 13. Cytotoxicity of Tri in freshly isolated rPT and rDT cells.

Freshly isolated rPT (**A**) and rDT (**B**) cells (5 to 10 x 10^6 cells/mL) were incubated with the indicated concentrations of Tri for 0, 1, and 2 hr and the percent LDH release was determined at each time point. Results are the means ± SD of at least 3 experiments. *Significant difference ($P < 0.05$) from control values.

A. PT Cells
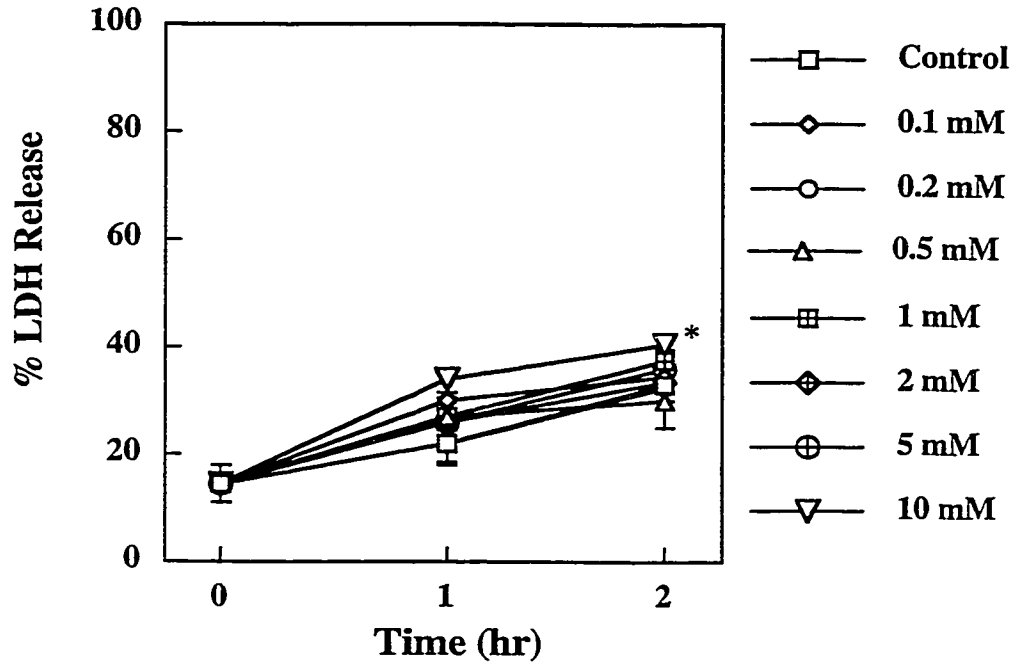
B. DT Cells
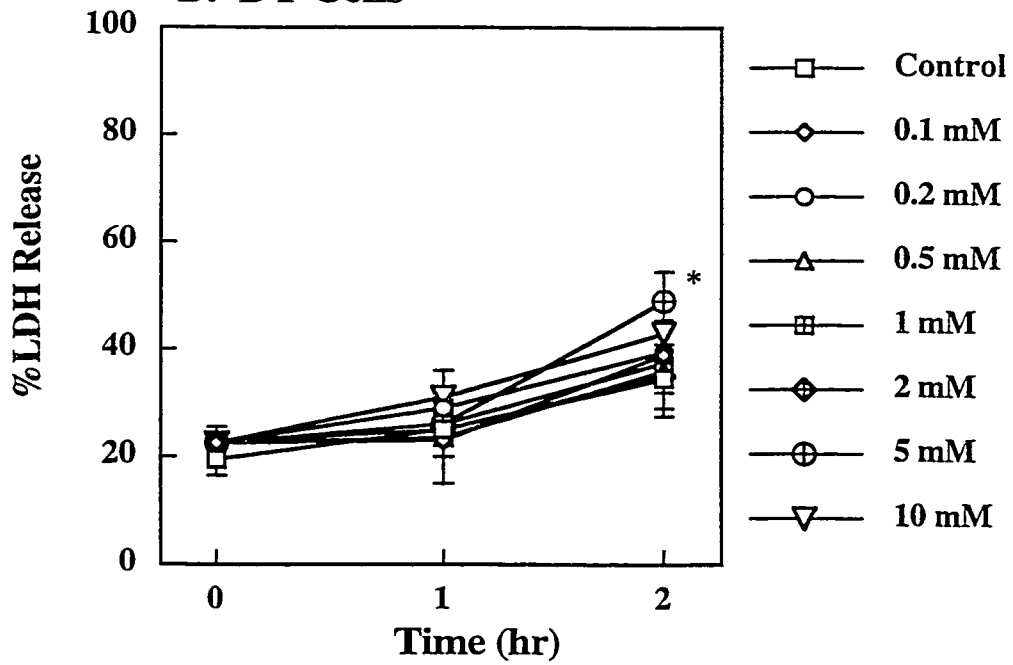
Figure 14. Effect of P450 inhibition on the cytotoxicity of Tri in freshly isolated rPT and rDT cells.

Freshly isolated rPT (A) and rDT (B) cells (0.5. to 10 x 10^6 cells/mL) were preincubated in the presence of either solvent control (i.e., 1.0%, v/v, acetone) or metyrapone (1 mM) for 15 min prior to the addition of Tri. At the indicated time points, the percent LDH release was determined. Results are the means $\pm$ SD of at least 3 experiments. *Significant difference ($P < 0.05$) from control. †Significant difference ($P < 0.05$) from same concentration without inhibitor.
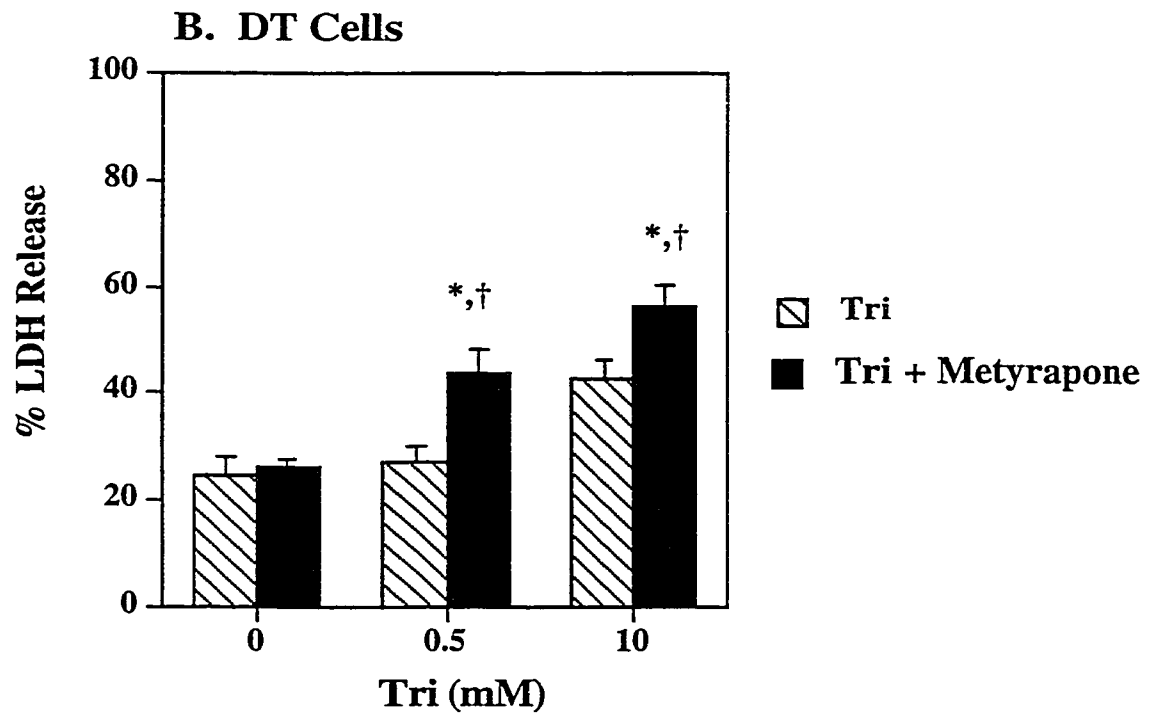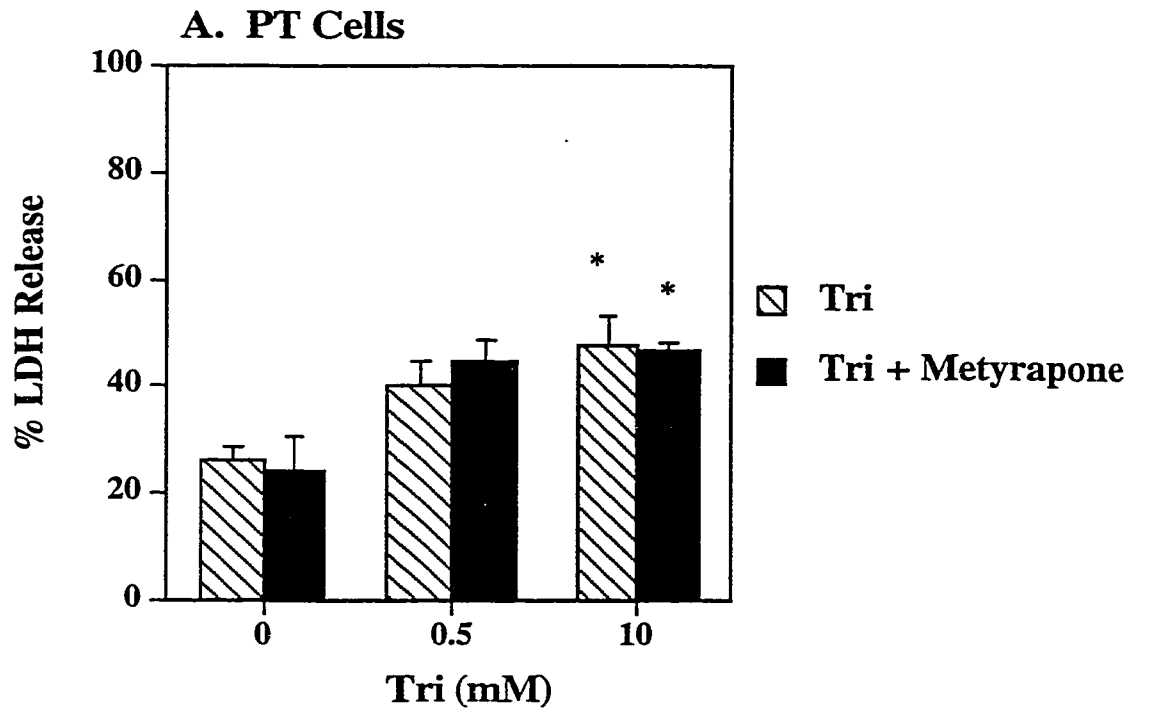
A. PT Cells

B. DT Cells

Figure 15. Metabolism of Tri to DCVG in freshly isolated rPT and rDT cells.

rPT (A) and rDT (B) cells (0.5 to 2 mg of protein/mL) were lysed with Triton (0.1% v/v), preincubated with either solvent control (i.e., 1.0%,v/v, acetone), SKF-525A (0.25 mM) or chlorzoxazone (1 mM) for 15 min prior to addition of 10 mM Tri in the presence of 5 mM GSH at 37°C for either 30 or 60 min. Metabolism was measured by quantitation of DCVG formation by HPLC after derivatization. Controls included the absence of Tri. Results are the means $\pm$ SD of at least 3 experiments. *Significant difference ($P < 0.05$) from cell not pretreated with inhibitor at the same time point.

A. PT Cells
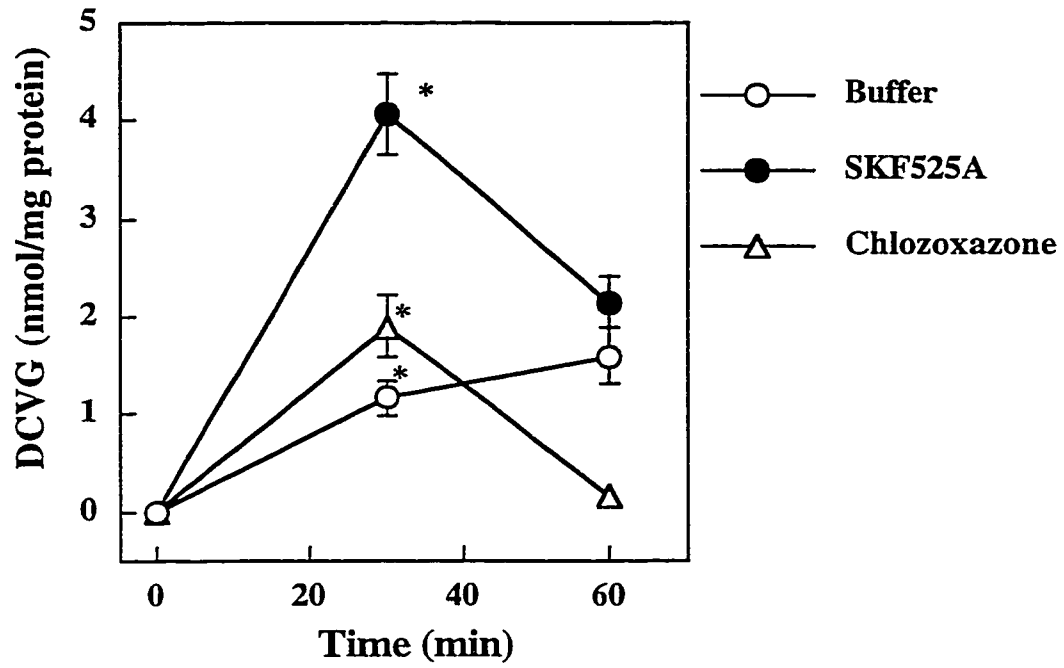
B. DT Cells
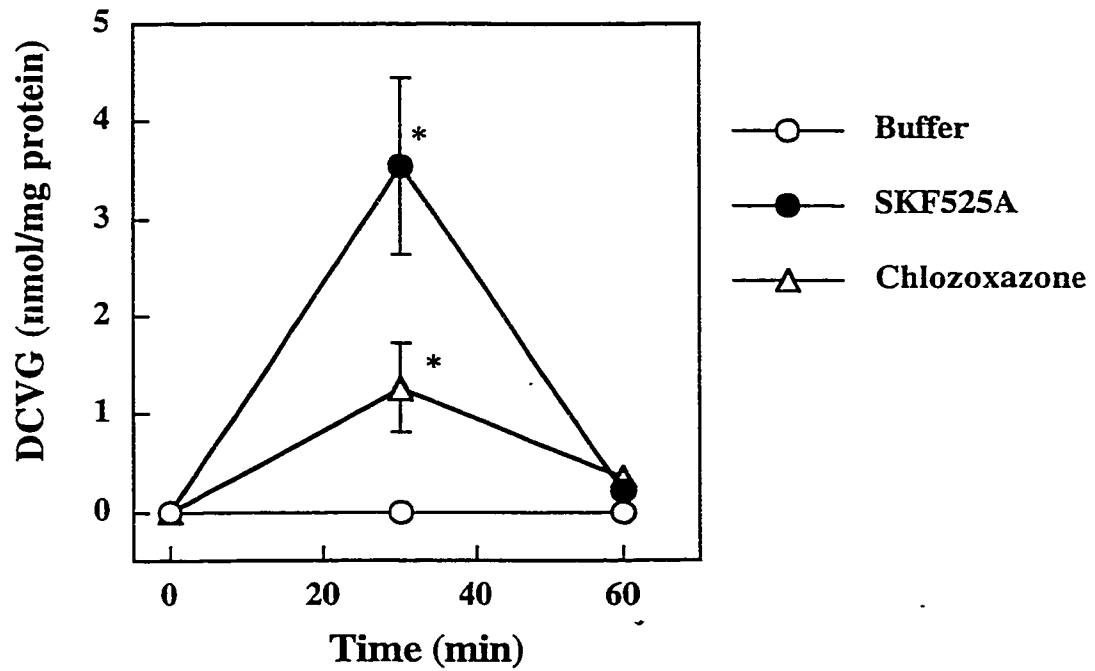
Kinetics of Tri metabolism to DCVG in freshly isolated rPT cells. The kinetics of Tri conjugation to GSH to form DCVG were determined in freshly isolated rPT cells (Figure 16). DCVG formation was detected with all concentrations of Tri used in rPT cells. DCVG formation was only detected in rDT cells at the highest concentrations used (15 and 20 mM), making analysis of kinetics of DCVG formation in these cells impossible. Lineweaver-Burke analysis of DCVG formation in rPT cells resulted in a single line (Figure 16A). In contrast, Eadie-Scatchard (or Eadie-Hofstee) analysis of DCVG formation in rPT cells resulted in a two-component model that yielded a high-affinity, low-capacity and a low-affinity, high-capacity process (Figure 16B). Kinetic parameters derived from these two analyses are summarized in Table 9. Higher concentrations of Tri (> 15 mM) significantly decreased DCVG levels (Figure 16C).

Metabolism of Tri by individual GSTα isoforms. As shown in Chapter 4, freshly isolated rPT and rDT cells both express high amounts of GSTα. The class of rat GSTα isoforms is made up of multiple members and GSTα1 and GSTα2 were chosen for study as they are two of the best characterized isoforms and were readily available commercially. These members can form homo- and heterodimers with each other, resulting in three isoforms, GSTα1-1, GSTα1-2, and GSTα2-2, and the ability of these isoforms to catalyze GSH conjugation of Tri in vitro was determined. Kinetic analysis of GSH conjugation of Tri by purified GSTα isoforms revealed that all three isoforms were active, although no DCVG formation was detected at 0.1 and 0.2 mM Tri with GSTα1-1. Lineweaver-Burke analysis (Figure 17 and Table 10) of these data yielded three different K_m values. GSTα1-2 had the highest K_m and V_{max} (7.51 mM and 1.5 nmol/min per mg protein, respectively) and GSTα2-2 had a 30- to 50-fold lower K_m (0.074 mM). In contrast, the K_m for GSTα1-1 (3.99 mM) was between GSTα1-2 and GSTα2-2.

Data on the time-dependence of DCVG formation catalyzed by these three isoforms revealed that DCVG formation was linear 10 to 20 min with 10 mM Tri. After

Figure 16. Kinetic analysis of GSH conjugation of Tri in freshly isolated rPT cells.

Freshly isolated rPT cells (0.5 to 2 mg of protein/mL) were lysed with Triton (0.1% v/v) and incubated in the presence of 0-20 mM Tri and 5 mM GSH at 37°C for 30 min. Metabolism was measured by quantitation of DCVG formation by HPLC after derivatization. Controls included the absence of Tri. Results were analyzed by Lineweaver-Burke (A) Eadie-Scatchard (B) or Michalis-Menten analysis. Results are the means ± SD of at least 3 experiments. Apparent K_m and V_{max} values are given in Table 9.

A. Lineweaver-Burke Analysis
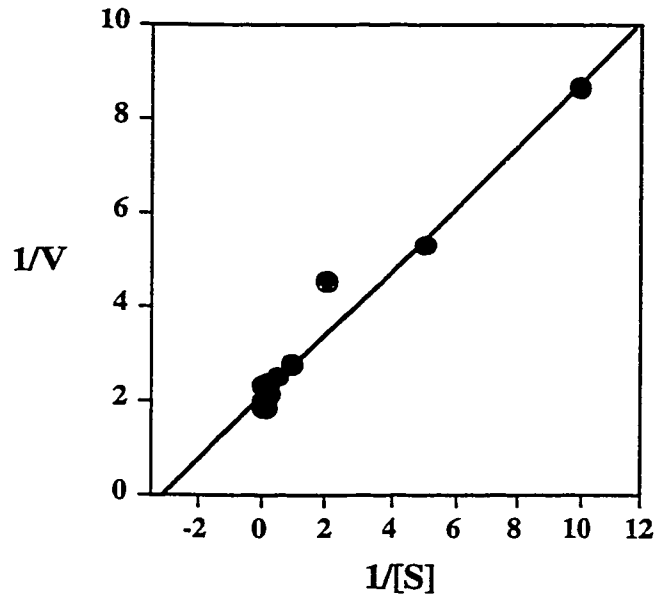
B. Eadie-Scatchard Analysis
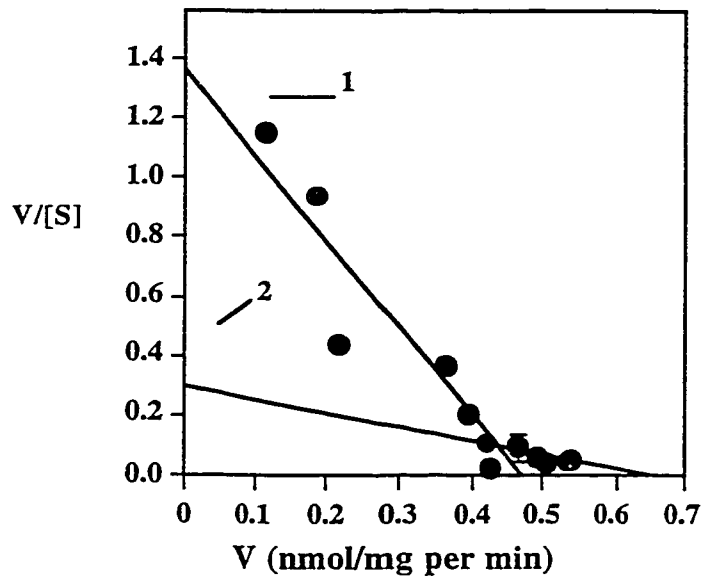
C. Michaelis-Menten Analysis
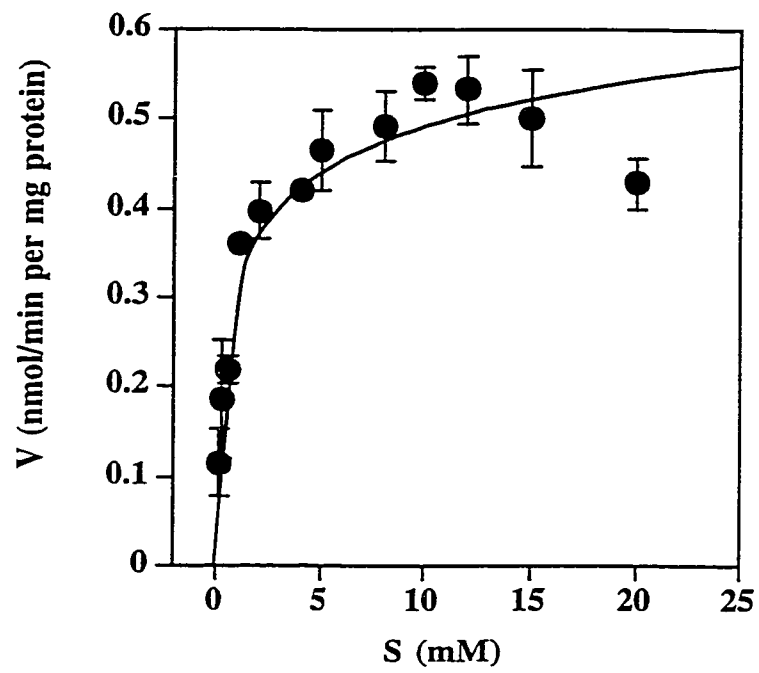
Table 9. Kinetics of Tri metabolism to DCVG in freshly isolated rPT cells.

Freshly isolated rPT cells were incubated in the presence of acivicin (0.25 mM) for 15 min to inhibit GGT. Tri (0.1-20 mM) and GSH (5 mM) were then added and reactions were allowed to proceed for 30 min. The reactions were stopped by addition of 100 μL of 70% (v/v) perchloric acid followed by 50 μL of bathophenanthroline disulfonate. Samples were then derivatized with 1-fluoro-2,4-dinitrobenzene and injected onto a Waters 10 μm μBondapak C18 amine column (8 mm X 100 mm) and were separated by a methanol-acetate mobile phase and gradient elution at 365 nm. Kinetic parameters were derived from linear transformations shown in Figure 16.

Method	K_m-1 (mM)	K_m-2 (mM)	V_{max}-1 (nmol/min per mg protein)	V_{max}-2 (nmol/min per mg protein)
Lineweaver-Burke	0.31	—	0.47	—
Eadie-Scatchard	0.46	2.91	0.47	0.65

Figure 17. Kinetic analysis of GSH conjugation of Tri to form DCVG by purified rat GSTα isoforms.

Purified rat GSTα1-1 (A), GSTα1-2 (B), or GSTα2-2 (C) (2-9 μg per preparation) were incubated with 0-10 mM Tri in the presence of 5 mM GSH for 10 min at 30°C. Metabolism was measured by quantitation of DCVG formation by HPLC after derivatization. Controls included the absence of enzyme, Tri, or GSH. Results were analyzed by Lineweaver-Burke analysis. Results are the means ± SD of at least 3 experiments. The K_m and V_{max} values for each GST isoform are given in Table 10.

A. GSTα1-1

B. GSTα1-2
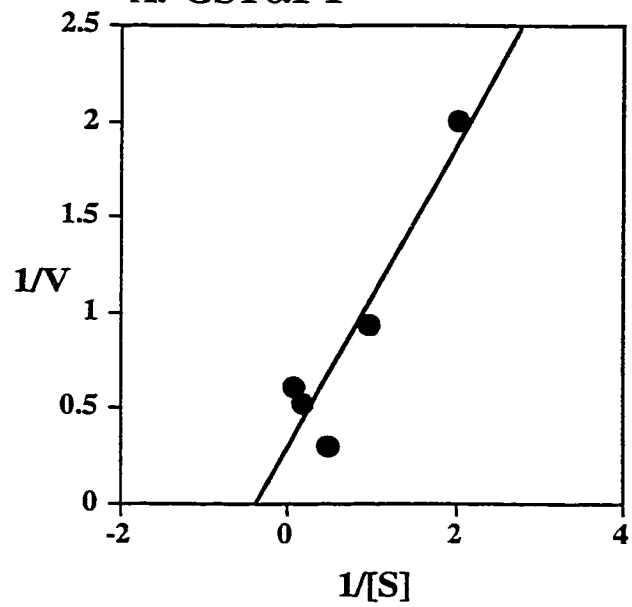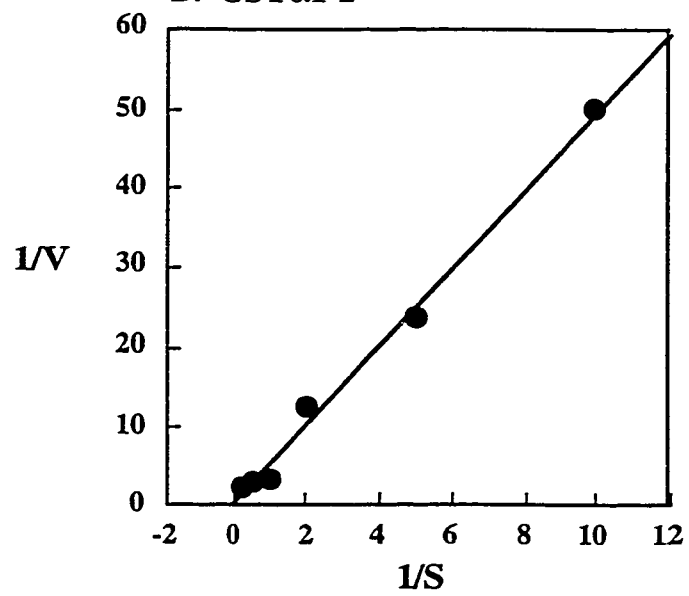
C. GSTα2-2
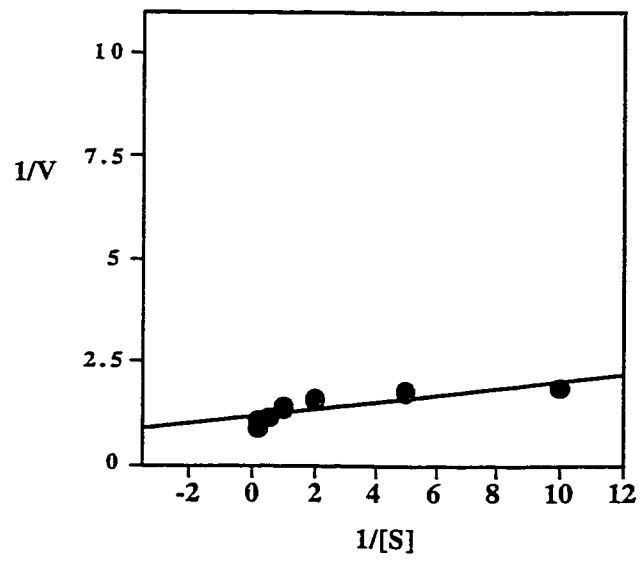
this time, DCVG formation significantly decreased (Figure 18). Thus, while all GSTα isoforms are capable of catalyzing GSH conjugation of Tri, GSTα2-2 had the highest affinity for Tri.

Inhibition of GSH conjugation of Tri by GSTα inhibitors. The ability of the GSTα inhibitors TETB and BSP to inhibit GSH conjugation of Tri by both purified rat GSTα isoforms and cytosol from rPT and rDT cells was tested. TETB and BSP are non-competitive inhibitors of CDNB metabolism by GSTα1-1 and GSTα2-2, respectively, with IC_{50} values of 3 and 2 μM, respectively (Mannervik, 1985). No studies could be found discussing the ability of these compounds to inhibit GSH conjugation of Tri by any enzyme or in any tissue. GSH conjugation of 1 mM Tri by rat GSTα1-1 was significantly inhibited by TETB (9 μM) but not by BSP (4 μM) (Figure 19). DCVG formation catalyzed by rat GSTα2-2 was significantly inhibited by both TETB (9 μM) and BSP (4 μM), with BSP causing more inhibition. Neither TETB nor BSP were able to inhibit the ability of GSTα1-2 to conjugate to catalyze GSH conjugation of Tri. It should be noted that both TETB and BSP can inhibit CDNB metabolism by GSTα1-2 if the concentration of each is raised (IC_{50} values of 100 and 10 μM, respectively (Mannervik, 1985). The concentrations of both TETB and BSP were kept below those needed to inhibit rat GSTα1-2 in order to better elucidate the effects of these inhibitors on the individual rat GSTα isoforms. Thus, as expected based on its ability to inhibit CDNB metabolism, TETB inhibited GSH conjugation of Tri by rat GSTα1-1. Rather surprisingly, both TETB and BSP inhibited GSH conjugation of Tri by rat GSTα2-2.

Inhibition of GSH conjugation of Tri in rPT and rDT cytosol. Data from the above study were used to test the ability of TETB and BSP to inhibit GSH conjugation of Tri in cytosol isolated from rPT and rDT cells. Cytosol was used instead of cells in order to study Tri metabolism in the absence of P450 isoforms. DCVG formation was measured in both rPT and rDT cytosol, and both TETB and BSP inhibited DCVG formation in rPT cytosol at high levels of Tri (10 mM) (Figure 20A). TETB and BSP were unable to inhibit

Figure 18. Time dependence of GSH conjugation by purified rat GSTα isoforms.

Purified rat GSTα1-1, GSTα1-2, or GSTα2-2 (2-9 μg per preparation) were incubated with 10 mM Tri in the presence of 5 mM GSH for the indicated times at 30°C. Metabolism was measured by quantitation of DCVG formation by HPLC after derivatization. Controls included the absence of enzyme, Tri, or GSH. Results are the means ± SD of at least 3 experiments. *Significant ($P < 0.05$) difference from DCVG levels at 10 min.
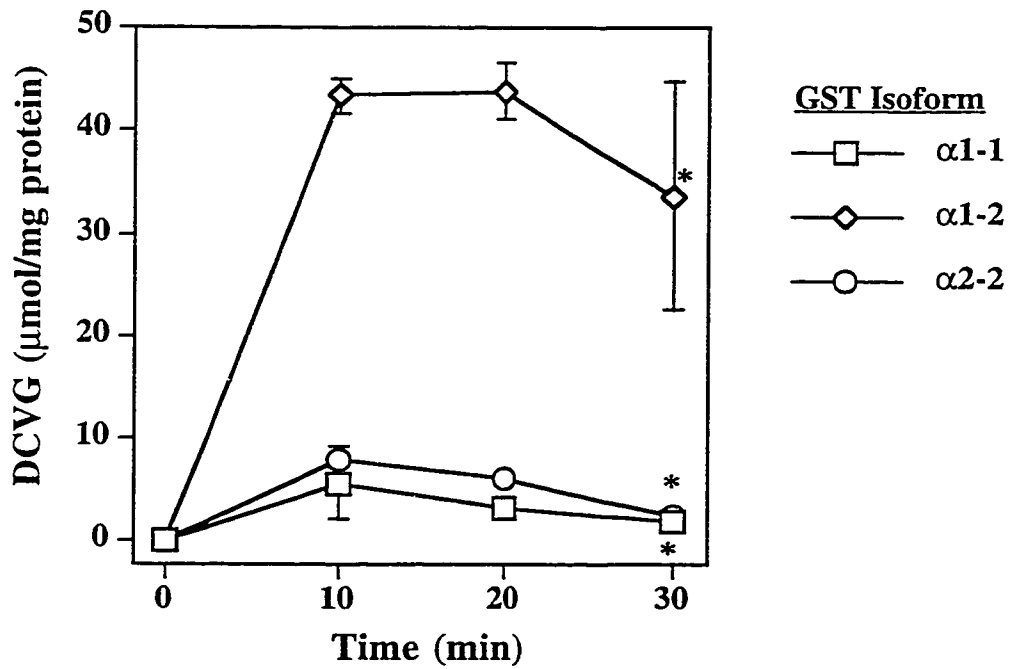
Table 10. Kinetics of Tri metabolism to DCVG by purified rat GSTα.

Purified enzyme plus Tri and GSH (5 mM) were mixed and reactions were allowed to proceed for 10 min. The reactions were stopped by addition of 100 μL of 70% (v/v) perchloric acid followed by 50 μL of bathophenanthroline disulfonate. Samples were then derivatized with 1-fluoro-2,4-dinitrobenzene and injected onto a Waters 10 μm μBondapak amine column (8 mm X 100 mm) and were separated by a methanol-acetate mobile phase and gradient elution at 365 nm. Kinetic parameters were derived from linear transformations shown in Figure 17.

Isoform	K_m (mM)	V_{max} (μmol/min per mg protein)
GSTα1-1	3.99	0.75
GSTα1-2	7.51	1.50
GSTα2-2	0.074	0.87

Figure 19. Effect of GSTα inhibitors on GSH conjugation of Tri to form DCVG by rat GSTα isoforms.

Purified rat GSTα1-1, GSTα1-2, or GSTα2-2 (2-9 µg per preparation) were preincubated for 15 min with the indicated inhibitor (TETB = 9 µM, BSP = 4 µM). Tri (1 mM) and 5 mM GSH were then added and the reaction was allowed to proceed for 10 min at 30°C. Metabolism was measured by quantitation of DCVG formation by HPLC after derivatization. Controls included the absence of enzyme, Tri, or GSH. Results are the means ± SD of at least 3 experiments. *Significant ($P < 0.05$) difference from enzyme with Tri alone.
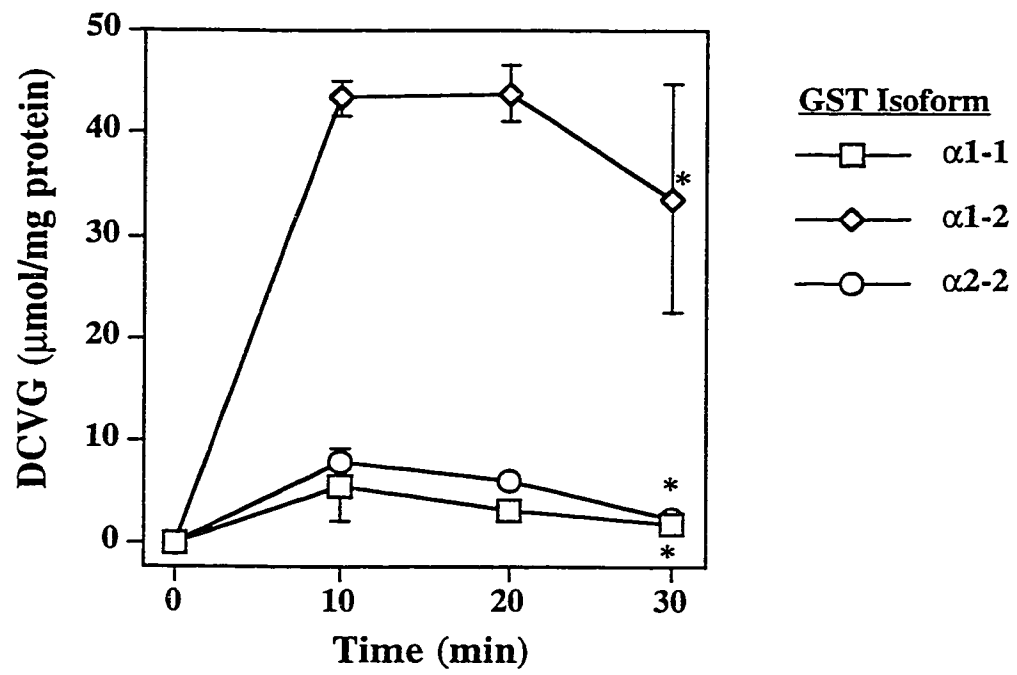
Figure 20. Effect of GSTα inhibitors on GSH conjugation of Tri by cytosol isolated from rPT (A) and rDT (B) cells.

Cytosol (5-10 mg/mL) isolated from freshly isolated rPT and rDT cells were preincubated for 15 min with the indicated inhibitor (TETB = 9 µM, BSP = 4 µM). Tri (0, 0.1, 1.0, or 10 mM) and 5 mM GSH were then added and the reaction was allowed to proceed for 30 min at 30°C. Metabolism was measured by quantitation of DCVG formation by HPLC after derivatization. Results are the means ± SD of at least 3 experiments. *Significant ($P <$ 0.05) difference from cytosol incubated with Tri alone.

A. PT Cytosol
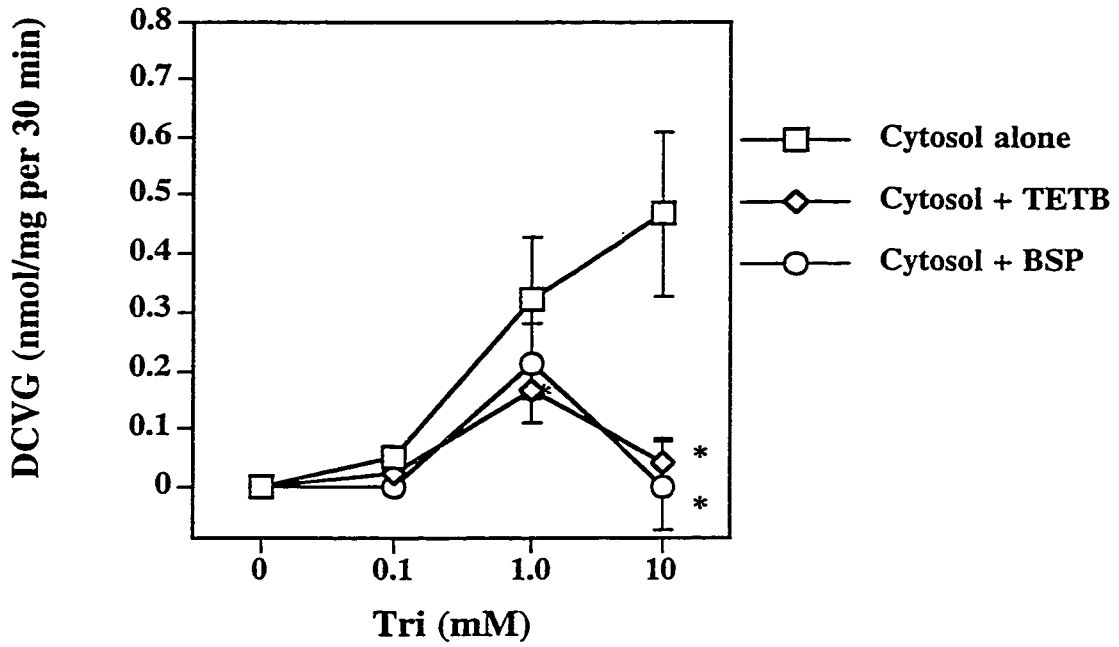
B. DT Cytosol
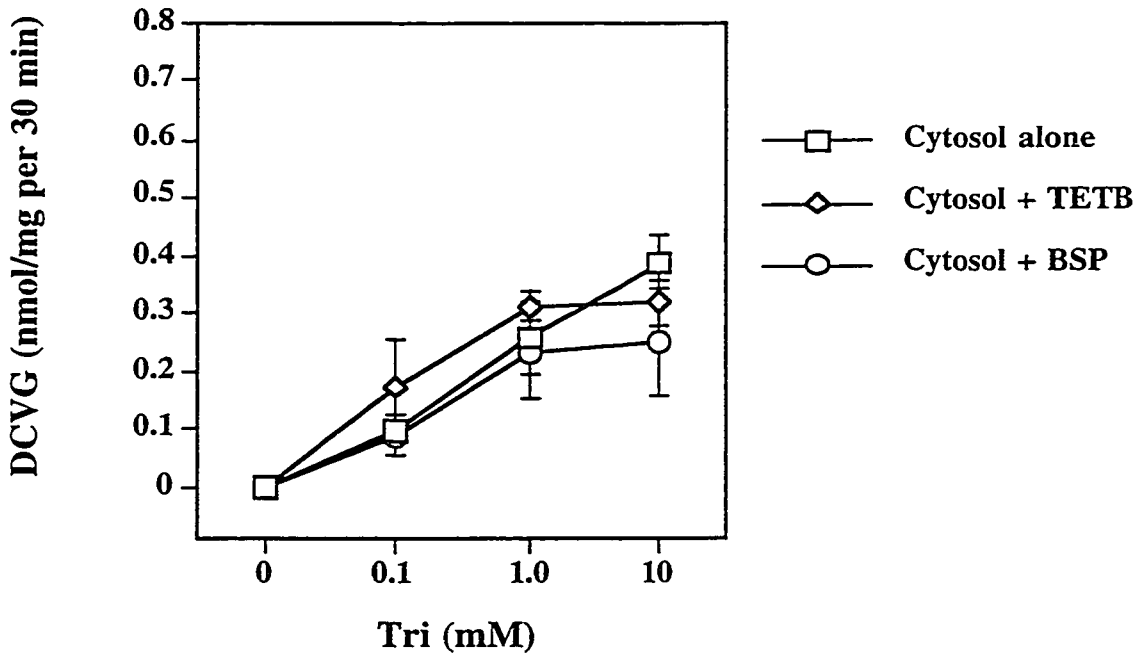
DCVG formation in cytosol isolated from rat renal DT cells at any concentration of Tri tested (Figure 20B). It was hypothesized that the ability of BSP and TETB to inhibit GSH conjugation to Tri in rPT cytosol, but not rDT cytosol, was perhaps a result of the lack of GSTα2-2 in rDT cells. To test this hypothesis the expression of GSTα2-2 in both rPT and rDT cytosol was tested by western blot analysis using a polyclonal rabbit-anti human antibody. GSTα2 has a higher molecular weight than GSTα1 (Armstrong, 1997) and thus had a reduced mobility on a 10% SDS-PAGE compared with GSTα1 (Figure 21A). Western blot analysis of rat kidney cytosol and cytosol isolated from rPT and rDT cells using a polyclonal rabbit anti-human GSTα1 antibody showed that all tissues tested expressed GSTα1 (Figure 21B). An additional faint band with higher mobility than the main band was also detected. These molecular weights of these bands correspond to GSTα1 (lower band) and GSTα2 (higher band). Western blot analysis of kidney cytosol and cytosol isolated from rPT and rDT cells using a polyclonal rabbit anti-human GSTα2 resulted in the detection of only one band in all of these tissue (Figure 21C). The mobility of this band corresponded to GSTα2. The expression of GSTα2 appeared to be higher in rPT cytosol than rDT cytosol.

Discussion

The metabolism and toxicity of Tri is complex and controversial. The ability of Tri to be metabolized by P450 and GSH-dependent pathways, in both liver and kidneys, and in other organs (e.g., lung, nasal mucosa) results in a number of possible toxic metabolites. The selective distribution of both P450 and GSH conjugation enzymes and of plasma membrane transporters are important determinants in the target organ toxicity of Tri (Lash et al., 1998). Tri is primarily conjugated in vivo to GSH in the liver to form DCVG, which is rapidly transported from the liver by interorgan translocation pathways and delivered to the kidneys as either DCVG or its metabolites NAcDCVC or DCVC (Davidson and Beliles, 1991). DCVG and its metabolites are transported to PT cells and are believed

Figure 21. Expression of GSTα1 and GSTα2 in cytosol isolated from rPT and rDT cells.

Cytosol was isolated from either kidney homogenate or from rPT and rDT cells and the expression of GSTα1 and GSTα2 was studied by western blot analysis using polyclonal rabbit anti-rabbit antibodies. Migrations of bands were compared to purified proteins. **A.** SDS-PAGE stained and analyzed for the migration of 1 μg of GSTα1 (lane 2) and GSTα1-2 (lane 3) by comparison of bands to standards (lane 1). **B.** Representative western blot using a polyclonal rabbit anti-human GSTα1 antibody showing the expression of GSTα in 60 μg of cytosol isolated from either rPT cells (lane 1) or rDT cells (lane 2). **C.** Representative western blot using a polyclonal rabbit anti-human GSTα2 antibody showing the expression of GSTα2 in 10 μg of cytosol isolated from rat renal cortical homogenate (lane 1) or 60 μg of cytosol isolated from either rPT cells (lane 2) or rDT cells (lane 3).

A

29 kDa ——→

20 kDa ——→

1   2   3

B

1   2

C

1   2   3
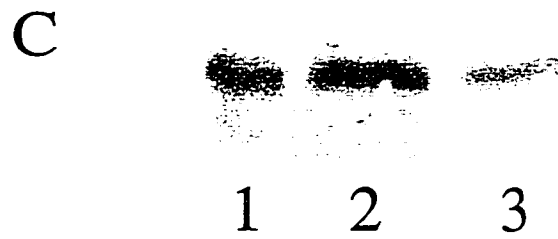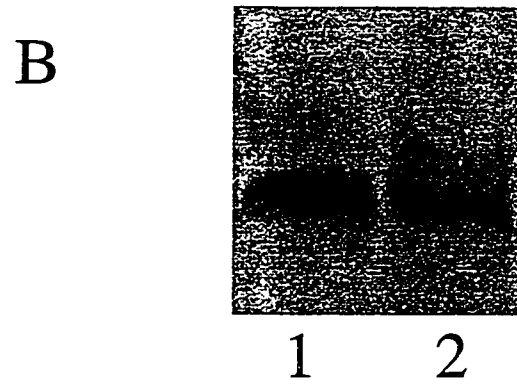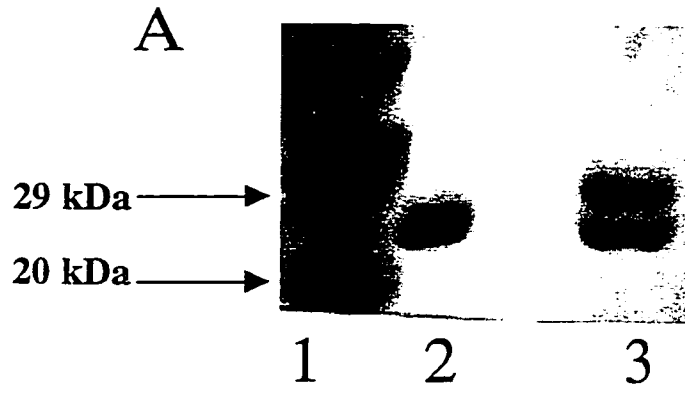
to undergo intracellular bioactivation. Tri may also be conjugated to GSH within the kidney cells, resulting in an intraorgan cycle of metabolism and toxicity (Lash et al. 1995b, 1998).

Controversy exists concerning the ability of Tri to cause both nephrotoxicity and nephrocarcinogenicity (Bloemen et al., 1995; Henschler et al, 1995; Swaen, 1995). Reasons for this controversy were discussed in Chapter 1, and include the belief that the amount of GSH conjugation of Tri is minor compared with other metabolic pathways, especially in humans. Regarding this point, cases of acute Tri poisoning have shown that the metabolites of the GSH conjugation pathway for Tri have been detected in the urine several days after ingestion of Tri (Brüning et al., 1998). Furthermore, DCVG was detected in the blood of humans exposed to small amounts of Tri via inhalation (Lash et al., 1999a). Finally, we have shown that both human liver and kidney microsomes and cytosol are capable of forming DCVG after exposure to Tri (Lash et al., 1999b). The recovery and identification of NAcDCVC as a urinary metabolite of Tri in rats, mice, and humans (Birner et al., 1993, Commandeur and Vermeulen 1990, Dekant et al., 1986, 1990) show that the kidney is a primary site for the accumulation of DCVG and formation of its subsequent metabolites. This correlates with the activity of GSH and GSH-conjugate metabolism within the liver and kidneys. Despite knowledge of this correlation, little work has been done to determine the exact enzymes responsible for GSH conjugation of Tri. This knowledge would significantly advance our ability to assess the relative human health hazard of not only Tri, but of many other chemicals that are metabolized by these enzymes.

The objective of this study was to determine the differences in Tri cytotoxicity and metabolism between rPT and rDT cells and to use these differences to assess further the human health hazard of Tri. As Tri-induced nephrocarcinogenicity is believed to be a result of long-term exposure, it was not surprising that Tri was not very toxic to freshly isolated rPT and rDT cells after acute exposures (Figure 13). Tri undergoes oxidative metabolism by P450 in both the liver and kidneys. It was not surprising, therefore, that inhibition of P450 altered Tri cytotoxicity in rPT and rDT cells. What was surprising was that inhibition

of P450 only increased Tri cytotoxicity in rDT cells. In the absence of P450 inhibition, DCVG formation was detected only in rPT cells at rates comparable to those measured in rat renal cortical cells (Figure 15) (Lash et al., 1995, 1998). Inhibition of P450 resulted in increases in DCVG formation in both rPT and rDT cells. The formation of DCVG in rDT cells after inhibition of P450 is consistent with the increases in cytotoxicity after P450 inhibition. Inhibition of P450 in rPT cells did not increase Tri cytotoxicity at any concentration despite increased DCVG formation. Reasons for this remain to be investigated but others factors controlling DCVG may be involved.

While both rPT and rDT cells express CYP2E1 and CYP2B, CYP2C11 was detected only in rPT cells and expression of CYP2E1 is slightly higher in rDT cells (Chapter 4). Inhibition of CYP2E1 in rPT and rDT cells using the CYP2E1 competitive substrate chlorzoxazone resulted in a slight increase in DCVG formation in rPT cells and a larger increase in rDT cells. This increase was transient, being measured at 30 min and decreasing back to control values, or lower, after 60 min. These data are the first to show the involvement of P450 in Tri metabolism in individual cells of the rat kidney. The fact that CYP2E1 is involved in Tri metabolism in these cells is not surprising as many studies have shown that CYP2E1 has a high affinity for Tri in the liver (Miller and Guengerich, 1983). The role of other P450 isoforms such as CYP2C11 and CYP2B in Tri metabolism and toxicity needs to be explored further.

The rates of DCVG formation in rPT cells compare favorably with those reported for rat renal cortical cells (Lash et al., 1995, 1998). Furthermore, the proposal of a two-component model for metabolizing Tri, as supported by the Eadie-Scatchard plot in Figure 16, is also supported by data on DCVG formation generated from human liver and kidney cytosol (Lash et al., 1999b). The two apparent K_m values reported in this study for DCVG formation in rPT cells (0.46 and 2.91 mM) are about an order of magnitude higher than those reported for DCVG formation in human kidney cytosol and microsomes (0.026 and 0.16 mM, respectively). The V_{max} values reported here are within the same range reported in

human kidney cytosol (0.65 and 0.47 nmol/min per mg protein vs. 0.81 nmol/min per mg protein, respectively (Lash et al., 1999a). Two possible explanations for the existence of two separate K_m values are more than one enzyme metabolizing Tri (i.e., multiple GST isoforms) or the possibility that DCVG is inhibiting Tri metabolism by GST at high concentrations of Tri. This would cause feedback inhibition, resulting in a two separate slopes. This possibility is discussed below. It should be pointed out that the data from human tissue is in cytosolic fractions, where the effects of P450 on Tri metabolism are absent. While the studies with human and rat kidney cytosol yield valuable information, data produced from rPT and rDT cells should more accurately reflect the *in vivo* situation where both cytosolic (mostly GSH-dependent pathways) and microsomal (P450 oxidative pathways) are metabolizing Tri.

Inhibition of P450 increased Tri metabolism to DCVG in rPT cells, but chlorzoxazone had only a small effect in these cells compared with that in rDT cells. Thus, other P450 isoforms besides CYP2E1 may be playing a role in Tri metabolism in rPT cells. Individual members of GSTα differed significantly in their catalysis of GSH conjugation of Tri (Figure 17, 18 and Table 9). GSTα2-2 had a significantly higher affinity for Tri as compared with GSTα1-1, and GSTα1-2. The V_{max} for these enzymes were all comparable, being within an order of magnitude of each other. The K_m for both GSTα1-1 is within the same order of magnitude determined in kinetics studies using freshly isolated rPT cells and Eadie-Scatchard analysis for Line 1 (3.99 and 2.34 vs. 2.91 mM, respectively). The K_m and V_{max} for GSTα1-2 is significantly higher than either GSTα1-1 or GSTα2-2. Thus, at higher concentration of Tri this enzyme would likely be responsible for GSH conjugation of Tri. Data reported in this study are the first data describing the conjugation of Tri to GSH by individual GST isoforms.

The decrease in DCVG levels after 60 min in rPT and rDT cells after P-450 inhibition (Figure 15), in rPT cells after exposure to high concentrations of Tri (Figure 16C), and in preparations containing purified rat GSTα after exposure to 10 mM Tri for 30

min is somewhat surprising. GSH S-conjugates can bind to GST *in vitro* with higher affinity than the second substrate or GSH has for GST *in vivo* (Hayes and Pulford, 1995; Meyer, 1993). It has been hypothesized that the binding of GSH S-conjugates to GST may prevent toxicity or stabilize the conjugates (Hayes and Pulford, 1995). Thus, the decreases in DCVG levels measured in Figures 15, 16, and 18 may be a result of DCVG binding to GST. This would result in lower levels of DCVG being available for derivatization. It is unlikely that DCVG is being processed further in rPT and rDT cells as the concentration of acivicin used almost completely inhibited GGT. No unidentified peaks were detected in any samples. The fact that decreases in DCVG were only seen at high levels of Tri after long time periods of incubation may be explained by the requirement for high levels of DCVG to affect GSH conjugation of Tri. The levels of DCVG formed in Figure 18 after 20 min are in the μM range. The possibility that DCVG is exhibiting feedback inhibition of Tri metabolism, is binding to GST, and the physiological relevance of either possibility needs to be explored further. If the above hypothesis is correct, than it would mean that the amount of Tri being metabolized by the GSH-dependent conjugation pathway may be underestimated as a significant portion of the GSH S-conjugate may be binding to GST and not available for detection.

Studies of the effect of inhibitors of GSTα on Tri metabolism by purified GSTα class members, and by cytosol from rPT and rDT cells, are important as they will aid in the determination in the role of these isoforms in Tri toxicity and metabolism. Data reported here demonstrate that while some of these compounds may follow the inhibition pattern seen with CDNB (i.e., TETB), some may not (i.e., BSP). The fact that these inhibitors were able to decrease DCVG formation in rPT cytosol but not rDT cytosol may explain some of the differences in DCVG formation seen in Figure 15. The concentration of inhibitors used was not sufficient to inhibit GSTα1-2 if CDNB was the substrate. Thus, it makes sense that no inhibition of DCVG formation was detected when GSTα1-2 was used. These findings suggest that GSTα1-1 is the primary isoform responsible for DCVG formation in

cytosol isolated from rPT cells. In contrast, neither GSTα1-1 nor GSTα2-2 seems to play a role in DCVG formation in cytosol isolated from rDT cells. The possible role of GSTα1-2 needs to be explored further. Data shown in Figure 21 demonstrate that GSTα2 is present in rPT and rDT cells. The level of GSTα2 expression appears higher in rPT cytosol than rDT cytosol. Thus, the ability of BSP and TETB to inhibit DCVG formation in rPT but not rDT cells may be caused by the increased amount of this enzyme in rPT and its absence in rDT cells.

In summary, the toxicity and metabolism of Tri in male Fischer 344 rPT and rDT cells and cytosol was determined to gain insight into the mechanism of Tri toxicity and metabolism. Tri was cytotoxic to both rPT and rDT cells but, under conditions in which P450 was not inhibited, DCVG formation was only detected in rPT cells. Inhibition of P450 resulted in increases in both cytotoxicity and metabolism of Tri to DCVG. Inhibition of CYP2E1 resulted in a small, transient increase in DCVG levels in rPT cells and a larger, transient increase in rDT cells. This observation is consistent with this P450 isoform plays a role in Tri toxicity and metabolism in individual cells of the rat kidney. The kinetics of GSH conjugation of Tri were determined in freshly isolated rPT cells and the apparent K_m and V_{max} values were within the range reported in other studies for rats and humans. This suggests that these cells may be useful as models to study the toxicity and metabolism of Tri. These results report on, for the first time, the metabolism of Tri by individual members of the GST superfamily. Members of the rat GSTα class conjugated Tri to GSH with different affinities. Furthermore, for the first time, the effect of various inhibitors of rat GSTα members on DCVG formation by both purified rat GSTα class members and in cytosol isolated from rPT and rDT cells was studied. These data suggest a possible explanation for differences in GSH conjugation of Tri between rPT and rDT cells. These data, especially those involving differences in P450 and GST activities, will aid in determination of the health hazard of Tri.

Chapter 6

P450 Oxidative Metabolism of Tri in the Rat Kidney

Introduction

As mentioned in Chapter 1, both P450 and GST isoforms metabolize Tri. The metabolism of Tri by conjugation to GSH was described in Chapter 5. The metabolism of Tri by P450 isoforms in the liver has been studied thoroughly. However, the role of P450 oxidative metabolism in renal Tri toxicity and metabolism has not been studied extensively. Data presented in Chapter 5 showed that P450 metabolism of Tri can definitely have a role in both renal metabolism and toxicity of Tri. However, the focus of Chapter 5 was on GSH conjugation of Tri by GST isoforms and not the oxidative metabolism of Tri by P450 isoforms. Based on the data shown in Chapter 5 it was hypothesized that Tri metabolism to either CH, TCA, DCA, or TCOH should be measurable in freshly isolated rPT and rDT cells as inhibition of P450 increased DCVG formation in both cells. These data suggest that P450 isoforms are contributing to Tri metabolism in some manner. Elfarra et al. (1998) have shown that Tri was oxidized in the liver to CH and TCOH. Elfarra et al. (1998) could only detect consistently CH and TCOH and did not detect significant amounts of DCA, TCA , oxalic acid, or TCOH glucuronide in either rat or human liver microsomes. This study also showed that Tri metabolism to CH in rat liver microsomes followed biphasic kinetics. This trend was not seen in mouse liver microsomes. The P450 isoforms involved in Tri metabolism in either rat or human kidneys were not determined nor was the extent of Tri oxidative metabolism in the kidney. The goal of this chapter is to determine the extent of P450 metabolism and the P450 isoforms involved in Tri metabolism in the kidney.

Results

Metabolism of Tri to CH in freshly isolated rat liver and kidney microsomes. To first verify that the method described by Elfarra et al. (1998) was reproducible, the metabolism of Tri to CH in freshly isolated rat liver microsomes was determined by gas chromatography using the methods given in Chapter 2. The rate of CH formation in rat liver microsomes was 2.55 nmol/min per mg protein compared to 3.45 nmol/min per mg protein reported in Elfarra et al. (1998) (Figure 22). Next, Tri metabolism by P450 oxidation was measured in freshly isolated rat kidney microsomes (Figure 23). In rat kidney microsomes CH was the only metabolite detected consistently. CH formation was linear up to 15 min and NADPH-dependent in both liver and kidney microsomes (data not shown). Lineweaver-Burke analysis resulted in apparent K_m and V_{max} values of 0.90 mM and 0.15 nmol/min per mg protein, respectively. Eadie-Scatchard analysis of CH formation in rat kidney microsomes indicated the presence of only one enzyme system contributing to CH formation in the rat kidney (data not shown).

Effect of P450 induction on CH formation in rat liver and kidney microsomes. The effect of pyridine and clofibrate on the oxidative metabolism of Tri was studied. Pyridine induces CYP2E1 in both rat liver and kidneys (Hotchkiss et al., 1992). Pyridine treatment (0.10 g/kg per day; 3 days i.p. injection) resulted in significant increases in CYP2E1 expression in both liver and kidney microsomes (Figure 24A and B), resulting in a 5-fold increase in CYP2E1 expression in liver microsomes and a 3-fold increase in kidney microsomes.

As shown in Chapter 4, clofibrate treatment (0.20 g/kg per day; 3 days) resulted in significant increases in CYP4A expression in both rat liver and kidney microsomes. Because data from Chapter 4 also showed that clofibrate can induce CYP2B, the effect of clofibrate treatment on the expression of CYP2C11 and CYP2E1 expression in both rat liver and kidney microsomes was studied. Clofibrate treatment did not increase CYP2E1 or CYP2C11 expression in liver microsomes but surprisingly did increase the expression of

Figure 22. CH formation in rat liver microsomes.

Rat liver microsomes (0.5 to 2.0 mg/mL) were incubated in the presence of Tri (2 mM) for 3 min at 37°C prior to the addition of NADPH (1 mM). After the indicated time, reactions were terminated by flash cooling, thawed, and extracted with 0.25 mL of ethyl acetate. Sample analysis was carried out on a Perkin Elmer Autosystem XL gas chromatograph fitted with a PE-210 30 m x 0.25 mm ID, 0.5 μM thickness column (Perkin Elmer) and an electron-capture detector. Metabolites were analyzed by injection of the ethyl acetate extracts into a split injector set at 200°C with a detector temperature of 300°C and a He flow rate of 24.8 cm/sec. The initial oven temperature was 35°C for 11 min. It was increased at 10°/min to 120°C, where it was held for 19 min. Retention time for Tri and CH were approximately 3.9 and 6 min, respectively. Results are the mean ± SD of at least 3 separate experiments.

Figure 23. Kinetic analysis of CH formation in rat kidney microsomes.

Rat kidney microsomes (0.5 to 2.0 mg/mL) were incubated with Tri for 3 min at 37°C prior to the addition of NADPH (1 mM). After 15 min, reactions were terminated by flash cooling, thawed, and extracted with 0.25 mL of ethyl acetate. Sample analysis was carried out on a Perkin Elmer Autosystem XL gas chromatograph fitted with a PE-210 30 m x 0.25 mm ID, 0.5 μM thickness column (Perkin Elmer) and an electron-capture detector. Metabolites were analyzed by injection of the ethyl acetate extracts into a split injector set at 200°C with a detector temperature of 300°C and a He flow rate of 24.8 cm/sec. The initial oven temperature was 35°C for 11 min. It was increased at 10°/min to 120°C, where it was held for 19 min. Retention time for Tri and chloral were approximately 3.9 and 6 min, respectively. Results 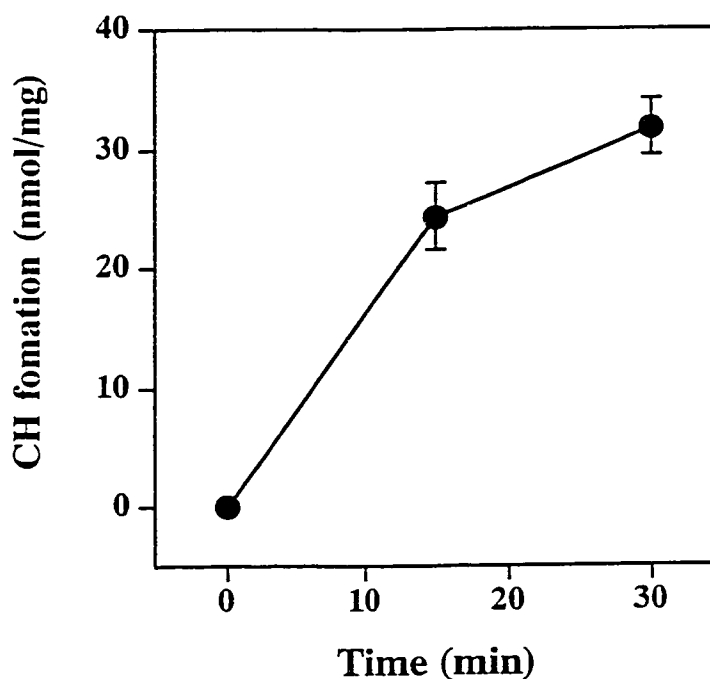are the mean ± SD of at least 3 separate experiments. K_m and V_{max} values for the analysis were 0.90 mM and 0.15 nmol/min per mg protein, respectively.

Figure 24. Effect of pyridine on CYP2E1 expression in rat liver and kidney microsomes.

A. Representative western blot using a polyclonal rabbit anti-human CYP2E1 antibody showing expression of CYP2E1 in 10 μg of rat liver microsomes (lanes 1 and 2) and 20 μg of rat kidney microsomes (lane 3 and 4). Lanes 1 and 3 indicate microsomes from saline-treated rats while lanes 2 and 4 indicate microsomes from pyridine-treated rats (0.10 g/kg per day; 3 days). **B.** Densitometric analysis of CYP2E1 protein expression.

A

Rat Liver Microsomes   Rat Kidney Microsomes

Pyridine   **-**   **+**   **-**   **+**
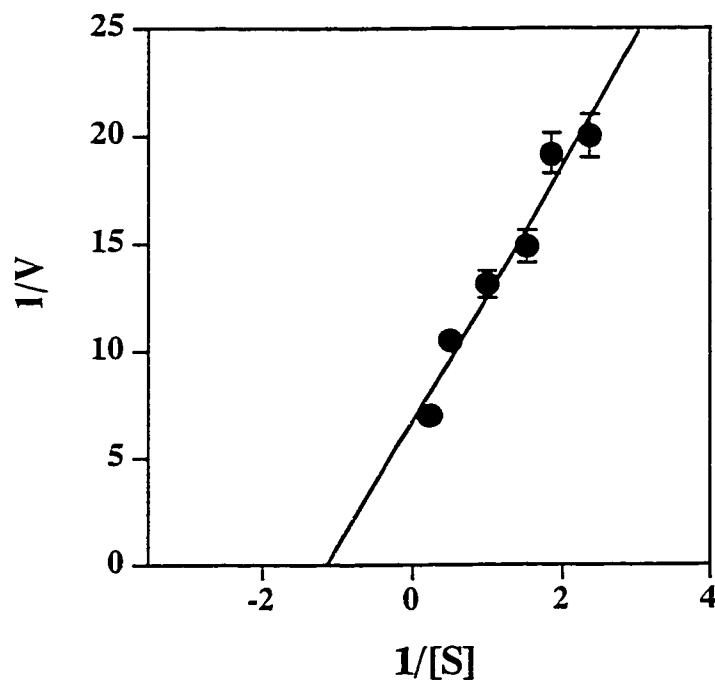
B
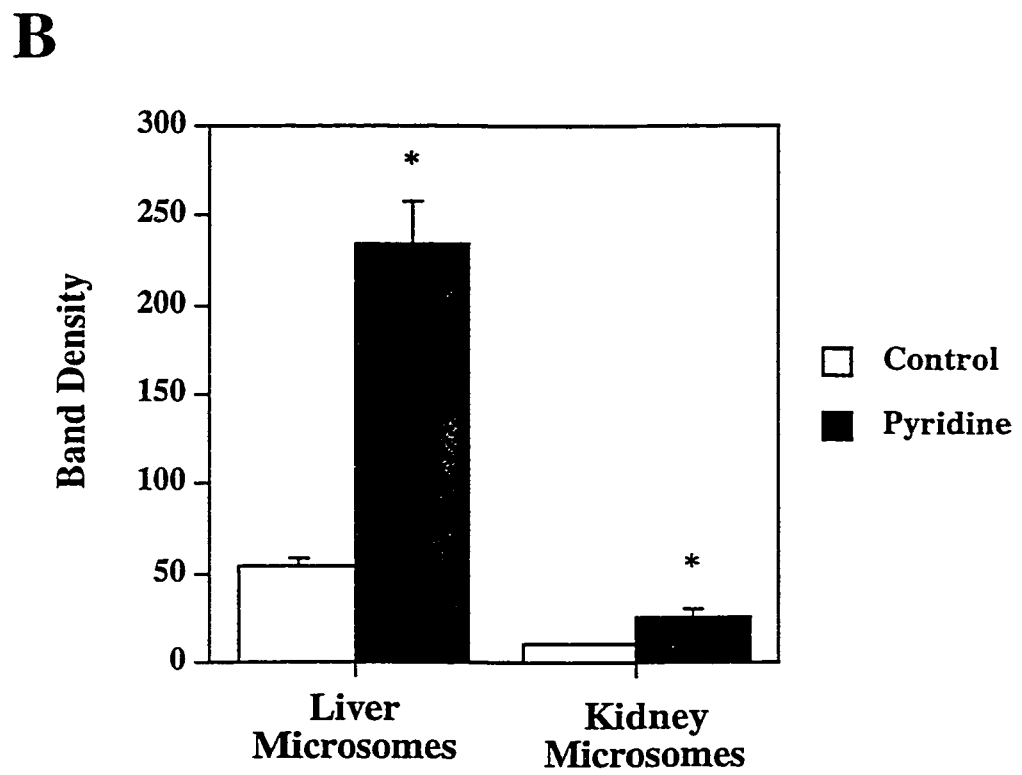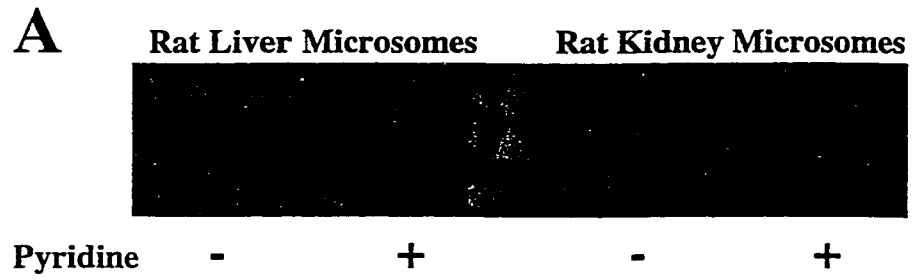
Figure 25. Effect of clofibrate on CYP2E1 and CYP2C11 expression in rat liver and kidney microsomes.

A. Representative western blot using a polyclonal rabbit anti-human CYP2E1 antibody showing expression of CYP2E1 in 10 μg of rat liver microsomes (lanes 1 and 2) and 20 μg of rat kidney microsomes (lane 3 and 4). Lanes 1 and 3 indicate microsomes from saline-treated rats while lanes 2 and 4 indicate microsomes from clofibrate-treated rats (0.20 g/kg per day; 3 days). **B.** Densitometric analysis of CYP2E1 protein expression. **C.** Representative western blot using a monoclonal mouse anti-rat CYP2C11 antibody showing expression of CYP2C11 in 10 μg of rat liver microsomes (lanes 1 and 2) and 20 μg of kidney microsomes (lane 3 and 4). Lanes 1 and 3 indicate microsomes from corn oil-treated rats while lanes 2 and 4 indicate microsomes from clofibrate-treated (0.20 mg/kg per day; 3 days) rats. **D.** Densitometric analysis of CYP2C11 protein expression.
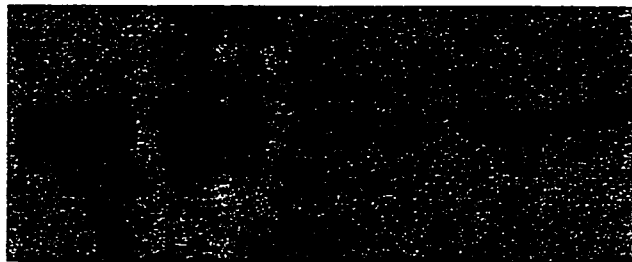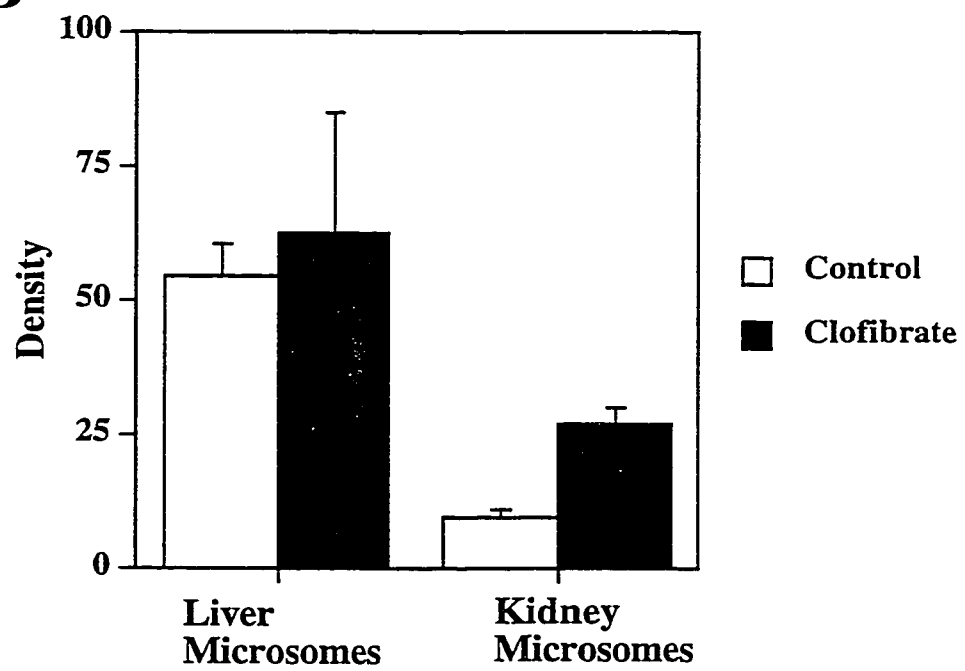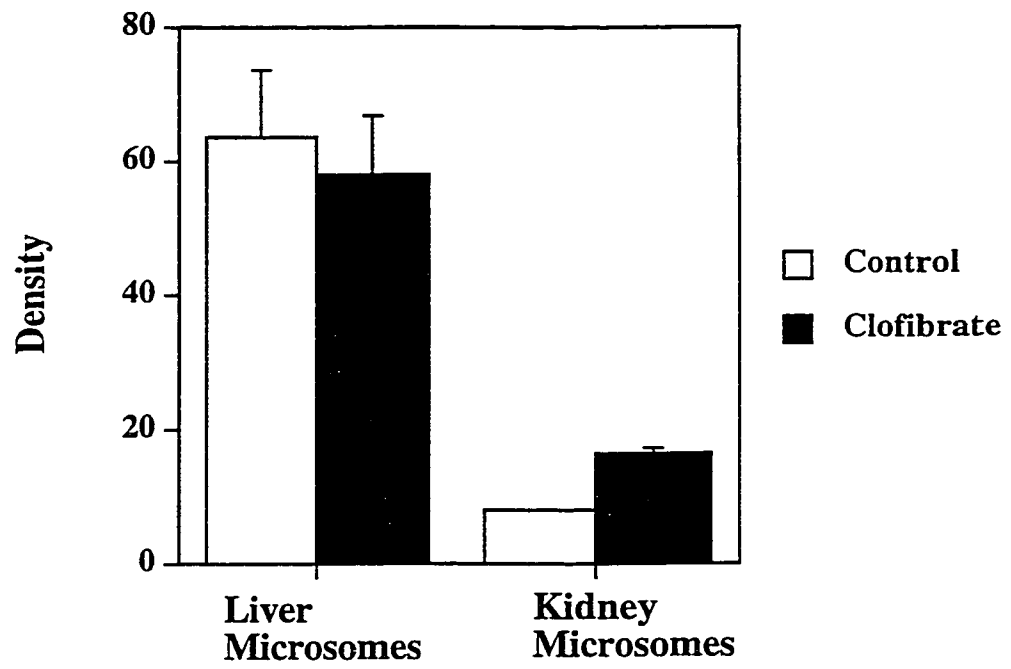
A

1 2 3 4

B

C

1 2 3 4

D

these isoforms in kidney microsomes (Figure 25A and C). Renal CYP2E1 expression was increased 2-fold while renal CYP2C11 expression was increased 3-fold (Figure 25B and D).

Pyridine treatment resulted in significant increases in CH formation in liver microsomes, causing a 4-fold increase in CH formation while clofibrate treatment did not result in a significant increase in CH formation in rat liver microsomes (Figure 26). In contrast, kidney microsomes isolated from rats treated with pyridine or clofibrate had significantly higher rates of CH formation (Figure 27). The increase in CH formation was greater in kidney microsomes isolated from rats treated with pyridine (3-fold) than kidney microsomes isolated from rats treated with clofibrate (1.5-fold).

Effect of inhibition of P450 on CH formation in liver and kidney microsomes. Rat liver and kidney microsomes were isolated from control, pyridine-treated, or clofibrate-treated rats and the formation of CH in the presence of either SKF525A (0.25 mM) or chlorzoxazone (1 mM) was measured. In both liver and kidney microsomes SKF-525A and chlorzoxazone resulted in significant decreases in CH formation (Figure 28A and B). The level of inhibition in liver microsomes by SKF525A was equal to that caused by chlorzoxazone while pretreatment of kidney microsomes with SKF525A resulted in significantly lower levels of CH than in kidney microsomes treated with chlorzoxazone. SKF525A and chlorzoxazone significantly decreased CH formation in microsomes isolated from pyridine- and clofibrate-treated rats (Figure 29A and B). Interestingly, SKF525A was only able to decrease CH to control levels, but not below, in liver microsomes from pyridine-treated rats (Figure 29A and B).

P450 oxidative metabolism of Tri in rPT and rDT cells. Tri oxidative metabolism was measured by analysis of CH formation in both rPT and rDT cells and was linear through 30-min of incubation and was NADPH-dependent (Figure 30A and B). Lineweaver-Burke analysis of CH formation in rPT cells resulted in a line that did not intercept the y-axis, making analysis of kinetics impossible (Figure 31A). Lineweaver-

Figure 26. **Effect of pyridine and clofibrate on CH formation in rat liver microsomes.**

Rat liver microsomes (0.5 to 2.0 mg/mL) isolated from control, pyridine-, or clofibrate-treated rats were incubated in the presence of Tri (2 mM) for 3 min at 37°C prior to the addition of NADPH (1 mM). After 15 min, reactions were terminated by flash cooling, thawed, and extracted with 0.25 mL of ethyl acetate. Sample analysis was carried out on a Perkin Elmer Autosystem XL gas chromatograph fitted with a PE-210 30 m x 0.25 mm ID, 0.5 μM thickness column (Perkin Elmer) and an electron-capture detector. Metabolites were analyzed by injection of the ethyl acetate extracts into a split injector set at 200°C with a detector temperature of 300°C and a He flow rate of 24.8 cm/sec. The initial oven temperature was 35°C for 11 min. It was increased at 10°/min to 120°C, where it was held for 19 min. Retention time for Tri and chloral were approximately 3.9 and 6 min, respectively. Results are the mean ± SD of at least 3 separate experiments. *Significant (P < 0.05) difference in CH formation as compared to control.

Figure 27. **Effect of pyridine and clofibrate on CH formation in rat kidney microsomes.**

Rat kidney microsomes (0.5 to 2.0 mg/mL) isolated from control, pyridine-, or clofibrate-treated rats were incubated in the presence of Tri (2 mM) for 3 min at 37°C prior to the addition of NADPH (1 mM). After 15 min, reactions were terminated by flash cooling, thawed, and extracted with 0.25 mL of ethyl acetate. Sample analysis was carried out on a Perkin Elmer Autosystem XL gas chromatograph fitted with a PE-210 30 m x 0.25 mm ID, 0.5 μM thickness column (Perkin Elmer) and an electron-capture detector. Metabolites were analyzed by injection of the ethyl acetate extracts into a split injector set at 200°C with a detector temperature of 300°C and a He flow rate of 24.8 cm/sec. The initial oven temperature was 35°C for 11 min. It was increased at 10°/min to 120°C, where it was held for 19 min. Retention time for Tri and chloral were approximately 3.9 and 6 min, respectively. Results are the mean ± SD of at least 3 separate experiments. *Significant (P < 0.05) difference in CH formation as compared to control.

Figure 28. Effect of P450 inhibition on CH formation in rat liver and kidney microsomes.

Rat liver (A) or kidney (B) microsomes (0.5 to 2.0 mg/mL) were incubated in the presence or absence of either SKF525A (250 μM), chlorzoxazone (1 mM), or solvent control (0.1 N NaOH < 1.0 % v/v) for 15 min prior to the addition of Tri (2 mM) and NADPH (1 mM). After 15 min, reactions were terminated by flash cooling, thawed, and extracted with 0.25 mL of ethyl acetate. Sample analysis was carried out on a Perkin Elmer Autosystem XL gas chromatograph fitted with a PE-210 30 m x 0.25 mm ID, 0.5 μM thickness column (Perkin Elmer) and an electron-capture detector. Metabolites were analyzed by injection of the ethyl acetate extracts into a split injector set at 200°C with a detector temperature of 300°C and a He flow rate of 24.8 cm/sec. The initial oven temperature was 35°C for 11 min. It was increased at 10°/min to 120°C, where it was held for 19 min. Retention time for Tri and chloral were approximately 3.9 and 6 min, respectively. Results are the mean ± SD of at least 3 separate experiments. *Significant (P < 0.05) difference in CH formation as compared to control.
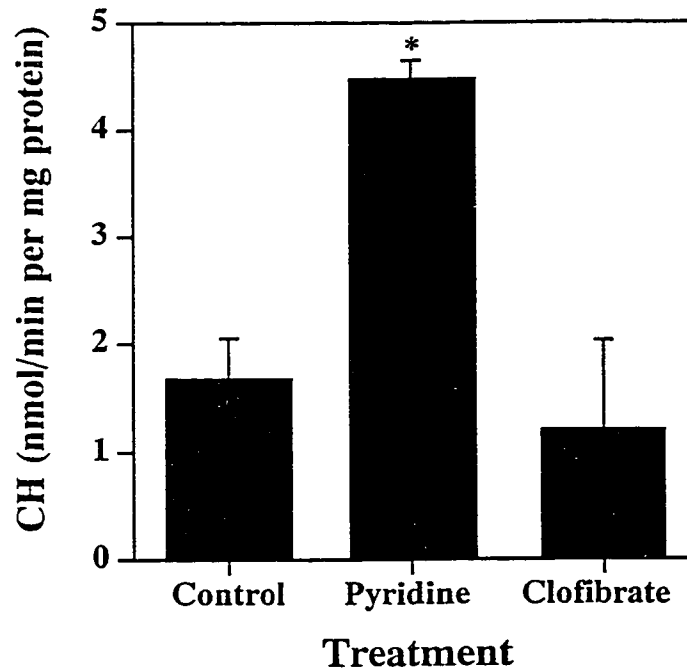
A. Liver Microsomes

B. Kidney Microsomes

Figure 29.   Effect of P450 inhibition on CH formation in liver and kidney microsomes from pyridine- and clofibrate-treated rats.

Liver (A) or kidney (B) microsomes (0.5 to 2.0 mg/mL) from pyridine-, or clofibrate-treated rats were incubated in the presence or absence of either SKF525A (250 μM), chlorzoxazone (1 mM), or solvent control (0.1 N NaOH < 1.0 % (v/v)) for 15 min prior to the addition of Tri (2 mM) and NADPH (1 mM).   After 15 min, reactions were terminated by flash cooling, thawed, and extracted with 0.25 mL of ethyl acetate.   Sample analysis was carried out on a Perkin Elmer Autosystem XL gas chromatograph fitted with a PE-210 30 m x 0.25 mm ID, 0.5 μM thickness column (Perkin Elmer) and an electron-capture detector.   Metabolites were analyzed by injection of the ethyl acetate extracts into a split injector set at 200°C with a detector temperature of 300°C and a He flow rate of 24.8 cm/sec.   The initial oven temperature was 35°C for 11 min.   It was increased at 10°/min to 120°C, where it was held for 19 min.   Retention time for Tri and chloral were approximately 3.9 and 6 min, respectively.   Results are the mean ± SD of at 3 least separate experiments.   *Significant (P < 0.05) difference in CH formation as compared to control.
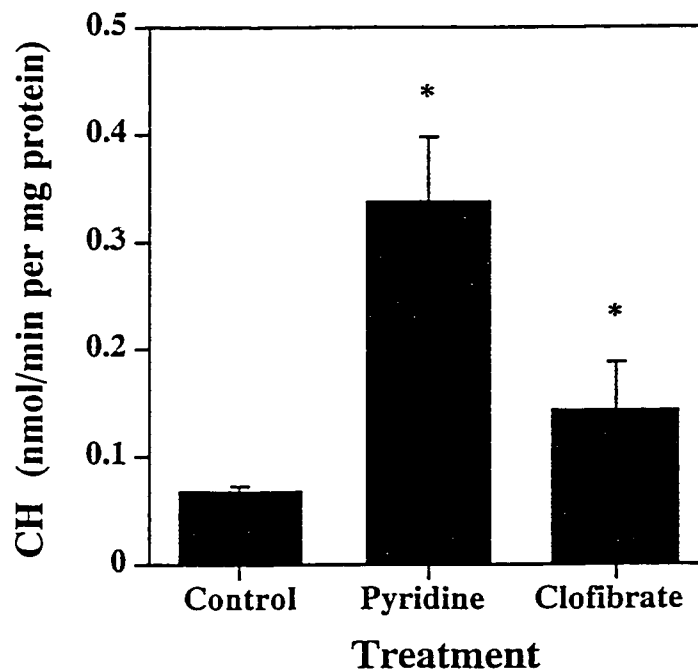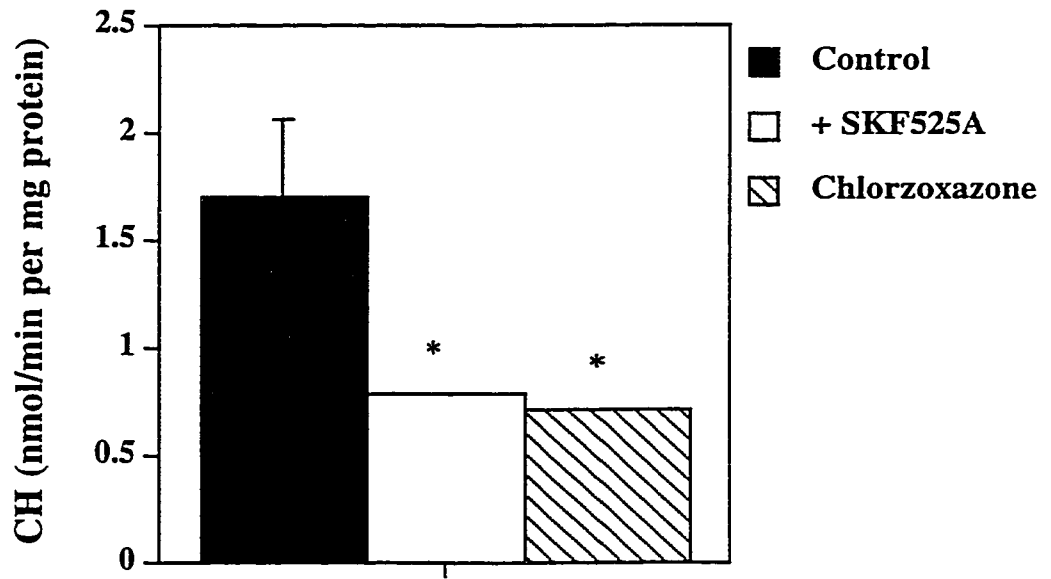
A. Liver Microsomes

B. Kidney Microsomes

Treatment

Pyridine

Pyridine + SKF525A

Pyridine + Chlorzoxazone

Clofibrate

Clofibrate + SKF525A

Clofibrate + Chlorzoxazone
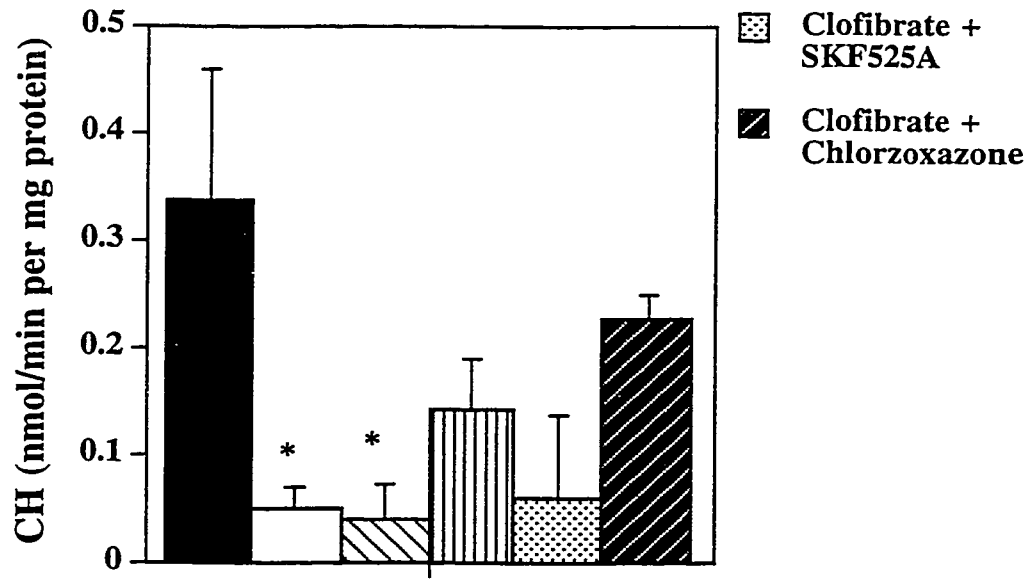
Figure 30. Time and NADPH dependence of CH formation in rPT and rDT cells.

A. Cells were incubated with Tri (10 mM) for 3 min at 37°C prior to the addition of NADPH (1 mM). At the indicated time, reactions were terminated by flash cooling, thawed, and extracted with 0.25 mL of ethyl acetate. B. Cells were incubated with Tri (10 mM) for 3 min at 37°C prior to the addition of NADPH (1 mM) or buffer control. After 30 min, reactions were terminated by flash cooling, thawed, and extracted with 0.25 mL of ethyl acetate. Sample analysis was carried out on a Perkin Elmer Autosystem XL gas chromatograph fitted with a PE-210 30 m x 0.25 mm ID, 0.5 µM thickness column (Perkin Elmer) and an electron-capture detector. Metabolites were analyzed by injection of the ethyl acetate extracts into a split injector set at 200°C with a detector temperature of 300°C and a He flow rate of 24.8 cm/sec. The initial oven temperature was 35°C for 11 min. It was increased at 10°/min to 120°C, where it was held for 19 min. Retention time for Tri and chloral were approximately 3.9 and 6 min, respectively. Results are the mean ± SD of at least 3 separate experiments.
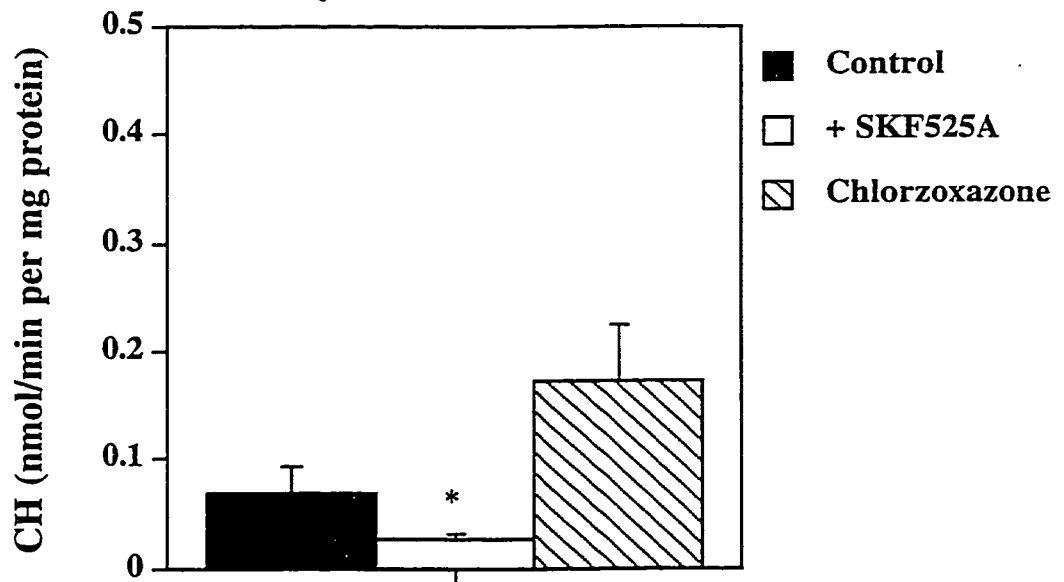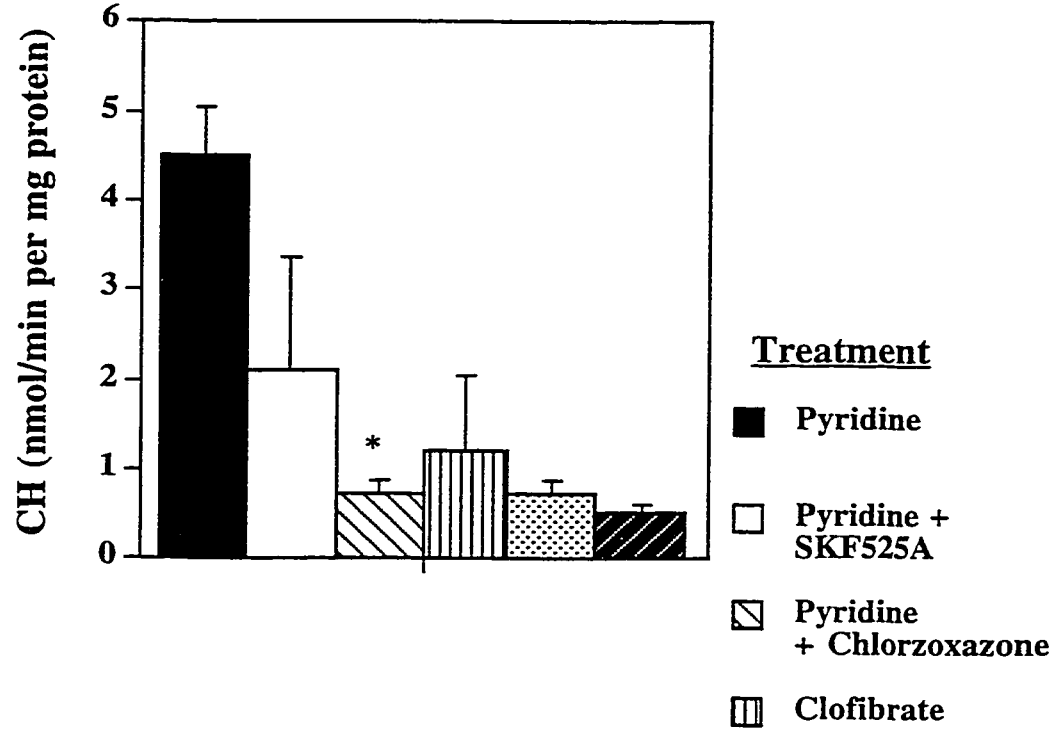
A. Time-Dependence

B. NADPH-Dependence

Figure 31. Kinetic analysis of CH formation in rPT and rDT cells.

rPT (A) and rDT cells (B) were incubated in the presence of Tri for 3 min at 37°C prior to the addition of NADPH (1 mM). After 30 min, reactions were terminated by flash cooling, thawed, and extracted with 0.25 mL of ethyl acetate. Sample analysis was carried out on a Perkin Elmer Autosystem XL gas chromatograph fitted with a PE-210 30 m x 0.25 mm ID, 0.5 μM thickness column (Perkin Elmer) and an electron-capture detector. Metabolites were analyzed by injection of the ethyl acetate extracts into a split injector set at 200°C with a detector temperature of 300°C and a He flow rate of 24.8 cm/sec. The initial oven temperature was 35°C for 11 min. It was increased at 10°/min to 120°C, where it was held for 19 min. Retention time for Tri and chloral were approximately 3.9 and 6 min, respectively.

A. PT Cells
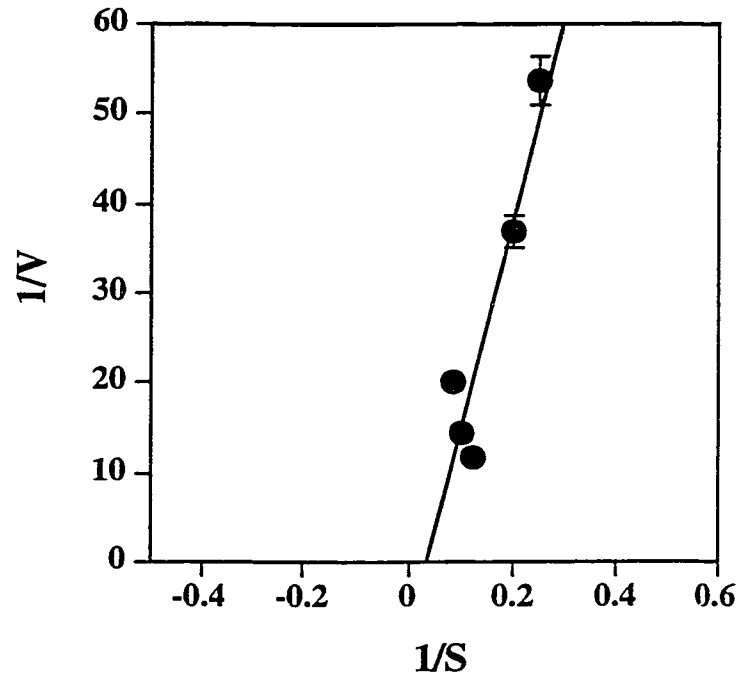
B. DT Cells
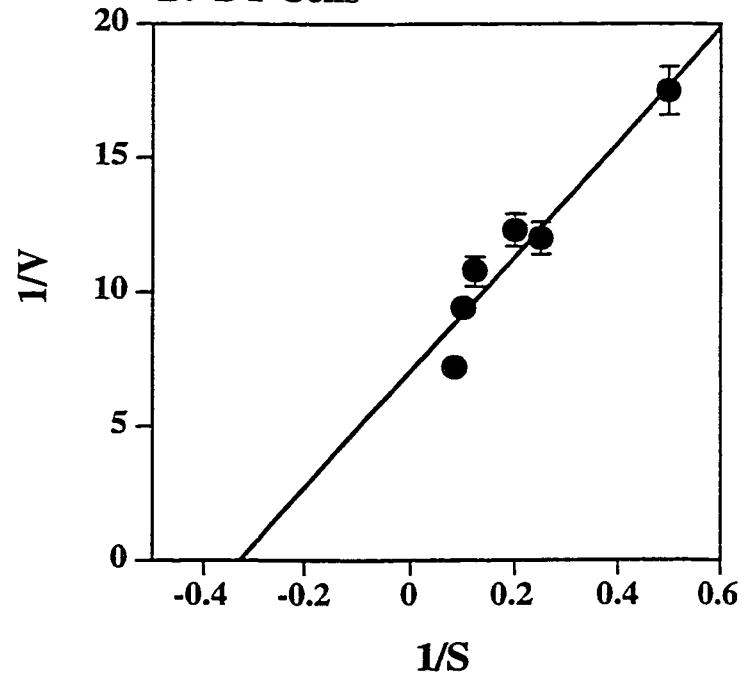
Burke analysis of CH formation in rDT cells resulted in apparent K_m and V_{max} values of 3.03 mM and 0.142 nmol/min per mg protein, respectively (Figure 31B). Eadie-Scatchard (Eadie-Hofstee) analysis of CH formation in both rPT and rDT cells indicated the contribution of only one enzyme system in CH formation (data not shown).

Effect of pyridine and clofibrate treatment on CH formation in rPT and rDT cells. As shown in Chapter 4, pretreatment of rats with clofibrate did not increase CYP4A2, CYP4A3, or CYP2B1/2 expression in microsomes isolated from rPT or rDT cells. Neither pyridine nor clofibrate treatment caused significant increases in the expression of either CYP2C11 or CYP2E1 in microsomes isolated from rPT and rDT cells (Figure 32A and B). CH formation was not significantly increased in rPT or rDT cells isolated from rats treated with either pyridine or clofibrate as compared to control (Figure 33A and B).

Effect of P450 inhibition on CH formation in rPT and rDT cells. rPT and rDT cells isolated from rats treated with either pyridine, clofibrate, or solvent control were isolated and the formation of CH in the presence or absence of SKF525A (0.25 mM) or chlorzoxazone was determined. Both SKF525A and chlorzoxazone significantly inhibited CH formation in rDT cells while SKF525A only inhibited CH formation in rPT cells (Figure 34A and B). Pretreatment of rPT cells, but not rDT cells, with SKF525A resulted in significantly lower levels of CH formation than in cells pretreated with chlorzoxazone. Pretreatment of rDT cells, but not rPT cells, with chlorzoxazone resulted in significantly lower levels of CH.

Discussion

CH formation in liver and kidney microsomes. The level of CH formation in rat liver microsomes measured in this study agrees with that previously reported for rat liver microsomes (Elfarra et al., 1998). Elfarra et al. (1998) reported a two-K_m model for Tri

Figure 32. Effect of clofibrate on CYP2E1 and CYP2C11 expression in rPT and rDT cells.

A. Representative western blot using a polyclonal rabbit anti-human CYP2E1 antibody showing expression of CYP2E1 in 20 µg of microsomes isolated from kidney homogenate (lane 1) or 60 µg microsomes isolated from rPT cells (lanes 2 and 3) and **rDT cells** (lane 4 and 5). Lanes 3 and 5 indicate microsomes from saline-treated rats while lanes 2 and 4 indicate microsomes from pyridine-treated rats (0.10 mg/kg per day; 3 days). **B.** Representative western blot using a monoclonal mouse anti-rat CYP2C11 antibody showing expression of CYP2C11 in 20 µg of microsomes isolated from kidney homogenate (lane 1) or 60 µg of microsomes isolated from rPT cells (lanes 2 and 3). Lanes 2 indicates microsomes from corn oil-treated rats while lane 3 indicates microsomes from clofibrate-treated (0.20 mg/kg per day; 3 days) rats.

Figure 33. Effect of pyridine and clofibrate on CH formation in rPT and rDT cells.

rPT (A) and rDT (B) cells isolated from control, pyridine-, or clofibrate-treated rats were incubated in the presence of Tri (10 mM) for 3 min at 37°C prior to the addition of NADPH (1 mM). After 30 min, reactions were terminated by flash cooling, thawed, and extracted with 0.25 mL of ethyl acetate. Sample analysis was carried out on a Perkin Elmer Autosystem XL gas chromatograph fitted with a PE-210 30 m x 0.25 mm ID, 0.5 µM thickness column (Perkin Elmer) and an electron-capture detector. Metabolites were analyzed by injection of the ethyl acetate extracts into a split injector set at 200°C with a detector temperature of 300°C and a He flow rate of 24.8 cm/sec. The initial oven temperature was 35°C for 11 min. It was increased at 10°/min to 120°C, where it was held for 19 min. Retention time for Tri and chloral were approximately 3.9 and 6 min, respectively. Results are the mean ± SD of at least 3 separate experiments.

A. PT Cells

B. DT Cells

Figure 34. Effect of P450 inhibition on CH formation in rPT and rDT cells.

rPT (A) or rDT (B) cells from control animals were incubated in the presence or absence of either SKF525A (250 µM), chlorzoxazone (1 mM), or solvent control (0.1 N NaOH < 1.0 % v/v) for 15 min prior to the addition of Tri (10 mM) and NADPH (1 mM). After 30 min, reactions were terminated by flash cooling, thawed, and extracted with 0.25 mL of ethyl acetate. Sample analysis was carried out on a Perkin Elmer Autosystem XL gas chromatograph fitted with a PE-210 30 m x 0.25 mm ID, 0.5 µM thickness column (Perkin Elmer) and an electron-capture detector. Metabolites were analyzed by injection of the ethyl acetate extracts into a split injector set at 200°C with a detector temperature of 300°C and a He flow rate of 24.8 cm/sec. The initial oven temperature was 35°C for 11 min. It was increased at 10°/min to 120°C, where it was held for 19 min. Retention time for Tri and chloral were approximately 3.9 and 6 min, respectively. Resu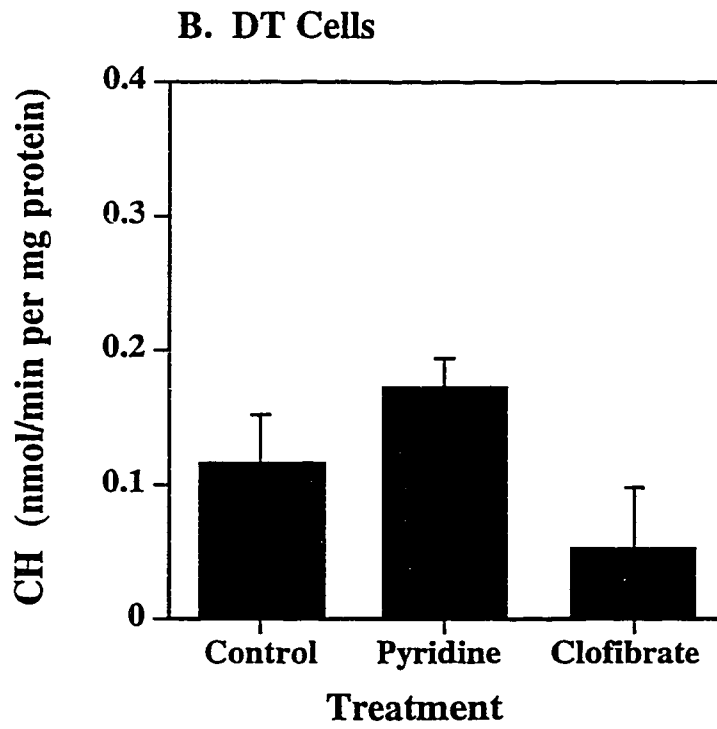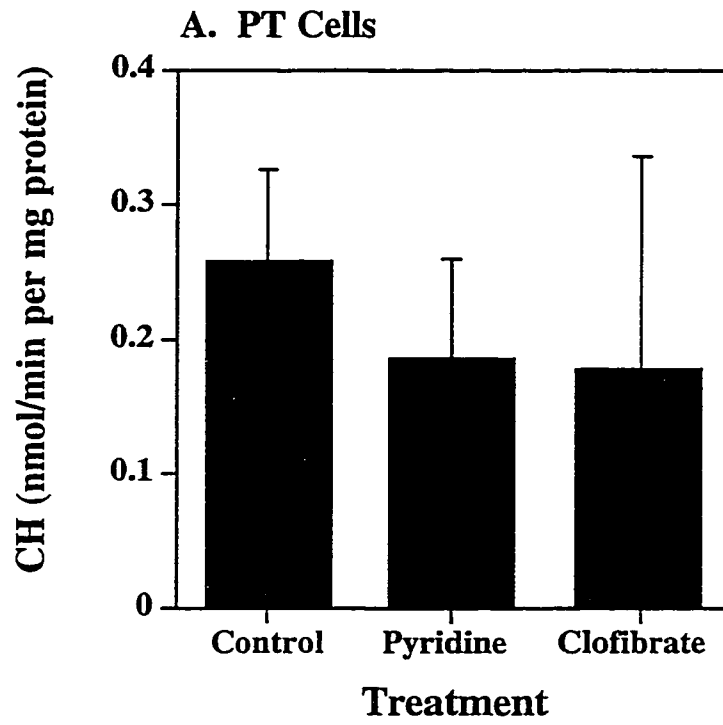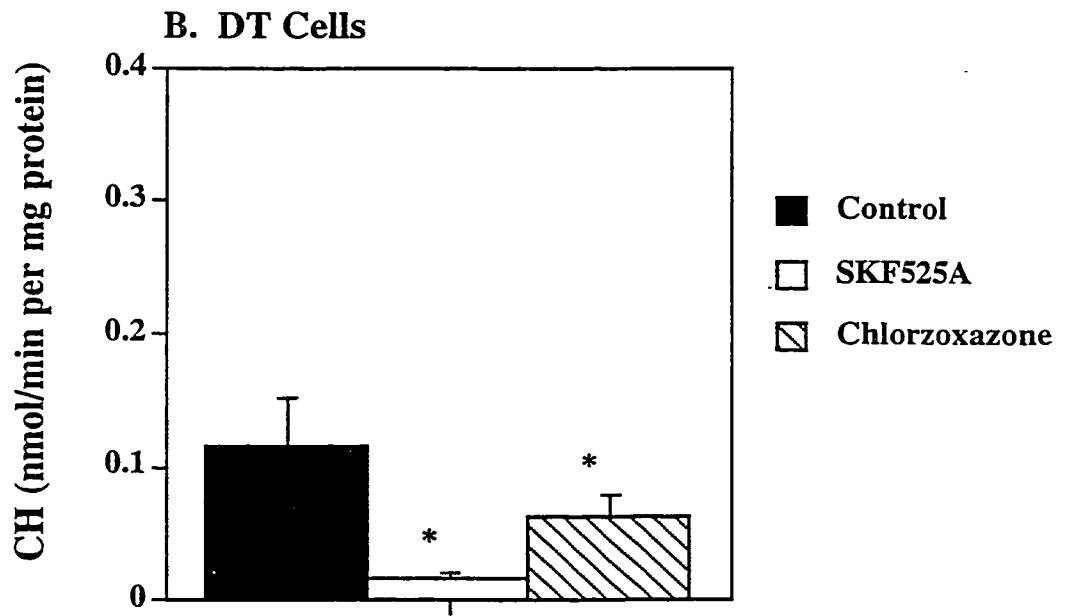lts are th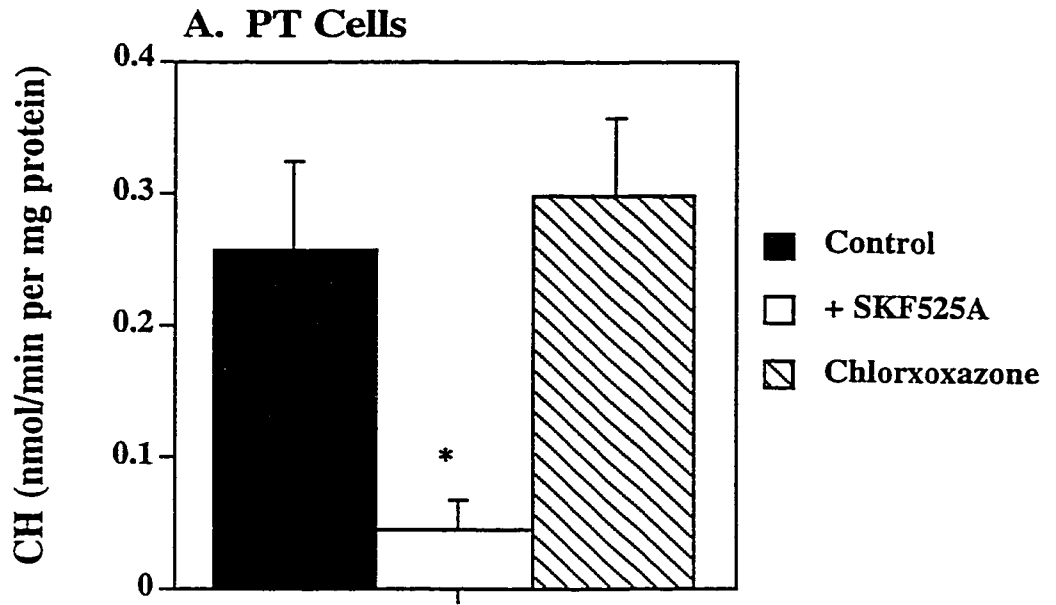e mean ± SD of at least 3 separate experiments. *Significant (P < 0.05) difference in CH formation as compared to control.

A. PT Cells

B. DT Cells

metabolism in the liver. CH was measured consistently in rat kidney microsomes and only one K_m was determined. The apparent K_m and V_{max} values for CH formation in rat kidney microsomes are approximately an order of magnitude lower than those reported for rat liver microsomes (approximately 0.5 mM and 2.4 nmol/min per mg protein, respectively) (Elfarra et al., 1998). It is surprising that only one enzyme appears to be contributing to the oxidative metabolism of Tri in the kidney as multiple P450 isoforms capable of metabolizing Tri are expressed in the rat kidney (Chapter 4). The apparent V_{max} for CH formation in rat kidney microsomes is very low while the apparent K_m is rather high compared to the liver. This results in a low-affinity, low-capacity system. This could result in an increased amount of Tri being shuttled to the GSH-conjugation pathway.

Effect of P450 induction and inhibition on CH formation in liver microsomes. Miller and Guengerich (1983) demonstrated that treatment of rats with either pyridine or phenobarbital resulted in increased CH formation from Tri in rat liver microsomes. Our data agree with this study. No studies could be found testing the effect of clofibrate on CH formation from Tri in any species. This is not surprising as clofibrate has mainly been used to study the effect of induction of CYP4A isoforms. Data from Chapter 4 combined with data from this study necessitate further study of the effect of clofibrate on drug metabolism. Despite the fact the clofibrate induced CYP2B in rat liver microsomes, no increase in CH formation was measured in liver microsomes isolated from clofibrate-treated rats (Figure 26). Treatment of rats with clofibrate did not increase either hepatic CYP2C11 or CYP2E1 levels (Figure 25). In contrast, treatment of rats with pyridine resulted in significant increases in both hepatic CYP2E1 expression and CH formation (Figures 25 and 26). Thus, the increase in CH formation in microsomes isolated from rats treated with pyridine correlates with the increase in CYP2E1 expression. This increase was reversed by pretreatment of liver microsomes with either SKF525A or chlorzoxazone (Figure 28). The level of inhibition of CH formation by SKF525A did not differ significantly from that seen with chlorzoxazone suggesting that CYP2E1 appears to be the

main enzyme involved in Tri oxidative metabolism in untreated rat liver microsomes. Furthermore, CH formation was inhibited equally in clofibrate-treated microsomes pretreated with either SKF525A or chlorzoxazone suggesting that similar enzymes are contributing to Tri metabolism in these treated microsomes. Neither SKF525A nor chlorzoxazone was able to completely inhibit CH formation in rat liver microsomes (Figure 27). Thus, other enzymes may be capable of the oxidative metabolism of Tri in the rat liver.

Effect pyridine and clofibrate on P450 induction in the rat kidney tissues. Similar to results seen in the liver, treatment of rats with pyridine resulted in significant increases in both CYP2E1 expression and CH formation in rat kidney microsomes (Figures 26 and 28). Unlike results seen in the liver, treatment of rats with clofibrate significantly increased expression of CYP2E1 and CYP2C11 in rat kidney microsomes (Figures 26). To our knowledge, this is the first time that clofibrate, or any similar compounds, have been shown to increase CYP2C11 expression in vivo. Studies (Zangar et al., 1995) have shown an increase in CYP2E1 in primary cultures of hepatocytes and renal cortical cells treated with ciprofibrate. Data from this study demonstrated that clofibrate can cause a kidney-selective induction of several P450 isoforms. The cause of this selectivity is not known. However, it should be pointed out that clofibrate induced every renal P450 studied in this work (for data on CYP2B and CYP4A, please see Chapter 4). Furthermore, the basal levels of expression of CYP2E1, CYP2B, and CYP2C11 in the kidneys are very low compared with the liver. This difference could account, in part, for the tissue-selective induction of these isoforms in the kidney and not the liver. The higher level of expression and activity of these isoforms in the liver may result in different modes of regulation of these isoforms than in the kidney. Thus, the effect of clofibrate on the expression of these isoforms may be overridden or ignored by the liver but not the kidney. Finally, the general increases in P450 expression caused by clofibrate in the kidney suggests a signaling pathway that caused an increase in over all renal P450 expression as opposed to a specific mechanism that involves each individual gene. For example, it is doubtful that clofibrate-induced

increases in CYP2C11, CYP2E1, or CYP2B1 are a result of direct interaction with each specific gene for each isoform. Rather, a general mechanism that may result in an up-regulation of total renal P450 expression in general seems more likely. The cause of this up-regulation may be an increase in a specific transcription factor or may be an increase in fatty acid metabolism. The latter hypothesis seems more likely as clofibrate, and similar compounds, have been shown to increase fatty acid metabolism in vivo (Ronnis et al, 1998). Furthermore, some of the products of increased fatty acid oxidation (e.g., ketone bodies) increase CYP2E1 in primary cultures of rat hepatocytes (Ronnis et al., 1998). Further study is needed to verify or refute these hypothesis. As seen in Chapter 4, treatment of rats with either pyridine or clofibrate did not increase the expression of any P450 isoform in microsomes isolated from rPT or rDT cells (Figure 32A and B). These data agree with data shown in Chapter 4 and once again suggest that the increase in P450 expression in the kidney by these chemicals does not occur in the renal epithelial tissue.

Pretreatment of rPT and rDT cells with both SKF525A and chlorzoxazone resulted in significant decreases in CH formation in rDT cells but not rPT cells (Figure 34A and B). Pretreatment of cells with SKF525A inhibited CH formation equally in rPT and rDT cells. In contrast, chlorzoxazone pretreatment resulted in significantly lower levels of CH in rDT cells than in rPT cells. These data correlate with data in Chapter 4 that showed that rPT cells express more isoforms of P450 than rDT cells. Thus, if chlorzoxazone fully inhibits CYP2E1 in rPT cells, Tri may be metabolized by CYP2C11. In contrast, CYP2C11 is not expressed in rDT cells (Chapter 4). As a result, Tri would be shuttled to different pathways for metabolism (possibly GSH-conjugation pathways). If this hypothesis is true, then chlorzoxazone pretreatment should result in a significant increase in DCVG in rDT cells over that in rPT cells. This in fact was shown to be true in Chapter 5. Thus, differences in the expression of drug metabolizing enzymes between rPT and rDT cells appear to be contributing to differences in the metabolism of Tri, supporting further the hypothesis of this work.

The fact that a decrease in CH at high concentrations of Tri was observed in rPT cells but not rDT cells is interesting (Figures 30 and 31). Tri has been shown to inhibit P450 activity in liver microsomes at high concentrations (Miller and Guengerich, 1983). This inhibition is believed to occur by destruction of the heme moiety of P450. It is not known if this is what is occurring in rPT cells. If this hypothesis is true, why were decreases not detected in rDT cells? Initial levels of CH formation were significantly higher in rPT cells then in rDT cells (Figures 30 and 31). Thus, it is possible that this increased level of CH formation in rPT cells results in inhibition of P450. The reasons this decrease was measured in rPT cells but not liver or kidney microsomes could be that lower levels of Tri were used in kidney and liver microsomes (2 mM vs. 10 mM). Furthermore, both liver and kidney microsomes have higher levels of P450 compared with the small amount expressed in rPT cells. It is also possible that CH is being metabolized further in rPT cells. This hypothesis seems unlikely as neither DCA, TCA, nor TCOH were detected at any time in any samples. Finally, it is possible that at high concentrations, Tri is being shuttled to alternative pathways, mainly the GSH-conjugation dependent pathway. Data in Chapter 5 showed that under normal conditions DCVG formation was not detected in rDT cells but was detected in rPT cells. This enabled kinetic analysis of DCVG formation in rPT cells but not rDT cells. The reverse situation appears to be occurring in this chapter. Kinetic analysis of CH formation is not possible in rPT cells but is in rDT cells. Thus, data presented in this chapter correlate with data presented earlier.

In summary, Tri metabolism to CH was measured in both rat liver and kidney microsomes and in rPT and rDT cells. The kinetics of CH formation were determined in both rat kidney microsomes and rDT cells. Kinetic analysis of CH formation in rPT cells was impossible due to a decrease in CH formation at high concentrations of Tri. This decrease was not measured in rDT cells. Treatment of rats with pyridine resulted in increases in CYP2E1 expression and CH formation in both rat liver and kidney microsomes but not in rPT or rDT cells. Treatment of rats with clofibrate resulted in increases in

CYP2E1 and CYP2C11 expression and CH formation in kidney microsomes but not in liver microsomes. Neither pyridine nor clofibrate treatment resulted in increased P450 expression or increased CH formation in rPT or rDT cells. Pretreatment of rat liver and kidney microsomes with either SKF525A or chlorzoxazone inhibited CH formation equally in control and treated animals, indicating that CYP2E1 appears the main enzyme responsible for Tri oxidative metabolism in both tissues. Pretreatment of rPT and rDT cells with SKF525A inhibited CH formation equally in both cell types. Chlorzoxazone pretreatment resulted in lower levels of CH in rDT cells than in rPT cells. These data for the first time describe the oxidative metabolism of Tri in the rat kidney. These results will be useful in determining how the absence or presence of P450 isoforms between different cell types may affect Tri metabolism. As an example, it is reported that human kidney does not express CYP2E1 (Amet et al., 1997b). As CYP2E1 is the major P450 isoform involved in Tri oxidative metabolism in the kidney it could be hypothesized that Tri oxidative metabolism in the human kidney would be lower than that in the rat. Finally, these data will be useful in determining how differences in the expression of drug metabolism enzymes among species affect the toxicity and metabolism of various chemicals.

Chapter 7

Toxicity of Tri and DCVC in Primary Cultures of rPT and rDT cells

Introduction

As mentioned in Chapter 1, and as demonstrated in Chapter 5, Tri is not very toxic in rPT and rDT cells after a short-term exposure. This is true of several chemicals, and chemical-induced injury to not only the kidney, but to many other organs is often the result of repeated exposures to a chemical over a longer period of time. Because of this, efforts have been made to develop models that can be used for the study of long term chemical-induced injury. These models would allow for the study of chemical-induced injury over a period of days instead of hours. Many studies have made use of *in vivo* models for the study of chemical-induced injury. While these studies are invaluable, they are expensive and time consuming. An in vitro model that mimics the in vivo state as closely as possible would greatly aid in the study of chemical-induced injury to the kidneys. The goal of this study was to develop an in vitro model to the study the effects of long-term (greater then 3 hr) toxicity of Tri in rPT and rDT cells. The criteria for this model were that it paralleled freshly isolated rPT and rDT cells as closely as possible in terms of the drug metabolism enzymes expressed. Especially important are those enzymes believed to be involved in GSH dependent metabolism (GGT, GST, GRD, GPX, and GGCS). Establishment of this model would aid greatly not only in the study of Tri toxicity, but in the study of chemical-induced nephrotoxicity induced by several other chemicals as well.

Results

Activity of GSH-dependent conjugation enzymes in primary cultures of rPT and rDT cells. Freshly isolated rPT and rDT cells were isolated and placed in primary

Figure 35. Photomicrograph of primary cultures of rPT and rDT cells after 5 days of cell growth.

Freshly isolated rPT (**A**) and rDT (**B**) cells were seeded onto a 35 mm polystyrene dish at a density of 0.5 to 1.0 x 10^6 cells/mL. Cells were grown for 5 days and photomicrographs were taken at 100x magnification on a Carl-Zeiss Confocal Laser Microscope.

A rPT Cells
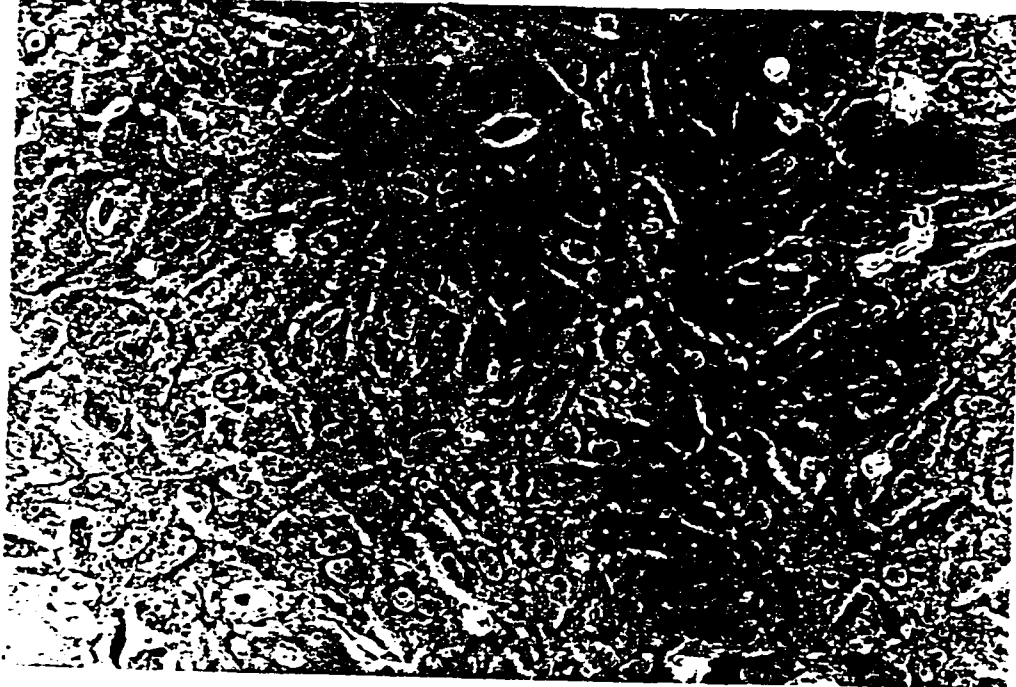
B. rDT Cells

culture as explained in Chapter 2. Cells took approximately 5-7 days to reach confluency (Figure 35). The activity of GGT, GRD, GPX, GST, GGCS, and hexokinase were measured in freshly isolated rPT and rDT cells (Day 0), and in cells isolated from 3 and 5 day old cultures. For the most part, the activity of all these enzymes did not change significantly over the time period tested with the exception of GGCS, which dropped initially but then recovered to Day 0 levels (Figure 36). In the rat kidney, GGT is a marker enzyme for rPT cells while hexokinase is marker enzyme for rDT cells (Lash and Tokarz, 1989). The activity of GGT is 3-5 times higher in freshly isolated rPT cells than in rDT cells. In contrast, hexokinase activity is 2-3 times higher in freshly isolated rDT cells than in rPT cells. Primary cultures of rPT and rDT cells maintained their ratios of GGT and hexokinase activity even after 5 days in culture.

Expression of P450 isoforms in primary cultures of rPT and rDT cells. The expression of P450 isoforms in primary cultures of rPT and rDT cells was studied. The P450 isoforms studied were those characterized in Chapter 4. Of all the P450 isoforms studied, and despite the use of inducers, no expression of CYP2E1, CYP2C11, CYP2B1/2, or CYP3A1/2 was detected by either northern or western blot analysis (data not shown). Northern blot analysis using a cDNA probe to CYP4A1 mRNA that recognizes all CYP4A mRNA forms detected CYP4A mRNA in primary cultures of rDT cells, but not rPT cells, after 5 days of culture (Figure 37A). Treatment of cultures for 3 days with the peroxisomal proliferator ciprofibrate (100 μM) resulted in increased expression of CYP4A mRNA in rDT cells only (Figure 37A). Differences in expression of CYP4A mRNA expression were not due to differences in loading as determined by the expression of 7S RNA (Figure 37B). Western blot analysis using a polyclonal antibody to rat CYP4A showed that a small amount of CYP4A was still expressed in microsomes prepared from primary cultures of rDT cells (Figure 38, lane 1). Interestingly, a small amount of CYP4A protein could still be detected in microsomes isolated from cultures of rPT cells (Figure 38, lane 2).

Figure 36. Activity of GSH-dependent enzymes and hexokinase in 0, 3, and 5 day old primary cultures of rPT and rDT cells.

Freshly isolated rPT and rDT cells were seeded at a density of 0.5 to 1.0 x 10^6 cells/mL and allowed to grow for 3, and 5 days. At each time period, cells were isolated and the activities of GGT, GRD, GPX, GST, GGCS, and hexokinase were determined and compared to activities in freshly isolated cells (Day 0). Data represent the mean ± the SD of at least three separate cell isolations.
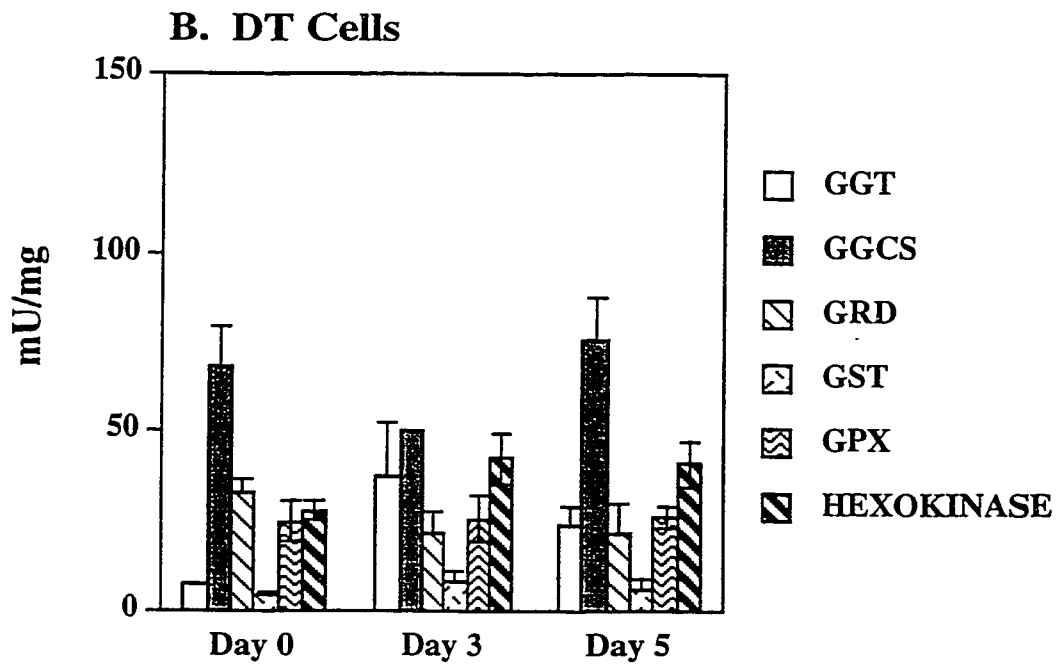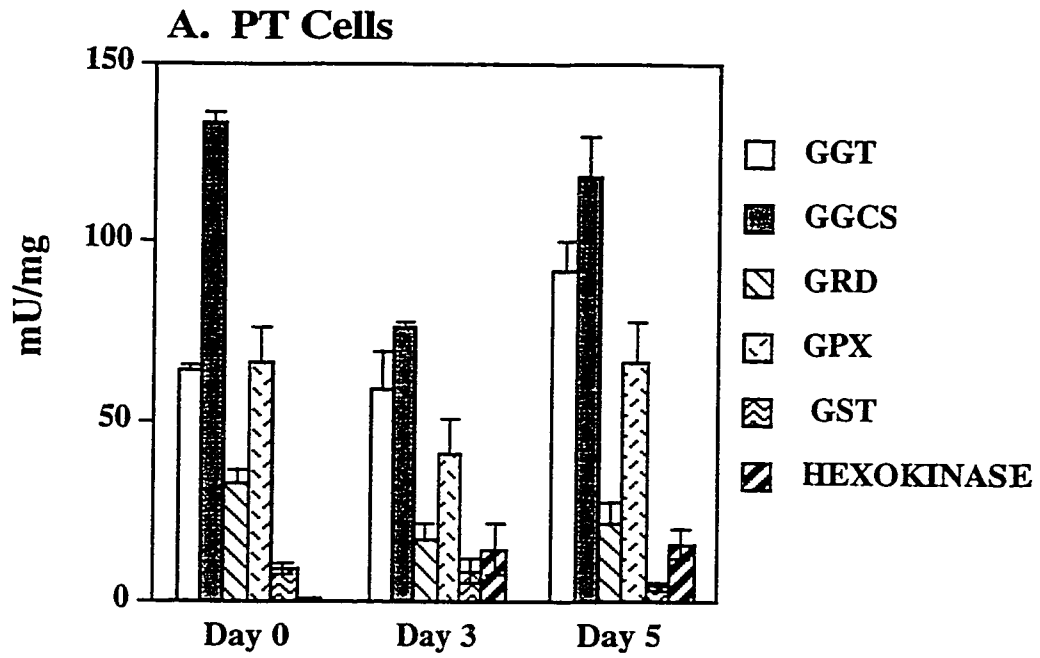
A. PT Cells

B. DT Cells

Figure 37. Effect of ciprofibrate on expression of CYP4A mRNA in primary cultures of rPT and rDT cells.

Freshly isolated rPT and rDT cells were seeded at an density of 0.5 to 1.0 x 10 ^{6} cells/mL and were allowed to grow for 24 hr. After 24 hr, the media were removed and replaced with media containing solvent control (EtOH < 1.0% v/v) or 100 μM ciprofibrate. Cultures were then allowed to grow for an additional 72 hr. Total RNA (10 μg/lane) was fractionated on a formaldehyde/agarose gel, transferred to a nylon membrane, probed with a cDNA complementary to rat CYP4A1 or mouse 7S RNA (loading standard) and autoradiographed.

A. CYP4A1 mRNA

Con Cipro Con Cipro

Kid. PT DT

B. 7S RNA

Con Cipro Con Cipro

Kid. PT DT
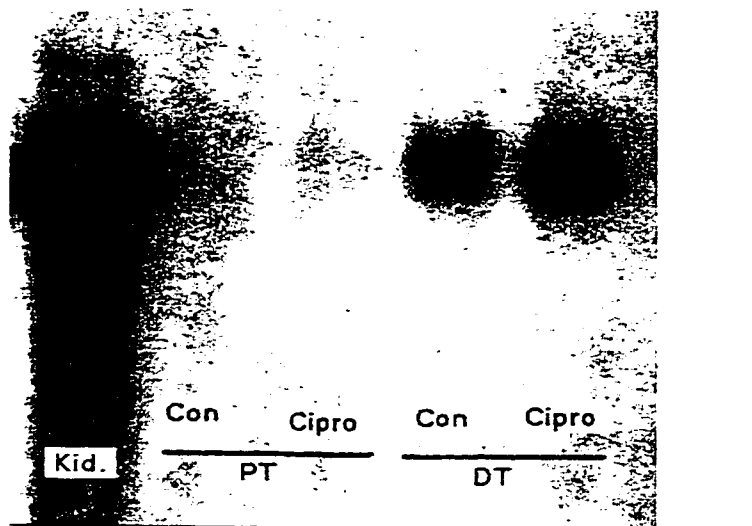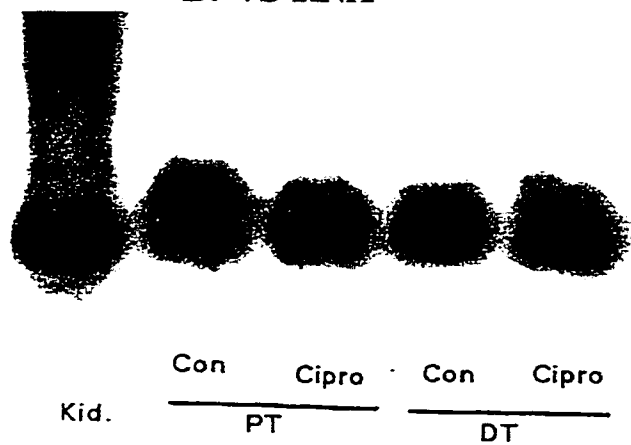
Figure 38. Western blot analysis of CYP4A expression in microsomes isolated from primary cultures of rPT and rDT cells.

Freshly isolated rPT (lane 2) and rDT (lane 1) cells were seeded at a density of 0.5 to 1.0 x 10^6 cells/mL. Cells were allowed to grow for 4 days, after which cells were isolated and microsomes were prepared. Microsomes (60 μg) were subjected to SDS-PAGE followed by transfer to a nitrocellulose membrane that was then incubated with a polyclonal goat anti-rat CYP4A antibody solution.

1   2
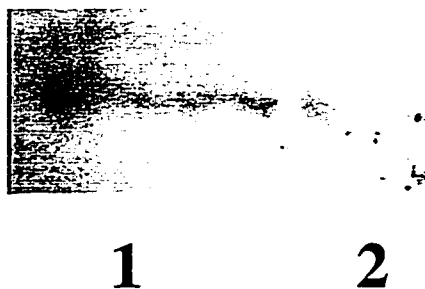
Toxicity of Tri and DCVC to primary cultures of rPT and rDT cells after short-term exposure. As primary cultures of rPT and rDT cells appeared to maintain their activity of GSH-dependent enzymes, and as the expression of at least one P450 isoform was maintained, the toxicity of Tri and DCVC to primary cultures of rPT and rDT cells was studied. The short-term (0 to 6 hr) toxicity of Tri (0, 0.1, 0.2, 0.5, 1, 2, 5, and 10 mM) to primary cultures of rPT and rDT cells was studied by assessment of LDH activity in these cultures (Figure 39A and B). Tri was not toxic at any concentration or time point tested. In contrast, DCVC (0, 0.1, 0.2, 0.5, and 1 mM) was highly toxic to primary cultures of rPT and rDT cells, causing significant increases in LDH release after only 1 hr of exposure to 0.2 mM DCVC (Figure 40A and B). Primary cultures of rDT cells were more susceptible to DCVC toxicity as 0.1 mM caused almost complete cell death after 3 hr of exposure compared to approximately 45% cell death in primary cultures of rPT cells. Furthermore, DCVC toxicity was time- and concentration-dependent in primary cultures of rPT cells and while time-dependent toxicity was observed with DCVC in primary cultures of rDT cells, the concentration-dependent effects of DCVC were not as straight forward. Maximum levels of LDH release were achieved after just 1 hr and were unaltered after 2 hr.

Toxicity of Tri and DCVC to primary cultures of rPT and rDT cells after long term exposures. The toxicity of Tri (0, 0.1, 0.2, 0.5, 1, 2, 5, and 10 mM) to primary cultures of rPT and rDT after 24 and 72 hr of exposure was assessed by measuring the %LDH release from these cultures. Tri was only mildly toxic to primary cultures of both rPT and rDT cells after 72 hr of exposure to high concentrations of Tri (5 and 10 mM) (Figure 41A and B). The toxicity of Tri was time-dependent. In contrast, DCVC was highly toxic to primary cultures of both rPT and rDT cells, causing significant increases in toxicity at concentrations as low as 0.1 mM after just 24 hr (Figure 42A and B). DCVC toxicity was time- and concentration-dependent in primary cultures of rPT cells. In primary

Figure 39. Toxicity of Tri in primary cultures of rPT and rDT cells after short-term exposure.

Freshly isolated rPT and rDT cells were seeded at a density of 0.5 to 1.0 x 10^6 cells/mL and allowed to grow to confluency (approximately 4 to 5 days). The toxicity of Tri at the indicated time points was then determined by assessment of LDH activity. %LDH equals (LDH activity in media)/(LDH activity in media + LDH activity in cells x 100%). LDH activity was determined by the decrease in NADH absorbance at 340 nm. Data are the mean ± SD of at least three separate measurements.

A. PT Cells

B. DT Cells

Exposure Time

—□— 0 Hr

—◇— 1 Hr

—○— 2 Hr

—△— 4 Hr

—⊞— 6 Hr

Figure 40. Toxicity of DCVC in primary cultures of rPT and rDT cells after short-term exposure.

Freshly isolated rPT and rDT cells were seeded at a density of 0.5 to 1.0 x 10^6 cells/mL and allowed to grow to confluency (approximately 4 to 5 days). The toxicity of DCVC at the indicated time points was then determined by assessment of LDH activity. %LDH equals (LDH activity in media)/(LDH activity in media + LDH activity in cells x 100%). LDH activity was determined by the decrease in NADH absorbance at 340 nm. Data are the mean ± SD of at least three separate measurements. *Significant ($P < 0.05$) difference from control.

A. PT Cells

B. DT Cells

Figure 41. Toxicity of Tri in primary cultures of rPT and rDT cells after long term- exposure.

Freshly isolated rPT and rDT cells were seeded at a density of 0.5 to 1.0 x 10^6 cells/mL and allowed to grow to confluency (approximately 4 to 5 days). The toxicity of Tri at the indicated time points was then determined by assessment of LDH activity. %LDH equals (LDH activity in media)/(LDH activity in media + LDH activity in cells x 100%). LDH activity was determined by the decrease in NADH absorbance at 340 nm. Data are the mean ± SD of at least three separate measurements. Control values for %LDH release in rPT cells at 1 and 3 days are 20.1 and 22.9%, respectively. Control values for %LDH release in rDT cells at 1 and 3 days are 19.2 and 25.9%, respectively. *Significant (P < 0.05) difference from control.
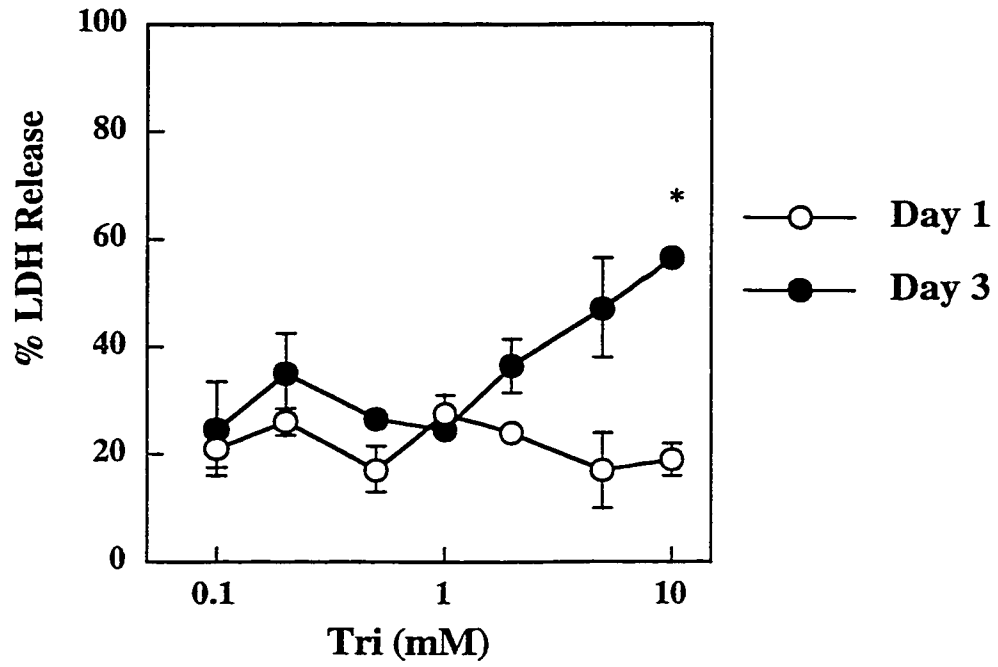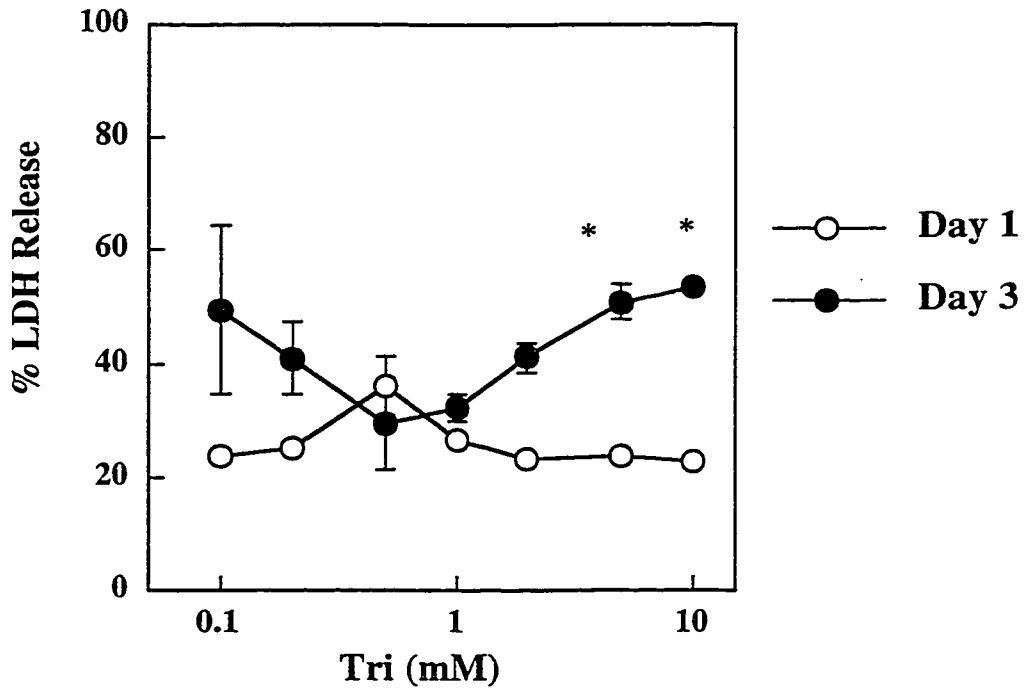
A. PT Cells

B. DT Cells

Figure 42. Toxicity of DCVC in primary cultures of rPT and rDT cells after long-term exposure.

Freshly isolated rPT and rDT cells were seeded at a density of 0.5 to 1.0 x 10^6 cells/mL and allowed to grow to confluency (approximately 4 to 5 days). The toxicity of DCVC at the indicated time points was then determined by assessment of LDH activity. %LDH equals (LDH activity in media)/(LDH activity in media + LDH activity in cells x 100%). LDH activity was determined by the decrease in NADH absorbance at 340 nm. Data are the mean ± SD of at least three separate measurements. *Significant (P < 0.05) difference from control.
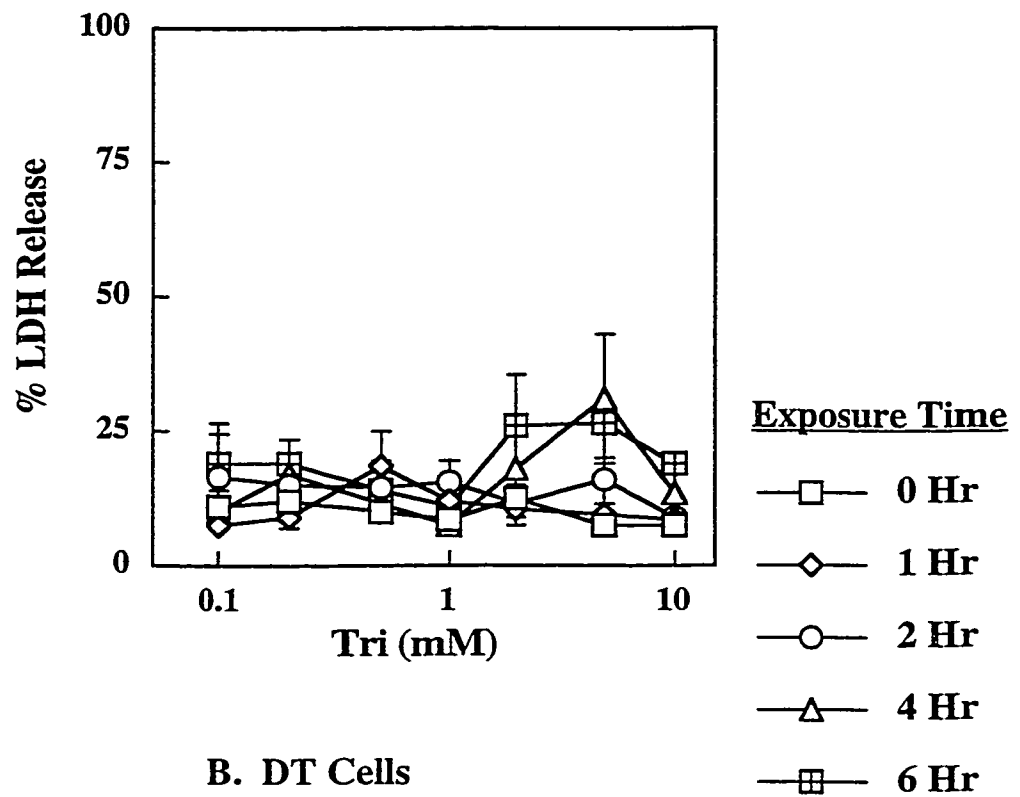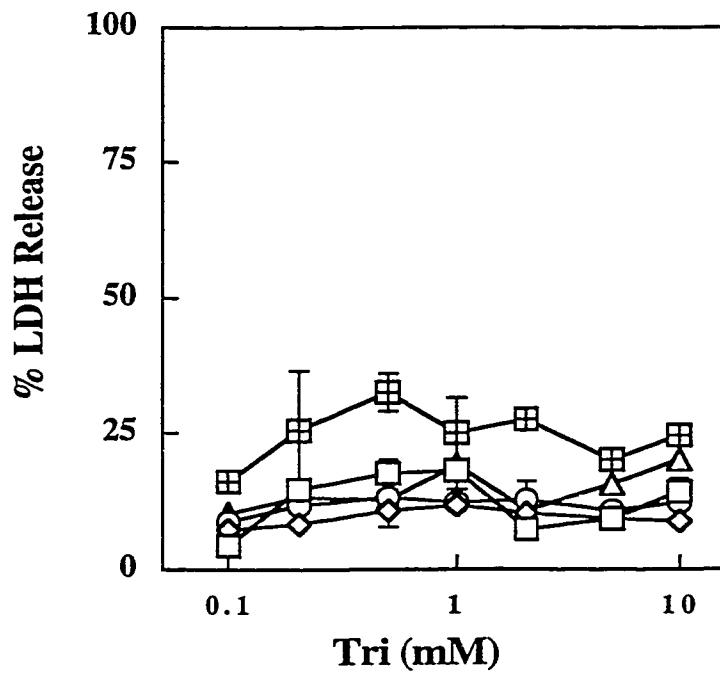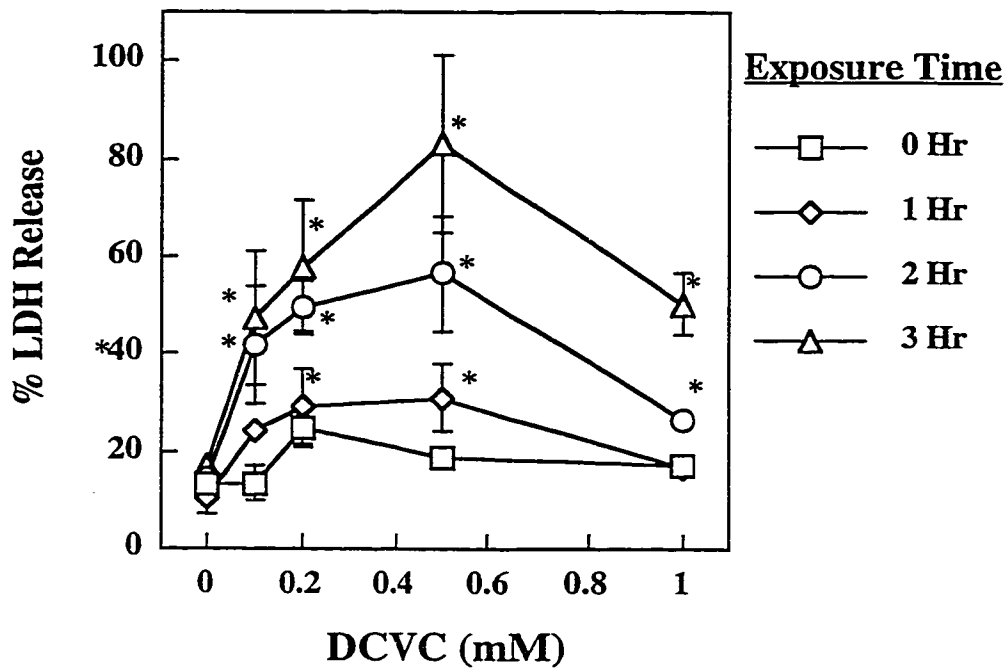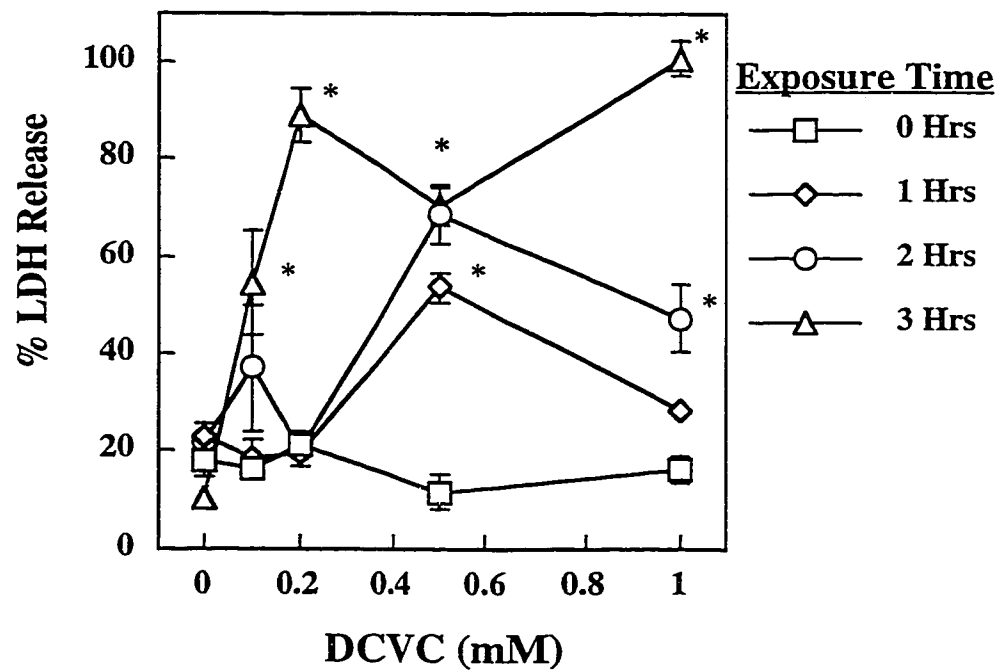
A. PT Cells

B. DT Cells

cultures of rDT cells, DCVC toxicity was time and concentration-dependent up to 5 mM, at which time total cell death occurred, and there was a decrease in total LDH activity. As in the case with short-term exposures (Figure 40A and B), primary cultures of rDT cells were more susceptible to DCVC toxicity as lower concentrations of DCVC caused significant increases in %LDH release and as concentrations above 5 mM caused total cellular death in rDT cells but not rPT cells.

Effect of Tri and DCVC on cellular protein and DNA levels. The alteration in both cellular protein and DNA levels in the cell culture dish as caused by Tri and DCVC was determined by the BCA protein assay kit from Sigma and by fluorescence spectroscopy, respectively. Tri did not alter either cellular protein or DNA levels after 72 hr of exposure to 0, 0.1, 0.2, 0.5, 1, 2, 5, and 10 mM concentrations of Tri (data not shown). In contrast, DCVC (0, 0.1, 0.2, 0.5, 1, 2, 5, and 10 mM) significantly decreased cellular protein and DNA levels after 72 hr of exposure (Figure 43A and B). Concentrations greater than 1 mM decreased cellular protein significantly and concentrations greater than 2 mM resulted in almost total cell death. DCVC at low concentrations (< 0.2 mM) actually resulted in a slight, but significant, increase in cellular DNA levels in rDT cells while concentrations greater than 2 mM resulted in significant decreases in these same cells (Figure 43B). In contrast, DNA levels in primary cultures of rDT cells were not significantly changed at any concentration, although it should be mentioned that the variability in DNA levels in primary cultures of rDT cells was high.

Effect of Tri and DCVC on cytokeratin and vimentin expression. The effect of Tri (10 mM) and DCVC (10 μM) on cytokeratin and vimentin expression in primary cultures of rPT and rDT cells was determined by immunohistochemical staining of the cultures using the methods described in Chapter 2. Freshly isolated rPT and rDT cells were seeded, allowed 24 hr to attach, and then were treated with either Tri or DCVC for 72 hr. After 72, hr the media containing Tri or DCVC were removed and the cells were allowed to recover for 3 hr in the appropriate media. After 3 hr of recovery, cells were washed and

Figure 43. Effect of DCVC on cellular protein and DNA levels in primary cultures of rPT and rDT cells.

Freshly isolated rPT and rDT cells were seeded at a density of 0.5 to 1.0 x 10^6 cells/mL and allowed 24 hr to attach, at which time DCVC at the indicated concentrations was added to the media. Cells were then allowed to grow for 72 hr. Cellular protein and DNA levels were determined as described in Chapter 2. Results are the mean ± SD of at least 3 separate experiments. *Significant ($P < 0.05$) difference from control.

A. Protein Levels
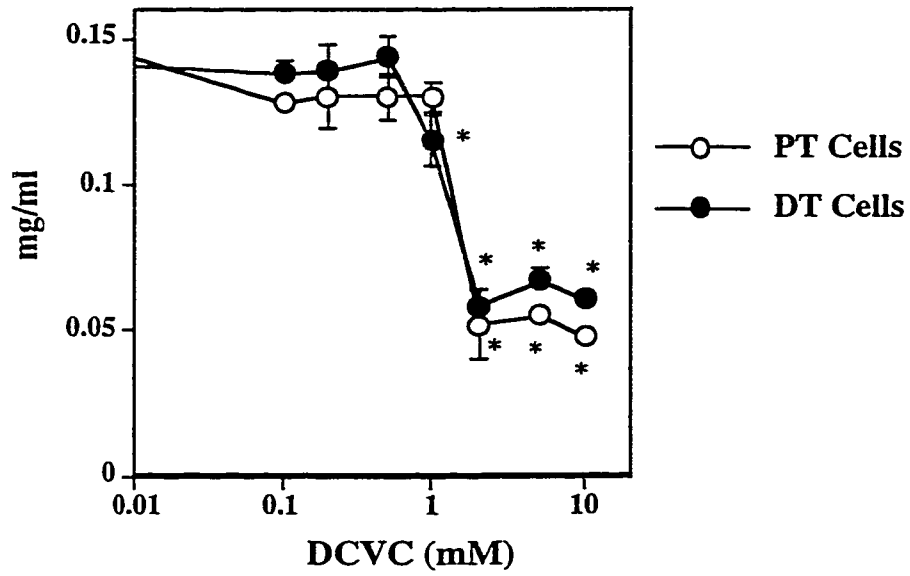
B. DNA Levels
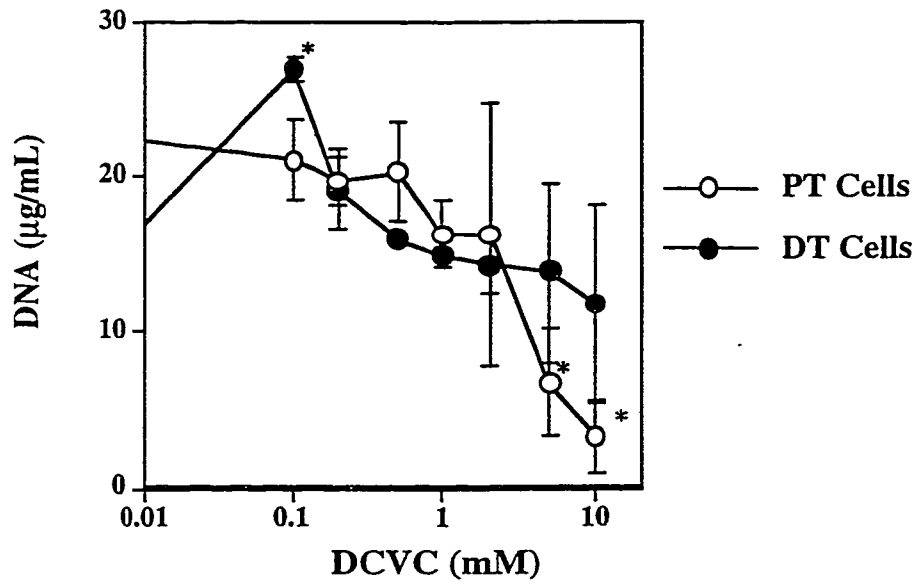
Figure 44. Effect of Tri on cytokeratin expression in primary cultures of rPT and rDT cells.

Freshly isolated rPT (**A**) and rDT (**B**) cells were seeded at a density of 0.5 to 1.0 x 10^6 cells/mL and allowed to grow for 24 hr prior to treatment with Tri (10 mM). After treatment for 72 hr, cells were washed twice with sterile PBS and allowed to recover in appropriate media for 3 hr. Cytokeratin expression was visualized using a monoclonal FITC-conjugated anti-mouse cytokeratin antibody. Photomicrographs were taken at 100X magnification on a Zeiss Confocal Laser Microscope.

A. rPT Cells

Control

Treated (10 mM)

B. rDT Cells

Control

Treated (10 mM)

Figure 45. Effect of Tri on vimentin expression in primary cultures of rPT and rDT cells.

Freshly isolated rPT (**A**) and rDT (**B**) cells were seeded at a density of 0.5 to 1.0 x 10^6 cells/mL and allowed to grow for 24 hr prior to treatment with Tri (10 mM). After treatment for 72 hr, cells were washed twice with sterile PBS and allowed to recover in appropriate media for 3 hr. Vimentin expression was visualizing Texas Red staining using an anti-mouse cytokeratin antibody. Photomicrographs were taken at 100X magnification on a Zeiss Confocal Laser Microscope.

A. rPT Cells
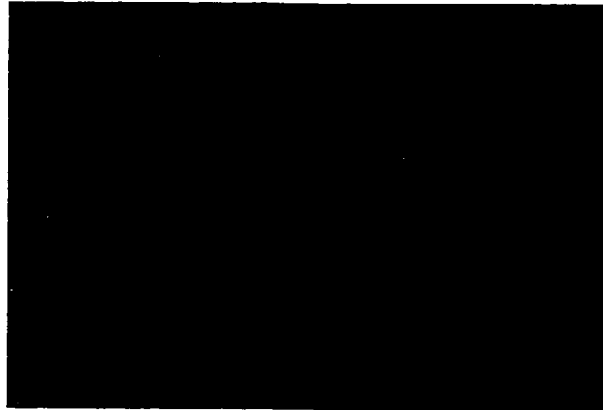
Control
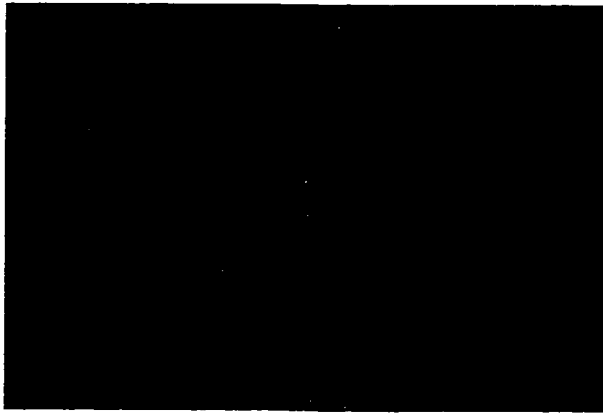
Treated (10 mM)

B. rDT Cells

Control

Treated (10 mM)
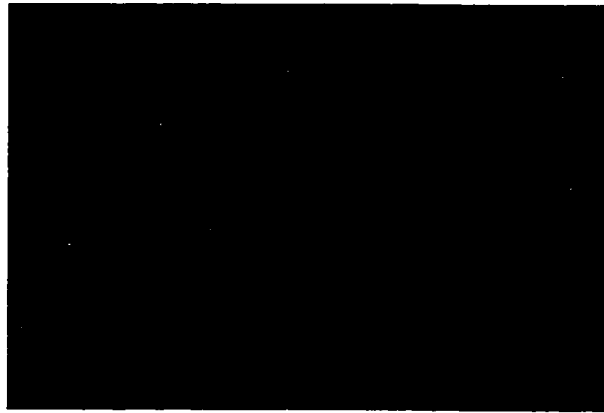
Figure 46. Effect of DCVC on cytokeratin expression in primary cultures of rPT and rDT cells.

Freshly isolated rPT (**A**) and rDT (**B**) cells were seeded at a density of 0.5 to 1.0 x 10^6 cells/mL and allowed to grow for 24 hr prior to treatment with DCVC (10 μM). After treatment for 72 hr, cells were washed twice with sterile PBS and allowed to recover in appropriate media for 3 hr. Cytokeratin expression was visualized using a monoclonal FITC-conjugated anti-mouse cytokeratin antibody. Photomicrographs were taken at 100X magnification on a Zeiss Confocal Laser Microscope.

A. rPT Cells

Control

Treated (10 μM)

B. rDT Cells

Control
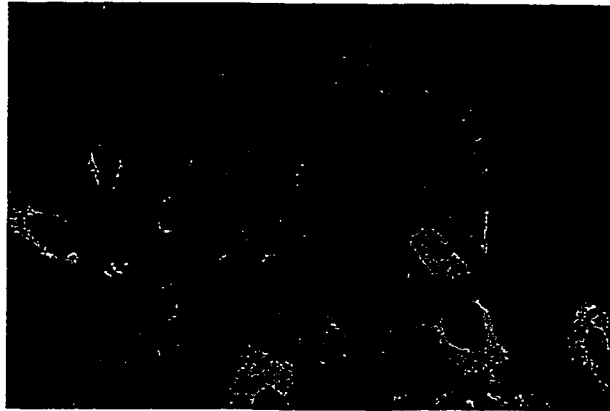
Treated (10 μM)

Figure 47. Effect of DCVC on vimentin expression in primary cultures of rPT and rDT cells.

Freshly isolated rPT (**A**) and rDT (**B**) cells were seeded at a density of 0.5 to 1.0 x 10^6 cells/mL and allowed to grow for 24 hr prior to treatment with DCVC (10 μM). After treatment for 72 hr, cells were washed twice with sterile PBS and allowed to recover in appropriate media for 3 hr. Vimentin expression was detected by Texas Red staining using an anti-mouse cytokeratin antibody. Photomicrographs were taken at 100X magnification on a Zeiss Confocal Laser Microscope.

A. rPT Cells
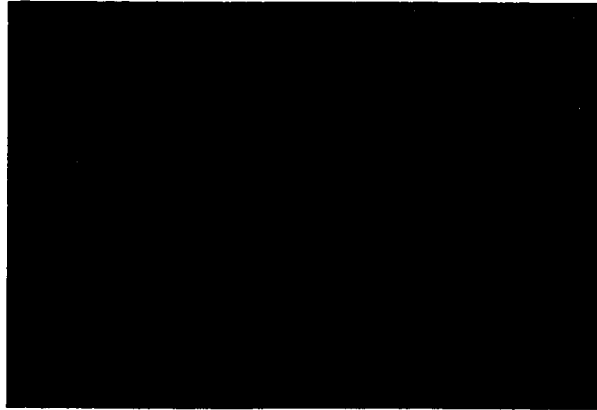
Control

Treated (10 μM)

B. rDT Cells

Control
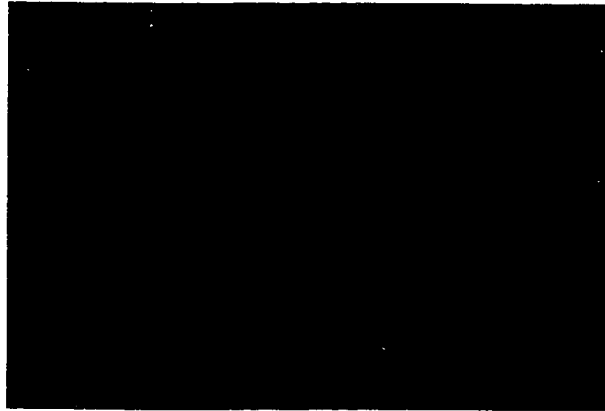
Treated (10 μM)

stained with the appropriate antibody. Treatment of primary cultures of either rPT or rDT cells with Tri or DCVC resulted in no apparent decreases in cytokeratin staining (Figures 44 and 45). Treatment of primary cultures of rPT and rDT cells with Tri caused increased vimentin expression in rDT cells only (Figure 46). DCVC slightly increased vimentin expression in cultures of both rPT and rDT cells (Figure 47). It should be noted that vimentin was not expressed in all control cells, as expected for normal epithelial cells.

Discussion

Data from this study showed that primary cultures of rPT and rDT cells are capable of maintaining most of their activity of GSH-dependent enzymes and hexokinase. More importantly, the ratio of GGT to hexokinase in these cultures was maintained as compared with freshly isolated rPT and rDT cells (Figure 36). Furthermore, primary cultures of rPT and rDT cells maintained cytokeratin and vimentin levels. (Figures 44-47). Thus, these cells appear to be epithelial in nature and appear to be valid models to study of chemical-induced nephrotoxicity involving GSH-dependent bioactivation enzymes. With the exception of CYP4A, the expression of all P450 isoforms tested was not detectable in primary cultures of rPT and rDT cells. Loss of P450 expression in primary cultures is not uncommon, as many studies have reported such a phenomenon (Zangar et al., 1995, Kocarek et al, 1993). The maintenance of CYP4A isoforms over that of others (CYP2C, CYP2B, CYP2E1) may be a result of the higher levels of expression in freshly isolated cells as compared to the other isoforms. The loss of CYP4A over time is obviously not a result of the loss of the gene as CYP4A was inducible with ciprofibrate (Figure 37). This fact, combined with the fact that mRNA for CYP2E1 and CYB2B could not be detected, suggests that a decrease in transcription, and not translation, causes the decrease in expression of these P450 isoforms.

Toxicity of Tri and DCVC in primary cultures of rPT and rDT cells. Tri toxicity after short-term exposure (less then 6 hr) in primary cultures of rPT and rDT cells

was less than that measured in freshly isolated rPT and rDT cells (Figures 13, 14, 39 and 40). Primary cultures of rPT and rDT cells are approximately 70-90% confluent at the start of the toxicity trials. In contrast, freshly isolated rPT and rDT cells are in suspensions. This difference may account for the difference in toxicity seen between the two studies. It should be noted that Tri is only modestly toxic to freshly isolated rPT and rDT cells, causing only approximately 20% increases in LDH release with a basal level of LDH release of approximately 20% at time zero. In contrast, primary cultures of rPT and rDT cells have had ample time to grow and to shed dead cells. As a result, the basal %LDH activity in cultures is much lower than that in freshly isolated cells. This may also account for the decreased toxicity of Tri in primary cultures of rPT and rDT cells. As expected, exposure of primary cultures of rPT and rDT cells to Tri for long time periods (greater then 24 hr) results in increased toxicity as assessed by %LDH release. Tri was toxic after three days of exposure to concentrations of at least 5 mM Tri (Figure 41). Tri was equally toxic to primary cultures of rPT and rDT cells.

Unlike Tri, DCVC caused significant increases in %LDH release in primary cultures of rPT and rDT cells after both long- and short-term exposure. Concentrations as low as 0.2 mM caused toxicity to primary cultures of rPT and rDT cells after only 1 hr of exposure (Figure 40). As seen in freshly isolated rPT and rDT cells (Lash et al., 1994), primary cultures of rDT cells were more susceptible to DCVC toxicity as the onset of toxicity was faster and occurred at lower concentrations of DCVC in these cells. Concentrations above 1 mM resulted in complete cell death in these cells. As expected, DCVC caused significant increases in %LDH release in primary cultures of rPT and rDT cells after longer-term exposure (Figure 42). DCVC was toxic at concentrations as low as 0.1 mM in rDT cells. Concentrations higher than 2 mM resulted in complete cell death, as determined by decreases in cellular protein (Figure 43). Interestingly, DCVC at low concentrations caused a significant increase in DNA levels, which was followed by significant decreases after exposure to higher concentrations (Figure 43). Alterations in

either cellular protein or DNA levels were not observed with Tri at any time or concentration (data not shown). These data support the hypothesis that DCVC is one, if not the major, metabolite responsible for the renal cellular toxicity of Tri.

Effect of Tri and DCVC on cytokeratin and vimentin expression. DCVC induces stimulation of cellular proliferation or repair processes (Eyre et al., 1995a,b; Hatzinger et al., 1988; Kays et al., 1995; Vamvakas et al., 1989). Cytokeratin and vimentin expression was used to study these processes in primary cultures of rPT and rDT cells. (Figures 44-47). Exposure of primary cultures of rPT and rDT cells to Tri (10 mM) or DCVC (10 μM) for 3 days followed by 3 hr of recovery did not result in any alteration in cytokeratin staining. These data suggest that neither Tri nor DCVC at the doses used or time tested are causing rPT and rDT cells to lose their epithelial status as based on cytokeratin staining. Vimentin can be a marker for cellular sub-lethal injury and repair (Hatzinger et al., 1988). Under normal conditions, primary cultures of rPT and rDT cells do not express vimentin (Figure 45 and 47). Exposure of primary cultures of rPT and rDT cells to Tri resulted in the detection of low levels of vimentin in rDT cells only while DCVC treatment resulted in increased expression of low levels of vimentin in both rPT and rDT cells. These data suggest that both Tri and DCVC may be causing sub-lethal injury and repair. Thus, both Tri and DCVC have the ability to alter genetic expression in these cells. The mechanisms causing the increase in vimentin expression in these cells are unknown.

In summary, primary cultures of rPT and rDT cells maintain their expression and ratio of GSH-dependent enzymes as compared to freshly isolated cells. Thus, these cells may prove useful as models for the study of chemical-induced injury to the kidney where the bioactivation mechanism involves these enzymes. Expression of every P450 isoform expressed in freshly isolated rPT and rDT cells decreased after 48 hrs of primary culture of these cells. The only P450 isoform whose expression could be maintained was CYP4A. Reasons for the decrease in expression were not determined. Tri and DCVC were toxic to both rPT and rDT cells after long periods of exposure, with DCVC being highly toxic.

Both Tri and DCVC appeared to cause sub-lethal injury and repair in these cells but the mechanism of this response was not studied. In conclusion, primary cultures of rPT and rDT cells appear to be valid models for the study of Tri and DCVC induced cytotoxicity. The lack of P450 isoforms in these models precludes their use for study of oxidative Tri metabolism.

Chapter 8

Isolation and Characterization of Human Renal Proximal Tubular Cells

Introduction

Results presented in the previous chapters have focused on drug metabolism and chemical-induced toxicity of Tri and thiophenes in the rat kidney. As stated previously, one of the goals of this research was to determine differences in the drug metabolism enzymes expressed between rat and human kidneys. Determination of the drug metabolism enzymes expressed in the human kidney along with data on their role in the toxicity and metabolism of several chemicals would decrease the uncertainty in the extrapolation to humans of data produced in animals. Furthermore, development of a in vitro model that mimics the in vivo human kidney cell would be a great benefit in the study of risk assessment, pharmacology, and toxicology, among other disciplines. Although several kidney models currently exist, the drug metabolism capability of these models has never been thoroughly studied. Furthermore, many of the models that do exist are transformed cells lines and by definition, are no longer suitable for comparison to the in vivo state. The goal of this chapter is to determine the drug metabolism enzymes expressed in the human kidney. The effect of the presence, or absence, of these enzymes on Tri metabolism and toxicity will then be studied. The enzymes studied will be similar to those characterized in the rat, as they can metabolize similar substrates and/or belong to the same gene family.

Please refer to Chapter 1 for a review of P450 and GST nomenclature in order to understand the differences in P450 isoforms studied in the human kidney compared with those studied in the rat. Previous studies have shown that human kidney microsomes express CYP3A5, CYP4F2, and CYP4A11, but not CYP2A6, CYP2C8, CYP2C9, CYP2C19, CYP2E1, or CYP3A4 (Powell et al., 1998). Of the P450 isoforms expressed in the human kidney, CYP4A11 was chosen for study as it metabolizes similar substrates in human liver

as CYP4A does in rat liver and kidney (i.e., lauric acid). CYP3A5 was not studied as CYP3A isoforms were found not to be expressed in the rat kidney. CYP4F2 substrate specificity is currently under study (Lasker et al., 1998) and at the current time no P450 isoform in the rat kidney has been isolated showing similar sequence identity to human CYP4F (i.e. same gene family such as human **CYP4A11** and rat **CYP4A1/2/3/8**).

Results

Isolation and characterization of hPT cells from human kidney cortical slices. Freshly isolated human kidney cortical slices were obtained from the Human Tissue Resources Core in the Department of Pathology at Harper Hospital (Detroit, MI). Slices were analyzed by a Pathologist and all slices were determined to be normal (healthy, non-cancerous, non-diseased, etc.) tissue. The age and gender of the subject from whom the tissue was isolated is listed in Table 11. Cause of death is not listed in Table 11 because in all cases just one kidney was removed for either biopsy or other purposes.

Activity of GSH-dependent enzymes in freshly isolated hPT cells. Freshly isolated hPT cells were prepared as described in Chapter 2. The activities of GGT, GGCS, GST, GRD, GPX, and hexokinase were then determined (Figure 48). Typical viability of these cells after isolation was approximately 90% as determined by Trypan Blue exclusion and LDH activity assays. Freshly isolated hPT cells had approximately ten times higher levels of GGT than hexokinase. Furthermore, levels of GGCS, GRD, and GPX were all relatively high compared to rat kidney cells. GST activity was approximately 4-fold lower than that measured in freshly isolated rat kidney cells.

CYP4A11 expression in freshly isolated hPT cells. Freshly isolated hPT cells from 4 male and 4 female patients ranging in age from 44 to 77 years of age were analyzed for the expression of CYP4A11 using a polyclonal rabbit anti-human antibody (Figure 50A and B). All of the patients tested expressed CYP4A11 (Figure 49A) and there was no

Table 11. Data on human kidney samples.

Freshly isolated human renal cortical slices were obtained from the Human Tissue Resources Core in the Department of Pathology in Harper Hospital (Detroit, MI). Slices were analyzed by a resident Pathologist and scored as normal tissue. All samples were weighed and rinsed in sterile PBS solution prior to analysis. Patient number corresponds to sample number at the Human Tissue Resources Core, which was used to obtain patient's age and gender.

Patient Number	Sex	Age	Patient Number	Sex	Age
97-532	F	58	97-534	M	62
97-540	F	50	97-541	F	54
97-542	F	68	98-001	M	72
98-002	M	77	98-026	M	44
98-037	M	56	98-045	F	63
98-057	F	45	98-058	F	63
98-077	F	45	98-105	F	47
98-183	M	56	98-240	F	69
98-349	F	51	98-352	M	70
98-355	F	75	98-358	M	66
98-415	F	77	99-026	F	77
98-015	M	68			

Figure 48. Activity of GSH-dependent enzymes in freshly isolated hPT cells.

Freshly isolated hPT cells were obtained from human renal cortical slices from three patients using enzymatic digestion in the presence of collagenase followed by differential centrifugation. Cells were either used immediately for enzymatic assays or frozen for future assays. Typically, 1-2 g of tissue yielded 50-80 x 10^6 cells. Typical viability was approximately 90% as based on Trypan Blue exclusion and LDH activity assays. Data represent the mean ± SD of at least 3 separate measurements.
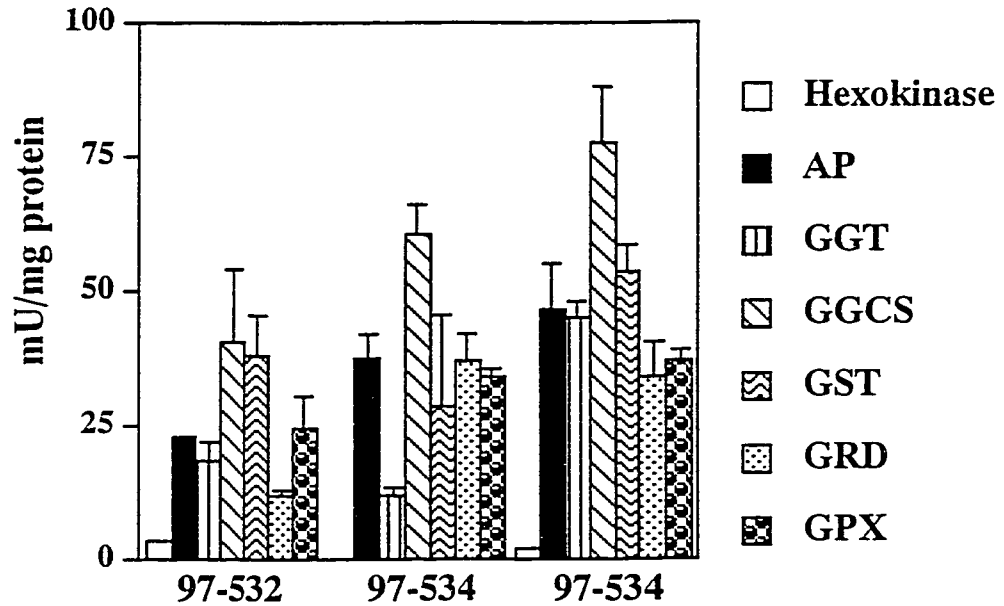
Figure 49. Western blot analysis of CYP4A11 expression in freshly isolated hPT cells.

A. Purified human liver CYP4A11 (1 μg) and freshly isolated hPT cells (60 μg) were subjected to SDS-PAGE and then transferred to a nitrocellulose blot that was then incubated with a polyclonal rabbit anti-human antibody to CYP4A11. Numbers refer to individual patient's samples. B. Densitometric analysis of CYP4A11 expression from samples represented in A. Densitometry was performed by scanning blots into a Power Macintosh 8100/100 computer using a Microtek ScanMaker IIsP scanner at a resolution of 150 lpi, using Adobe photoshop 5.0 and NIH Scan Image software.

A

B
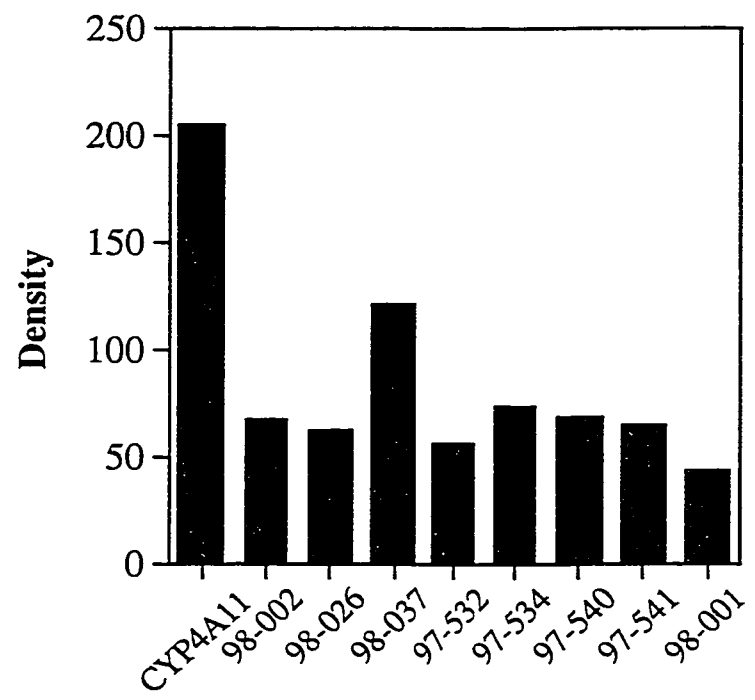
significant difference in expression levels between patients, with the exception of patient 98-037, as determined by densitometric analysis (Figure 49B). There was also no observable difference in expression of CYP4A11 between male and female patients as determined by densitometric analysis (Figure 49B), although it should be pointed out that the sample size is relatively low. The activity of CYP4A11 was assessed by measurement of lauric acid hydroxylation using HPLC analysis as described in Chapter 2. In microsomes prepared from homogenates of human renal cortical slices, ω-lauric acid formation was linear up to 30 min with rates of approximately 0.4 to 0.5 nmol/min per mg protein (Figure 50).

Expression of GST isoforms in freshly isolated hPT cells. The expression of GST isoforms corresponding to those studied in freshly isolated rPT and rDT cells (GSTα, GSTμ, and GSTπ) was studied in freshly isolated hPT cells. Freshly isolated hPT cells from 2 male and 3 female patients ranging in age from 44 to 63 years of age were analyzed for expression of GSTA using a polyclonal goat anti-rat GSTα antibody that also recognizes human GSTA (Figure 51A and B). All of the patients tested expressed GSTA (Figure 51A). Males appeared to express lower levels of GSTA than females based on densitometric analysis (Figure 51B). GSTP expression was measured in 2 male and 3 female patients ranging in age from 44 to 63 years of age using a polyclonal rabbit anti-human GSTP antibody (Figure 52A and B). There was high variability in GSTP expression among the patients tested, with patient number 97-532 expressing low levels of GSTP and patient number 98-037 expressing no detectable level of GSTP (Figure 52A). There was no significant difference in GSTP expression between male and female patients as determined by densitometric analysis (Figure 52B). The expression of GSTM in 2 male and 4 female patients was analyzed by western blot analysis using a polyclonal goat anti-rat antibody that also recognizes human GSTM. GSTM was not detected in either cytosol isolated from whole human kidney cortical slices or in freshly isolated hPT cells from any patient (data not shown). Finally, GSTT expression was analyzed by

Figure 50. ω-Lauric acid hydroxylation in microsomes from homogenates of human renal cortical slices.

Activity of CYP4A11 was determined by analysis of the appearance of ω-lauric acid by HPLC analysis as described in Chapter 2. Results are the means ± SD of measurements from 3 separate preparations of microsomes.
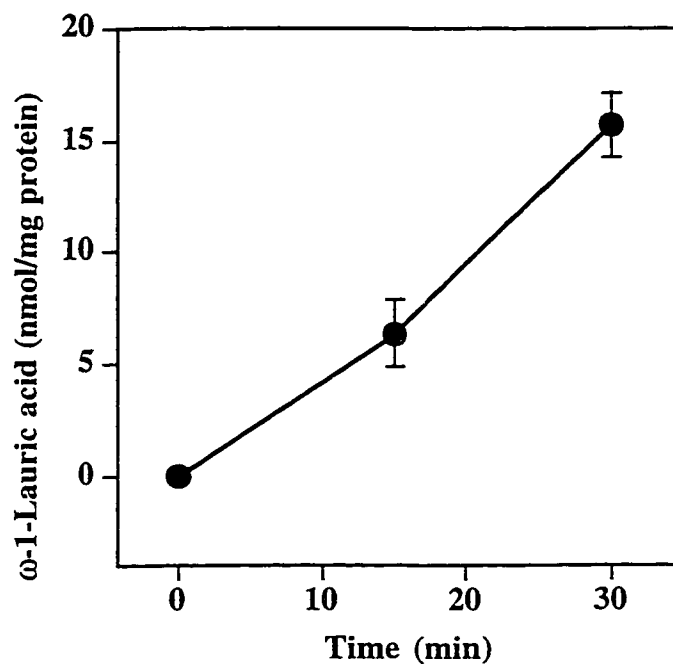
Figure 51. Western blot analysis of GSTA expression in freshly isolated hPT cells.

A. Human kidney cytosol (5 µg) and hPT cells (60 µg) were subjected to SDS-PAGE and then transferred to a nitrocellulose blot that was then incubated with a polyclonal goat anti-rat antibody to GSTα that also recognized human GSTA. Numbers refer to individual patient samples. **B.** Densitometric analysis of GSTP expression from samples represented in **A.** Densitometry was performed by scanning blots into a Power Macintosh 8100/100 computer using a Microtek ScanMaker IIsP scanner at a resolution of 150 lpi, using Adobe photoshop 5.0 and NIH Scan Image software.
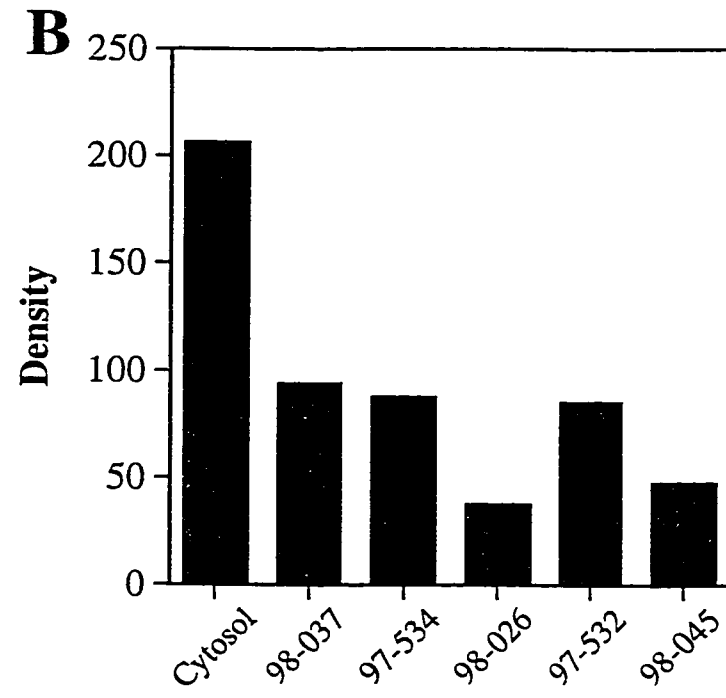
Figure 52. Western blot analysis of GSTP expression in freshly isolated hPT cells.

A. Human kidney cytosol (5 µg) and freshly isolated hPT cells (60 µg) were subjected to SDS-PAGE and then transferred to a nitrocellulose blot that was then incubated with a polyclonal rabbit anti-human antibody to GSTP. Numbers refer to individual patient samples. **B.** Densitometric analysis of GSTP expression from samples represented in A. Densitometry was performed by scanning blots into a Power Macintosh 8100/100 computer using a Microtek ScanMaker IIsP scanner at a resolution of 150 lpi, using Adobe photoshop 5.0 and NIH Scan Image software.
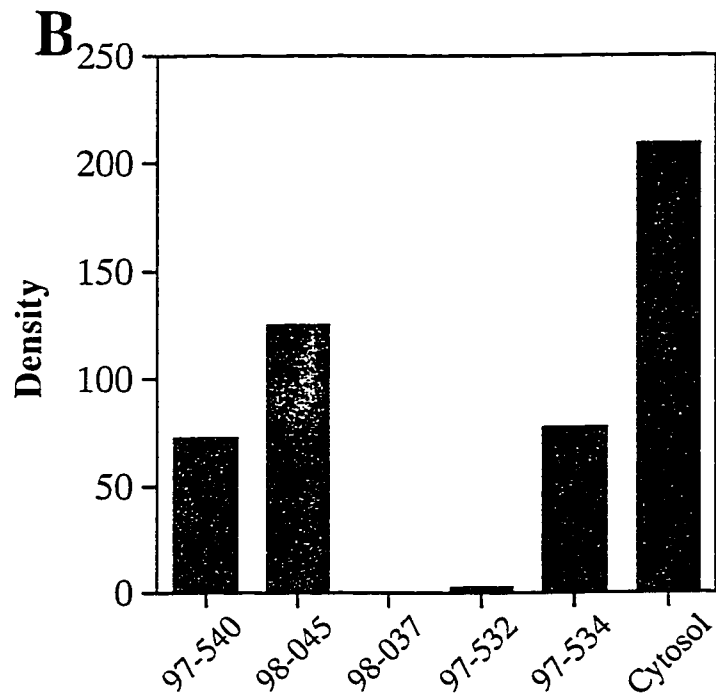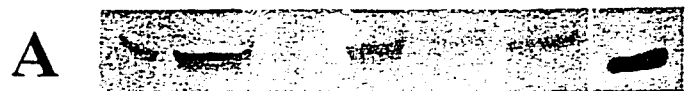
Figure 53. Western blot analysis of GSTT expression in freshly isolated hPT cells.

A. Human kidney cytosol (5 μg) and freshly isolated hPT cells (60 μg) were subjected to SDS-PAGE and then transferred to a nitrocellulose blot that was then incubated with a polyclonal rabbit anti-human antibody to GSTT. Numbers refer to individual patient samples. B. Densitometric analysis of GSTT expression from samples represented in A. Densitometry was performed by scanning blots into a Power Macintosh 8100/100 computer using a Microtek ScanMaker IIsP scanner at a resolution of 150 lpi, using Adobe photoshop 5.0 and NIH Scan Image software.

A

B
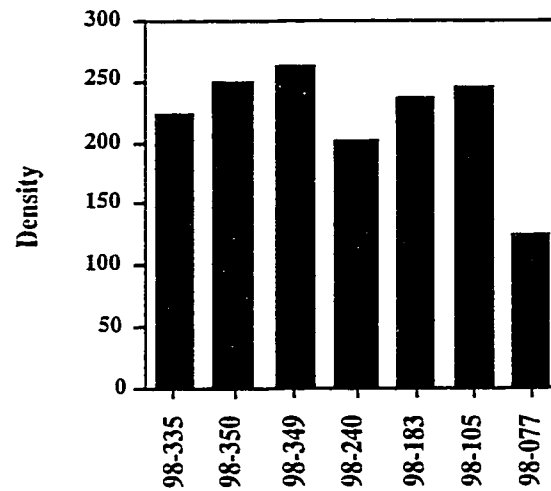
western blot analysis using a polyclonal human anti-rabbit GSTT antibody. GSTT was detected in all patients tested (Figure 53A) and levels did not vary significantly between the patients tested (Figure 53B).

Toxicity of Tri in freshly isolated hPT cells. The toxicity of Tri in hPT cells was assessed by measurement of the LDH activity in duplicate samples from two separate patient samples (99-015 and 99-026, n = 4 total). The concentrations of Tri used were equal to those tested in rPT cells in Chapter 5. Testing a range of concentrations similar to those tested in rPT cells (Chapter 5) was not done due to the lack of sufficient tissue. Tri at both 0.5 mM and 10. mM was toxic to hPT cells as determined by decreases in LDH activity after 2 hr (Figure 54). Pretreatment of cells with metyrapone (0.25 mM) did not alter the toxicity of Tri at either concentration.

GSH Conjugation of Tri in freshly isolated hPT cells. GSH conjugation of Tri was measured in 3 separate patient samples (97-415, 98-077, 98-078) by determining the formation of DCVG after incubation with 0, 0.25, 0.5, 1, 2, 4, 8 and 10 mM Tri for 30 min. Lineweaver-Burke analysis of DCVG formation in these three samples resulted in a curve yielding an r^2 of 0.934 (Figure 55A). This curve resulted in apparent K_m and V_{max} values of 1.3 mM and 0.20 nmol/min per mg protein, respectively. Eadie-Scatchard analysis of DCVG formation in hPT cells resulted in two distinct curves with r^2 values of 0.937 and 0.963 (Figure 54B, lines 1 and 2, respectively). Line 1 resulted in apparent K_m and V_{max} values of 0.58 mM and 0.11 nmol/min per mg protein, respectively. Line 2 resulted in apparent K_m and V_{max} values of 29.4 mM and 1.35 nmol/min per mg protein, respectively.

Oxidative metabolism of Tri by P450 in freshly isolated hPT cells. Tri metabolism to CH was studied in human renal cortical microsomes from 2 male and 2 female patients, ranging in age from 40 to 63 years. CH formation was only detected in one patient (Female, Patient # 98-077) at the highest concentration of Tri tested (2 mM). The rate of formation of CH was 0.127 ± 0.01 nmol/min per mg protein (n = 3).

Figure 54. Effect of P-450 inhibition on the cytotoxicity of Tri in freshly isolated hPT cells.

Freshly isolated hPT cells (0.5. to 10 x 10^6 cells/mL) were preincubated in the presence of either solvent control (i.e., 1.0%, v/v, acetone) or metyrapone (0.25 mM) for 15 min prior to the addition of Tri. At the indicated time points, the activity of LDH was determined. Results are the means $\pm$ SD of at least 3 separate kidney samples. *Significant difference ($P < 0.05$) from control.
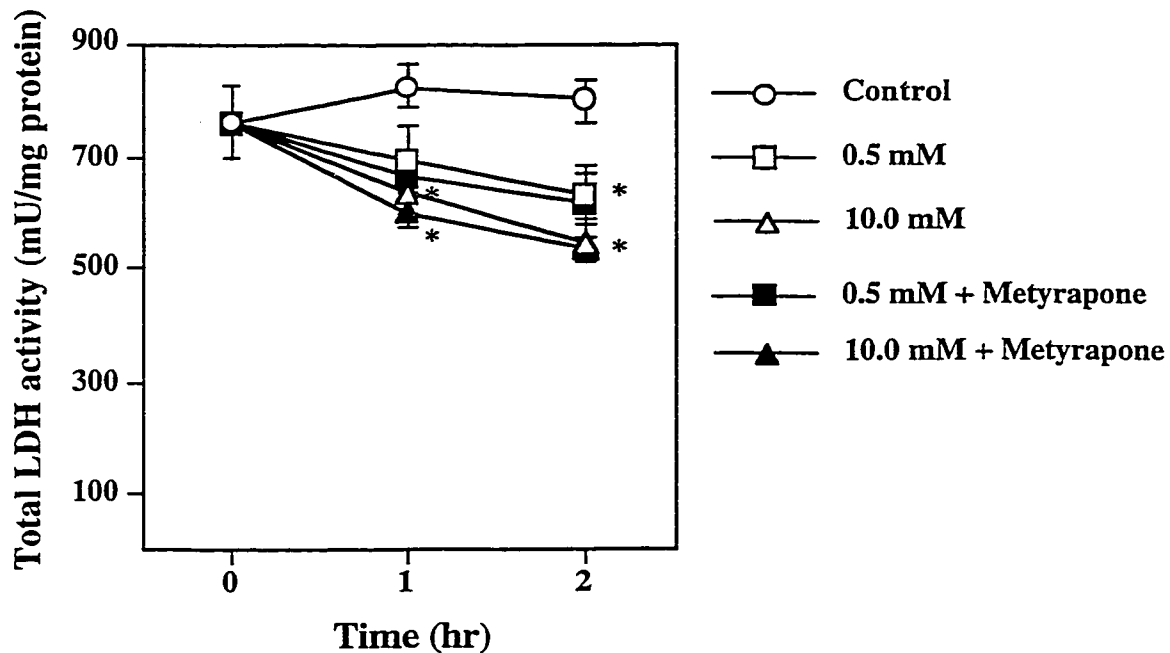
Figure 55. Kinetic analysis of GSH conjugation of Tri in freshly isolated hPT cells.

Freshly isolated hPT cells (0.5 to 2 mg of protein/mL) were lysed and incubated in the presence of 0-10 mM Tri and 5 mM GSH at 37°C for 30 min. Metabolism was measured by quantitation of DCVG formation by HPLC after derivatization. Controls included the absence of Tri. Results were analyzed by both Lineweaver-Burke (**A**) or Eadie-Scatchard (**B**) analysis. Results are the means ± SD of 3 separate samples.

A. Lineweaver-Burke Plot
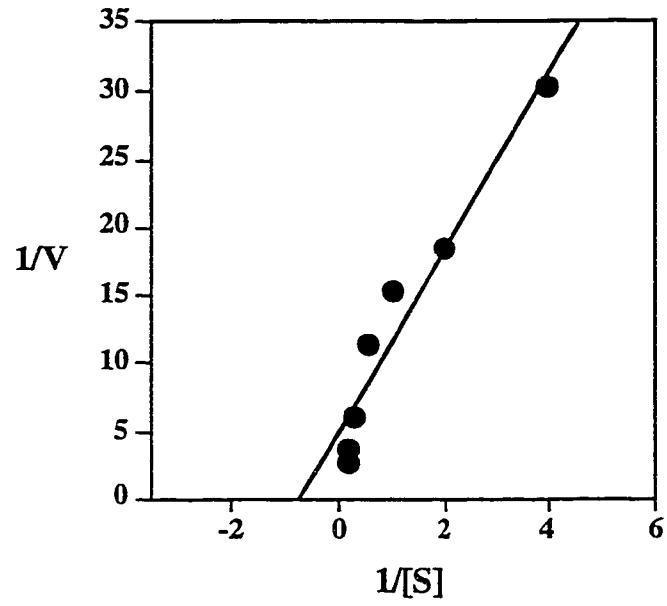
B. Eadie-Scatchard Plot
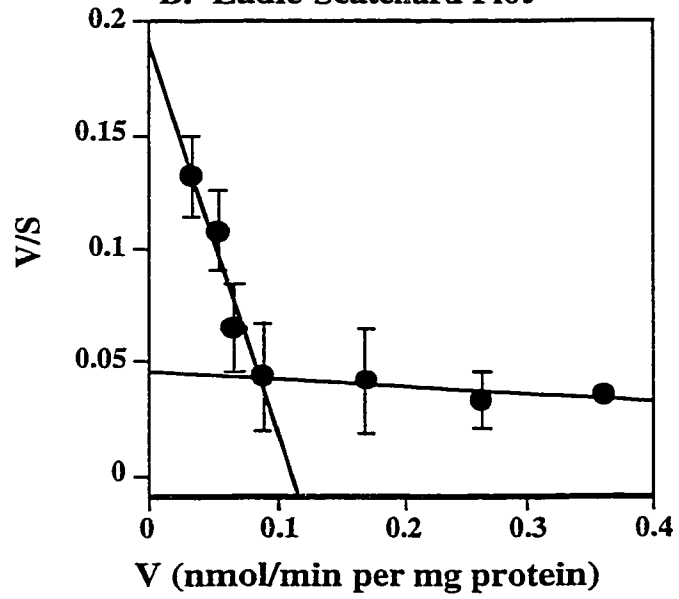
Toxicity of DCVC in freshly isolated hPT cells. Freshly isolated hPT cells were preincubated with aminooxyacetic acid (AOAA) (0.1 mM), an cysteine S-conjugate β-lyase inhibitor, or solvent control ([EtOH] < 1.0 % v/v) for 15 min prior to the addition of 0.5 or 1 mM DCVC. These concentrations were used as they had been shown to be toxic in freshly isolated rPT cells (Lash et al., 1994). Toxicity was assessed by measurement of LDH activity. DCVC caused both time- and concentration-dependent toxicity to hPT cells, causing approximately 60-75% LDH release after 2 hr of exposure to 1 mM DCVC (Figure 56). DCVC did not cause any decrease in LDH activity. Pretreatment of cells with AOAA did not alter the toxicity of DCVC at any time point or with any concentration used.

Effect of duration of cell culture on activity of GSH-dependent enzymes. Freshly isolated hPT cells were seeded at 0.5 to 1.0 x 10^6 cells/mL in the same media used for primary cultures of rPT cells. Cells were grown to confluency (approximately 4 to 5 days) and isolated by trypsin-EDTA digestion. At each passage, one half of the cells were harvested and the other half was passaged. Figure 57 displays the activity of GSH-dependent enzymes in freshly isolated hPT cells (passage # 0) and 4 subsequent passages. The ratios of GGT to hexokinase dropped slightly compared with freshly isolated cells but GGT activities were still 4-5 times higher than hexokinase activity. Hexokinase activity was not detected in passage 1 but was detected in passages 2-4. GRD activity significantly increased in passage 1 but dropped significantly in passages 2-4. GGT activity remained relatively constant until passage 4, where a significant increase was detected. The activities of GST and GPX remained unchanged until passage 2, after which a significant decrease was measured. GGCS activities remained unchanged throughout the experiment.

Effect of duration of cell culture on expression of CYP4A11 in hPT cells. Freshly isolated hPT cells were seeded at a density of 0.5 to 1.0 x 10^6 cells/mL. After 24 hr, media were removed and media containing either solvent control ([EtOH] < 1.0%, v/v)

Figure 56. Toxicity of DCVC in freshly isolated hPT cells.

Freshly isolated hPT cells (0.5. to 10 x 10^6 cells/mL) were preincubated in the presence of either solvent control (i.e., 1.0%, v/v acetone) or AOAA (0.1 mM) for 15 min prior to the addition of DCVC. At the indicated time points, the percent LDH release was determined. Results are the means ± SD of at least 3 separate kidney samples. *Significant difference ($P < 0.05$) from control.
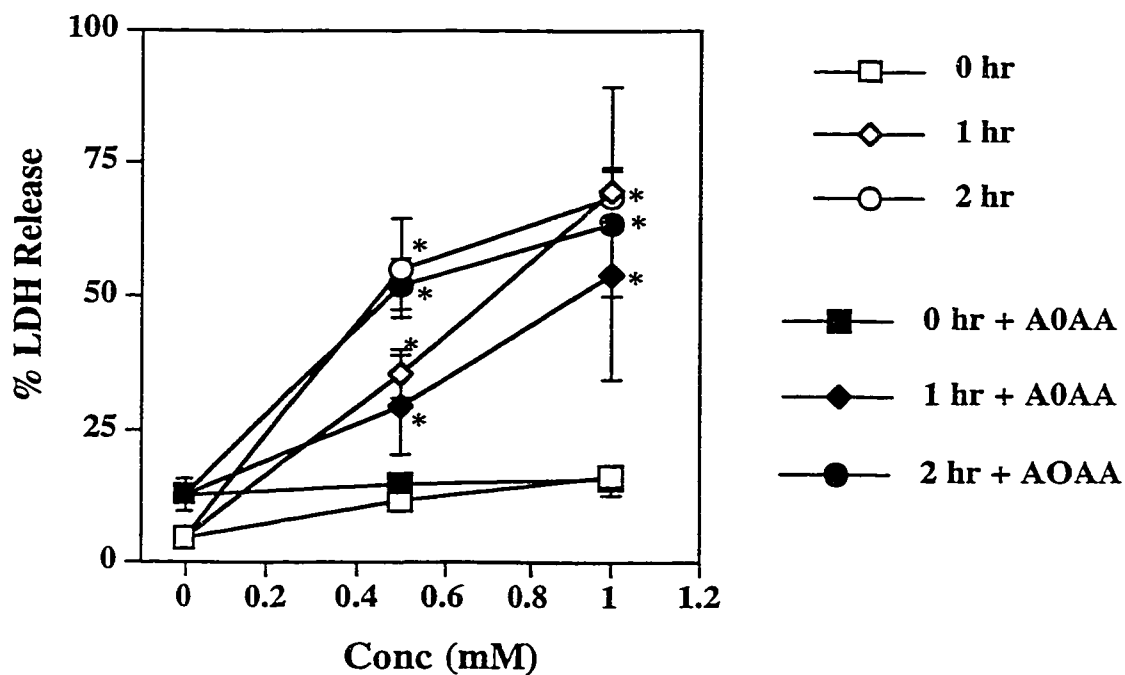
Figure 57. Effect of passage of hPT cells on GSH-dependent enzymes.

Freshly isolated hPT cells were isolated and seeded at a density of 0.5 to 1.0 x 10⁶ cells/mL and allowed to grow to confluency (approximately 4 to 5 days). At each time point, half of the cells were harvested and the other half was passaged. GSH-dependent conjugation enzymes and hexokinase enzymatic activity were determined by using spectrophotometric methods. Passage 0 equals freshly isolated hPT cells. Data represent the mean ± SD of at least 3 separate experiments.
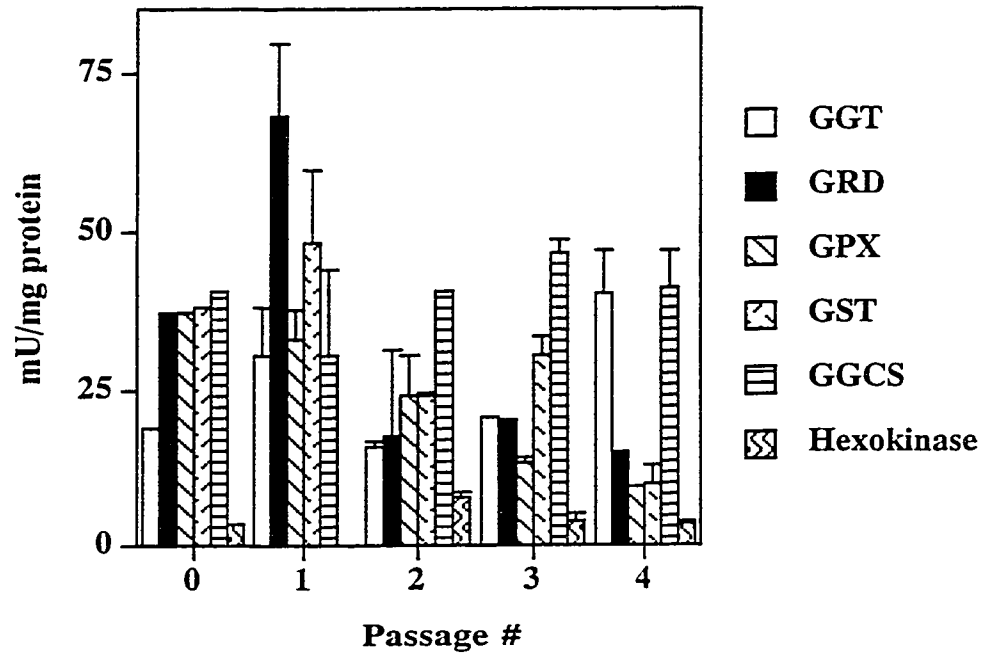
Figure 58. Effect of primary culture and ciprofibrate on CYP4A11 expression in hPT cells.

Freshly isolated hPT cells were seeded at a density of 0.5 to 1.0 x 10^6 cells/ml and allowed to grow for 24 hr prior to treatment with ciprofibrate or solvent control (EtOH < 1.0% v/v), and then allowed to grow for an additional 24 or 48 hr. At the indicated time, cells were harvested and CYP4A11 expression was measured by western blot analysis using a polyclonal rabbit anti-human CYP4A11 antibody. A. Representative western blot showing the expression of CYP4A11 in 50 μg of either freshly isolated hPT cell lysates or cell lysates from primary cultures of hPT cells. B. Densitometric analysis of CYP4A11 expression in primary cultures of hPT cells from panel A.

A

100 μM
Ciprofibrate

| + | + | - | - |

| Hours in Culture | 72 | 48 | 72 | 48 | Freshly Isolated |
| Hours of Ciprofibrate Treatment | 48 | 24 | | | |

B

- ☐ 72 hr + Ciprofibrate
- ■ 48 hr + Ciprofibrate
- 72 hr + Solvent Control
- 48 hr + Solvent Control
- Freshly Isolated
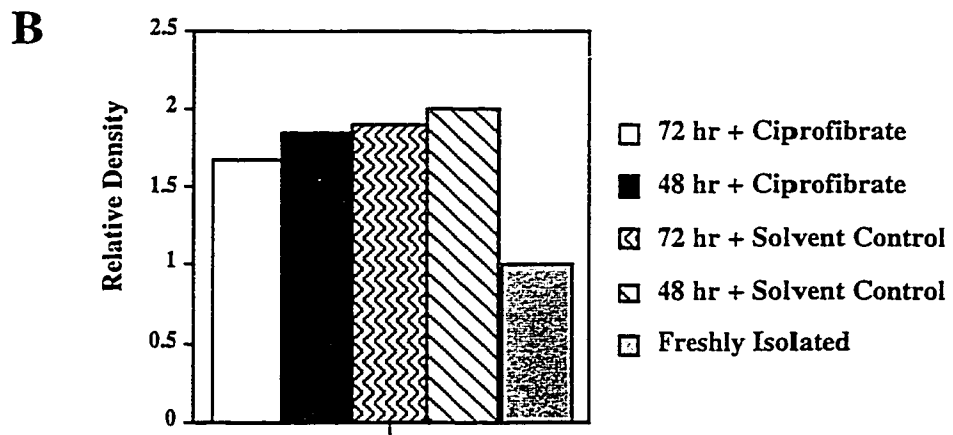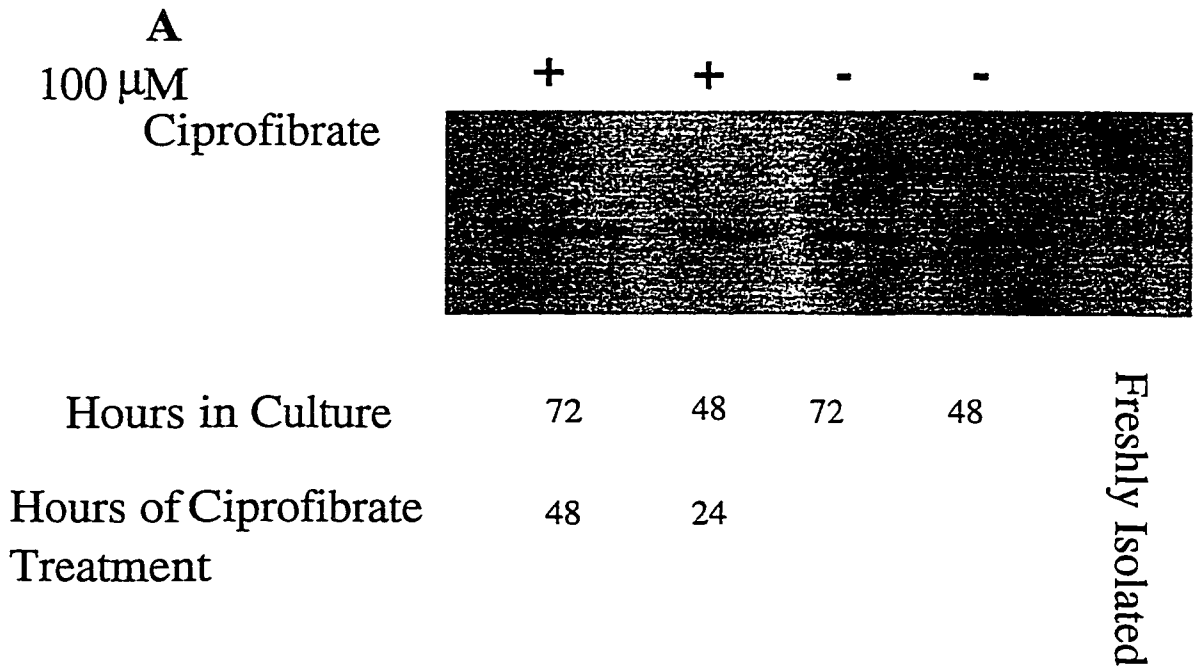
or ciprofibrate (100 μM), and peroxisomal proliferating agent similar to clofibrate, was added. Cells were allowed to grow for an additional 24 or 48 hr, after which they were isolated and analyzed for the expression of CYP4A11 by western blot analysis using an polyclonal rabbit anti-human CYP4A11 antibody (Figure 58A and B). CYP4A11 expression was maintained in primary cultures of hPT cells after both 48 and 72 hr of culture (Figure 58A). Ciprofibrate had no effect on CYP4A11 expression at any time point tested (Figure 58B). Interestingly, the levels of CYP4A11 expression in primary cultures of hPT cells appeared to be higher than those in freshly isolated hPT cells. This was not due to loading differences, as equal amounts of protein were loaded onto the SDS-PAGE and this was verified by running a corresponding gel that was stained. Because of this, the effect of EtOH alone on CYP4A11 expression in primary cultures of hPT cells was tested (Figure 59A and B). Treatment of primary cultures of hPT cells with 25 mM EtOH did not result in an increase in CYP4A11 expression compared with control cells while treatment of cells with 50 mM EtOH resulted in a slight increase in CYP4A11 expression compared to control. Finally, the effect of dexamethasone in the presence and absence of EtOH on CYP4A11 expression in primary cultures of hPT cells was determined (Figure 59C and D). Dexamethasone (7.0 nM) increased CYP4A11 expression over control after 48 hrs of treatment (Figure 58C, lanes 1 and 2). EtOH (50 mM) treatment also resulted in a slight increase in CYP4A11 expression compared with control (Figure 59C, lanes 1 and 3). Cells treated with both EtOH and dexamethasone had significantly higher levels of CYP4A11 expression then control cells or cells treated with EtOH alone (Figure 59C, lanes 1, 3, and 4). Cells treated with both EtOH and dexamethasone had only slightly higher levels of CYP4A11 expression than cells treated with only dexamethasone (Figure 59C, lanes 2 and 4).

Expression of GSTA, GSTP, and GSTT in primary cultures of hPT cells. Freshly isolated hPT cells were seeded at a density of 0.5 to 1.0 x 10^6 cells/mL and allowed to grow to confluency (approximately 4 to 5 days). Cells were than harvested

and expression of GSTA, GSTP, and GSTT were determined using western blot analysis and polyclonal rabbit anti-human and goat anti-rat and for GSTA and GSTP and GSTT antibodies, respectively. GSTA was detected in 30 μg of cytosol isolated from 6 separate cultures, representing two different patients, after 4 days of growth (Figure 60A, lanes 2-7). The expression of GSTP and GSTT in cytosol isolated from hPT cells after 4 days of growth was also determined by western blot analysis (Figure 60B and C). Unlike GSTA, the expression of both GSTP and GSTT decreased from levels seen in freshly isolated human kidney cytosol.

Expression of cytokeratin and vimentin in primary cultures of hPT cells. Cytokeratin expression and vimentin expression in confluent primary cultures of hPT cells were determined by immunohistochemical staining using monoclonal FITC-conjugated mouse antibody to cytokeratin and a monoclonal Texas Red-conjugated mouse antibody to vimentin. Primary cultures of hPT cells expressed high levels of cytokeratin after 4 days of cell growth (Figure 61). In contrast, no vimentin staining was detected in these cells (data not shown).

Flow cytometry analysis of primary cultures of hPT cells. Flow cytometry analysis of primary cultures of hPT cells was performed in order to assess the proportion of these cells in different phases of the cells cycle (Figure 62). This method can also tell if there are any cells undergoing apoptosis. The results demonstrate that the confluent (4 days of cells growth) hPT cells are all diploid, viable, and predominantly in the G_o/G_1 phase of the cell cycle, with less than 10% of the cells in the S phase. Any cells undergoing apoptosis would show up to the left of the G_o/G_1 peak in the subdiploid region.

Discussion

The role of the human kidney in the physiological processes of the body such as filtering blood, and regulation of blood pressure has been intensely studied for a number

Figure 59. Effect of EtOH and dexamethasone on CYP4A11 expression in primary culture of hPT cells.

Freshly isolated hPT cells were seeded at a density of 0.5 to 1.0 x 10^6 cells/mL and allowed to grow for 24 hr prior to treatment with either 25 or 50 mM EtOH, or dexamethasone (7.0 nM) and then allowed to grow for an additional 24 or 48 hr. At the indicated time cells were harvested and CYP4A11 expression was measured by western blot analysis using a polyclonal rabbit anti-human CYP4A11 antibody. A. Western blot showing the expression of CYP4A11 in 50 µg of either freshly isolated hPT cell lysates or cell lysates from primary cultures of hPT cells. B. Densitometric analysis of CYP4A11 expression in primary cultures of hPT cells from panel A. C. Western blot showing the expression of CYP4A11 in 50 µg of either freshly isolated hPT cell lysate or cells lysates from primary cultures of hPT cells treated with either buffer, EtOH (50 mM), dexamethasone (1 mM), or EtOH and dexamethasone. D . Densitometric analysis of CYP4A11 expression in primary cultures of hPT cells shown in panel C.

A

EtOH (mM)	0	25	50
Hours of Culture	72	72	72
Hours of Treatment	0	48	48

B
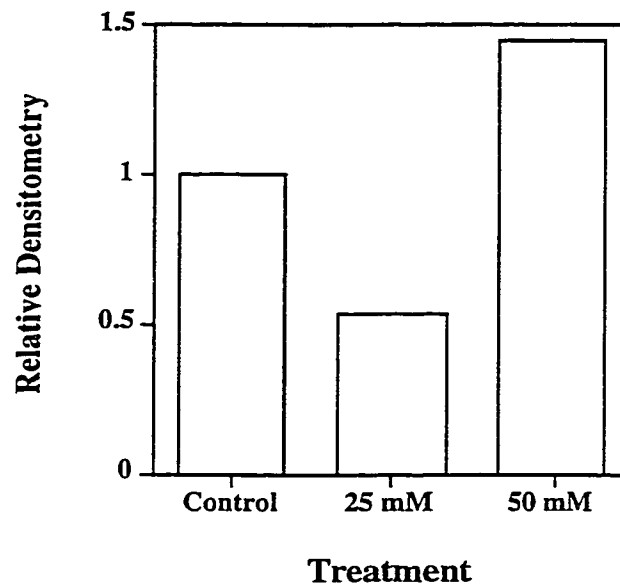
C
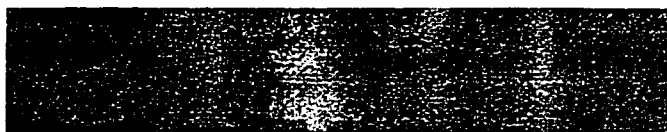
Hours in culture	0	72	72	72	72
Hours of treatment		48	48	48	48
Dex (7 nM)		−	+	−	+
EtOH (50 mM)		−	−	+	+

D

- ☐ Freshly Isolated
- ■ Control
- ▨ Dex
- ◨ EtOH
- ▦ EtOH + Dex
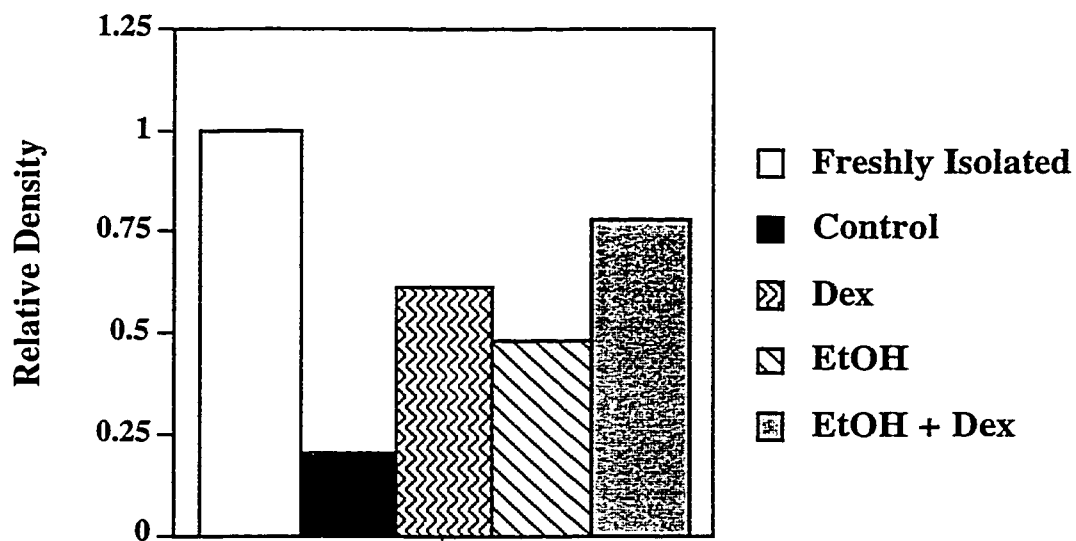
Figure 60. Expression of GSTA, GSTP, and GSTT in cytosol isolated from primary cultures of hPT cells.

Freshly isolated hPT cells were seeded at a density of 0.5 to 1.0 x 10^6 cells/mL and allowed to grow to confluency (approximately 4 to 5 days). GSTA, GSTP, or GSTT expression was measured by western blot analysis using a polyclonal rabbit anti-human antibody or polyclonal goat anti-rat GSTP and GSTT antibodies. **A.** GSTA expression. Lane 1 is cytosol (5 µg) from freshly isolated hPT cells while lanes 2-7 are cytosol (30 µg) from 6 separate preparations from two different patients. **B.** GSTP expression. Lane 1 is cytosol (5 µg) isolated from freshly isolated hPT cells while lanes 2-4 are cytosol (30 µg) isolated from 2 separate preparations from two different patients. **C.** GSTT expression. Lane 1 is cytosol (5 µg) from freshly isolated hPT cells while lanes 3-5 are cytosol (30 µg) isolated from 2 separate preparations from two different patients.
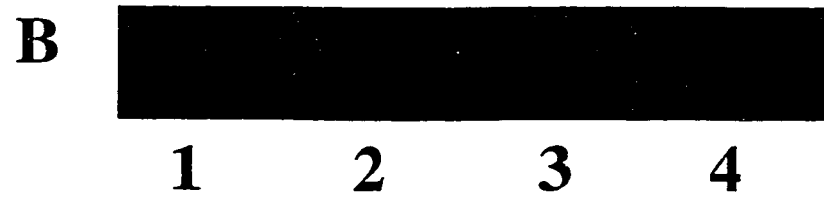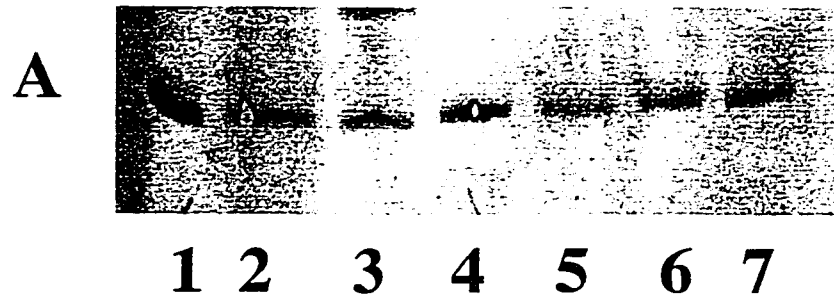
Figure 61. Expression of cytokeratin in primary cultures of hPT cells.

Freshly isolated hPT cells were seeded at a density of 0.5 to 1.0 x 10^6 cells/mL and allowed to grow to confluency (approximately 4 to 5 days). Cells were incubated with a monoclonal FITC-conjugated mouse cytokeratin antibody and cytokeratin staining was visualized on a Carl-Zeiss Laser Scanning Microscope at 340 nM. Magnification equal 100X.

A. Primary Cultured hPT Cells

B. Cytokeratin Staining

Figure 62. Flow cytometry analysis of primary cultures of hPT cells.

Freshly isolated hPT cells were seeded at a density of 0.5 to 1.0 x 10^6 cells/mL and allowed to grow to confluency (approximately 4 to 5 days). Cell were then harvested by trypsin-EDTA digestion, washed in sterile PBS, and fixed overnight in EtOH. Cells were stained by propidium iodide staining and analyzed by flow cytometry using a Becton Dickinson FACS*Calibur* Flow Cytometer.
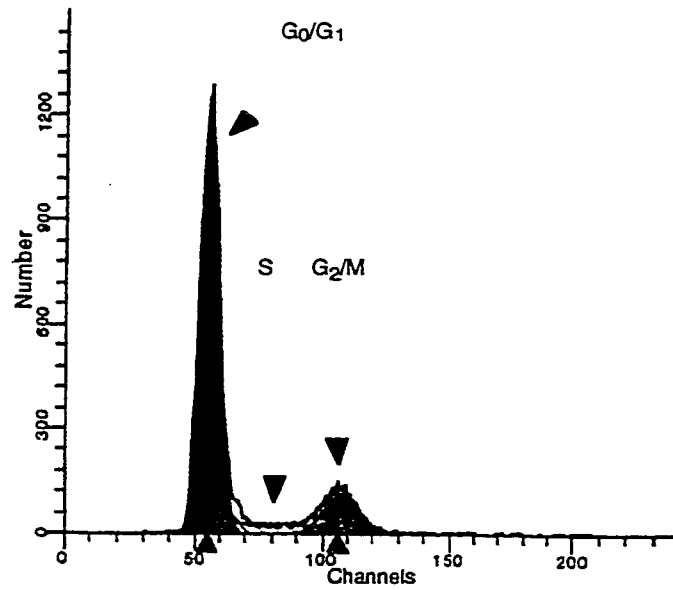
DIPLOID: 100.00 %
  Dip G0-G1: 76.13 % at 55.36
  Dip G2-M: 13.98 % at 107.54
  Dip S: 9.89 % G2/G1: 1.94
  Dip %CV: 6.16

Total S-Phase: 9.89 %

Extra Pop: %
Debris: 0.44 %
Aggregates: 0.00 %
Modeled Events: 14090
RCS: 2.962

Diploid B.A.D.: 0.08 %   no aggs

of years. The role of the human kidney in the metabolism of xenobiotics is not as well understood. The results presented in this chapter describe the isolation, characterization, and development of freshly isolated and primary cultures of hPT cells for the purpose of the study of chemical-induced nephrotoxicity. This chapter first showed the activity of GSH-dependent enzymes in freshly isolated hPT cells. Next, the P450 isoforms expressed in human kidney microsomes and in freshly isolated hPT cells were determined. The GST isoforms expressed in human kidney cytosol and freshly isolated hPT cells were then studied. Finally, the toxicity and metabolism of Tri in human kidney microsomes, cytosol, and freshly isolated hPT cells was determined.

Primary cultures of hPT cells were established and the effect that duration of culture had on the expression of both P450 and GST isoforms in these cells was determined. The effect of primary culture, and passage of hPT cells on the activity of several GSH-dependent enzymes were also determined. Cytokeratin and vimentin expression were also studied along with FACS analysis to verify that primary cultures of hPT cells were epithelial and diploid, respectively, in nature.

Freshly isolated hPT cells express high levels of several GSH-dependent enzymes (Figure 48). Although these cells have been isolated and used for study in several laboratories for a numbers of years, these are the first data reporting on the activity of these enzymes in these cells. The level of activity of several of these enzymes (GGCS, GPX, GRD) was higher than that measured in rat kidney cells while several other enzymes activities were lower (GST, GGT, and hexokinase). It is interesting to note that the activity of GST was lower in hPT cells than in rat kidney cells but hPT cells expressed GSTA, GSTP, and GSTT while only GSTα and GSTμ could be detected in rat kidney cells (Figures 51, 52 and 12, respectively). The difference between the activity levels of GST as measured by spectrophotometric assays and the expression of GST isoforms in these cell types could be due to the substrate used in the activity assays (CDNB). CDNB has been used as a model substrate for GST isoforms and different

isoforms have different affinities for this substrate. The expression of GSTA and GSTP, but not GSTM, in freshly isolated hPT cells is in agreement with previous studies showing that GSTA and GSTP are expressed in the human kidney (Campbell et al., 1991; Hilley et. al., 1994; Rodilla et al., 1998; Terrier et al., 1990). These studies also showed a small amount of GSTM expression in some patients studied, especially when the other two isoforms were absent. It is also not surprising that GSTM was not detected in any of the patients tested as a genetic polymorphism results in approximately 50 to 60% of the human population not expressing this isoform (Hayes and Pulford, 1995). All of these studies showed that GSTA was the major GST isoform expressed in the human kidney. The results in this study agree with those results. GSTM expression has been shown to be increased in several kidneys displaying neoplasia and tumor growth (Rodilla et al., 1998). Within this study, the levels of GSTA were higher in male than in female patients (Figure 51) while no variation was measured in GSTP expression between male and female patients (Figure 52). It is very important to point out that the sample size for this study was too low to make conclusions about the expression of these isoforms in the human population. Finally, analysis of the expression of GST isoforms between rat and human kidney showed that kidneys from male Fischer 344 rats expressed GSTα and GSTμ (Figure 12) while GSTA, GSTP, and GSTT were expressed in the human kidney samples tested (Figures 51, 52, and 53). As mentioned in Chapter 4, the expression of GST isoforms in the kidneys of the strain of rat tested in this study differed from that reported for another strain of rat (Sprague-Dawley rats). As a result of these data, and the data reported in this study, considerable time and care should be taken when choosing a rat model for the study of chemical-induced nephrotoxicity of chemicals metabolized by GST isoforms. This is especially true if the chemical is intended for human use. GSTT was detected in samples from all patients tested (Figure 53). To the best of our knowledge, this is the first time GSTT expression has been detected in the human kidney, let alone in hPT cells. The levels of GSTT did not differ significantly among the patients tested. The level of expression of

GSTT in the human kidney is similar to that of GSTA. The potential role that GSTT has in the human kidney needs to be studied further. GSTτ was not detected in rat liver or kidney cytosol (Chapter 4). It is not known if this is because this human polyclonal antibody will not detect rat GSTτ or if GSTτ is not expressed in the rat. The manufacturer of this antibody (Biotrin, Newton, MA) had not previously determined the antibody specificity. No data on the expression of GSTτ in the rat could be found.

Data from this study and studies from Powell et al. (1998) showed that CYP2A6, CYP2C8, CYP2C9, CYP2C19, CYP2E1, and CYP3A4 were not expressed in human kidney microsomes. CYP4F2, CYP4A11, and CYP3A5 were detected in human kidney microsomes by Powell et al. (1998). CYP2E1 was not detected in any sample of human kidney microsomes that we tested (data not shown). These data are in agreement with a previous study that showed that CYP2E1 was not expressed in 18 samples of human kidney microsomes tested by Amet et al. (1997a). This study also identified the presence of one CYP4A electrophoretic band using a polyclonal sheep anti-rat antibody. The authors of that study believed that the polyclonal antibody to rat CYP4A was detecting CYP4A11. The activity of CYP4A in human kidney microsomes, as measured by lauric acid hydroxylation, was significantly lower than that reported by Amet et al., (1997a) (0.4 to 0.5 nmol/min per mg protein vs. 2.38 nmol/min per mg protein, respectively). It should be pointed out that the activity of lauric acid hydroxylase reported by Amet et al. (1997a) varied greatly between 0.51 nmol/min per mg protein to 5.78 nmol/min per mg protein. The activity of lauric acid hydroxylase reported in Figure 50 is on the lower end of this range. Amet et al. (1997b) reported no difference in either CYP4A expression levels or in the activity of lauric acid hydroxylase between male and female patients. This agrees with the data reported in Figure 49, which also showed that CYP4A11 expression did not differ between male and female patients. Powell et al. (1996, 1998) showed that in human liver and kidney microsomes, CYP4A11 is very active in ω-lauric acid hydroxylation, accounting for approximately 85% of total ω–lauric acid hydroxylation. Powell et al. (1998) also showed that both CYP4F2

and CYP4A11 are expressed in human kidney microsomes, however no studies measuring the amount of ω-lauric acid formation or its location within the kidney were reported. Data reported in this study show for the first time that CYP4A11 is expressed in hPT cells. The rates of formation of ω-lauric acid are comparable to those reported in other studies (Amet et al., 1997a), however no ω-1-lauric acid formation was detected despite the use of a radioactive substrate. CYP4F2 expression was not studied due to reasons discussed above.

From the data presented in Chapters 4 and 8, it is obvious that rat and human kidneys differ significantly in the expression of both GST and P450 isoforms. The importance of this information cannot be underestimated. For example, several chemicals, such as acetaminophen, chloroethylenes, and low-molecular-weight hydrocarbons are metabolized by CYP2E1 (Guengerich, 1991; Nakajima et al., 1991). Although a majority of metabolism of these chemicals is thought to occur in the liver, it is possible, especially in cases of exposure to high concentrations of chemicals such as in suicide attempts, that the kidneys may be exposed to the parent form of these chemicals. In such cases, the differences in CYP2E1 expression between the rat and human may prove critical. A majority of studies on the nephrotoxicity and metabolism of several chemicals have been done in the rat. Thus, investigations in the rat studying the nephrotoxicity of chemicals metabolized by CYP2E1 may not applicable to human due to the lack of CYP2E1 in the human kidney. On the other hand, both rat and human kidney express high amounts of CYP4A isoforms and have relatively high levels of ω-lauric acid hydroxylase activity. Thus, the rat kidney may be a valid model for study of CYP4A function for human purposes. Finally, the rat kidney appears to have higher amounts of P450 than humans (0.14 nmol P450/ per mg protein vs. 0.042 nmol P450/mg protein, (Lohr et al., 1998; Amet et al., 1997a) and express more forms of P450 compared with the human kidneys (CYP2B, CYP2C11, CYP2E1, CYP4A2, and CYP4A3 Vs. CYP4F2, CYP4A11, and CYP3A5). These differences could prove vital in extrapolation of toxicity studies using

rat kidneys to humans.

Tri toxicity and metabolism in freshly isolated hPT cells. Data from Chapter 5 demonstrated that Tri toxicity in rPT and rDT cells could be altered by P450 inhibition, at least in rDT cells. Those data also showed that the differences in Tri toxicity between rPT and rDT cells correlated with differences in DCVG formation between these two cell types. Thus, in the rat kidney, P450 metabolism of Tri appears to be a route of detoxification. The fact that Tri was toxic to hPT cells (Figure 54) was not surprising given that no P450 isoform capable of metabolizing Tri was found in the human kidney and that GST isoforms were detected. The suggestion that P450 oxidative metabolism does not play a role in Tri toxicity in hPT cells is supported by data showing that inhibition of P450 isoforms with metyrapone did not alter Tri toxicity. This is supported further by the fact that P450 oxidative metabolism of Tri could not be measured in 3 out of the 4 human kidney microsome samples tested. Furthermore, DCVG formation was detected in all human patients tested (Figure 55).

Data from Figure 55 suggest that Tri metabolism in hPT cells is a result of at least 2 separate enzyme systems. The apparent K_m and V_{max} values for these curves are distinctly different (0.51 mM and 0.10 nmol/min per mg protein vs. 24.9 mM and 1.0 nmol/min per mg protein) suggesting the presence of a relatively high-affinity low-capacity enzyme system and a low-affinity high-capacity enzyme system. It should be mentioned that at the concentrations tested, the low-affinity, high-capacity enzyme system would not be saturated. GSTA, GSTP, and GSTT were all expressed in hPT cells (Figures 51, 52, and 53). Thus, it is possible that all of these enzymes are metabolizing Tri. It is also possible that different isoforms of the same enzyme may be metabolizing Tri, such as GSTA1-1 and GSTA2-2. This possibility is supported by data shown in Chapter 5, which demonstrates that different subclasses of the same enzyme family can have different affinity for Tri. However, it is highly unlikely that these enzymes would differ in kinetic properties as much as shown in Figure 55B. DCVG formation at high

concentrations of Tri (8 and 10 mM) decreased in a manner similar to that reported in Chapter 5. Data from Chapter 5 suggested that inhibition of Tri metabolism by either feedback inhibition or conjugation of DCVG to GST may be occurring in both rPT cells and to purified GSTα isoforms. If this same phenomenon is occurring in hPT cells, it could result in the curve shown in Figure 54B. Whether or not the two distinct slopes measured in Figure 54 are a result of two distinct enzyme systems or a decrease in DCVG formation needs to be determined.

The level of Tri metabolism detected in hPT cells was significantly lower than that measured in human kidney cytosol and in the blood and urine of male and female patients exposed to low concentrations of Tri (Lash et al., 1999a,b). The maximum levels of DCVG measured in the blood after 4 hr of exposure to 100 ppm Tri in male and female patients were 46.1 ± 14.2 and 13.4 ± 6.6 nmol/ml, respectively (Lash et al., 1999a). DCVG was not measured in the urine of any patient tested but NAcDCVC was. Studies presented in this chapter are important as they will aid in the determination of the role of drug metabolism enzymes in the formation of DCVG. Comparison of the kinetics of DCVG formation in hPT cells compared with those determined in human kidney cytosol (Lash et al., 1999b) reveals several similarities. First, both models displayed biphasic kinetics in terms of Tri metabolism. The apparent K_m values for Tri metabolism in human kidney cytosol (0.026 and 0.16 mM) were significantly lower than the apparent K_m values determined in this study for hPT cells (0.51 and 24.9 mM). The apparent V_{max} value for Tri metabolism in human kidney cytosol (0.81 nmol/min per mg protein) was higher then the apparent V_{max} value determined by Lineweaver-Burke analysis for Tri metabolism in hPT cells (0.20 nmol/min per mg protein). The V_{max} values for Tri metabolism in hPT cells as determined by Eadie-Scatchard analysis (0.50 and 1.0 nmol/min per mg protein) are within the range reported for Tri metabolism in human kidney cytosol. Differences in these values can be attributed to either the concentration of GST isoforms in human kidney cytosol vs. hPT cells or the presence of non-GST enzymes metabolizing Tri. Unlike the

interpretation of studies in rPT cells, a role for P450 oxidation of Tri in hPT cells cannot be proposed as Tri was not oxidized to CH in almost every patient tested. The difference in concentrations of GST isoforms between human kidney cytosol and hPT cells seems a more likely explanation

Toxicity of DCVC in hPT cells. DCVC was highly toxic in hPT cells at concentrations as low as 0.5 mM after just 1 hr (Figure 56). Pretreatment of cells with AOAA did not alter DCVC toxicity as it had been previously shown to do in rPT and rDT cells (Lash et al., 1994). Lash et al. (1990) showed that human kidney cytosol possesses cysteine-S-conjugate β-lyase activity. The activity levels for this enzyme in the human kidney, however are lower than that reported for both the rat and mouse but AOAA was able to inhibit activity in all three species equally. Thus, these data indicate that other pathways for DCVC toxicity besides metabolism by the cysteine-S-conjugate β-lyase, may be occurring in hPT cells. These alternative pathways should be investigated as they might help to explain the greater susceptibility of rodents to Tri-induced kidney cancer as compared with the susceptibility in humans.

Primary cultures of hPT cells. As stated in Chapter 1, primary cultures of hPT cells have been studied more than 10 years. Much work with these cultures has centered on non-drug metabolism issues with a few exceptions. To date, a comprehensive study detailing the expression of drug metabolism enzymes in primary cultures of hPT cells has not been published. Data from this study, for the first time, describe the changes occurring in the drug metabolism capability of primary cultures of hPT cells.

Activity and expression of GSH-dependent enzymes in primary cultures of hPT cells. Similar to primary cultures of rPT and rDT cells, primary cultures of hPT cells maintained their activity of all GSH-dependent enzymes studied (Figure 57). Hexokinase activity was also maintained in primary cultures of hPT cells. Interestingly, GSH-dependent enzyme activity was not maintained after passage of these cells. Many studies have reported data using passages of these cells as high as 6 or 7. Data from this

study show that these cells would not be viable models for the study of drug metabolism after the primary culture. The expression of GSTA was maintained in primary cultures of hPT cells while the expression of GSTP and GSTT decreased. Both GSTP and GSTT were still detected after 4 days of culture but the levels were far below those measured in freshly isolated human kidney cytosol. The difference between the expression levels of these GST isoform may reflect the role of each individual GST isoforms in kidney function or may be a result of differences in the regulation of expression of each GST isoform.

Unlike primary cultures of rPT and rDT cells, primary cultures of hPT cells seem to maintain their expression of most drug metabolism enzymes. CYP4A11 expression was maintained without the aid of an inducer for up to 4 days in culture (Figure 58). Furthermore, EtOH, and dexamethasone were able to induce CYP4A11 expression in these cultures (Figure 59). CYP4A11 expression began to decrease in these cultures after 4 days, which usually coincided with the cells reaching confluency. These findings are of importance for a number of reasons. First, the maintenance of CYP4A11 in cell culture, for even as little as 4 to 5 days, allows for the study of the mechanism of induction of CYP4A11. This area is virtually unstudied. Second, there is strong link between kidney disease and alcoholism. The dose of EtOH used in these studies (50 mM) is not that high much over the legal limit for driving under the influence in most states (17 mM). Thus, the dose used in this study is easily obtainable in the human population. The effect of dexamethasone on CYP4A11 expression in these cultures suggests that CYP4A11 expression may be hormonally regulated, perhaps by a glucocorticoid receptor. This hypothesis needs to be studied further. Finally, this model could be used to study CYP4A11 involvement in the arachidonic acid cascade. It should be mentioned that CYP4F2 expression in either freshly isolated hPT cells or in primary cultures of hPT cells was not studied. It would be interesting to know if CYP4F2 expression is also maintained. It is interesting that the only P450 isoform whose expression could be

maintained in primary cultures of rPT and rDT, and hPT cells was CYP4A. The maintenance of expression of this subfamily in these cells may be a result of the vital role it plays in normal kidney physiological function.

Maintenance of cytokeratin and vimentin expression was observed in primary cultures of hPT cells up to 5 days in culture (Figure 61). These data indicate that primary cultures of hPT cells are epithelial in nature. Primary cultures of hPT cells at confluencey are normal as determined by flow cytometry (Figure 62). As would be expected for hPT cells functioning in vivo, primary cultures of hPT cells are diploid, primarily in the resting phase, and not undergoing cells death either by necrosis or apoptosis. Thus, these cells would be valuable models to study the effect of chemicals on the alterations of the kidney cell cycle or agents that induce apoptosis.

In summary, the expression of several drug metabolism enzymes in freshly isolated hPT cells and primary cultures of hPT cells was determined. The difference in the expression of these enzymes before and after culture was determined. All drug metabolism enzymes detected in freshly isolated hPT cells were detected in primary cultures of hPT cells. Thus, primary cultures of hPT cells appear to be good models for the study of chemical-induced nephrotoxicity. Data on the effect of inducers on CYP4A11 expression is the first of its kind to study the regulation of CYP4A11. Data on the toxicity and metabolism of Tri and DCVC will be extremely useful in assessment of the human health risk of Tri or of any other chemicals metabolized by these enzymes. Finally, these data validate a new model for the use of primary cultures of hPT cells for the study of chemical-induced injury and the physiological functions of the human kidney.

Chapter 9

Summary and Conclusions

The purpose of this chapter is to summarize the data presented in Chapters 3-8 and to expand further how these data support the hypothesis presented in Chapter 1. The hypothesis of this study was that the difference in the toxicity of nephrotoxicants to both rat and human kidney cells are caused by differences in the expression of drug metabolizing enzymes. A review of the specific aims of this study that were to prove this hypothesis is given below.

1. Determine if freshly isolated rPT and rDT cells differ significantly enough in the expression of drug metabolism enzymes to be of use for the testing of chemical-induced nephrotoxicity.

2. Determine the difference in the expression and distribution of P450 and GST isoforms in rPT and rDT cells. Determine how these differences affect chemical-induced nephrotoxicity in these cells.

3. Establish, characterize, and validate primary cultures of rPT and rDT cells for use in the testing of chemical-induced nephrotoxicity.

4. Determine the expression of drug metabolism enzymes in freshly isolated and primary cultures of hPT cells. Correlate differences in the expression of drug metabolism enzymes in these cells to differences in the toxicity and metabolism of chemicals tested in rPT and rDT cells.

Chapter 3 showed that differences in thiophene-induced toxicity in freshly isolated rPT and rDT cells were caused, in part, by differences in the activity of P450 in these two cell types. These data demonstrate that these two cells types would be valuable tools for use in determining the mechanism of chemical-induced nephrotoxicity of several chemicals. Thus, Specific Aim 1 was completed. Data in Chapter 3 supported the hypothesis that differences in the expression of drug metabolism enzymes

217

contribute to differences in the susceptibility of different cells to chemical-induced nephrotoxicity. Furthermore, these data suggested that these cells could be used as models to study the effect that differences in P450 expression may have on the toxicity of environmental pollutants such as Tri. This was of prime interest as differences in the expression of drug metabolism between the rodent and human have been suggested to contribute to the increased susceptibility of rodents to Tri. Further use of these cells meant that the exact differences in the expression of drug metabolism enzymes must be determined.

Chapter 4 described in detail the differences in expression of P450 and GST isoforms between freshly isolated rPT and rDT cells. This specific aim was difficult because of the low amount of most P450 isoforms expressed in these cells. Study of P450 expression using the cell lysate of rPT and rDT cells, while capable of being done, was impractical due to the high amounts of tissue needed to be isolated for study (at least 3 rats equaling 6 kidneys). Isolation of microsomes from rPT and rDT cells allowed for the recovery of fractions containing high concentrations of P450 and also allowed for direct comparison with P450 expression in microsomes prepared from whole liver and kidney homogenates. Using these microsomes CYP2B1/2, CYP2C11, CYP2E1, and CYP4A2/3 were shown to be expressed in freshly isolated rPT and rDT cells. CYP2B1/2 and CYP4A2/3 expression was approximately equal in microsomes isolated from rPT and rDT cells while CYP2C11 was only detected in microsomes isolated from rPT cells. CYP3A1/2 was not detected in microsomes isolated from either rPT or rDT cells. CYP4A2/3 and CYP2B1/2 were induced by clofibrate (0.20 g/kg per day; 3 days) in both liver and kidney microsomes but not in microsomes isolated from rPT and rDT cells. These data suggest that induction of P450 expression in the kidney does not occur in every cell in the kidney. Furthermore, for the first time CYP2B, CYP2C11, and CYP4A2/3 expression was shown in rDT cells. CYP2E1 expression was consistently higher in rDT cells than in rPT cells. Finally, GSTα, and GSTμ expression was detected

in rPT and rDT cells while GSTτ and GSTπ was not. These data proved that there are differences in the expression of drug metabolism enzymes between rPT and rDT cells, and thus completed specific aim 2. Data from this aim served as valuable data for use in the explanation of differences in Tri toxicity and metabolism between not only rPT and rDT cells but between human and rat kidney cells.

Data from Chapter 5 further proved that freshly isolated rPT and rDT cells differ significantly in their response to chemical-induced nephrotoxicity. This time the chemical used was Tri and like thiophene-induced nephrotoxicity, the toxicity of Tri in rPT and rDT cells could be altered by inhibition of P450. Furthermore, differences in the metabolism of Tri could be correlated with differences in the expression of CYP2E1 and GSTα between rPT and rDT cells. Data from this chapter showed that both CYP2E1 and GSTα contribute significantly to Tri metabolism in rPT and rDT cells. Data from this chapter also showed measured GSH conjugation of Tri in rPT and rDT cells for the first time. Finally, data in this chapter determined what isoforms of GST are capable of metabolizing Tri in the rat kidneys. These data will aid tremendously in the determination of human health risk of Tri as GST isoforms are believed to catalyze the initial step in the bioactivation of Tri. Thus, data from this chapter support the hypothesis that differences in chemical-induced toxicity and metabolism in the different cell types are a result of differences in the drug metabolism enzymes expressed in these cells.

Chapter 5 reported on the GSH-conjugation of Tri in the rat kidney. Chapter 6 reported on the oxidative metabolism of Tri by P450 isoforms. Data from this chapter showed that P450 oxidative metabolism of Tri does occur in the kidney. This was not surprising as data shown in Chapter 5 supported this possibility. Data reported in Chapter 6 also showed that Tri was metabolized to CH in both rPT and rDT cells. One P450 isoform shown to be involved in Tri metabolism in the rat kidney was CYP2E1. Data reported in Chapter 6 expanded on the result shown in Chapter 4 by demonstrating that CYP2C11 and CYP2E1 are induced by clofibrate in kidney but not in liver microsomes.

The levels of CH formation in the kidney correlated with increases in expression of both these isoforms. Data from Chapter 6 supported the findings shown in Chapter 5. Thus data from Chapter 5 and 6 prove that CYP2E1 and GSTα have major roles in the genesis of Tri toxicity and metabolism in freshly isolated rPT and rDT cells.

Chapters 5 and 6 reported on the toxicity and metabolism of Tri in freshly isolated rPT and rDT cells after short-term of exposure. Tri nephrotoxicity, like that of many other chemicals, is believed to be a result of repeated exposures to chemicals over an extended length of time. In order to study these types of exposures, a cell culture model using primary cultures of rPT and rDT cells was characterized. Chapter 7 reports data generated towards this goal. Primary cultures of rPT and rDT cells do not mimic freshly isolated rPT and rDT cells in terms of expression of P450 isoforms. The only P450 isoform detectable in these cultures was CYP4A. CYP4A was inducible and thus, these cultures may serve useful for the study of the regulation of this isoform. Primary cultures of rPT and rDT cells did maintain the expression of all GSH-dependent enzymes studied. Because of this, Tri and DCVC toxicity was studied. Both Tri and DCVC were toxic in these cells with DCVC producing significantly higher levels of toxicity than Tri. Both Tri and DCVC were able to cause sub-lethal injury and repair as determined by increases in vimentin expression in these cells. Data from Chapter 7 thus characterized primary cultures of rPT and rDT cells for the study of chemical-induced nephrotoxicity.

Chapter 8 shows data used to study Specific Aim 4. Data from the first part of this chapter proves that the rat and human kidney differ significantly in the expression of both P450 and GST isoforms. These differences were shown to be important in terms of differences in the toxicity of Tri to hPT and rPT cells. No P450 isoforms believed to be capable of the metabolism of Tri to CH were found in human kidney microsomes. Thus, it makes sense that Tri metabolism to CH was only measured in samples from 1 out of 4 human kidney patients tested. The lack of P450 oxidation combined with the fact that hPT cells express multiple isoforms of GST, suggest the Tri should be metabolized in these cells

and should be toxic. This in fact was shown to be true. Data reported in Chapter 8 correlates with data on Tri metabolism and toxicity reported in Chapters 5 and 6. For example, data in Chapter 5 showed that Tri was toxic to both rPT and rDT cells and inhibition of P450 increased Tri toxicity in rDT cells. Data shown in Chapter 8 showed that P450 isoforms capable of metabolizing Tri were not detected in hPT cells so it could be hypothesized that P450 inhibition should not alter Tri toxicity in these cells. This is in fact what was shown. These data support the hypothesis that the difference in the toxicity of nephrotoxicants in both rat and human kidney cells are caused by differences in the expression of drug metabolizing enzymes. Data from Chapters 4 and 8 also showed the specific differences that exist in P450 and GST expression between the rat and human kidney. These data will be invaluable in decreasing uncertainty in the extrapolation to the human kidney of toxicity data produced in the rat kidney. The second half of Chapter 8 reports on the characterization of primary cultures of hPT cells for use in the study of chemical-induced toxicity and metabolism. Data reported here showed that primary cultures of hPT cells are far better models than primary cultures of rPT and rDT cells as all the P450 and GST isoforms studied in freshly isolated hPT cells were detected in primary cultures of hPT cells. Furthermore, data from Chapter 8 showed primary cultures of hPT cells are epithelial in nature, diploid, and normal, as determined by FACS analysis of cell cycle status.

In conclusion, data reported in this thesis support the hypothesis that differences in cell- and species-dependent toxicity of both thiophenes and Tri are caused by differences in the drug metabolism enzymes expressed in these cells. Determination of these drug metabolism enzymes in these cells resulted in a database of information that will be useful for not only determination of the mechanism of toxicity of a number of chemicals, but also for reducing the uncertainty in the extrapolation of toxicity data from animals to human. Establishment and characterization of primary cultures of rPT, rDT, and hPT cells gives researchers new models for the study chemical-induced nephrotoxicity. Furthermore, the

maintenance of expression of several P450 isoforms in these cultures creates new models in which to study the regulation of these P450 isoforms.

References

Abelson PH (1993) Health risk assessment. *Regul Toxicol Pharmacol* **17**: 219-23.

Aleo MD, Taub ML, Nickerson PA and Kostyniak PJ (1989) Primary cultures of rabbit renal proximal tubule cells: I. Growth and biochemical characteristics. *In Vitro Cell Dev Biol* **25**: 776-783.

Amet Y, Berthou F, Fournier G, Dreano Y, Bardou L, Cledes J and Menez J-F (1997a) Cytochrome P450 4A and 2E1 expression in human kidney microsomes. *Biochem Pharmacol* **53**: 765-771.

Amet Y, Zerilli A, Goasduff T, Dreano Y and Berthou F (1997b) Noninvolvement of CYP2E1 in the (ω-1)-hydroxylation of fatty acids in rat kidney microsomes. *Biochem Pharmacol* **53**: 947-952.

Anders MW, Lash LH, Dekant W, Elfarra AA and Dohn DR (1988) Biosynthesis and metabolism of glutathione conjugates to toxic forms. *Crit Rev Toxicol* **18**: 311-341.

Armstrong RN (1997) Structure, catalytic mechanism, and evolution of glutathione transferases. *Chem Res Toxicol* **10**: 2-18.

Ashwell JD, Cuningham RE, Noguchi PD and Hernandez D (1987) Cell growth cycle block of T cell hybridomas upon activation with antigen. *J Exp Med* **165**: 173-194.

Beaune PH, Dansette PM, Mansuy D, Kiffel L, Finck M, Amar C, Leroux JP and Homberg JC (1987) Human antiendoplasmic reticulum autoantibodies appearing in a drug induced hepatitis are directed against a human liver cytochrome that hydroxylates the drug. *Proc Natl Acad Sci USA* **84**: 551-555.

Beaune PH, Pessayre D, Dansette P, Mansuy D and Manns M (1994) Autoantibodies against cytochrome P450: Role in human diseases. *Adv. Pharmacol* **30**: 199-245.

Bebri K, Boobis AR, Davies DS and Edward RJ (1995) Distribution and induction of CYP3A1 and CY3A2 in rat liver and extrahepatic tissue. *Biochem Pharmacol* **50**: 2047-2056.

Bessey OA, Lowry OH, and Brock ML (1946) A method for the rapid determination of alkaline phosphatase with five cubic milliliters of serum. *J Biol Chem* **164**: 321-329.

Birner G, Vamvakas S, Dekant W and Henschler D (1993) Nephrotoxic and genotoxic N-acetyl-S-dichlorovinyl-L-cysteine is a urinary metabolite after occupational 1,1,2-trichloroethene exposure in humans: Implications for the risk of trichloroethene exposure. *Environ Health Perspect* **99**: 281-284.

Bloemen LJ and Tomenson J (1995) Increased incidence of renal cell tumors in a cohort of cardboard workers exposed to trichloroethene. *Arch Toxicol* **70**: 129-130.

Brown LP, Rarrar DG and de Rooij CG (1990) Health risk assessment of environmental exposure to trichloroethylene. *Regul Toxicol Pharmacol* **11**: 24-41.

Brüning T, Vamvakas S, Makropoulos M and Birner G (1998) Acute intoxication with

trichloroethylene: Clinical symptoms, toxicokinetics, metabolism, and development of biochemical parameters for renal damage. *Toxicol Sciences* **41:** 157-165.

Bulger RE and Dobyan DC (1982) Recent advances in renal morphology. *Annu Rev Physiol* **44:** 147-179.

Butler TC (1949) Metabolic transformation of trichloroethylene. *J Pharmacol Exp Ther* **97:** 84-92.

Cambell JAH, Corrigall AV, Guy A and Kirsch RE (1991) Immunohistological localization and alpha, mu, and pi class glutathione s-transferases in human tissues. *Cancer* **67:** 1608-1613.

Carroll MA, Garcia MP, Falck JR and McGiff JC (1990) 5,6-Epoxyeicosatrienoic acid, a novel arachidonate metabolite: Mechanism of vasoactivity in the rat. *Circ Res* **67:** 1082-1088.

Chen Q, Jones TW and Steven JL (1994) Early cellular events couple covalent binding of reactive metabolites to cell killing by nephrotoxic cysteine conjugates. *J Cell Physiol* **161:** 293-302.

Chen Q, Yu K, Holbrook NJ and Stevens JL (1992) Activation of the growth arrest and DNA damage-inducible gene gadd153 by nephrotoxic cysteine conjugates. *J Biol Chem* **267:** 8207-8212.

Chen JC, Stevens JL, Trifillis AL and Jones TW (1990) Renal cysteine conjugate beta-lyase-mediated toxicity studied with primary cultures of human proximal tubular cells. *Toxicol Appl Pharmacol* **267:** 463-473.

Chopra DP, Sullivan J, Wille JJ and Siddiqui KM (1987) Propagation of differentiating normal human tracheobronchial epithelial cells in serum-free medium. *J Cell Physiol* **130:** 173-181.

Chung SD, Alavi N, Livingston D, Hiller S and Taub M (1982) Characterization of primary rabbit kidney cultures that express proximal tubule functions in a hormonally defined medium. *J Cell Biol* **95:** 118-126.

Commandeur JNM and Vermeulen NPE (1990) Identification of N-acetyl(2,2-dichlorovinyl)- and N-acetyl(1,2-dichlorovinyl)-L-cysteine as two regioisomeric mercapturic acids of trichloroethylene in the rat. *Chem Res Toxicol* **3:** 212-218.

Cui X-L and Douglas JG (1997) Arachidonic acid activates c-jun N-terminal kinase through NADPH oxidase in rabbit proximal tubular epithelial cells. *Proc Natl Acad Sci USA* **94:** 3771-3776.

Dansette PM, Thang DC, Amri HE and Mansuy D (1992) Evidence for thiophene-S-oxide as a primary reactive metabolite of thiophene in vivo: Formation of a dihydrothiophene sulfoxide mercapturic acid. *Biochem Biophys Research Comm* **186:** 1624-1630.

Dansette PM, Amar C, Smith C, Pons C and Mansuy D (1990) Oxidative activation of the thiophene ring by hepatic enzyme. Hydroxylation and formation of electrophilic metabolites during metabolism of tienilic acid and its isomer by rat liver microsomes. *Biochem Pharmacol* **39:** 911-918.

David NJ, Wolman R, Milne FJ and van Niekerk I (1989) Acute renal failure due to trichloroethylene poisoning. *Brit J Indus Med* **46**: 347-349.

Davidson IW and Beliles RP (1991) Consideration of the target organ toxicity of trichloroethylene in terms of metabolite toxicity and pharmacokinetics. *Drug Metab Rev* **23**: 493-599.

Dean PN (1987) Data analysis in cell kinetics research. In Techniques In Cell Cycle Research (J W Gray and Z Darzynkiewicz, eds), pp. 207-253. *Human Press Clifton* NJ.

Dekant W, Koob M and Henschler D (1990) Metabolism of trichloroethylene-In vivo and in vitro evidence for activation by glutathione conjugation. *Chem-Biol Interact* **73**: 89-101.

Dekant W, Metzler M and Henschler D (1986) Identification of S-(1,2-dichlorovinyl)-N-acetyl-cysteine as an urinary metabolite of trichloroethylene: A possible explanation for its nephrocarcinogenicity in male rats. *Biochem Pharmacol* **35**: 2455-2458.

Detrisac CJ, Sens MA, Garvin AJ, Spicer SS and Sens DA (1984) Tissue culture of human kidney epithelial cells of proximal tubule origin. *Kidney Int* **25**: 383-390.

Doniger J, O'Neil R, Noguchi P and DiPaolo JA (1983) Initiation of carcinogenesis dependence upon MNNG-induced release of the G1 block of density-inhibited Syrian hamster cells. *Teratogen, Carcinogen, and Mutagen* **3**: 123-131.

Eklöw L, Moldeus P, and Orrenius S(1984) Oxidation of glutathione during hydroperoxide metabolism: A study using isolated hepatocytes and the glutathione reductase inhibitor 1,3,-bis(2-chlorethyl)-1-nitrosoerea. *Eur J Biochem* **138**: 459-463.

Elfarra AA, Krause RJ, Last AR, Lash LH and Parker JC (1998) Species- and sex-related differences in metabolism of trichloroethylene to yield chloral and trichloroethylene in mouse, rat, and human liver microsomes. *Drug Metab Dispos* **26**: 779-785.

Escalante B, Erlij D, Falck JR and McGiff JC (1991) Effect of Cytochrome P450 arachidonate metabolites on ion transport in rabbit kidney loop of Henle. *Science* **251**: 799-802.

Escalante B, Sessa WC, Falck JR, Yadagiri P and Schwartzman M (1989) Vasoactivity of 20-hydroxyeicosatetraenoic acid is dependent on metabolism by cyclooxygenase. *J Pharmacol Exp Ther* **248**: 229-232.

Estabrook RW (1967) Mitochondrial respiratory control and the polargraphic measurements of ADP:O ratios. *Methods Enzymol* **10**: 41-47.

Eyre RJ, Stevens DK, Parker JC and Bull RJ (1995a) Acid-labile adducts to protein can be used as indicators of the cytseine S-conjugate pathway of trichloroethene metabolism. *J Toxicol Environ Health* **46**: 443-464.

Eyre RJ, Steven DK, Parker JC and Bull RJ (1995b) Renal activation of trichloroethene and S-(1,2-dichlorovinyl)-L-cysteine and cell proliferative responses in the kidneys of F344 rats and B6C3F1 mice. *J Toxicol Environ Health* **46**: 465-481.

Fleischer S and Fleischer B (1967) Removal and binding of polar lipids in mitochondria and other membrane systems. *Methods Enzymol* **10**: 406-433.

Goeptar AR, Commandeur JNM, van Ommen B, van Bladeren PJ and Vermeulen NPE (1995) Metabolism and kinetics of trichloroethylene in relation to toxicity and carcinogenicity. Relevance of the mercapturic acid pathway. *Chem Res Toxicol* **8**: 3-21.

Gorski JC, Jones DR, Wrighton SA and Hall SA (1997) Contribution of human CYP3A subfamily members to the 6-hydroxylation of chlorzoxazone. *Xenobiotica* **27**: 243-256.

Green T (1990) Chloroethylenes: A mechanistic approach to human risk evaluation. *Annu Rev Pharmacol Toxicol* **30**: 73-89.

Green T and Prout MS (1985) Species differences in response to trichloroethylene. II. Biotransformation in rats and mice. *Toxicol Appl Pharmacol* **79**: 401-411.

Groves Ce, Hayden PJ, Lock EA, and Schnellmann RG (1993) Differential cellular effects in the toxicity of haloalkene and haloalkane cysteine conjugates to rabbit renal proximal tubules. *J Biochem Toxicol* **8**: 49-56.

Groves CE, Lock EA and Schnellman RG (1991) Role of lipid peroxidation in renal proximal tubule cell death induced by haloalkene cysteine conjugates. *Toxicol Appl Pharmacol* **107**: 54-62.

Guder W G and Ross B D (1984) Enzyme distribution along the nephron. *Kidney Int* **26**: 101-111.

Guengerich FP (1991) Oxidation of toxic and carcinogenic chemicals by human cytochrome P450 enzymes. *Chem Res Toxicol* **2**: 391-407.

Guengerich FP (1990) Enzymatic oxidation of xenobiotic chemicals. *Biochem Mol Biol* **25**: 97-118.

Guengerich FP, Kim D-H and Iwasaki M (1991) Role of cytochrome P-450 IIE1 in the oxidation of many low molecular weight cancer suspects. *Chem Res Toxicol* **4**: 168-179.

Habig EA (1974) Activity of glutathione-S-transferase in porcine liver microsomes and cytosol. J *Biol Chem* **249**: 7130-7139.

Hanioka N, Omae R, Yoda R, Jinno H, Nishimura T and Ando M (1997) Effect of trichloroethylene on cytochrome P450 enzymes in the rat liver. *Bull Environ Contamin Toxicol* **58**: 628-635.

Hatzinger PB, Chen Q, Dong LQ and Stevens JL (1988) Alterations in intermediate filament proteins in rat kidney proximal tubule epithelial cells. *Biochem Biophys Res Commun* **157**: 1316-1322.

Hayden PJ, Welsh CJ, Yang Y, Schaefer WH, Ward AJ and Stevens JL (1992) Formation of mitochondrial phospholipid adducts by nephrotoxic cysteine conjugate metabolites. *Chem Res Toxicol* **5**: 232-237.

Hayden PJ and Stevens JL (1990) Cysteine conjugate toxicity, metabolism and binding to macromolecules in isolated rat kidney mitochondria. *Mol Pharmacol* **37:** 468-476.

Hayes JD and Pulford DJ (1995) The glutathione S-transferase supergene family: Regulation of GST and the contribution of the isoenzyme to cancer chemoprotection and drug resistance. *CRC Crit Rev Biochem Mol Biol* **30:** 445-600.

Henschler D, Vamvakas S, Lammert M, Dekant W, Kraus B, Thomas B and Ulm K (1995) Increased incidence of renal cell tumors in a cohort of cardboard workers exposed to trichloroethene. *Arch Toxicol* **69:** 291-299.

Henschler D, Vamvakas S, Lammert M, Dekant W, Kraus B, Thomas B and Ulm K (1995) Increased incidence of renal cell tumors in a cohort of cardboard workers exposed to trichloroethene. *Arch Toxicol* **70:** 131-133.

Hiley CG, Otter M, Bell J, Strange RC and Keeling JW (1994) Immunohistochemical studies of the distribution of alpha and pi isoforms of glutathione s-transferase in cystic renal disease. *Pediatric Path* **14:** 497-504.

Hirt D, Capdevila J, Falck JR, Breyer MD and Jacobson HR (1991) Cytochrome P450 metabolites of arachidonic acid are potent inhibitors of vasopressin action on rabbit cortical collecting duct. *J Clin Invest* **84:** 1805-1812.

Hotchkiss JA, Kim H, Hahn FF, Novak RF and Dahl AR (1995) Pyridine induction of Sprague-Dawley rat renal cytochrome P4502E1: Immunohistochemical localization and quantitation. *Toxicol Lett* **78:** 1-7.

Ito O, Alonso-Galicia M, Hopp KA and Roman RJ (1998) Localization of cytochrome P-450 4A isoforms along the rat nephron. *Am J Physiol* **274:** F395-F404.

Jayyosi Z, Knoble D, Muc M, Erick J, Thomas PE and Kelley M (1995) Cytochrome P-450 2E1 is not the sole catalyst of chlorzoxazone hydroxylation in rat liver microsomes. *J Pharmacol Exp Ther* **273:** 1156-1161.

Joshi MD and Jagannathan V (1966) Hexokinase. *Methods Enzymol* **9:** 371-375.

Kays SE and Schnellmann RG (1995) Regeneration of renal proximal tubule cells in primary culture following toxicant injury : response to growth factors. *Toxicol Appl Pharmacol* **132:** 273-280.

Kempson SA, McAteer JA, Al-Mahrouq HA, Dousa TP, Dougherty GS and Evans AP (1989) Proximal tubule characteristics of cultured human renal cortex epithelium. *J Lab Clin Med* **112:** 285-296.

Kocarek TA, Scheutz EG and Guzelian PS (1993) Expression of multiple forms of cytochrome P450 mRNAs in primary cultures of rat hepatocytes maintained on Matrigel. *Mol Pharmacol* **43:** 328-334.

Koop DR, Crump BL, Nordblom GD and Coon MJ (1985) Immunochemical evidence for induction of the alcohol-oxidizing cytochrome P-450 of rabbit liver microsomes by diverse agents: Ethanol, imidazole, trichloroethylene, acetone, pyrazole, and isoniazid. *Proc Nat Acad Sci USA* **82:** 4065-4069.

Lash LH (1997) Glutathione status and other antioxidant defense mechanisms. In:

Comprehensive Toxicology, (Goldstein, RS eds.), *Elsevier Science Inc.*, New York, NY. pp. 403-428.

Lash LH, Brashear WT, Abbas R, Parker JC and Fisher JW (1999a) Identification of S-(1,2-dichlorovinyl)glutathione in the blood of human volunteers exposed to trichloroethylene. *J Toxicol Environ Health* **56:** 1-21.

Lash LH, Lipscomb JC, Putt DA and Parker JC (1999b) Glutathione conjugation of trichloroethylene in human liver and kidney: Kinetics and individual variation. *Drug Metab Dispos*, in press.

Lash LH, Qian W, Putt DA, Jacobs K, Elfarra AA, Krause RJ and Parker JC (1998) Glutathione conjugation of trichloroethylene in rats and mice: Sex-, species-, and tissue-dependent differences. *Drug Metab Dispos* **26:** 12-19.

Lash LH, Xu Y, Elfarra AA, Duescher RJ and Parker JC (1995a) Glutathione-dependent metabolism of trichloroethylene in isolated liver and kidney cells of rats and its role in mitochondrial and cellular toxicity. *Drug Metab Dispos* **23:** 846-853.

Lash LH, Tokarz JJ and Pegouske DM (1995b) Susceptibility of primary cultures of proximal and distal tubular cells from rat kidney to chemically induced toxicity. *Toxicology* **103:** 85-103.

Lash LH and Tokarz JJ (1995) Oxidative stress and cytotoxicity of 4-(2-thienyl)butyric acid in isolated rat renal proximal tubular and distal tubular cells. *Toxicology* **103:** 167-175.

Lash LH, Sausen PJ, Duescher RJ, Cooley AJ and Elfarra AA (1994) Roles of cysteine conjugate β-lyase and S-oxidase in nephrotoxicity: Studies with S-(1,2-dichlorovinyl)-L-cysteine and S-(1,2-dichlorovinyl)-L-cysteine sulfoxide. *J Pharmacol Exp Ther* **269:** 374-383.

Lash LH, Nelson RM, VanDyke RA and Anders MW (1990) Purification and characterization of human kidney cytosolic cysteine conjugate β-lyase activity. Drug Metab Dispos **18:** 50-54.

Lash LH and Tokarz JJ (1990) Oxidative stress in isolated rat renal proximal and distal tubular cells. *Am J Physiol* **259:** F338-F347.

Lash LH and Anders MW (1987) Mechanism of S-(1,2-dichlorovinyl)-L-cysteine- and S-(1,2-dichlorovinyl)-L-homocysteine-induced renal mitochondrial toxicity. *Mol Pharmacol* **32:** 549-556.

Lawrence RA and Burk RF (1976) Glutathione peroxidase activity in selenium-deficient rat liver. *Biochem Biophys Res Commun* **71:** 952-958.

Lock EA and Schnellman RG (1990) The effect of haloalkene cysteine conjugation on rat renal glutathione reductase of lipoyl dehydrogenase activities. *Toxicol Appl Pharmacol* **104:** 180-190.

Lohr JW, Willsky GR and Acara A (1998) Renal Drug Metabolism. *Pharmacol Rev* **50:** 107-141.

Lopez-Garcia MP, Dansette PM, Valadon P, Aman C, Beaune PH, Guengerich FP and

Mansuy D (1993) Human-liver cytochrome P-450 expressed in yeast as tools for reactive-metabolites formation studies, oxidative of tienilic acid by cytochrome P-450 2C9 and 2C10. *Eur J Biochem* **213**(1): 223-232.

Mahn, SE (1992) Toxicological Chemistry, 2th ed., Lewis Publishers Inc.,

Makita K, Falck JR Capdevila JH (1996) Cytochrome P450, the arachidonic acid cascade, and hypertension: new vistas for an old enzyme system. *FASEB J* **10**: 1456-1463.

Meyer DJ (1993) Significance of an unusually low K_m for glutathione in glutathione transferase of the α, μ, and π classes. *Xenobiotica* **23**: 823-834.

Miller JH (1986) Restricted growth of rat kidney proximal tubule cells cultured in serum-supplemented and defined media. *J Cell Physiol* **129**: 264-272.

Miller RE and Guengerich FP (1983) Metabolism of trichloroethylene in isolated hepatocytes, microsomes, and reconstituted enzyme systems containing cytochrome P-450. *Cancer Res* **43**: 1145-1152.

Miranda CL, Wang J-L, Henderson MC, Williams DE and Buhler DR (1990) Regiospecificity in the hydroxylation of lauric acid by rainbow trout hepatic cytochrome P450 isozymes. *Biophys Res Commun* **171**: 537-542.

Nagaya T, Ishikawa N. and Hata H. (1989) Urinary total protein and beta-2-microglobulin in workers exposed to trichloroethylene. *Environ Res* **50**: 86-92.

Nakajima T, Wang R-S, Elovaara E, Park SS, Gelboin HV and Vainio H (1993) Cytochrome P450-related differences between rats and mice in the metabolism of benzene, toluene and trichloroethylene in liver microsomes. *Biochem Pharmacol* **45**: 1079-1085.

Nakajima T, Wang R-S, Elovaara E, Park SS, Gelboin HV and Vainio H (1992a) A comparative study on the contribution of cytochrome P450 isozymes to metabolism of benzene, toluene and trichloroethylene in rat liver. *Biochem Pharmacol* **43**: 251-257.

Nakajima T, Wang R-S, Katakura Y, Kishi R, Elovaara E, Park SS, Gelboin HV and Vaino H. (1992b) Sex-, age- and pregnancy-induced changes in metabolism of toluene and trichloroethylene in rat liver in relation to the regulation of cytochrome P450IIEI and P450IIC11 content. *J Pharmacol Exp Ther* **261**: 869-874.

Nakajima T, Wang R-S, Murayama N and Sato A (1990) Three forms of trichloroethylene-metabolizing enzymes in rat liver induced by ethanol, phenobarbital, and 3-methylchloranthrene. *Toxicol Appl Pharmacol* **102**: 546-552.

Nakajima T, Okino T, Okuyama S, Kaneko T, Yonekura I and Sato A (1988) Ethanol-induced enhancement of trichloroethylene metabolism and hepatotoxicity: Difference from the effect of phenobarbital. *Toxicol Appl Pharmacol* **94**: 227-237.

National Toxicology Program (NTP) (1990) Carcinogenesis studies of trichloroethylene (with out epichlorohydrin) (CAS No. 79-01-6) in F344/N rats and BC63F1 mice (gavage study). *NTP TR 243 U.S. DHEW*, Research Triangle Park, NC.

National Toxicology Institute (1982) Carcinogenesis bioassay of trichloroethylene.

National Cancer Inst Carcinogenesis Tech Rep Ser 2. Bethesda: U.S. DHEW Publ. No. (NIH) 76-802.

Neau E, Dansette PM, Andronick V and Mansuy D (1990) Hydroxylation of the thiophene ring by hepatic monooxygenases. Evidence for 5-hydroxylation of 2-aryolthiophene as a general metabolic pathway using a simple UV-visible assay. *Biochem Pharmacol* **39:6:** 1101-1107.

Nelson DR, Koymans L, Kamataki T, Stegeman JJ, Feyereisen R, Waxman DJ, Waterman MR, Gotoh O, Coon MJ, Estabrook RW, Gunsalus IC and Nebert DW (1996) P450 superfamily: Update on new sequences, genemapping, accession numbers, early trivial names of enzymes, and nomenclature. *Pharmacogenetics* **6:** 1-42.

Ochoa S (1955) Malic dehydrogenase from pig heart. *Methods Enzymol* **1:** 735-739.

Okita JR, Johnson SB, Castle PJ, Cezellem SC and Okita RT (1998) Improved separation and immunodetection of rat cytochrome P450 4A forms in liver and kidney. *Drug Metab Dispos* **25:** 1008-1012.

Orlowski M and Meister A (1963) γ-Glutamyl-*p*-nitroanilide: A new convenient substrate for determination and study of L- and D-γ-glutamyltranspeptidase activities. *Biochim Biophys Acta* **73:** 679-681.

Pluznik DH, Cunningham RE and Noguchi PD (1984) Colony stimulating factor (CSF) controls proliferation of CSF-dependent cells by acting during the G1 phase of the cell cycle. *Proc Nat Acad Sci USA* **81:** 7451-7455.

Powell JF (1945) Trichloroethylene: Absorption, elimination and metabolism. *Brit J Indus Med* **2:** 142-145.

Powell PK, Wolf I, Jin R and Lasker JM (1998) Metabolism of arachidonic acid to 20-hydroxy-5,8,11,14-eicosatetraenoic acid by P450 enzymes in human liver: Involvement of CYP4F2 and CYP4A11. *J Pharmacol Exp Ther* **285:** 1327-1336.

Powell PK, Wolf I and Lasker JM (1996) Identification of CYP4A11 as the major lauric acid ω-hydroxylase in human liver microsomes. *Arch Biochem Biophys* **335:** 219-226.

Reichert, D (1983) Biological actions and interactions of tetrachloroethylene. *Mutat Res* **123:** 411-429.

Rodilla v, Benzie AA, Veitch JM, Murray GI, Rowe JD and Hawksworth GM (1998) Glutathione S-transferase in human renal cortex and neoplastic tissue: enzymatic activity, isoenzyme profile and immunohistochemical localization. *Xenobiotica* **28:** 443-456.

Romero MF, Madhun ZT, Hopfer U and Douglas JG (1991) An epoxygenase metabolite of arachidonic acid 5,6-epoxy-eicosatrienoic acid mediates angiotensin-induced natriuresis in proximal tubular epithelium. *Adv Prost Thromb Leuk Res* **21A:** 205-208.

Ronnis MJJ, Huang J, Longo V, Tindberg N, Ingelman-Sundberg M and Badger TM (1998) Expression and distribution of cytochrome P450 enzymes in male rat kidney: Effects of ethanol acetone and dietary conditions. *Biochem Pharmacol* **55:** 123-129.

Salhad AS, Applewhite J, Couch MW, Okita RT and Shiverick KT (1987) Extraction of ω- and ω-1-hydroxylauric acid with ethyl acetate results in formation of acetoxy

products. *Drug Metab Dispos* 15: 233-236.

Schmidt E and Schmidt W (1983) Glutamate dehydrogenase. In H.U. Bergmeyer (ED.) *Methods of Enzymatic Analysis* 3rd ed. Vol. III, Verlag Chemie, Weinheim pp. 216-227.

Schuetz EG, Schuetz JD, Grogan WM, Naray-Fejes-Toth A, Fejes-Toth G, Raucy J, Guzelian P, Gionela K and Watlington CO (1992) Expression of cytochrome P450 3A in amphibian, rat, and human kidney. *Arch Biochem Biophys* 294: 206-217.

Seelig GF and Meister A (1984) γ-Glutamylcysteine synthetase from erythrocytes. *Anal Biochem* 141: 510-514.

Sorger T and Germinario RJ (1983) A direct solubilization procedure for the determination of DNA and protein in cultured fibroblast monolayers. *Anal Biochem* 131: 254-256.

Sundseth SS and Waxmann DJ (1992) Sex-dependent expression and clofibrate inducibility of P450 4A fatty acid ω-hydroxylase. *J Biol Chem* 267: 3915-3921.

Swaen GMH (1995) Increased incidence of renal cell tumors in a cohort of cardboard workers exposed to trichloroethene. *Arch. Toxicol* 70: 127-128.

Taub ML., Yang IS, and Wang Y (1989) Primary rabbit kidney proximal tubule cell cultures maintain differentiated functions when cultured in a hormonally defined serum-free medium. *In Vitro Cell Dev Biol* 25: 770-775.

Terrier P, Townsend AJ, Coindre JM, Triche TJ and Cowan KH (1990) An immunohistochemical study of pi class glutathione s-transferase expression in normal human tissue. *Amer J Path* 137: 845-853.

Tisher CC and Madsen KM (1996) Anatomy of the kidney. In: *The Kidney*, (Brenner, BM eds.), WB Sander Co., Philadelphia, PA. 8-18.

Todd JH, McMartin KE and Sens DA (1995) Enzymatic isolation and serum-free culture of human renal cells. In: *Methods in Molecular Medicine*: Human Cell Culture Protocols. Eds. Jones GE, Humana Press Inc. Totowa, NJ Chapter 32.

Trifillis AL, Regec AL and Trump BF (1985) Isolation, culture and characterization of human renal tubular cells. *J Urol* 133: 324-329.

Tune BM (1986) The nephrotoxicity of cephalosporin antibiotics: Structure-activity relationships. *Comments Toxicol* 1: 145-170.

Tune BM and Fravert D (1980) Mechanism of cephalosporin nephrotoxicity: A comparison of cephaloridine and chepaloglycin. *Kidney Int* 18: 591-600.

Valadon P, Dansette PM, Girault JP, Amar C and Mansuy D. (1996) Thiophene sulfoxides as reactive metabolites: Formation upon microsomal oxidation of a 3-hydroxytienlic acid. *Chem Res Toxicol* 9: 1403-1413.

Vamvakas S, Bittner D, Dekant W and Anders MW (1992) Events that precede and that follow S-(1,2-dichlorovinyl)-L-cysteine-induced release of mitochondrial Ca+2 and their association with cytotoxicity to renal cells. *Biochem Pharmacol* 44: 1131-1138.

Vamvakas S, Sharma VK, Sheu SS and Anders MW (1990) Perturbation of intracellular calcium distribution in kidney cells by nephrotoxic haloalkenyl cysteine S-conjugates. *Mol Pharmacol* **38:** 455-61.

Vamvakas S, Dekant W and Henschler D (1989) Assessment of unscheduled DNA synthesis in a cultured line of renal epithelial cells exposed to cysteine S-conjugates of haloalkenes and haloalkanes. *Mutat Res* **222:** 329-335.

Vamvakas S, Elfarra AA, Dekant W, Henschler D and Anders MW (1988) Mutagenicity of amino acid and glutathione-S-conjugates in the Ames test. *Mutat Res* **206:** 83-90.

Wallin A, Zhang G, Jones TW, Jaken S and Stevens JL (1992) Mechanism of the nephrogenic repair response. Studies on proliferations and vimentin expression after 35S-1,2-dichlorovinyl-L-cysteine nephrotoxicity in vivo and in cultured proximal tubule epithelial cells. *Lab Invest* **66:** 474-484.

Waxman DJ, Lapenson DP, Park SS, Attisano C and Gelboin HV (1987) Monoclonal antibodies inhibitory to rat hepatic cytochrome P-450: P-450 form specificity's and use as probes for cytochrome P-450-dependent steroid hydroxylations. *Mol Pharmacol* **32:** 615-635.

Weiss NS (1996) Cancer in relation to occupational exposure to trichloroethylene. *Occup Environ Med* **53:** 1-5.

Wilson PD (1986) Use of cultured renal tubular cells in the study of cell injury. *Mineral Electrolyte Metab* **12:** 71-83.

Wrighton SA and Stevens JC (1992) The human hepatic cytochromes P450 involved in drug metabolism. *Crit Rev Toxicol* **22:** 11-21.

Yamazaki H, Guo Z and Guengerich FP 1995) Selectivity of cytochrome P4502E1 in chlorzoxazone 6-hydroxylation. *Drug Metab Dispos* **23:** 438-440.

Yu K, Chen Q, Liu H, Zhan Y and Stevens JL (1994) Signaling the molecular stress response to nephrotoxic and mutagenic cysteine conjugates: differential roles for protein synthesis and calcium in the induction of c-fos and c-myc mRNA in LLC-PK1 cells. *J Cell Physiol* **161:** 303-311.

Zangar RC, Woodcroft KJ, Kocarek TA and Novak RF (1995) Xenobiotic-enhanced expression of cytochrome P450 2E1 and 2B1/2B2 in primary cultured rat hepatocytes. *Drug Metab Dispos* **23:** 681-687.

Zerilli A, Lucas D, Dréano Y, Picart D and Berthou F (1998) Effect of pyrazole and dexamethasome administration on cytochrome P450 2E1 and 3A isoforms in rat liver and kidney: Lack of specificity of p-nitrophenol as a substrate of P450 2E1. *Alcohol Clin Exp Res* **22:** 652-657.

Zerilli A, Ratanasavanh D, Lucas D, Goasduff T, Dréano Y, Menard C, Picart D and Berthou F (1997) Both cytochromes P450 2E1 and 3A are involved in the O-hydroxylation of p-nitrophenol, a catalytic activity known to be specific for P450 2E1. *Chem Res Toxicol* **10:** 1205-1212.

Zimmerman HJ, Lewis JH, Ishak KG and Maddrey W (1984) Ticrynafen-associated hepatic injury: Analysis of 340 cases. *Hepatology* **4:** 315-323.

ABSTRACT

EFFECT OF CELL- AND SPECIES-DIFFERENCES IN THE EXPRESSION OF DRUG METABOLISM ENZYMES ON CHEMICAL-INDUCED INJURY TO THE RAT AND HUMAN KIDNEY

by

BRIAN S. CUMMINGS

May, 1999

Advisor: Dr. Lawrence H. Lash

Major: Pharmacology

Degree: Doctor of Philosophy

Differences in the expression of drug metabolizing enzymes between cells of the rat and human kidney on chemical-induced nephrotoxicity were studied. Rat renal proximal tubular (rPT) and distal tubular (rDT) cells differed in their susceptibility to trichloroethylene (Tri) and thiophene-containing compounds. These differences were caused in part by differences in the activity of cytochrome P450 monooxygenase (P450) between the two cell types. rPT cells expressed cytochrome P450 (CYP) 2B1/2, CYP2C11, CYP2E1, CYP4A2/3, and GSTα, but not CYP3A1/2, GSTμ, GSTπ, or GSTτ. rDT cells expressed CYP2B1/2, CYP2E1, and CYP4A2/3, GSTα, and GSTμ, but not CYP2C11, CYP3A1/2, GSTπ, or GSTτ. Expression of CYP2E1 was significantly higher in rDT cells than in rPT cells. Pyridine induced CYP2E1 in both liver and kidney microsomes but not in rPT and rDT cells. Clofibrate induced CYP4A and CYP2B only in liver and kidney microsomes and also CYP2E1 and CYP2C11 in kidney microsomes. The GST isoforms responsible for GSH conjugation of Tri were also determined. Pyridine treatment increased CH formation in rat liver and kidney microsomes. Clofibrate treatment only increased CH formation in kidney microsomes. Primary cultures of rPT and rDT cells maintained their expression of GSH-dependent enzymes

233

but not P450 isoforms. Freshly isolated human proximal tubular (hPT) cells expresses CYP4A11, GSTA, GSTP, and GSTT but not GSTM. Tri and DCVC were toxic to freshly isolated hPT cells in a manner not affected by P450 or cysteine S-conjugate β-lyase inhibition. Tri was metabolized to its GSH conjugate but not to CH in hPT cells. Primary cultures of hPT cells maintained their expression of GSH-dependent enzymes and CYP4A11. Treatment of cultures with ethanol or dexamethasone altered expression of CYP4A11. These data support the hypothesis that differences in the susceptibility of rPT, rDT, and hPT cells to chemical-induced nephrotoxicity are caused by difference in the expression of drug metabolism enzymes.

AUTOBIOGRAPHICAL STATEMENT
BRIAN S. CUMMINGS

Education:

Wayne State University   1999
Department of Pharmacology
Detroit, MI 48201
Doctor of Philosophy

Eastern Michigan University   1994
Ypsilanti, MI 48197
Bachelor of Science
Double Major: Biochemistry/Toxicology

Associations:

Michigan Regional Chapter of the Society of Toxicology   1995-Present
- Served on the executive council as the student representative October 1995 to October 1996.

Member National Society of Toxicology   1997-Present

Manuscripts:

B.S. Cummings, R.C. Zangar, R.F. Novak, and L.H. Lash. Cellular Distribution of cytochromes P450 in the Rat Kidney. *Drug Metab. Dispos.* In press.

Submitted Manuscripts:

B.S. Cummings and L.H. Lash. Role of cytochrome P450 2E1 and GSTα in trichloroethylene toxicity and metabolism in rat renal proximal tubular and distal tubular cells. Submitted to *Biochem Pharmacol* 2/99.

Manuscripts in Preparation:

B.S. Cummings, J.M. Lasker, and L.H. Lash. Expression of drug metabolism enzymes in freshly isolated and primary cultures of human renal proximal tubular cells. Expected date of submission is 2/99 to *Biochem Pharmacol*.

B.S. Cummings and L.H. Lash. Effect of pyridine and clofibrate on trichloroethylene metabolism in chloral hydrate in the rat liver and kidney. Expected date of submission is 2/99 to *Drug Metab and Dispos*.

B.S. Cummings and L.H. Lash. Effect of structure and differences in drug metabolism enzyme expression on thiophene-induced cytotoxicity in rat renal proximal tubular and distal tubular cells. Expected date of submission is 3/99 to *Toxicol Appl Pharmacol*.

B.S. Cummings and L.H. Lash. Use of primary cultures of rat renal proximal tubular and distal tubular cells for trichloroethylene and S-(1,2-dichlorovinyl)-L-cysteine cytotoxicity assays. Expected date of submission is 3/99 to *Toxicology*.